



**Properties and Applications of Bio-nanocomposite Films from  
Fish and Squid Skin Gelatins**

**Muralidharan Nagarajan**

**A Thesis Submitted in Fulfillment of the Requirements for the Degree of  
Doctor of Philosophy in Food Science and Technology**

**Prince of Songkla University**

**2014**

**Copyright of Prince of Songkla University**

**Thesis Title** Properties and Applications of Bio-nanocomposite Films from  
Fish and Squid Skin Gelatins  
**Author** Mr. Muralidharan Nagarajan  
**Major Program** Food Science and Technology

---

**Major Advisor:**

.....  
(Prof. Dr. Soottawat Benjakul)

**Examining Committee:**

.....Chairperson  
(Asst. Prof. Dr. Manee Vittayanont)

**Co-Advisors:**

.....  
(Asst. Prof. Dr. Thummanoon Prodpran)

.....Committee  
(Prof. Dr. Soottawat Benjakul)

.....  
(Dr. Ponusa Jitphuthi)

.....Committee  
(Asst. Prof. Dr. Thummanoon Prodpran)

.....Committee  
(Dr. Supachai Pisuchpen)

.....Committee  
(Assoc. Prof. Dr. Rungsinee Sothornvit)

The Graduate School, Prince of Songkla University, has approved this thesis as partial fulfillment of the requirements for the Degree of Doctor of Philosophy in Food Science and Technology.

.....  
(Assoc. Prof. Dr. Teerapol Srichana)  
Dean of Graduate School

This is to certify that the work here submitted is the result of the candidate's own investigations. Due acknowledgement has been made of any assistance received.

.....Signature

(Prof. Dr. Soottawat Benjakul)

Major Advisor

.....Signature

(Mr. Muralidharan Nagarajan)

Candidate

I hereby certify that this work has not been accepted in substance for any degree, and is not being currently submitted in candidature for any degree.

.....Signature

(Mr. Muralidharan Nagarajan)

Candidate

**Thesis Title** Properties and Applications of Bio-nanocomposite Films from Fish and Squid Skin Gelatins  
**Author** Mr. Muralidharan Nagarajan  
**Major Program** Food Science and Technology  
**Academic Year** 2014

## ABSTRACT

Gelatin from splendid squid (*Loligo formosana*) skin extracted at different temperatures (50-80 °C) and their corresponding films were characterised. Gelatin extracted at 80 °C showed the highest yield (45.3%, dry weight basis) with relatively higher free amino group content ( $P<0.05$ ). However, gelatin extracted at 50 °C (G50) had the highest gel strength ( $P<0.05$ ). G80 had the higher  $a^*$  value, compared with others ( $P<0.05$ ). When films from those gelatins were prepared, tensile strength (TS) and elongation at break (EAB) of films decreased, but water vapour permeability (WVP) increased ( $P<0.05$ ) as the extraction temperature increased. Increase in transparency value with coincidental decrease in lightness was observed with increasing extraction temperatures. Thermogravimetric analysis (TGA) indicated that film prepared from G80 (F80) exhibited the higher heat susceptibility and weight loss. Loosen structure was observed in film prepared from gelatin with increasing extraction temperatures.

Gelatins obtained from bleached (0-8%  $H_2O_2$  w/v) squid skin and films from those gelatins were characterised. Gelatin from skin bleached with higher  $H_2O_2$  concentrations had higher yield, lower free amino group and carbonyl group contents than the control gelatin ( $P<0.05$ ). Gel strength of gelatin generally decreased as  $H_2O_2$  concentrations increased ( $P<0.05$ ). Gelatin prepared from skin bleached with 2%  $H_2O_2$  showed the highest  $L^*$ , but lowest  $\Delta E^*$ -values ( $P<0.05$ ).  $H_2O_2$  at higher concentrations yielded gelatin with increasing  $b^*$ -value. TS and WVP of films decreased, but EAB increased ( $P<0.05$ ) as the concentration of  $H_2O_2$  increased. TGA indicated that heat susceptibility and weight loss of different films varied with  $H_2O_2$  concentrations. Rougher surface was obtained in gelatin films prepared from skin bleached with  $H_2O_2$  concentrations above 4%.

The impacts of hydrophilic and hydrophobic montmorillonite (MMT) nanoclays at various levels (0-10%, w/w) on properties of tilapia skin gelatin films were investigated. Generally, mechanical properties were improved by the addition of Cloisite Na<sup>+</sup> in the range of 0.5-5% (w/w). The lowest WVP was observed for films incorporated with Cloisite Na<sup>+</sup> and Cloisite 20A at a level of 1% (w/w) (P<0.05). Wide angle X-ray diffraction (WAXD) and scanning electron microscopic (SEM) analyses revealed the intercalated/exfoliated structure of films. Homogeneity and smoothness of film surface decreased with the addition of both nanoclays. The incorporation of nanoclays enhanced the rigidity and heat stability of films.

Tilapia skin gelatin films incorporated with hydrophilic and hydrophobic nanoclays with the aid of homogenisation using different pressure levels (1000 to 4000 psi) and passes (2 and 4) were characterised. YM, TS and EAB of films decreased and WVP increased with increasing pressure levels and number of passes. Films incorporated with Cloisite 20A exhibited the lower WVP than those with Cloisite Na<sup>+</sup>. Transparency of films increased when homogenisation pressure and number of passes increased. Nanocomposite films prepared using homogenisation had exfoliated structure, whilst those prepared without homogenisation exhibited intercalated structure. TGA and DSC analyses indicated that thermal stability of nanocomposite films varied with homogenisation condition.

Effects of various pHs (4-8) of film forming suspensions (FFS) on the properties of nanocomposite film based on tilapia skin gelatin and Cloisite Na<sup>+</sup> were investigated. In general, mechanical and water vapour barrier properties of nanocomposite films were improved when FFS having pH 6 was used. Intercalated/exfoliated structure of nanocomposite films was revealed by WAXD analysis. Homogeneity and smoothness of film surface were obtained for nanocomposite films with pH 6 as confirmed by SEM micrographs. Thermal stability of nanocomposite films varied with different pH levels.

Effects of ethanolic extract from coconut husk (EECH) at 0-0.4% (w/w) on properties of films and nanocomposite films from tilapia skin gelatin were investigated. YM, TS and EAB of both films decreased with addition of EECH

( $P < 0.05$ ). The lowest WVP was obtained for gelatin film and nanocomposite film containing 0.05% and 0.4% EECH (w/w), respectively ( $P < 0.05$ ). Generally,  $a^*$  value of films increased ( $P < 0.05$ ) with increasing levels of EECH, regardless of nanoclay incorporation. Intercalated or exfoliated structure of nanocomposite films was revealed by WAXD analysis. Based on SEM analysis, the rougher surface was found when EECH was added. EECH had varying impact on thermal stability of films.

When tilapia and squid skin gelatin films and nanocomposite films incorporated without and with EECH were used to cover mackerel meat powder, quality changes were monitored in comparison with that covered with polyethylene (PE) film and the control (without covering) during storage of 30 days at 28-30 °C. The powder covered with nanocomposite film incorporated with EECH at 0.4% (w/w) (SGF-Na-EECH) generally had the lower moisture content than those covered with other gelatin films throughout the storage. The lower PV, TBARS, TVB and pH were observed for SGF-Na-EECH sample than PE sample and the control ( $P < 0.05$ ). Based on SPME-GC-MS analysis, SGF-Na-EECH sample contained the lower volatile lipid oxidation products. Higher overall likeness score was observed for SGF-Na-EECH sample on day 30 of storage.

Therefore, fish and squid gelatins could be used as biomaterials for film preparation. The improvement of film properties could be achieved by incorporation of nanoclay, especially in combination with EECH. The film could extend the shelf-life of dried mackerel powder, mainly via the prevention of lipid oxidation.

## ACKNOWLEDGEMENT

First of all, I would like to express my heartfelt gratefulness, deepest gratitude, sincere appreciations and honor to the “Almighty God” for showering enormous blessings and kindness towards me in every stage of my life.

It is my profound privilege to express my deep sense of gratitude, admiration and intense appreciation to my respected advisor, Prof. Dr. Soottawat Benjakul of Department of Food Technology, Faculty of Agro-Industry, Prince of Songkla University who showed me the path and helped to get me started on the right direction to this degree. His enthusiasm, encouragement, kindness and faith in me throughout have been extremely helpful. He was always available for me and he was optimistic and gave generously of his time and vast knowledge. He always knew where to look for the solutions to obstacles while leading me to the right source, theory, and perspective. His workaholic nature, energy level, intellectual dimension, experience, height of confidence, guidance style and numerous publications have always highly inspired and motivated me to next level of my career part. His patience to correct my writings and facilitation to improve my skills are profoundly appreciated. I realised this is one of the greatest blessings in my life that I worked under his supervision.

It is my great pleasure to express my sincere and heartfelt thanks and regards to my co-advisors, Asst. Prof. Dr. Thummanoon Prodpran and Dr. Ponusa Jitphuthi of the Department of Material Product Technology, Faculty of Agro-Industry, Prince of Songkla University for their invaluable comments, suggestions and timely help. I would like to specially thank Dr. Thummanoon Prodpran for his keenness, tolerance and kind help to improve the quality of my writings.

I am using this opportunity to record my sincere and deepest thanks and regards to chairperson and members of my examining committee, Asst. Prof. Dr. Manee Vittayanont of the Department of Food Technology, Faculty of Agro-Industry, Prince of Songkla University, Dr. Supachai Pisuchpen of the Department of Material Product Technology, Faculty of Agro-Industry, Prince of Songkla University and



Assoc. Prof. Dr. Rungsinee Sothornvit of the Department of Food Engineering, Faculty of Engineering, Kasetsart University, Kamphaengsaen Campus for their critical and very useful comments, kindness, patience and helpful suggestions.

I would like to express my special appreciation and thanks to Dr. Phanat Kittiphattanabawon, Dr. Rossawan Intarasirisawat, Dr. Palanivel Ganesan, Dr. Suthasinee Yarnpakdee, Dr. Sirima Takeungwongtrakul, Dr. Yasir Ali Arfat, Dr. Yaowapa Thiansilakul, Dr. Tanaji G. Kudre, Dr. Samart Sai-Ut, Mr. Sitthichoke Sinthusamran, Mr. Theeraphol Sephan, Mr. Thanasak Sae-leaw, Mr. Phakawat Tongnuanchan, Ms. Anisa Adeen, Ms. Jaksuma Pongsetkul, Mr. Sira Chuaychan, Mr. Naveen Kumar, Ms. Supatra Karnjanapratum, Mr. Natchapol Buamard, Mr. Passakorn Kingwascharapong, Mr. Sulaiman Mad-ali, Mr. Krisna Nilsuwan, Ms. Pimchanok Kaewudom, Ms. Onuma Kaewdang, Ms. Phangam Kaewruang, Ms. Sochaya Chanarat and all other Thai and International friends and colleagues of Seafood Chemistry and Biochemistry Laboratory (2205) for their kindness, unfailing support and invaluable suggestions. It would have been a lonely lab without them.

I wish to thank Dr. Kongkarn Kijroongrojana for her precious time and consistent help to obtain raw material throughout this study. I would like to thank all faculty members and staffs of Agro-Industry for their kind co-operation during my study period. Dedicate, active and accurate services of all professional scientist and technical personnel in Scientific Equipment Center, Prince of Songkla University, are extremely appreciated. My research would not have been possible without their helps.

I find countless words to express my thanks and love to my friends especially Mr. B. Sivaraman, Mr. G. Jayaraman, Mr. L. Ranjith, Dr. J. Biju Sam Kamalam, Mr. P. Antony Jesu Prabhu, Mr. K. Elavarasan, Mrs. K. Nagalakshmi and Dr. S. Saravanan.

It's my great pleasure to acknowledge Dr. Karthikeyan Venkatachalam, who always stood beside me and supported me in all seasons of life, without him I would have felt lonesome in Thailand.

I am extremely thankful to Ms. Nisachon Sakunchannarong for her great support, affection, concern, wishes and suggestions. I specially acknowledge her caring. I also thank Mr. Pitoon Thongchim, Mr. Sarawut Lertlamtraiphop, Ms. Wimol Ngamyinyuad, Ms. Arunporn Atimarmaitree, Ms. Phonpimon Daewa, Dr. Lavanya Goodla and Ms. Panyanan Thongbour for their friendliness, kind support and hospitality.

Words can't express how grateful I am to Ms. Rejini Simpson who supported me in making this thesis and incited me to strive towards my goal. I solely acknowledge her fondness, moral support, sacrifices, prayers and all.

From the depth of my heart, I take the right to express my deepest humbleness, faithfulness and affection to my Amma, Appa, my sisters Kani Mozhi, Surya and Banu Priya, my brothers Mohanraj and Ajayanand, my brother-in-laws Venkatesan, Kuppan and Santhosh Kumar, my nephew Kavin and niece Sanah Sri and all my relatives and friends for their love, affection, ample faith and confidence in me, unrelenting support and inspiration to move always on the right direction, which helped my dreams come true.

Finally, this study could not be succeeded without the financial support from the Indian Council of Agricultural Research (ICAR), New Delhi, India under the ICAR-International Fellowship Program. I gratefully acknowledge this financial support.

I also place on record, my sense of gratitude to one and all, who directly or indirectly, have lent their helping hand in this venture.

I wholly dedicate this thesis to Almighty God, respected ICAR, my beloved advisor and lovable family.

Muralidharan Nagarajan

## CONTENTS

	<b>Page</b>
Abstract.....	v
Acknowledgement.....	viii
Contents.....	xi
List of Tables.....	xxv
List of Figures.....	xxix
<b>Chapter</b>	
<b>1. Introduction and Review of Literature</b>	
1.1 Introduction.....	1
1.2 Review of literature.....	4
1.2.1 Collagen .....	4
1.2.2 Gelatin .....	8
1.2.2.1 Gelatin structure .....	9
1.2.2.2 Fish gelatin .....	10
1.2.2.3 Gelatin extraction .....	15
1.2.2.3.1 Pre-treatment of raw material .....	15
1.2.2.3.2 Extraction of gelatin .....	25
1.2.2.3.3 Purification and drying .....	26
1.2.2.3.4 Improvement of gelling property .....	26
1.2.3 Biodegradable films .....	28
1.2.3.1 Protein.....	30
1.2.3.2 Plasticisers .....	32
1.2.3.3 Formation of protein based-films .....	35

## CONTENTS (Continued)

<b>Chapter</b>	<b>Page</b>
1.2.3.4 Fish gelatin films .....	36
1.2.4 Nanofilms .....	42
1.2.4.1 Nanoclay.....	44
1.2.4.2 Formation and morphology of polymer/clay nanocomposites...	46
1.2.4.3 Gelatin/nanoclay composites .....	52
1.2.5 Improvement of the properties of gelatin films .....	53
1.2.6 Applications of protein based films.....	57
1.2.6.1 Protection and gas/water barrier for food storage.....	61
1.2.6.2 Active packaging for shelf-life extension of foods.....	61
1.3 Objectives .....	64
<b>2. Characteristics and functional properties of gelatin from splendid squid</b>	
<b>(<i>Loligo formosana</i>) skin as affected by extraction temperatures</b>	
2.1 Abstract.....	65
2.2 Introduction.....	66
2.3 Material and methods.....	67
2.3.1 Chemicals.....	67
2.3.2 Collection and preparation of squid skin .....	67
2.3.3 Extraction of gelatin from squid skin .....	68
2.3.4 Analyses .....	69
2.3.4.1 Determination of proximate composition.....	69
2.3.4.2 Electrophoretic analysis and free amino group content.....	69
2.3.4.3 Amino acid analysis.....	70
2.3.4.4 Fourier transform infrared (FTIR) spectroscopic analysis.....	70
2.3.4.5 Measurement of $\zeta$ -potential.....	71
2.3.4.6 Colour measurement .....	71

## CONTENTS (Continued)

<b>Chapter</b>	<b>Page</b>
2.3.4.7 Determination of gel strength .....	71
2.3.4.8 Determination of emulsifying properties.....	72
2.3.4.9 Determination of foaming properties.....	72
2.3.5 Statistical analysis.....	73
2.4 Results and discussion.....	73
2.4.1 Yield and proximate composition.....	73
2.4.2 Protein patterns and free amino group content.....	75
2.4.3 Amino acid composition.....	77
2.4.4 ATR- FTIR spectra.....	79
2.4.5 $\zeta$ - potential.....	82
2.4.6 Colour.....	83
2.4.7 Gel strength.....	83
2.4.8 Emulsifying properties.....	85
2.4.9 Foaming properties.....	87
2.5 Conclusion.....	88
<b>3. Properties of film from splendid squid (<i>Loligo formosana</i>) skin gelatin with various extraction temperatures</b>	
3.1 Abstract.....	89
3.2 Introduction.....	89
3.3 Material and methods.....	91
3.3.1 Chemicals.....	91
3.3.2 Collection and preparation of squid skin.....	91
3.3.3 Extraction of gelatin from squid skin.....	91
3.3.4 Preparation of films.....	92

## CONTENTS (Continued)

<b>Chapter</b>	<b>Page</b>
3.3.5 Analyses.....	93
3.3.5.1 Thickness.....	93
3.3.5.2 Mechanical properties.....	93
3.3.5.3 Water Vapour Permeability.....	93
3.3.5.4 Colour, light transmission and transparency.....	94
3.3.5.5 Electrophoretic analysis.....	95
3.3.5.6 Free amino group content.....	95
3.3.5.7 Attenuated total reflectance-Fourier transform infrared (ATR-FTIR) spectroscopic analysis.....	96
3.3.5.8 Thermo-gravimetric analysis (TGA).....	96
3.3.5.9 Microstructure.....	96
3.3.6 Statistical analyses.....	97
3.4 Results and discussion.....	97
3.4.1 Thickness.....	97
3.4.2 Mechanical properties.....	97
3.4.3 Water vapour permeability (WVP).....	98
3.4.4 Colour.....	99
3.4.5 Light transmission and transparency values.....	100
3.4.6 Protein patterns.....	102
3.4.7 FTIR spectra analysis.....	104
3.4.8 Thermogravimetric analysis (TGA).....	106
3.4.9 Microstructure .....	108
3.5 Conclusion.....	110
<b>4. Effects of bleaching on characteristics and gelling property of gelatin from splendid squid (<i>Loligo formosana</i>) skin</b>	
4.1 Abstract.....	111

## CONTENTS (Continued)

<b>Chapter</b>	<b>Page</b>
4.2 Introduction.....	112
4.3 Materials and methods.....	112
4.3.1 Chemicals.....	112
4.3.2 Collection and preparation of squid skin.....	113
4.3.3 Extraction of gelatin from squid skin bleached with H <sub>2</sub> O <sub>2</sub> at various concentrations.....	113
4.3.4 Yield and Characterisation of gelatin.....	114
4.3.4.1 Yield of gelatin.....	114
4.3.4.2 Determination of carbonyl content.....	114
4.3.4.3 Determination of free amino group content.....	115
4.3.4.4 Electrophoretic analysis.....	115
4.3.4.5 Attenuated total reflectance-Fourier transform infrared (ATR-FTIR) spectroscopic analysis.....	116
4.3.4.6 Measurement of ζ-potential.....	116
4.3.4.7 Colour measurement.....	117
4.3.4.8 Determination of gel strength.....	117
4.3.5 Statistical analyses.....	117
4.4 Results and discussion.....	118
4.4.1 Extraction yield.....	118
4.4.2 Carbonyl content.....	120
4.4.3 Free amino group content.....	120
4.4.4 Protein patterns.....	121
4.4.5 ATR-FTIR spectra.....	122
4.4.6 ζ- potential analysis.....	124
4.4.7 Colour.....	126
4.4.8 Gel strength.....	126
4.5 Conclusion.....	128

## CONTENTS (Continued)

<b>Chapter</b>	<b>Page</b>
<b>5. Film forming ability of gelatins from splendid squid (<i>Loligo formosana</i>) skin bleached with hydrogen peroxide</b>	
5.1 Abstract.....	129
5.2 Introduction.....	129
5.3 Materials and methods.....	131
5.3.1 Chemicals.....	131
5.3.2 Collection and preparation of squid skin.....	131
5.3.3 Extraction of gelatin from squid skin.....	131
5.3.4 Preparation of gelatin films.....	132
5.3.5 Analyses.....	133
5.3.5.1 Thickness.....	133
5.3.5.2 Mechanical properties.....	133
5.3.5.3 Water Vapour Permeability.....	133
5.3.5.4 Colour.....	134
5.3.5.5 Light transmission and transparency.....	134
5.3.5.6 Electrophoretic analysis.....	135
5.3.5.7 Attenuated total reflectance-Fourier transform infrared (ATR-FTIR) spectroscopic analysis .....	135
5.3.5.8 Thermo-gravimetric analysis (TGA).....	136
5.3.5.9 Microstructure analysis.....	136
5.3.6 Statistical analyses.....	136
5.4 Results and discussion.....	137
5.4.1 Thickness.....	137
5.4.2 Mechanical properties.....	137
5.4.3 Water Vapour Permeability (WVP).....	139



## CONTENTS (Continued)

<b>Chapter</b>	<b>Page</b>
5.4.4 Colour.....	139
5.4.5 Light transmission and transparency values.....	140
5.4.6 Protein patterns.....	142
5.4.7 FT-IR spectra analysis.....	143
5.4.8 Thermogravimetric analysis.....	145
5.4.9 Microstructure.....	148
5.5 Conclusion.....	150
<b>6. Characteristics of bio-nanocomposite films from tilapia skin gelatin incorporated with hydrophilic and hydrophobic nanoclays</b>	
6.1 Abstract.....	151
6.2 Introduction.....	151
6.3 Materials and methods.....	153
6.3.1 Chemicals.....	153
6.3.2 Preparation of gelatin films.....	155
6.3.3 Analyses.....	156
6.3.3.1 Thickness.....	156
6.3.3.2 Mechanical properties.....	156
6.3.3.3 Water Vapour Permeability.....	156
6.3.3.4 Colour.....	157
6.3.3.5 Light transmission and transparency.....	157
6.3.4 Characterisation of selected gelatin films.....	158
6.3.4.1 Wide angle x-ray diffraction (WAXD) analysis.....	158
6.3.4.2 Scanning electron microscopic (SEM) analysis.....	158

## CONTENTS (Continued)

<b>Chapter</b>	<b>Page</b>
6.3.4.3 Thermo-gravimetric analysis (TGA).....	158
6.3.4.4 Differential Scanning Calorimetry (DSC).....	159
6.3.5 Statistical analyses.....	159
6.4 Results and discussion.....	159
6.4.1 Thickness.....	159
6.4.2 Mechanical properties.....	160
6.4.3 Water Vapour Permeability (WVP).....	163
6.4.4 Colour.....	164
6.4.5 Light transmission and transparency.....	166
6.4.6 Characterisation of selected gelatin nanocomposite films.....	168
6.4.6.1 Wide angle x-ray diffraction (WAXD) analysis.....	168
6.4.6.2 Scanning electron microscopy (SEM).....	170
6.4.6.3 Thermogravimetric analysis (TGA).....	173
6.4.6.4 Differential Scanning Calorimetry (DSC).....	175
6.5 Conclusion.....	177
<b>7. Properties of bio-nanocomposite films from tilapia skin gelatin as affected by different nanoclays and homogenising conditions</b>	
7.1 Abstract.....	178
7.2 Introduction.....	178
7.3 Materials and methods.....	180
7.3.1 Chemicals.....	180
7.3.2 Preparation of gelatin films containing nanoclays with different homogenising conditions.....	181
7.3.3 Analyses.....	183

## CONTENTS (Continued)

<b>Chapter</b>	<b>Page</b>
7.3.3.1 Thickness.....	183
7.3.3.2 Mechanical properties.....	183
7.3.3.3 Water Vapour Permeability.....	184
7.3.3.4 Colour.....	184
7.3.3.5 Light transmission and transparency.....	185
7.3.4 Characterisation of selected films.....	185
7.3.4.1 Wide angle x-ray diffraction (WAXD) analysis.....	185
7.3.4.2 Thermo-gravimetric analysis (TGA) .....	186
7.3.4.3 Differential scanning calorimetry (DSC).....	186
7.3.5 Statistical analyses.....	186
7.4 Results and Discussion.....	187
7.4.1 Properties of films.....	187
7.4.1.1 Thickness.....	187
7.4.1.2 Mechanical properties.....	187
7.4.1.3 Water vapor permeability (WVP).....	191
7.4.1.4 Colour.....	192
7.4.1.5 Light transmission and transparency.....	194
7.4.2 Characteristics of selected nanocomposite films.....	196
7.4.2.1 WAXD analysis.....	196
7.4.2.2 TGA analysis.....	198
7.4.2.3 DSC analysis.....	200
7.5 Conclusions.....	203

## CONTENTS (Continued)

Chapter	Page
<b>8. Effects of pHs on properties of bio-nanocomposite based on tilapia skin gelatin and Cloisite Na<sup>+</sup></b>	
8.1 Abstract.....	204
8.2 Introduction.....	204
8.3 Materials and methods.....	206
8.3.1 Chemicals.....	206
8.3.2 Study on $\zeta$ - potential of gelatin solution as affected by pHs .....	206
8.3.3 Characteristics of gelatin films containing nanoclay as influenced by pHs .....	207
8.3.3.1 Preparation of nanocomposite films.....	207
8.3.3.2 Analyses.....	208
8.3.3.2.1 Wide angle x-ray diffraction (WAXD) pattern.....	208
8.3.3.2.2 Thickness .....	208
8.3.3.2.3 Mechanical properties.....	208
8.3.3.2.4 Water vapour permeability.....	209
8.3.3.2.5 Colour.....	209
8.3.3.2.6 Light transmission and transparency.....	210
8.3.3.2.7 Scanning electron microscopic (SEM) image.....	210
8.3.3.2.8 Thermo-gravimetric curve.....	210
8.3.3.2.9 Differential scanning calorimetric (DSC) thermograms ...	211
8.3.4 Statistical analyses.....	211
8.4 Results and discussion.....	211
8.4.1 Effect of pHs on $\zeta$ - potential of gelatin solution.....	211

## CONTENTS (Continued)

<b>Chapter</b>	<b>Page</b>
8.4.2 Characteristics of gelatin films containing nanoclay as influenced by pHs .....	212
8.4.2.1 Wide angle x-ray diffraction patterns.....	212
8.4.2.2 Thickness.....	214
8.4.2.3 Mechanical properties.....	215
8.4.2.4 Water vapour permeability (WVP) .....	218
8.4.2.5 Colour .....	218
8.4.2.6 Light transmission and transparency.....	220
8.4.2.7 Microstructure .....	222
8.4.2.8 Thermogravimetric curves .....	224
8.4.2.9 Differential scanning calorimetric thermograms .....	225
8.5 Conclusion.....	229
<b>9. Properties and characteristics of nanocomposite films from tilapia skin gelatin incorporated with ethanolic extract from coconut husk</b>	
9.1 Abstract.....	230
9.2 Introduction.....	230
9.3 Materials and methods.....	232
9.3.1 Chemicals.....	232
9.3.2 Extraction of ethanolic extract from coconut husk.....	233
9.3.2.1 Collection and preparation of coconut husk.....	233
9.3.2.2 Preparation of the ethanolic extract.....	233
9.3.3 Preparation of gelatin films and nanocomposite films.....	234
9.3.4 Analyses.....	236
9.3.4.1 Thickness.....	236

## CONTENTS (Continued)

<b>Chapter</b>	<b>Page</b>
9.3.4.2 Mechanical properties.....	236
9.3.4.3 Water vapour permeability.....	237
9.3.4.4 Colour.....	237
9.3.4.5 Light transmission and transparency.....	238
9.3.5 Characterisation of selected films.....	238
9.3.5.1 Wide angle x-ray diffraction (WAXD) analysis.....	238
9.3.5.2 Scanning electron microscopic (SEM) analysis.....	238
9.3.5.3 Thermo-gravimetric analysis (TGA).....	239
9.3.5.4 Differential scanning calorimetry (DSC).....	239
9.3.6 Statistical analyses.....	239
9.4 Results and discussion.....	240
9.4.1 Properties of gelatin films and nanocomposite films as affected by EECH addition.....	240
9.4.1.1 Thickness.....	240
9.4.1.2 Mechanical properties.....	240
9.4.1.3 Water vapour permeability (WVP).....	243
9.4.1.4 Colour.....	245
9.4.1.5 Light transmission and transparency.....	246
9.4.2 Characteristics of selected gelatin film and nanocomposite film added with EECH.....	248
9.4.2.1 Wide angle x-ray diffraction (WAXD) analysis.....	249
9.4.2.2 Microstructure.....	251
9.4.2.3 TGA thermograms.....	253
9.4.2.4 DSC thermograms.....	256
9.5 Conclusion.....	259

## CONTENTS (Continued)

<b>Chapter</b>	<b>Page</b>
<b>10. Effects of bio-nanocomposite films from tilapia and squid skin gelatins incorporated with ethanolic extract from coconut husk on storage stability of mackerel meat powder</b>	
10.1 Abstract.....	260
10.2 Introduction.....	260
10.3 Materials and methods.....	262
10.3.1 Chemicals.....	262
10.3.2 Preparation of squid skin and extraction of gelatin.....	263
10.3.3 Extraction of ethanolic extract from coconut husk.....	263
10.3.3.1 Collection and preparation of coconut husk.....	263
10.3.3.2 Preparation of the ethanolic extract.....	263
10.3.4 Preparation of gelatin films and nanocomposite films.....	264
10.3.5 Study on shelf-life extension of mackerel meat powder using gelatin films and nanocomposite films.....	264
10.3.5.1 Preparation of mackerel meat powder.....	264
10.3.5.2 Storage of mackerel meat powder covered with films.....	265
10.3.5.3 Analyses.....	265
10.3.5.3.1 Moisture content.....	265
10.3.5.3.2 pH measurement.....	265
10.3.5.3.3 Determination of peroxide value (PV).....	267
10.3.5.3.4 Determination of thiobarbituric acid reactive substances (TBARS).....	267
10.3.5.3.5 Determination of total volatile base (TVB) content.....	268
10.3.5.3.6 Determination of colour.....	268
10.3.5.3.7 Sensory evaluation.....	268

## CONTENTS (Continued)

<b>Chapter</b>	<b>Page</b>
10.3.5.3.8 Measurement of volatile compounds.....	268
10.3.5.3.8.1 Extraction of volatile compounds by SPME fibre.....	269
10.3.5.3.8.2 GC–MS analysis.....	269
10.3.5.3.8.3 Analyses of volatile compounds.....	270
10.3.6 Statistical analyses.....	270
10.4 Results and discussion.....	270
10.4.1 Chemical changes of mackerel meat powder during storage.....	270
10.4.1.1 Moisture content.....	270
10.4.1.2 pH.....	273
10.4.1.3 PV.....	273
10.4.1.4 TBARS value.....	274
10.4.1.5 TVB content.....	276
10.4.2 Changes in colour of mackerel meat powder during storage.....	278
10.4.3 Changes in sensory property of mackerel meat powder during storage.....	280
10.4.4 Changes in volatile compounds of mackerel meat powder during storage.....	282
10.5 Conclusion.....	284
11. Summary and future works.....	285
11.1 Summary.....	285
11.2 Future works.....	286
References.....	287
Vitae.....	340



## LIST OF TABLES

<b>Table</b>	<b>Page</b>
1. Sources of collagen from different fish species .....	5
2. Different sources of fish gelatin.....	12
3. Procedures employed for pretreatment and extraction of fish gelatin.....	16
4. Properties of gelatin-based film from different fish species.....	38
5. Chemical formula and characteristics of commonly used 2:1 phyllosilicates.....	45
6. Characteristics of nanoclays and organoclays .....	47
7. Properties of nanocomposite films from different sources.....	50
8. Properties of gelatin nanocomposite films from different sources.....	54
9. Properties of gelatin films incorporated with plant extracts.....	58
10. Extraction yield, proximate composition, colour and gel strength of gelatin from the skin of splendid squid extracted at different temperatures.....	74
11. Amino acid composition of gelatin from the skin of splendid squid extracted at different temperatures.....	78
12. Emulsifying and foaming properties of gelatin from the skin of splendid squid extracted at different temperatures.....	86
13. Tensile strength (TS), elongation at break (EAB), water vapour permeability (WVP) and thickness of films from squid skin gelatin extracted at different temperatures.....	99
14. Colour of films from squid skin gelatin extracted at different temperatures.....	100
15. Light transmittance (%) and transparency values of films from squid skin gelatin extracted at different temperatures.....	101

### LIST OF TABLES (Continued)

<b>Table</b>	<b>Page</b>
16. Thermal degradation temperature ( $T_d$ , °C) and weight loss ( $\Delta w$ , %) of films from squid skin gelatin extracted at different temperatures.....	107
17. Yield, carbonyl content, free amino group content and colour of gelatins from the splendid squid skin bleached with $H_2O_2$ at various concentration.....	119
18. Tensile strength (TS), elongation at break (EAB), water vapour permeability (WVP) and thickness of gelatin films from the splendid squid skin bleached with $H_2O_2$ at various concentrations.....	138
19. Colour, light transmittance and transparency values of gelatin films from the splendid squid skin bleached with $H_2O_2$ at various concentrations.....	141
20. Thermal degradation temperature ( $T_d$ , °C) and weight loss ( $\Delta w$ , %) of gelatin films from the splendid squid skin bleached with $H_2O_2$ at various concentrations.....	147
21. Characteristics of hydrophilic and hydrophobic nanoclays.....	154
22. Young's modulus (YM), tensile strength (TS), elongation at break (EAB), water vapour permeability (WVP) and thickness of films from tilapia skin gelatin incorporated with different types of nanoclays at various levels.....	161
23. Colour of films from tilapia skin gelatin incorporated with different types of nanoclays at various levels.....	165
24. Light transmittance and transparency values of films from tilapia skin gelatin incorporated with different types of nanoclays at various level.....	167

### LIST OF TABLES (Continued)

<b>Table</b>		<b>Page</b>
25.	Thermal degradation temperature ( $T_d$ , °C), weight loss ( $\Delta w$ , %) and glass transition temperature ( $T_g$ , °C) of films from tilapia skin gelatin incorporated with different types of nanoclays.....	174
26.	Young's modulus (YM), tensile strength (TS), elongation at break (EAB), water vapour permeability (WVP) and thickness of films from tilapia skin gelatin incorporated with hydrophilic and hydrophobic nanoclays using different homogenisation conditions.....	190
27.	Colour of films from tilapia skin gelatin incorporated with hydrophilic and hydrophobic nanoclays using different homogenisation conditions.....	193
28.	Light transmittance and transparency values of films from tilapia skin gelatin incorporated with hydrophilic and hydrophobic nanoclays using different homogenisation conditions.....	195
29.	Thermal degradation temperature ( $T_d$ , °C), weight loss ( $\Delta w$ , %), and glass transition temperature ( $T_g$ , °C) of films from tilapia skin gelatin incorporated with hydrophilic and hydrophobic nanoclays using different homogenisation conditions.....	200
30.	Young's Modulus (YM), tensile strength (TS), elongation at break (EAB), water vapour permeability (WVP) and thickness of nanocomposite films from tilapia skin gelatin incorporated with Cloisite Na <sup>+</sup> prepared from FFS at different pH levels.....	217
31.	Colour of nanocomposite films from tilapia skin gelatin incorporated with Cloisite Na <sup>+</sup> prepared from FFS at different pH levels.....	219
32.	Light transmittance (%) and transparency values of nanocomposite films from tilapia skin gelatin incorporated with Cloisite Na <sup>+</sup> prepared from FFS at different pH levels.....	221

### LIST OF TABLES (Continued)

<b>Table</b>		<b>Page</b>
33.	Thermal degradation temperature ( $T_d$ , °C), weight loss ( $\Delta w$ , %) and glass transition temperature ( $T_g$ , °C) of nanocomposite films from tilapia skin gelatin incorporated with Cloisite Na <sup>+</sup> prepared from FFS at different pH levels.....	226
34.	Young's Modulus (YM), tensile strength (TS), elongation at break (EAB), water vapour permeability (WVP) and thickness of gelatin films and nanocomposite films incorporated with EECH at different levels.....	241
35.	Colour of gelatin films and nanocomposite films incorporated with EECH at different levels.....	246
36.	Light transmittance and transparency values of gelatin films and nanocomposite films incorporated with EECH at different levels.....	248
37.	Thermal degradation temperature ( $T_d$ , °C), weight loss ( $\Delta w$ , %), residue (%) and glass transition temperature ( $T_g$ , °C) of gelatin films and nanocomposite films incorporated with EECH at different levels..	255
38.	Likeness score of mackerel meat powder covered with gelatin films and nanocomposite films incorporated without and with EECH in comparison with that covered PE film and the control during storage at 28-30 °C.....	281
39.	Volatile compounds of mackerel meat powder at day 0 and powder covered with nanocomposite film from squid skin gelatin incorporated with 0.4% EECH (w/w) in comparison with PE film and the control after 30 days of storage at 28-30 °C.....	283

## LIST OF FIGURES

<b>Figure</b>	<b>Page</b>
1. Classification of the biodegradable polymers .....	29
2. Processing methods of film formation: wet (or solvent) and dry process.....	36
3. Schematic illustration of formation of “tortuous path” in nanocomposite .....	43
4. Potential applications of nanotechnology in the food and food-packaging industries .....	44
5. The crystal structure of the phyllosilicates .....	45
6. Types of composite derived from the interaction between clays and polymers.....	46
7. Formation of bio-nanocomposites and bio-degradation.....	49
8. A scheme illustrating the impact of herb extracts without and with oxidation of the cross-linking of gelatin molecules in the film matrix	56
9. Preparation of antioxidant/antimicrobial nanocomposite films using a solvent casting method.....	62
10. Protein patterns (a) and free amino group content (b) of gelatins from the skin of splendid squid extracted at different temperatures.....	76
11. Proposal scheme for gelatin extraction from squid skin at low and high temperatures.....	77
12. ATR-FTIR spectra of gelatins from the skin of splendid squid extracted at different temperatures. ....	80
13. $\zeta$ -potential of gelatins from the skin of splendid squid extracted at different temperature.....	82

### LIST OF FIGURES (Continued)

<b>Figure</b>	<b>Page</b>
14. Protein patterns (a) and free amino group content (b) of films from splendid squid skin gelatin extracted at different temperatures.....	103
15. ATR-FTIR spectra of films from splendid squid skin gelatin extracted at different temperatures.....	105
16. Thermogravimetric curves of films from splendid squid skin gelatin extracted at different temperatures.....	106
17. SEM micrographs of surface (A) and cryo-fractured cross-section (B) of films from splendid squid skin gelatin extracted at different temperatures.....	109
18. Protein patterns of gelatins from the splendid squid skin bleached with H <sub>2</sub> O <sub>2</sub> at various concentrations.....	121
19. ATR-FTIR spectra of gelatins from the splendid squid skin bleached with H <sub>2</sub> O <sub>2</sub> at various concentrations.....	123
20. ζ-potential of gelatins from the splendid squid skin bleached with H <sub>2</sub> O <sub>2</sub> at various concentrations.....	125
21. Gel strength of gelatins from the splendid squid skin bleached with H <sub>2</sub> O <sub>2</sub> at various concentrations. ....	127
22. Protein patterns of gelatin films from the splendid squid skin bleached using H <sub>2</sub> O <sub>2</sub> at various concentrations.....	142
23. ATR-FTIR spectra (a) and TGA curves (b) of gelatin films from splendid squid skin bleached with H <sub>2</sub> O <sub>2</sub> at various concentrations.....	144
24. SEM micrographs of surface (A) and cryo-fractured cross-section (B) of gelatin films from the splendid squid skin bleached with H <sub>2</sub> O <sub>2</sub> at various concentrations.....	149

### LIST OF FIGURES (Continued)

<b>Figure</b>	<b>Page</b>
25. WAXD patterns of nanoclays (a) and films from tilapia skin gelatin incorporated with different nanoclays (b).....	169
26. SEM micrographs of surface (A and B) and cryo-fractured cross-section (C) of films from tilapia skin gelatin incorporated with different nanoclays .....	171
27. Thermogravimetric curves of films from tilapia skin gelatin incorporated with different nanoclays.....	173
28. DSC thermograms of films from tilapia skin gelatin incorporated with different nanoclays.....	176
29. Scheme for preparation of film formig suspensions of fish gelatin and MMT nanoclays using different homogenisation conditions.....	182
30. WAXD patterns of nanoclay (a) and films from tilapia skin gelatin incorporated with Cloisite Na <sup>+</sup> using different homogenisation conditions (b).....	197
31. Thermogravimetric curves of films from tilapia skin gelatin incorporated with Cloisite Na <sup>+</sup> using different homogenisation conditions.....	199
32. DSC thermograms of first (a) and second (b) heating scan of films from tilapia skin gelatin incorporated with Cloisite Na <sup>+</sup> using different homogenization conditions.....	201
33. Proposed scheme of nanoclay incorporated gelatin film matrix as affected by different homogenisation conditions.....	202
34. ζ- potential value of tilapia skin gelatin.....	212
35. WAXD patterns of Cloisite Na <sup>+</sup> (a) and nanocomposite films from tilapia skin gelatin incorporated with Cloisite Na <sup>+</sup> prepared from FFS at different pH levels (b).....	213

### LIST OF FIGURES (Continued)

Figure		Page
36.	SEM micrographs of surface (A) and cryo-fractured cross-section (B) of nanocomposite films from tilapia skin gelatin incorporated with Cloisite Na <sup>+</sup> prepared from FFS at different pH levels.....	223
37.	Thermogravimetric curves of nanocomposite films from tilapia skin gelatin incorporated with Cloisite Na <sup>+</sup> prepared from FFS at different pH levels.....	225
38.	DSC thermograms of nanocomposite films from tilapia skin gelatin incorporated with Cloisite Na <sup>+</sup> prepared from FFS at different pH levels.....	228
39.	Proposed scheme of nanoclay incorporation with gelatin chains at different pH levels of FFS.....	229
40.	Scheme for preparation of gelatin film-forming solutions and nanocomposite film-forming suspensions incorporated with EECH..	235
41.	WAXD patterns of Cloisite Na <sup>+</sup> (a) and gelatin films and nanocomposite films incorporated with EECH at different levels (b)..	250
42.	SEM micrographs of surface (A) and cryo-fractured cross-section (B) of gelatin films and nanocomposite films incorporated with EECH at different levels.....	252
43.	Thermogravimetric curves of gelatin films and nanocomposite films incorporated with EECH at different levels.....	254
44.	DSC thermograms of gelatin films and nanocomposite films incorporated with EECH at different levels.....	256
45.	Proposed scheme of possible interaction between gelatin, phenolic compounds, and nanoclay in film matrix.....	258
46.	Scheme for preparation of mackerel meat powder covered with different films.....	266



**LIST OF FIGURES (Continued)**

<b>Figure</b>		<b>Page</b>
47.	Moisture content (a) and pH (b) of mackerel meat powder covered with gelatin films and nanocomposite films incorporated without and with EECH in comparison with that covered polyethylene (PE) film and the control during storage at 28-30 °C.....	272
48.	PV (a) and TBARS values (b) of mackerel meat powder covered with gelatin films and nanocomposite films incorporated without and with EECH in comparison with that covered PE film and the control during storage at 28-30 °C.....	275
49.	TVB content of mackerel meat powder covered with gelatin films and nanocomposite films incorporated without and with EECH in comparison with that covered PE film and the control during storage at 28-30 °C.....	277
50.	Colour of mackerel meat powder covered with gelatin films and nanocomposite films incorporated without and with EECH in comparison with that covered PE film and the control during storage at 28-30 °C.....	279

## CHAPTER 1

### INTRODUCTION AND REVIEW OF LITERATURE

#### 1.1 Introduction

Nowadays, biodegradable films are gaining increasing attention as the important non-toxic and eco-friendly packaging materials over synthetic thermoplastic films (Wang *et al.*, 2015). Most synthetic films are non-biodegradable and may cause environmental pollution and serious ecological problems. Moreover, biodegradable materials have several desirable physico-chemical characteristics over synthetic counterpart. Renewable biopolymers such as proteins, lipids and polysaccharides have been used as potential film-forming material (Tharanathan, 2003).

Gelatin is a well known biopolymer among the animal proteins for its film-forming ability and applicability for food packaging and storage (Gomez-Guillen *et al.*, 2009). Gelatin is a water soluble protein obtained by partial hydrolysis of collagen, the main fibrous protein constituent in bones, cartilages and skins (Benjakul *et al.*, 2012a). Gelatin can be used as foaming, emulsifying and wetting agent in food, pharmaceutical, medical and technical applications due to its surface-active properties (Balti *et al.*, 2011). Gelatin from cuttlefish skin had the improved emulsifying property when modified by oxidized fatty acids (Aewsiri *et al.*, 2011). Functional properties of gelatin are governed by many factors such as chain length or molecular weight, amino acid composition and hydrophobicity, etc (Gomez-Guillen *et al.*, 2002). Due to the constraints for the use of bovine and porcine gelatin associated with religious prohibition, gelatin from aquatic animal has gained increasing attention (Karim and Bhat, 2009). In addition, there is increasing concern whether land animal tissue-derived collagens and gelatins are capable of transmitting pathogenic vectors such as prions (Wilesmith *et al.*, 1991). As a consequence, fish gelatin has gained increasing interest as the potential alternative for land animal counterpart. Fish processing discards such as skin, fin, scale and bones, etc., accounting for 70–85% of

the total weight of catch (Shahidi, 1994), have been used as the starting material for gelatin extraction.

Apart from gelling property, gelatin has been used for film formation with the superior gas barrier property. Gelatins from the skin of cuttlefish (Jridi *et al.*, 2014a), tilapia (Pranoto *et al.* 2007; Tongnuanchan *et al.*, 2013) and bigeye snapper (Rattaya *et al.*, 2009) have been used for making transparent, colourless, and flexible films. Additionally, it can be used as the active packaging, in which the antioxidants or antimicrobials can be incorporated (Gomez-Estaca *et al.*, 2014; Jongjareonrak *et al.*, 2008; Tongnuanchan *et al.*, 2012). Owing to the superior oxygen barrier property, fish gelatin based film could prevent the lipid oxidation in food systems (Jongjareonrak *et al.*, 2006b). However, gelatin has the hydrophilicity in nature and the film from gelatin generally shows low water vapour barrier property. Furthermore, gelatin film has the relatively poor mechanical properties, in comparison with traditional synthetic polymeric films (McHugh and Krochta, 1994). This more likely leads to the limitation for commercial uses. To tackle this problem, several approaches have been developed to improve the barrier property, e.g. the incorporation of essential oils (Tongnuanchan *et al.*, 2013) and fatty acid (Limpisophon *et al.*, 2010). The mechanical properties of fish gelatin film were also improved by the incorporation of nano-clays (Bae *et al.*, 2009a; Farahnaky *et al.*, 2014).

Thailand and other Southeast Asian countries have consumed a large amount of squid and have exported squid and their products all over the world (Hoque *et al.*, 2010). During processing, skin is generated and constitutes around 3-5% of total weight. Skin has a low market value and is generally used as animal feed. Recently, gelatin has been extracted from skin of giant squid (Uriarte-Montoya *et al.*, 2011; Gimenez *et al.*, 2009). Gelatins from fish and cuttlefish skin have been demonstrated to render the biodegradable films with the superior UV barrier properties (Houque *et al.*, 2011a; Jridi *et al.*, 2014a; Rattaya *et al.*, 2009). Nevertheless, the pigments in squid skin pose a colour problem in the resulting gelatin. To tackle such a limitation, bleaching squid skin prior to extraction of gelatin can be an effective means to bring about the gelatin with acceptable colour for wider

applications, especially for film preparation. Additionally, the better understanding of extracting procedures associated with molecular property can lead to the better preparation of gelatin film with desirable characteristics. The use of nanoclay to improve water barrier property of gelatin film is another approach to broaden the use of gelatin film or packaging for shelf-life extension of food products. The incorporation of plant extracts into gelatin film along with nanoclay can enhance the use of the film as smart packaging, which can extend the shelf-life of foods, particularly perishable fish and fish products. The information gain will be of benefit for squid processing industry, in which the value-added products, such as gelatin can be produced and the smart bio-nanocomposite films can be obtained as green and smart packaging.

## 1.2 Review of Literature

### 1.2.1 Collagen

Collagen is abundant in animal connective tissues. It has a triple helix structure with three long polypeptide chains. Each polypeptide is a left handed triple helix; but the three helices are wrapped around each other towards right. Each polypeptide is made up of roughly 1000 amino acid residues with a repeated Glycine-X-Y sequence (Benjakul *et al.*, 2012b; Mathew, 2002). Glycine-X-Y repeat with the frequent occurrence of proline and hydroxyproline in the X and Y position, respectively. Both imino acids, hydroxyproline and hydroxylysine, are found only in position Y, while proline can be found in either the X- or Y- position (Fratzl, 2008). Proline and hydroxyproline form bends in polypeptide chains and are not compatible with  $\alpha$ -helix structure (Lehninger, 1982). Imino acids have been reported to affect thermal stability of collagen molecules (Karim and Bhat, 2009; Piez and Gross, 1960). Amino acid composition directly has the impact on property of collagens (Brinckman, 2005).

Apart from mammalian skin and bones, the discards from fish processing including skin, scales and bones can be used as starting materials for collagen extraction (Table 1). Recently, swim bladder has been reported as the excellent source of collagen (Bama *et al.*, 2010; Sinthusamran and Benjakul, 2013). Collagen content in fish varies with the species, muscle parts, age, season, nutritional condition, time of catch, etc. (Sato *et al.*, 1998). The proportion of collagen in the connective tissue is 88-98%. Collagen and elastin contents were reported to be 0.68-1.35% of the total proteins in fish. The total collagen ranged from 76.2% of whole body collagen for Japanese eel to 91.1% for red seabream (Yoshinaka *et al.*, 1990). Collagen can be extracted with the aid of acid, which is able to solubilise the collagen termed 'acid soluble collagen' (ASC) (Skierka and Sadowska, 2007). Due to crosslinking of collagen fibrils, at telopeptide regions, the use of pepsin, which specifically cleaves at telopeptide can increase the extraction yield. The resulting collagen is termed 'pepsin soluble collagen' (PSC). Nalinanon *et al.* (2007) extracted

**Table 1.** Sources of collagen from different fish species

<b>Fish species</b>	<b>Sources</b>	<b>Extracted collagen</b>	<b>Yield (%)</b>	<b>References</b>
Grass carp ( <i>Ctenopharyngodon idella</i> )	Skin	ASC	46-91	Liu <i>et al.</i> (2015)
Skipjack tuna ( <i>Katsuwonus pelamis</i> )	Spine	ASC	2.47	Di <i>et al.</i> (2014)
		PSC	5.62	
	Skull	ASC	3.57	
		PSC	6.71	
Silvertip shark ( <i>Carcharhinus albimarginatus</i> )	Skeletal	PSC	NR	Jeevithan <i>et al.</i> (2014)
	Head bone	PSC	NR	
Amur sturgeon ( <i>Acipenser schrenckii</i> )	Cartilage	SSC	2.18	Liang <i>et al.</i> (2014)
		ASC	27.04	
		PSC	55.92	
Squid ( <i>Doryteuthis singhalensis</i> )	Skin	ASC	56.8	Veeruraj <i>et al.</i> (2014)
		PSC	24.6	
Spanish mackerel ( <i>Scomberomorus niphonius</i> )	Skin	ASC	13.68	Li <i>et al.</i> (2013)
		PSC	3.49	
	Bone	ASC-1	12.54	
		ASC-2	14.27	

**Table 1.** (Continued)

<b>Fish species</b>	<b>Sources</b>	<b>Extracted collagen</b>	<b>Yield (%)</b>	<b>References</b>
Sea bass ( <i>Lates calcarifer</i> )	Skin	ASC	15.8	Sinthusamran and Benjakul (2013)
	Swim bladder	ASC	28.5	
Bighead carps ( <i>Hypophthalmichthys nobilis</i> )	Skin	PSC	17.5	Liu <i>et al.</i> (2012)
	Swim bladder	PSC	14.6	
Walleye pollock ( <i>Theragra chalcogramma</i> )	Skin	ASC	NR	Yan <i>et al.</i> (2012)
Balloon fish ( <i>Diodon holocanthus</i> )	Skin	ASC	4	Huang <i>et al.</i> (2011)
		PSC	19.5	
Ornate threadfin bream ( <i>Nemipterus hexodon</i> )	Skin	PSC	NR	Nalananon <i>et al.</i> (2011)
Striped catfish ( <i>Pangasianodon hypophthalmus</i> )	Skin	ASC	5.1	Singh <i>et al.</i> (2011)
		PSC	7.7	
Skate ( <i>Raja kenoei</i> )	Skin	ASC	4.84-11.5	Shon <i>et al.</i> (2011)
Catfish ( <i>Tachysurus maculatus</i> )	Swim bladder	PSC	40	Bama <i>et al.</i> (2010)
Brownbanded bamboo shark ( <i>Chiloscyllium punctatum</i> )	Skin	ASC	9.38	Kittiphattanabawon <i>et al.</i> (2010a)
		PSC	8.86	

**Table 1.** (Continued)

<b>Fish species</b>	<b>Sources</b>	<b>Extracted collagen</b>	<b>Yield (%)</b>	<b>References</b>
Jumbo squid ( <i>Dosidicus gigas</i> )	Skin	ASC	70	Uriarte-Montoya <i>et al.</i> (2010)
Common carp ( <i>Cyprinus carpio</i> )	Skin	ASC	41.3	Duan <i>et al.</i> (2009)
	Bone	ASC	1.06	
Nile tilapia ( <i>Oreochromis niloticus</i> )	Skin	ASC	39.4	Zeng <i>et al.</i> (2009)
Largefin longbarbel catfish ( <i>Mystus macropterus</i> )	Skin	ASC	16.8	Zhang <i>et al.</i> (2009)
		PSC	28.0	
Silver carp ( <i>Hypophthalmichthys molitrix</i> )	Skin	NR	NR	Rodziewicz-Motowidło <i>et al.</i> (2008)
Walleye pollock ( <i>Theragra chalcogramma</i> )	Skin	ASC	NR	Yan <i>et al.</i> (2008)
Channel catfish ( <i>Ictalurus punctatus</i> )	Skin	ASC	25.8	Liu <i>et al.</i> (2007)
		PSC	38.4	
Bigeye snapper ( <i>Priacanthus tayenus</i> )	Skin	ASC	5.31	Nalinanon <i>et al.</i> (2007)
		PSC	18.74	

ASC: Acid Soluble Collagen; PSC: Pepsin Soluble Collagen; SSC: Salt Soluble Collagen.

NR: Not Reported.



both ASC and PSC from the skin of bigeye snapper with yields of 5.31 and 18.74%, respectively and both ASC and PSC showed similar properties.

Fish collagen was characterised to have very low denaturation temperature (Td) (Lewis and Piez, 1964). Ikoma *et al.* (2003) stated that the Td values were found to be more dependent on hydroxyproline rather than proline. The total imino acid content of fish collagen was found proportional to the Td values (Piez and Gross, 1960). Td values were also found to vary with the structural parts of fish (Kimura *et al.*, 1988).

Fish muscle Type I collagen exhibited higher Td values because of higher degree of proline hydroxylation when compared to skin Type I collagen (Kimura *et al.*, 1988). Td values of bone collagen of skipjack tuna and yellow seabream were much higher than those of skin collagen that ranged from 29.5-30 °C and 25-26.5 °C, respectively (Nagai and Suzuki, 2000). In contrast to previous reports, higher Td value of 36 °C for collagen of Nile perch skin was reported by Muyonga *et al.* (2004a). Collagens from elasmobranchs were found to have 5 °C higher Td values than those from teleosts (Bae *et al.*, 2008). Collagen from ray skin had a Td value of 33 °C. Wang *et al.* (2008) observed Td values of 16.1, 17.7 and 17.5 °C for deep-sea red fish skin, scale and bone collagen, respectively. Td value of collagen obtained from tropical water fish is higher than that of temperate water fish (Wang *et al.*, 2008).

### **1.2.2 Gelatin**

Gelatin is not a naturally occurring protein and it can be obtained by thermal denaturation and partial hydrolysis of fibrous protein collagen (Benjakul *et al.*, 2012a; United States Pharmacopeia, 1990). During the collagen-to-gelatin transition, many non-covalent bonds are broken along with some covalent inter- and intra-molecular bonds (Schiff's base and aldo condensation bonds). This results in conversion of the helical collagen structure to a more amorphous form, known as gelatin (Foegeding *et al.*, 1996). It is a high molecular weight polypeptide and serves

as an important hydrocolloid with a wide range of applications in food products because of its gelling and thickening properties (Karim and Baht, 2009). The strength of the gel formed is proportional to the concentration of gelatin and its molecular weight (Cho *et al.*, 2004). Gelatin differs from other hydrocolloids because most of them are polysaccharides, whereas gelatin is a digestible protein containing all essential amino acids except tryptophan (Hao *et al.*, 2009). Furthermore, gelatin can be used as foaming, emulsifying and wetting agents in food, pharmaceutical, medical and technical applications due to its surface-active properties (Balti *et al.*, 2011).

### **1.2.2.1 Gelatin structure**

Gelatin generally consists of a large number of glycine, proline and 4-hydroxyproline residues (Johnston-Banks, 1990). Gelatin can be classified into two types, depending on denaturation processes or pre-treatment conditions of native collagen. Type A and type B gelatins are derived from acid and alkaline pre-treatment of native collagen, respectively (Cole and Roberts 1997).

The primary structure of gelatin closely resembles the parent collagen. This similarity has been substantiated for several tissues and species. Small differences are due to raw material sources together with pretreatment and extraction procedures. These can be summarized as follows (Johnston-Banks, 1990):

- 1) Partial removal of amide groups of asparagine and glutamine, resulting in an increase in the contents of aspartic acid and glutamic acid. This increases the number of carboxyl groups in the gelatin molecule and thus lowers the isoelectric point. The degree of conversion is related to the severity of the pretreatment process (Ofori, 1999).
- 2) Conversion of arginine to ornithine in more prolonged treatments experienced during long liming processes. This takes place by removal of a urea group from the arginine side-chain (Ofori, 1999).

- 3) There is a tendency for trace amino acids, such as cysteine, tyrosine, isoleucine, serine, etc., to be found in lower proportions than in their parent collagens. This is due to the inevitable removal of some telopeptide during cross-link cleavage, which is then lost in the pretreatment solutions (Ofori, 1999).

Gelatin is not completely polydispersed, but has a definite molecular weight distribution pattern corresponding to the  $\alpha$ -chain and its oligomers (Johnston-Banks, 1990). One to eight oligomers may be detected in solution, but it is possible that higher numbers exist. Doublets, known as  $\beta$ -chains, are formed from both  $\alpha_1$ - and  $\alpha_2$ -chains, giving rise to  $\beta_{11}$ - and  $\beta_{12}$ -molecules (Johnston-Banks, 1990). Oligomers of three  $\alpha$ -chains will mainly exist as intact triple helix, but a certain proportion will exist as extended  $\alpha$ -polymers bonded randomly by end-to-end or side-to-side bonds (Johnston-Banks, 1990). The structure of oligomers of greater than four  $\alpha$ -chain units obviously become increasingly more complex (Gimenez *et al.*, 2005a). Molecular-weight spectra normally relate to physical properties of gelatin (Karim and Bhat, 2009). In general, the sum of the  $\alpha$ - and  $\beta$ -fractions, together with their larger peptides, is proportional to the bloom strength, and the percentage of higher molecular weight material is related to the viscosity (Karim and Bhat, 2009). The setting time is increased for the peptide fractions below  $\alpha$ -chain, but fractions with very high molecular weight have the reduced setting time (Johnston-Banks, 1990). Kittiphattanabawon *et al.* (2010b) reported that gelatin extracted from shark skin at higher temperature with a lower portion of  $\alpha$ -chain or  $\beta$ -chain had the longer setting time, compared with those extracted at lower temperature. The melting point also increases with higher molecular weight content (Cho *et al.*, 2004; Karim and Bhat, 2009).

#### **1.2.2.2 Fish gelatin**

Gelatin from beef is not acceptable for Hindu and porcine gelatin is prohibited for Judaism and Islam (Karim and Bhat, 2009). Due to the outbreak of Foot

and Mouth Disease (FMD) or Bovine Spongiform Encephalopathy (BSE), land animal tissue-derived collagens and gelatins are questionable for transmitting pathogenic vectors such as prions (Wilesmith *et al.*, 1991). As a consequence, fish gelatin has gained increasing interest as the potential alternative for land animal counterpart. Fish processing discards such as skin, fin, scale and bones, etc., accounts for 70–85% of the total weight of catch (Shahidi, 1994). Disposal of these wastes poses serious environmental problem. Those resources have been reported as promising raw material for gelatin production (Gomez-Guillen *et al.*, 2002).

Gelatin from fish can be derived from four groups of fish as follows (Ofori, 1999):

- 1) Elasmobranchs (Sharks, dogfishes and rays)
- 2) Cold-water fishes (Cod, halibut and plaice)
- 3) Warm-water fishes (Sturgeons, carp, coelacanth and threadfins)
- 4) Hot-water fishes (Lungfishes)

The gelatins from these groups cover a wide range of composition with varying gel strength (Table 2). Fish gelatins derived from cold water fishes have lower gelling properties. On the other hand, gelatins from warm-water fishes have gelling properties more comparable with mammalian gelatins (Karim and Baht, 2009).

Gelling and melting temperatures of cold water fish/mammalian gelatins are in general lower than the warm water fish/mammalian gelatins (Muyonga *et al.*, 2004b). Gomez-Guillen *et al.* (2002) reported that low melting point is related to the lower imino acid content and decreased proline hydroxylation degree in the cold water fish gelatin. The lower imino acid content in cold water fishes reduces the propensity for intermolecular helix formation (Gilsenan and Ross Murphy, 2000). Gelling and melting temperatures are also influenced by the change in ionic strength and pH of gelatin. They decreased with the increase in ionic strength of  $> 0.5 \text{ mol / L}$ ,

**Table 2.** Different sources of fish gelatin

<b>Fish species</b>	<b>Sources</b>	<b>Extraction condition</b>	<b>Gel strength (g)</b>	<b>References</b>
Barbel ( <i>Barbus callensis</i> )	Skin	50 °C for 18 h	NR	Sila <i>et al.</i> (2015)
Sea bream	Bone	60 °C for 12 h	81.7-87.3	Akagunduz <i>et al.</i> (2014)
	Scale		126	
African catfish ( <i>Clarias gariepinus</i> )	Skin	33 °C for 9 h	234	Alfaro <i>et al.</i> (2014)
Cuttlefish	Skin	40 °C for 14 h	192.01	Jridi <i>et al.</i> (2014b)
Yellowfin tuna ( <i>Thunnus albacares</i> )	Skin	55 °C for 1 h	289.8	Karayannakidis and Zotos (2014)
Zebra blenny ( <i>Salaria basilisca</i> )	Skin	50 °C for 8 h	170.2	Ktari <i>et al.</i> (2014)
Thornback ray	Skin	50 °C for 5 h	140	Lassoued <i>et al.</i> (2014)
Unicorn leatherjacket ( <i>Aluterus monoceros</i> )	Skin	45, 55, 65 and 75 °C, 12 h	~60-180	Kaewruang <i>et al.</i> (2013)
Pink perch ( <i>Nemipterus japonicus</i> )	Skin	45 °C for 12 h	140	Koli <i>et al.</i> (2012)
	Bone		130	
Tiger-toothed croaker ( <i>Otolithes ruber</i> )	Skin		170	
	Bone		150	
Marine snail ( <i>Hexaplex trunculus</i> )	Meat	60 °C for 9 h	103	Zarai <i>et al.</i> (2012)
Grey triggerfish ( <i>Balistes capriscus</i> )	Skin	50 °C for 18 h	168.3	Jellouli <i>et al.</i> (2011)

**Table 2.** (Continued)

<b>Fish species</b>	<b>Sources</b>	<b>Extraction condition</b>	<b>Gel strength (g)</b>	<b>References</b>
Red tilapia ( <i>Oreochromis nilotica</i> ),	Skin	48 °C for 12 h	384.9	Jamilah <i>et al.</i> (2011)
walking catfish ( <i>Clarias batrachus</i> ),	Skin		147.4	
striped catfish ( <i>Pangasius sutchi fowler</i> )	Skin		238.9	
Giant squid ( <i>Dosidicus gigas</i> )	Skin	65 °C for 12 h	NR	Uriarte-Montoya <i>et al.</i> (2011)
Giant catfish ( <i>Pangasianodon gigas</i> )	Skin	45 °C for 12 h	153	Jongjareonrak <i>et al.</i> (2010)
Bamboo shark ( <i>Chiloscyllium punctatum</i> ),	Skin	45, 60 and 75 °C,	~30-220	Kittiphattanabawon <i>et al.</i> (2010b)
blacktip shark ( <i>Carcharhinus limbatus</i> )	Skin	6 and 12 h		
Cuttlefish ( <i>Sepia pharaonis</i> )	Skin	60 °C for 12 h	126 (DS) 137 (VS)	Aewsiri <i>et al.</i> (2009)
Greater Lizard ( <i>Saurida tumbil</i> )	Skin	40-50 °C for 12 h	159.1	Taheri <i>et al.</i> (2009)
Baltic cod ( <i>Gadus morhua</i> ),	Bone	45, 70 and 100 °C,	NR	Kolodziejska <i>et al.</i> (2008)
salmon ( <i>Salmo salar</i> ),	Skin	15-120 min		
herrings ( <i>Clupea harengus</i> )	Skin			
Catfish ( <i>Ictalurus punctatus</i> )	Skin	45 °C, 7 h	243-256	Liu <i>et al.</i> (2008a)
Bigeye snapper ( <i>Priacanthus tayenus</i> )	Skin	45 °C for 12 h	138.6	Nalinanon <i>et al.</i> (2008)
Atlantic salmon ( <i>Salmo salar</i> )	Skin	56 and 65 °C, 2 h	108	Arnesen and Gildberg (2007)

**Table 2.** (Continued)

<b>Fish species</b>	<b>Sources</b>	<b>Extraction condition</b>	<b>Gel strength (g)</b>	<b>References</b>
Sin croaker ( <i>Johnius dussumieri</i> ),	Skin	40-50 °C, 12 h	124.9	Cheow <i>et al.</i> (2007)
Shortfin scad ( <i>Decapterus macrosoma</i> )	Skin		176.9	
Grass carp ( <i>Ctenopharyngodon idella</i> )	Skin	40- 80 °C	267	Kasankala <i>et al.</i> (2007)
Skate ( <i>Raja kenoei</i> ),	Skin	40-80 °C, 1-9 h	426	Cho <i>et al.</i> (2006)
Bigeye snapper ( <i>Priacanthus macracanthus</i> ),	Skin	45 °C, 12 h	105.7	Jongjareonrak <i>et al.</i> (2006a)
brownstripe red snapper ( <i>Lutjanus vitta</i> )	Skin		218.6	
Nile perch ( <i>Lates niloticus</i> )	Skin	50, 60 and 70 °C, 5 h	81-229	Muyonga <i>et al.</i> (2004b)
	Bone		134-179	
Alaska pollock ( <i>Theragra chalcogramma</i> )	Skin	50 °C for 3 h	460	Zhou and Regenstein (2004)
Flounder ( <i>Platichthys flesus</i> )	Skin	50 °C	~150-200	Fernandez-Diaz <i>et al.</i> (2003)
Alaska pollock ( <i>Theragra chalcogramma</i> )	Skin	50 °C, 3 h	98	Zhou and Regenstein (2003)
Megrim ( <i>Lepidorhombus boscii</i> ) (Risso),	Skin	45 °C, over night	340	Gomez-Guillen <i>et al.</i> (2002)
hake ( <i>Merluccius merluccius</i> ),	Skin		~110	
dover sole ( <i>Solea vulgaris</i> )	Skin		350	
Black tilapia ( <i>Oreochromis mossambicus</i> ),	Skin	45 °C, 12 h	180.7	Jamilah and Harvinder (2002)
red tilapia ( <i>Oreochromis nilotica</i> )	Skin		128.1	

NR: Not reported

which was probably due to the reduced electrostatic interaction, thereby preventing attractive ionic inter-chain bridging and gelation of fish gelatin (Haug *et al.*, 2004). The melting temperature of tropical fish gelatins was generally high with 22.5-28.9 °C for tilapia skin (Jamilah and Harvinder, 2002), 25-26 °C for red snapper and grouper bone gelatins (Shakila *et al.*, 2012a), 26.5-25.9 °C for Nile perch bone gelatin (Muyonga *et al.*, 2004b) and the cold water cod fish with 8-10 °C (Gudmundsson and Hafsteinsson, 1997). Gelling temperatures of fish gelatins were 6 °C lower than that of mammalian gelatin. Gelling temperatures reported for Nile perch bone gelatin were 18.5-19.0 °C (Muyonga *et al.*, 2004b) and rohu and common carp skin gelatin were 18.52 °C and 17.96 °C, respectively (Ninan *et al.*, 2011a,b). This difference was also related to the imino acid composition of gelatin. The imino acids were found to stabilise the ordered conformation when gelatin forms the gel network during gelling (Muyonga *et al.*, 2004a,b).

### **1.2.2.3 Gelatin extraction**

The ultimate goal in gelatin production is to convert the different insoluble collagenous raw material into a maximum quantity of soluble and highly purified gelatin with good physico-chemical properties (Ofori, 1999). High gel strength, high clarity, and viscosity are the major characteristic that the producers pay attention and determine application of gelatin.

Production of gelatin consists of three main stages (Karim and Bhat, 2009) including pre-treatment of the raw material, extraction of the gelatin and purification and drying. The gelatin from different aquatic resources with different pretreatment and extraction methods are summarised in Table 3.

#### **1.2.2.3.1 Pre-treatment of raw material**

Depending on the method in which the collagens are pretreated, two different types of gelatin (each with differing characteristics) can be produced. Type A gelatin (isoelectric point at pH ~6–9) is produced from acid-treated collagen, and type B gelatin (isoelectric point at approximately pH ~ 5) is produced from alkali-



**Table 3.** Procedures employed for pretreatment and extraction of fish gelatin

Sources	Pretreatment	Extraction condition	References
Skin of amur sturgeon ( <i>Acipenser schrenckii</i> )	1) Soak in 0.1 M NaOH (1:10 w/v) at 4 °C and continuously stir for 6 h. Change solution every 2 h. 2) Defat the skin using butyl alcohol (1:10 w/v) for 18 h at 4 °C and change the solvent every 6 h 3) Treat the skin with 0.05, 0.10 and 0.20 M acetic acid (1:10 w/v) for 3 and 6 h at 4 °C. Change the solution every 1 h	Distilled water at a ratio of 1:5 (w/v) at 50 °C for 1 h with continuous stirring	Nikoo <i>et al.</i> (2014)
Scale of bighead carp ( <i>Hypophthalmichthys nobilis</i> )	Decalcifying by soaking in 0.5 M HCl (1:25 w/v) for 1 h	Distilled water at a ratio of 1:15 (w/v) at 80 °C for 2 h	Sha <i>et al.</i> (2014)
Skins of skipjack tuna ( <i>Katsuwonus pelamis</i> ), dog shark ( <i>Scoliodon sorrakowah</i> ) and rohu ( <i>Labeo rohita</i> )	1) Soak in 0.1 M NaOH (1:10 w/v) for 2 h with continuous stirring at ambient temperature. Change solution every 1 h 2) Soak in 0.2 M acetic acid (1:10 w/v) for 24 h at 4 °C. Change solution every 12 h	Distilled water at a ratio of 1:10 (w/v) at 45 °C for 12 h	Shyni <i>et al.</i> (2014)
Skin of cobia ( <i>Rachycentron canadum</i> )	1) Soak in 3 M NaOH (1:1 ratio) with slow agitation for 15 min at room temperature. Change the solution and wait for 60 min. Drain the solution 2) Soak in 3 M HCl (1:1 ratio). Stir the mixture for 15 min at room temperature	Distilled water at 52 °C for 2 h	Silva <i>et al.</i> (2014)

**Table 3.** (Continued)

Sources	Pretreatment	Extraction condition	References
Skin of unicorn leather jacket ( <i>Aluterus monoceros</i> )	1) Soak in 0.05 M NaOH (1:10 w/v) for 4 h at room temperature 2) Soak in 0.1 M phosphoric acid (1:10 w/v) for 12 h	Distilled water at a ratio of 1:5 (w/v) at different temperatures (45, 55, 65 and 75 °C) in the absence and presence of trypsin inhibitor (100 units/1 g skin)	Kaewruang <i>et al.</i> (2013)
Skin of blacktip shark ( <i>Carcharhinus limbatus</i> )	1) Soak in 0.1 M NaOH (1:10 w/v) for 2 h at 20 °C 2) Demineralise by soaking in 1 N HCl (1:10 w/v) for 1 h at 20 °C 3) Swell by soaking in 0.2 M acetic acid (1:10 w/v) for 15 min at room temperature (26-28 °C)	Distilled water at a ratio of 1:2 (w/v) at 45 °C and continuously stir for 6 h	Kittiphattanabawon <i>et al.</i> (2012)
Skin of cuttlefish ( <i>Sepia officinalis</i> )	1) Soak in 0.05 M NaOH (1:10 w/v) with stirring for 2 h at room temperature. Change solution every 30 min 2) Soak in 0.2 M acetic acid (1:10 w/v). Stir the mixtures for 48 h at 4°C	Distilled water at 50 °C for 18 h with continuous stirring	Balti <i>et al.</i> (2011)
Skin of carps ( <i>Cyprinus carpio</i> )	1) Soak in 0.1 M NaOH (1:8 w/v) for 6 h with continuous stirring. Change solution every 3 h 2) Soak in 10% butyl alcohol (1:10 w/v) for overnight to remove fat, and then wash with cold distilled water repeatedly	Distilled water at a ratio of 1:15 (w/v) at 60, 70 and 80 °C for 4 h	Duan <i>et al.</i> (2011)

**Table 3.** (Continued)

Sources	Pretreatment	Extraction condition	References
Skins of red tilapia ( <i>O. nilotica</i> ), walking catfish ( <i>C. batrachus</i> ) and striped catfish ( <i>P. sutchifowler</i> )	1) Soak in 2.7% saturated lime solution [ $\text{Ca}(\text{OH})_2$ ] (1:2 w/v) at 20 °C for 14 h 2) Wash with abundant tap water (1:10 w/v) to remove excessive $\text{Ca}(\text{OH})_2$	Distilled water at 48 °C for over night	Jamilah <i>et al.</i> (2011)
Skins of bamboo shark ( <i>Chiloscyllium punctatum</i> ) and blacktip shark ( <i>Carcharhinus limbatus</i> )	1) Soak in 0.1M NaOH (1:10 w/v) with gentle stirring for 6 h 2) Demineralise by soaking in 1M HCl (1:10 w/v) with gentle stirring for 1 h 3) Swell by soaking in 0.2 M acetic acid (1:10 w/v) for 15 min	Distilled water at 45, 60 and 75 °C for 6 and 12 h with a continuous stirring	Kittiphattanabawon <i>et al.</i> (2010b)
Skin of cuttlefish ( <i>Sepia pharaonis</i> )	1) Soak in 0.05 N NaOH (1:10 w/v) for 6 h with gentle stirring at 26–28 °C 2) Bleach in 2% and 5% $\text{H}_2\text{O}_2$ (1:10 w/v) for 24 and 48 h at 4 °C	Distilled water at a ratio of 1:2 (w/v) at 60 °C for 12 h with continuous stirring	Aewsiri <i>et al.</i> (2009)
Skins of bigeye snapper, ( <i>Priacanthus tayenus</i> ) and ( <i>Priacanthus macracanthus</i> )	1) Soak in 0.025 M NaOH (1:10 w/v) with gentle stirring for 2 h. Change solution every hour 2) Soak in 0.2 M acetic acid (1:10 w/v) with gentle stirring for 2 h. Change solution every 40 min	Distilled water at a ratio of 1:10 (w/v) at 45 °C for 12 h with continuous stirring	Benjakul <i>et al.</i> , (2009)

**Table 3.** (Continued)

Sources	Pretreatment	Extraction condition	References
Skin of saithe ( <i>P. virens</i> )	1) Soak in 0.1 M NaOH (1:10 w/v) for 24 h with gentle shaking followed by washing with MILLLI-Q water 2) Bleach skins in 1% (v/v) H <sub>2</sub> O <sub>2</sub> (1:10 w/v) for 30 min	0.01 and 0.1 M acetic acid for 12, 18 and 24 h at 22, 45 and 65 °C	Eysturskra <i>et al.</i> (2009)
Skin of channel catfish ( <i>Ictalurus punctatus</i> )	Soak in 0.05 M acetic acid (1:8 w/v) at 15 °C for 18 h, then wash with distilled water	Distilled water at 45 °C for 7 h	Liu <i>et al.</i> (2008a)
Skin of bigeye snapper ( <i>Priacanthus tayenus</i> )	1) Soak in 0.025M NaOH (1:10 w/v) and stir for 2 h at 25–28 °C. Change solution every hour 2) Soak in 0.2 M acetic acid (1:10 w/v) in the presence of BSP (0-15 units/g skin), then stir at 4 °C for 48 h	Distilled water at 45 °C for 12 h with continuous stirring	Nalinanon <i>et al.</i> (2008)
Skin of yellowfin tuna ( <i>Thunnus albacares</i> )	1) Soak in 0.5 M NaCl for 5 min at 5°C 2) Soak in 0.1 M NaOH for 40 min at 20 °C	0.1 N acetic acid solution at 50 °C for 18 h	Rahman <i>et al.</i> (2008)
Skin of atlantic salmon ( <i>Salmo salar</i> )	1) Soak in cold 0.04 N NaOH solution (1:3 w/v) for 30 min 2) Soak in 0.12 M H <sub>2</sub> SO <sub>4</sub> (1:3 w/v) for 30 min 3) Soak in 0.005 M citric acid solution (1:3 w/v) and then wash with cold-water to remove acid	Distilled water at a ratio of 1:1 (w/v) at 56 °C and then at 65 °C for 2 h	Arnesen and Gildberg (2007)
Skin of grass carp ( <i>Ctenopharyngodon idella</i> )	Soak in 0.1–3.0% HCl at 7 °C	Distilled water at 40–80 °C in a shaking hot water bath (180 rpm)	Kasankala <i>et al.</i> (2007)

**Table 3.** (Continued)

Sources	Pretreatment	Extraction condition	References
Skins of sin croaker ( <i>Johnius dussumeiri</i> ) and shortfin scad ( <i>Decapterus macrosona</i> )	1) Soak in 0.2% (w/v) NaOH solution for 40 min 2) Soak in 0.2% (w/v) H <sub>2</sub> SO <sub>4</sub> for 40 min 3) Soak in 1.0% (w/v) citric acid for 2 h (repeat 3 times each step)	Distilled water at 40–50 °C for 12 h	Cheow <i>et al.</i> (2007)
Skin of channel catfish ( <i>Ictalurus punctatus</i> )	1) Soak in NaOH (1:6 w/v) for variable time 2) Soak in acetic acid (1:6 w/v) for varying times	Deionised water extraction in a water bath for varying times	Yang <i>et al.</i> (2007)
Skin of atlantic cod ( <i>Gadus morhua</i> )	Soak in dilute NaOH (pH 11) and HCl (pH 2–2.6) at room temperature	Distilled water at different temperature and pH	Arnesen and Gildberg (2006)
Skins of bigeye snapper ( <i>Priacanthus macracanthus</i> ) and brownstripe red snapper ( <i>Lutjanus vitta</i> )	1) Soak in 0.2 M NaOH (1:10 w/v) at 4 °C with a gentle stirring. Change solutions every 30 min for 3 times 2) Soak in 0.05 M acetic acid (1:10 w/v) for 3 h at 25–28 °C with a gentle stirring	Distilled water at a ratio of 1:10 (w/v) at 45 °C for 12 h with a continuous stirring	Jongjareonrak <i>et al.</i> (2006b)
Skin of yellowfin tuna ( <i>Thunnus albacares</i> )	1) Soak in 1–3% NaOH (1:8 w/v) at 10 °C with shaking (200 rpm for 1–5 days) 2) Soak in 6 N HCl	Distilled water at a ratio of 1:6 (w/v) at 40–80 °C for 1–9 h	Cho <i>et al.</i> (2005)
Skin of dover sole ( <i>Solea vulgaris</i> )	1) Soak in absolute ethanol or 80–20 absolute ethanol– glycerol mixture 2) Dry using marine salt 3) Soak in 0.05 M acetic acid	Distilled water at 45 °C	Gimenez <i>et al.</i> (2005a)

**Table 3.** (Continued)

Sources	Pretreatment	Extraction condition	References
Skin of dover sole ( <i>Solea vulgaris</i> )	1) Soak in different 0.8 M salt solutions (NaCl, KCl, MgCl <sub>2</sub> and MgSO <sub>4</sub> ) (1:6 w/v) at 5 °C for 2 min 2) Soak in 50 mM acetic acid or 25 mM lactic acid	Distilled water at 45 °C	Gimenez <i>et al.</i> (2005b)
Skin of dover sole ( <i>Solea vulgaris</i> )	1) Treat with high pressure at 250 and 400 MPa, for 10 or 20 min 2) Soak in 0.05 M acetic acid for 3 h	Distilled water at 45 °C for 16-18 h	Gomez-Guillen <i>et al.</i> (2005)
Skin of alaska Pollock	Soak in NaOH or Ca(OH) <sub>2</sub> (1:6 w/v) with varying OH concentrations (0.01, 0.1, 0.2, and 0.5 M) for 60 min, or treated with 0.05 M acetic acid (1:6 w/v) with H <sup>+</sup> concentration for 60 min	Distilled water at 50 °C for 180 min in the absence or presence of a mixture of protease inhibitors, consisting of 5 mM EDTA disodium salt, 0.2 mM phenylmethanesulfonyl fluoride and 2 μM pepstatin	Zhou and Regenstein (2005)
Skin of baltic cod ( <i>Gadus morhua</i> )	-	Distilled water at a ratio of 1:6 (w/v) at 45 °C for 15–120 min	Kołodziejska <i>et al.</i> (2004)
Skin of nile perch ( <i>Lates niloticus</i> )	Soak in 0.01 M H <sub>2</sub> SO <sub>4</sub> (1:2 w/v) and wash with abundant water	Distilled water at 50, 60 and 70 °C, followed by boiling for 5 h	Muyonga <i>et al.</i> (2004b)
Skin of pollock ( <i>Alaskan pollock</i> )	1) Soak in Ca(OH) <sub>2</sub> (1:6 w/v) at varying OH- concentrations 2) Soak in acetic acid (1:6 w/v)	Distilled water at different temperatures for various times	Zhou and Regenstein (2004)
Skin of flounder ( <i>Platichthys flesus</i> )	Soak in acid	Distilled water at temperatures below 50 °C	Fernandez-Diaz <i>et al.</i> (2003)

**Table 3.** (Continued)

Sources	Pretreatment	Extraction condition	References
Skins of megrim ( <i>Lepidorhombus boscii</i> ), Cod ( <i>Gadus morhua</i> ), dover sole ( <i>Solea vulgaris</i> ), hake ( <i>Merluccius merluccius</i> ) and squid ( <i>Dosidicus gigas</i> )	Soak in 0.05 M acetic acid	Distilled water at 45 °C and for squid at 80 °C for overnight	Gomez-Guillen <i>et al.</i> (2002)
Skins of black tilapia ( <i>Oreochromis mossambicus</i> ) and red tilapia ( <i>Oreochromis nilotica</i> )	1) Soak in 0.2% (w/v) NaOH solution for 40 min 2) Soak in 0.2% H <sub>2</sub> SO <sub>4</sub> 3) Soak in 1.0% citric acid	Distilled water at 45 °C for 12 h	Jamilah and Harvinder (2002)
Skin of megrim ( <i>Lepidorhombus boscii</i> )	1) Soak in 0.2 N NaOH (1:6 w/v) at 5 °C for 30 min 2) Soak in 0.05, 0.1 and 0.5 M of different acid solutions like formic, acetic, propionic, lactic, malic, tartaric and citric acid (1:20 w/v), respectively at 20 °C for 16-18 h	Distilled water at a concentration of 6.67% (w/v) at 45 °C for 30 min	Gomez-Guillen and Montero (2001)
Skin of megrim ( <i>Lepidorhombus boscii</i> )	1) Soak in cold (2 °C) 0.2 N NaOH (1:6 w/v) for 40 min 2) Soak in 0.2 N sulphuric acid (1:6 w/v) for 40 min (both repeated 3 times) 3) Soak in 0.7% citric acid for 40 min with continuous stirring (GM1) 4) Clean with 0.8 N NaCl and then soak in 0.05 N acetic acid (1:10 w/v) at 25-28 °C for 3 h (GM2)	Distilled water overnight at 45 °C	Montero and Gómez-Guillén (2000)

treated collagen (Stainsby, 1987). Acidic pretreatment is most suitable for the less covalently cross-linked collagens found in pig and fish, while alkaline treatment is suitable for the more complex collagens found in bovine hides.

Gelatin can be extracted from many fish species by non-collagenous protein elimination, demineralisation and swelling with acid solution prior to gelatin extraction (Foegeding *et al.*, 1996). For raw material constituting high content of lipid, it is more important to degrease before pre-treatment and extraction (Holzer, 1996). The extraction process can influence the length of the polypeptide chains and the functional properties of the gelatin. Processing parameters (temperature, time, and pH), the pre-treatment, the properties and preservation method of the starting raw material affect chain length of gelatin (Karim and Bhat, 2009). Type of acid used, ionic strength and pH strongly influence swelling process and solubilisation of collagen as well as the extraction of gelatin (Gimenez *et al.*, 2005b). Type of acid used for swelling has been reported to determine the properties of resulting gelatin. Yield and gel strength of Amur sturgeon skin gelatin were decreased as the acid concentration and pretreatment time increased (Nikoo *et al.*, 2014). Ahmad and Benjakul (2011) reported that swelling of skin of unicorn leather jacket using phosphoric acid rendered gelatin with higher gel strength than acetic acid. Gomez-Guillen and Montero (2001) reported that acetic and propionic acid pretreated skin of megrim (*Lepidorhombus boscii*) rendered the gelatins with the highest elastic modulus, viscous modulus, melting temperature, and gel strength.

Additionally, bleaching during pretreatment for colour improvement also had the impact on gelatin extraction as well as characteristics of the resulting gelatin. Aewsiri *et al.* (2009) reported that pretreatment of cuttlefish skin using H<sub>2</sub>O<sub>2</sub> at higher concentrations resulted in the increased yield. H<sub>2</sub>O<sub>2</sub> was found to break the hydrogen bond of collagen (Courts, 1961). Perkins (1996) stated that hydroperoxyl anion is a strong nucleophile which, during bleaching, is able to break the chemical bonds that make up the chromophore. This might lead to the formation of different substances, which either did not contain a chromophore, or contained a chromophore



that did not absorb visible light. Bleaching using 2% and 5% H<sub>2</sub>O<sub>2</sub> could improve not only the colour of gelatin by increasing the *L\**-value and decreasing *a\**-value but also enhanced the bloom strength, and the emulsifying and foaming properties of the resulting gelatin from dorsal and ventral skin of cuttlefish (Aewsiri *et al.*, 2009).

Endogenous proteases in fish skin show the profound impact on degradation of  $\alpha$ -chains of gelatin during extraction. Serine proteinase was formed as dominant proteinase in skin of bigeye snapper (Intarasirisawat *et al.*, 2007). Gelatin was extracted from the bigeye snapper (*Priacanthus macracanthus*) skin in water without and with 0.001 mM soybean trypsin inhibitor (SBTI) using a skin/water ratio of 1:7 at different temperatures (35, 40, 45, 50, 55 and 60 °C) for 12 h. In the presence of SBTI, the degradation was markedly inhibited. However,  $\beta$ -chain disappeared and  $\alpha$ -chains underwent degradation to some extent at temperature above 50 °C (Intarasirisawat *et al.*, 2007). Moreover, the degradation of gelatin components was markedly prevented, when SBTI at a concentration of 0.1  $\mu$ M was incorporated during the gelatin extraction from bigeye snapper (*Priacanthus tayenus*) skin (Nalinanon *et al.*, 2008).

Ultra-high pressure (UHP) was applied as a pretreatment to extract gelatins with 1% HCl as the transmission medium. The effects of various pressures (0.1-500 MPa) on the gelatinisation of collagen and the properties of the extracted gelatins were investigated by Chen *et al.* (2014). The UHP-treated gelatins exhibited higher yield and better physical properties, such as gel strength and rheological indexes, because they contained more subunit components than the gelatin obtained from an acid pretreatment process. The UHP treatment could destabilise the triple-helix structure and facilitate the conversion of collagen to gelatin. Pressure above the optimum point (400 MPa) led to poor properties of resulting gelatin (Chen *et al.*, 2014). It has been reported that UHP can induce protein denaturation by disturbing the balance of the non-covalent interactions that stabilise the native conformations of many proteins (Qin *et al.*, 2013; Torrezan *et al.*, 2007). Kaewruang *et al.* (2014) reported that phosphorylation could be achieved by incorporating sodium tripolyphosphate (STPP) at appropriate level during pretreatment (0.2%) or extraction

(0.08%) of gelatin from the skin of unicorn leatherjacket and the resulting gelatins showed the better properties than the control (without addition of STPP).

#### 1.2.2.3.2 Extraction of gelatin

After pretreatment, the material is subjected to heat treatment, in which bondings stabilising the triple helix are disrupted and gelatin can be solubilised and collected. Extraction temperature and time strongly influenced the total yield and rheological properties of pollack skin gelatin (Zhou and Regenstein, 2003). Yield of gelatin from the skin of giant squid was 7.5% (Uriarte-Montoya *et al.*, 2011). Gomez-Guillen *et al.* (2002) reported that the extraction of gelatin from the skin of squid, *Dosidicus gigas* at 45 °C was not possible. Even at high temperature (80 °C), very low yield was gained (2.6%). Jamilah and Harvinder (2002) stated that the difference in gelatin recovery from different species could be attributed to the intrinsic characteristics of the skin and collagen molecules, the collagen content, the amount of soluble components in the skins, the loss of extracted collagen through leaching during the series of washing steps, etc. The degree of conversion of collagen into gelatin depends on various parameters (Karim and Bhat, 2009). Increasing temperature directly provided more energy to disrupt bondings stabilising the collagen structures as well as peptide bonds of  $\alpha$ -chains. As a result, a larger amount of gelatin could be extracted as the temperature was elevated (Kaewruang *et al.*, 2013; Sinthusamran *et al.*, 2014). Higher yields were obtained when gelatin was extracted from seabass skin at 55 °C, in comparison with 45 °C for all extraction times (3, 6 and 12 h). The highest yield from seabass skin (66.4%) was obtained when the extraction was carried out at 55 °C for 12 h (Sinthusamran *et al.*, 2014).

A strong decrease in the percentage of  $\beta$ -chain was observed for giant squid skin gelatin extracted at higher temperature (80 °C) (Gomez-Guillen *et al.*, 2002). Extraction temperatures played a major role in protein components of resulting gelatin. Aewsiri *et al.* (2009) and Hoque *et al.* (2011a) also reported that no proteins with MW of 70 and 76 kDa were retained in gelatin extracted from skin bleached with H<sub>2</sub>O<sub>2</sub>, regardless of concentration used. Very low content of  $\beta$ - components and an

almost disappearance of higher molecular aggregates was observed in squid gelatin. Gelatins with higher content of  $\alpha$ -chain were reported to possess better functional properties including gel strength, emulsifying and foaming properties (Gomez-Guillen *et al.*, 2002). In general, the formation of fragments is associated with lower viscosity, low melting point, low setting point, high setting time, as well as decreased bloom strength of gelatin (Muyonga *et al.*, 2004b). Protein degradation fragments may reduce the ability of  $\alpha$ -chains to anneal correctly by hindering the growth of the existing nucleation sites (Ledward, 1986).

#### **1.2.2.3.3 Purification and drying**

Gelatin extracted with distilled water was purified by different methods such as centrifugation (Aewsiri *et al.*, 2011; Balti *et al.*, 2011; Hoque *et al.*, 2011a; Kołodziejska *et al.*, 2008; Ktari *et al.*, 2014; Lassoued *et al.*, 2014) and filtration (Jongjareonrak *et al.*, 2006a). After extraction process, residual skin was separated by filtration using a double layer cheese cloth (Jongjareonrak *et al.*, 2010; Nikoo *et al.*, 2014). Filtrate was further filtered by filter paper to obtain a pure gelatin solution (Arnesen and Gildberg, 2007; Cheow *et al.*, 2007; Kaewruang *et al.*, 2013; Kittiphattanabawon *et al.*, 2010b; Muyonga *et al.*, 2004b; Nalinanon *et al.*, 2008; Sinthusamran *et al.*, 2014). For further purification, Eysturskard *et al.* (2009) dialysed the gelatin solution prior to drying.

Drying of gelatin solution was done by vacuum drying (Binsi *et al.*, 2009), freeze drying (Hoque *et al.*, 2011a; Kaewruang *et al.*, 2014; Kwak *et al.*, 2009; Lassoued *et al.*, 2014; Shakila *et al.*, 2012a), spray drying (Kwak *et al.*, 2009) and oven drying (Aleman *et al.*, 2011; Kwak *et al.*, 2009; Rahman *et al.*, 2008). In some cases, gelatin solution was concentrated by rotary-evaporator before drying (Arnesen and Gildberg, 2007; Liu *et al.*, 2009; Shyni *et al.*, 2014; Zhang *et al.*, 2011).

#### **1.2.2.3.4 Improvement of gelling property**

Gelation is one of most important functional property of gelatin and determines the price and application. Gomez-Guillen *et al.* (2002) compared the

rheological characteristics (visco-elasticity and gel strength) and chemical/structural properties (amino acid composition, molecular weight distribution and triple helix formation) of different fish skin gelatins. The stability of the triple helical structure in renatured gelatins has been reported to be proportional to the total content of imino acids. Hydroxyproline plays a key role in the stabilisation of the triple-stranded collagen helix due to its hydrogen bonding ability through its hydroxyl group. Proline and hydroxyproline are thought to be responsible for the stability of the triple-helix of collagen structure through hydrogen bonding between free water molecules and the hydroxyl group of the hydroxyproline in gelatin (Fernandez-Diaz *et al.*, 2001). The lower content of proline and hydroxyproline generally gives fish gelatin a low gel modulus, and low gelling and melting temperatures (Balti *et al.*, 2011). The super-helix structure of the gelatin gel, which is critical for the gel properties, is stabilised by steric restrictions. These restrictions are imposed by both the pyrrolidine rings of the imino acids in addition to the hydrogen bonds formed between amino acid residues (Sikorski, 2001).

Various chemicals and enzymes have been used to improve the gelatin properties. Karayannakidis and Zotos (2014) added four compounds ( $\text{NaH}_2\text{PO}_4$ ,  $\text{MgCl}_2$ ,  $\text{CaCl}_2$  and glycerol) at various concentrations in order to improve physical properties of fish gelatin. Gelatin gels exhibited the highest gel strength, when  $\text{NaH}_2\text{PO}_4$  at concentrations of 0.3 and 0.5 mol/L were added. Gelatin from unicorn leather jacket skin incorporated with STPP at 0.08% STPP during extraction showed the highest gel strength (Kaewruang *et al.*, 2014). When gelatin from bighead carp (*Hypophthalmichthys nobilis*) scale with the gel strength of  $415.7 \pm 9.9$  g was subjected to ammonium sulfate fractional precipitation (ASFP) at different saturations (20%, 25%, 30%, 35% and 40%, respectively), various fractions showed different gel strengths ( $469.7 \pm 12.0$ ,  $419.7 \pm 9.9$ ,  $181.9 \pm 17.7$ ,  $83.9 \pm 9.9$  and  $15.3 \pm 2.1$  g, respectively) (Sha *et al.*, 2014).

Microbial transglutaminase is one of cross-linking enzyme, which can be used for enhancement of gelatin gel strength. Gelatin from the skin of Baltic cod (*Gadus morhua*) was modified using transglutaminase. A gelatin solution (5%)

formed gel at room temperature in the presence of microbial transglutaminase (MTGase) (0.15- 0.7 mg of enzyme protein/ml) and the reaction time also affected gel properties (Kolodziejska *et al.*, 2004). The addition of MTGase at concentration up to 0.005% and 0.01% (w/v) increased the bloom strength of gelatin gel from bigeye snapper (*Priacanthus macracanthus*) and brownstripe red snapper (*Lutjanus vitta*), respectively. SDS-PAGE of gelatin gel added with MTGase showed the decrease in band intensity of protein components, especially  $\beta$  and  $\gamma$ -components (Jongjareonrak *et al.*, 2006a). Gelatin gel contained  $\alpha$ -chains but with higher concentration of transglutaminase, these protein bands disappeared. Chiou *et al.* (2006) reported that Alaska pollock (*Theragra chalcogramma*) and Alaska pink salmon (*Oncorhynchus gorbuscha*) skin gelatins had the improved gelation and melting behavior as well as cross-linking behavior upon the addition of genipin and glutaraldehyde. Pollock skin gelatin was cross-linked faster with glutaraldehyde than with genipin (Chiou *et al.*, 2006). Gel strength of gelatin from walleye pollock (*Theragra chalcogramma*) skin increased with increasing gallic acid concentration up to 20 mg/g dry gelatin, and then decreased at further elevated gallic acid concentration. However, gel strength continuously increased with increasing levels of rutin upto 8 mg/g dry gelatin (Yan *et al.*, 2011).

### 1.2.3 Biodegradable films

Until the early 2000's, the high cost of biopolymers has been a major factor limiting their utilisation. So, plastics are one of the most commonly used materials in the food packaging industry due to their ability to preserve the sensory properties and nutritional values in food products. The market size of rigid and flexible plastics was about 45% of the total packaging industry in 2009 (Barnett, 2010). However, the current increase in crude oil price has allowed biopolymer films to be more cost competitive and there has been a widespread interest in films made from renewable and natural polymers which can degrade naturally and more rapidly than petroleum-based plastics. Biopolymers are considered as alternatives to synthetic plastics since they are typically derived from renewable and abundant resources.

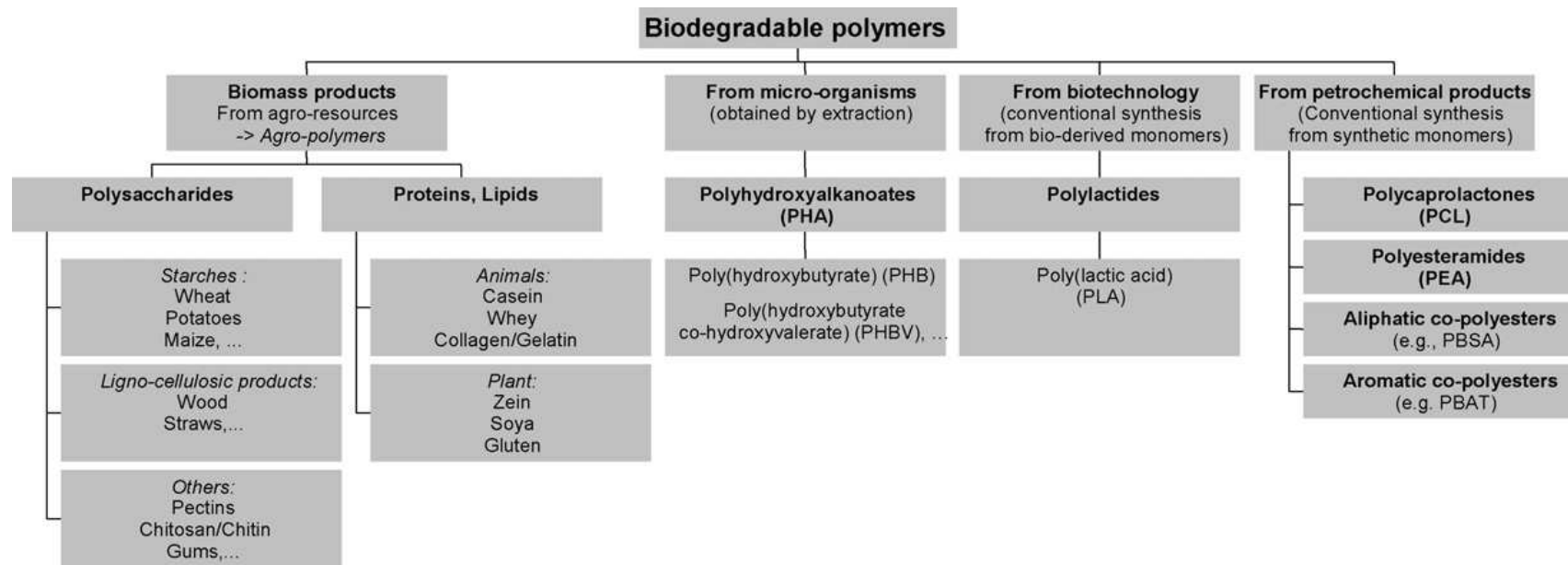


**Figure 1.** Classification of the biodegradable polymers

Source: Averous (2004)

Much research has been done on the application of biopolymers in food packaging (Byun *et al.*, 2012). Biopolymeric materials used for biodegradable films or packaging can be divided into 4 categories: biopolymer hydrocolloids (proteins and polysaccharides), lipids, resins and composites (Krochta *et al.*, 1994). Physical and chemical characteristics of the biopolymers greatly influence the properties of resulting films (Sothornvit and Krochta, 2000). Biodegradable films can be made from renewable biopolymers such as proteins, lipids and polysaccharides (Tharanathan, 2003). Additionally, biodegradable films can be obtained from different sources (Figure 1). Among them, edible films of proteins are supposed to provide nutritional value and also have impressive mechanical properties and gas barrier property (Ou *et al.*, 2004).

### **1.2.3.1 Protein**

Proteins are biopolymers capable of forming the film and their properties can be varied with proteinaceous materials. The most distinctive characteristics of proteins compared to other film-forming materials are conformational denaturation, electrostatic charges, and amphiphilic nature (Han *et al.*, 2005). In addition, stronger intermolecular binding potential, via covalent bonds, is found in protein-based films and not in films from homopolymer polysaccharides (Cuq *et al.*, 1995). Protein used as film-forming materials are derived from both animal and plant sources, such as animal tissues, milks, eggs, grains, and oilseeds (Krochta, 2002). Several proteins have been used for film preparation. Those include myofibrillar protein (Tongnuanchan *et al.*, 2011), soy protein (Rhim *et al.*, 2006), corn zein (Arcan and Yemenicioglu, 2011), wheat gluten (Gennadios *et al.*, 1994), milk protein (McHugh and Krochta, 1994), gelatin (Jongjareonrak *et al.*, 2006a,b; Weng *et al.*, 2014) and egg white (Gennadios *et al.*, 1996).

Edible films can be produced from myofibrillar protein (Tongnuanchan *et al.*, 2011) and muscle protein (Hamaguchi *et al.*, 2007). Myofibrillar proteins are salt soluble proteins, comprising 54% of total protein. Generally, acid or alkaline solubilisation is required for preparation of film forming-solution. Films prepared

from myofibrillar proteins are flexible and semi-transparent and their mechanical properties are altered with pH used for solubilisation (Hamaguchi *et al.*, 2007; Shiku *et al.*, 2003). Artharn *et al.* (2007) reported that the removal of undesirable components and increasing concentration of myofibrillar proteins by washing could improve the properties of films.

Soy proteins are composed of a mixture of albumins and globulins, 90% of which are storage proteins with globular structure (Kinsella, 1979). Soy protein films have received considerable attention due to their excellent film-forming abilities, low cost and barrier properties against oxygen permeation, but they have poor mechanical properties and heat sealability, compared to synthetic polymer (Rhim *et al.*, 2006). Guerrero *et al.* (2010) stated that soy protein isolate (SPI) based films are eco-friendly because they are biodegradable and come from renewable sources but they are brittle.

Zein, is a corn protein and a valuable co-product from ethanol production. Zein has many functional properties including film forming capabilities. Zein is a relatively hydrophobic and thermoplastic material; this hydrophobicity is related to its high content of non-polar amino acids as leucine, alanine and proline (Shukla and Cheryan, 2001). The packaging films made from an alcohol-soluble protein like corn zein have relatively high barrier properties, compared to films from other proteins.

Wheat gluten has not received as much study as other proteins for its film-forming potential (Gennadios *et al.*, 1994). Wheat gluten films were produced by drying cast aqueous ethanol solutions of wheat gluten and a plasticiser, usually glycerin, was added to reduce film brittleness and ensure the formation of free standing films. Wheat gluten films in a dry state were very effective oxygen barriers (Gennadios *et al.*, 1994). However, wheat gluten films are poor water vapor barriers because of the inherent hydrophilicity of the proteins (Krochta, 2002).



Milk protein, can be divided into two types, whey protein and casein. Milk protein based edible films have good mechanical strength and are excellent oxygen, lipid, and aroma barriers; however, due to their hydrophilic nature, they have poor moisture barrier properties (Chick and Ustunol, 1998). Improved physical properties through heat denaturation were reported in whey protein films (Stuchell and Krochta, 1994) and whey protein films are transparent and flexible. Casein has also been used for film-forming material because its inexpensive, readily available, non-toxic and highly stable and casein film exhibited high tensile strength (Diak *et al.*, 2007).

Egg white consists primarily of about 90% water into which is dissolved 10% proteins (including albumins, mucoproteins and globulins) (Woodward, 1990). Ovalbumin, which constitutes more than of egg white protein by weight, is the only fraction that contains free sulphhydryl (SH) groups. Other proteins, such as ovotransferrin, ovomucoid, and lysozyme contain disulphide (S-S) bonds (Mine, 1995). Preparation of egg white protein films involve denaturation of egg white protein in aqueous solution by alkaline solubilisation or heat treatment (Gennadios *et al.*, 1996). Cast albumen films with added lysozyme inhibited bacterial growth, showing potential as active packagings (Padgett *et al.*, 1995). Gennadios *et al.* (1996) have been studied the mechanical and water vapour barrier properties of cast albumen films plasticised with glycerin, sorbitol, or polyethylene glycol.

Gelatin has been used as a potential biopolymer for film preparation. Gelatin films have been used in various fields such pharmaceutical (as the delivery system for a wide range of medicine) and food industry (as a packaging material), etc. (Donhowe and Fenema, 1994). Protein content, plasticisers type and concentration have been reported to affect the properties of gelatin based films (Vanin *et al.*, 2005).

### **1.2.3.2 Plasticisers**

Plasticisers play a vital role in the preparation of edible films and coatings, especially from polysaccharides and proteins. Those films are often brittle

and stiff due to extensive interactions between polymer molecules (Krochta, 2002). Plasticisers are low molecular weight agents incorporated into the polymeric film-forming materials, which helps to decrease inherent brittleness of films by reducing intermolecular forces and decrease the glass transition temperature of the polymers. They are able to position themselves between polymer molecules and to interfere with the polymer-polymer interaction to increase flexibility and processability by increasing the mobility of polymeric chains (Guilbert and Gontard, 1995; Krochta, 2002). Most plasticisers are very hydrophilic and hygroscopic. Water molecules in the films function as plasticisers. Water is actually a very good plasticiser, but it can easily be lost by dehydration at a low relative humidity (Guilbert and Gontard, 1995). Therefore, the addition of hydrophilic chemical plasticisers to films can reduce water loss through dehydration, increase the amount of bound water, and maintain a high water activity.

There are two main types of plasticisers (Sothornvit and Krochta, 2005):

- 1) Agents capable of forming many hydrogen bonds, thus interacting with polymers by interrupting polymer-polymer bonding and maintaining the farther distance between polymer chains.
- 2) Agents capable of interacting with large amounts of water to retain more water molecules, thus resulting in higher moisture content and larger hydrodynamic radius.

Owing to the hydrophilic nature of water, biopolymers, and plasticisers, and due to the abundant existing hydrogen bonds in their structures, it is very difficult to separate these two mechanisms. Four theories have been proposed to explain the mechanism of the plasticiser effect (Sothornvit and Krochta, 2005) shown as follows:

- 1) Lubricity theory – a plasticiser is considered as a lubricant to facilitate the movements of the macromolecules over each other.

- 2) Gel theory– a plasticiser disrupts the polymer–polymer interactions including hydrogen-bonds and Van der Waals and ionic forces.
- 3) Free volume theory– a plasticiser may depress the glass transition temperature by increasing polymer free volume and mobility of polymeric chains. The fundamental concept underlying these theories is that a plasticiser can interpose itself between the polymer chains and decrease the forces holding the chains together.
- 4) Coiled spring theory– plasticising effects from the point of view of tangled macromolecules.

Currently, hydroxyl compounds and polyols are often cited as good plasticisers for protein based materials. Among them, glycerol is the most widely used (Audic and Chaufer, 2005). In general, plasticisers such as glycerol, sorbitol, etc are required for making flexible films. Glycerol and sorbitol were found to show considerable plasticising effect on protein-based film, so the two plasticisers were mostly used to plasticise polymers (Sobral *et al.*, 2001). Different kinds of plasticisers have been used for protein based films. Different plasticisers with varying amounts directly determine the property of resulting films. Also, lipids and waxes were used as hydrophobic plasticisers, which can be used to lower water vapour permeability of resulting films. Pommet *et al.* (2003) produced films from gluten using saturated fatty acids with different carbon chain lengths as plasticisers. Bertan *et al.* (2005) have been used triacetin as plasticiser. Plasticised gelatin films had glycerol at low and middle concentrations, about 0–50% (Cuq *et al.*, 1997; Jongjareonrak *et al.*, 2006b; Tongnuanchan *et al.*, 2012), however a few studies were undertaken on films with higher glycerol content (Audic and Chaufer, 2005). Vanin *et al.* (2005) studied plasticisation of gelatin film by using four polyols, i.e., glycerol, propylene glycol, diethylene glycol and ethylene glycol. Jongjareonrak *et al.* (2006b) compared the effects of glycerol, ethylene glycerol, sorbitol, polyethylene glycol 200 and 400 on properties of gelatin films and found that different plasticisers showed varying effect

on properties of resulting films. The combination of sorbitol and glycerol was also used as plasticiser for gelatin film (Thomazine *et al.*, 2005).

### **1.2.3.3 Formation of protein based-films**

There are two categories of film formation processes; dry and wet (Guerrero *et al.*, 2010; Guilbert *et al.*, 1997) (Figure 2). The dry process of edible film production does not use solvent medium, such as water or alcohol. Molten casting, extrusion and heat pressing are good examples of dry processes. For the dry process, heat is applied to the film-forming materials to increase the temperature to above the melting point of the film-forming materials, to cause them to flow. The wet process uses solvents for the dispersion of film-forming materials, followed by drying to remove the solvent and form a film structure. In the wet process, the selection of solvents is one of the most important factors. Since the film-forming solution should be edible and biodegradable, only water, ethanol and their mixtures are appropriate as solvents (Krochta, 2002). All the ingredients of film-forming materials should be dissolved or homogeneously dispersed in the solvents to produce film-forming solutions (Cuq *et al.*, 1995).

Most of protein based films made from different fish, including bigeye snapper and brown stripe red snapper (Jongjareonrak *et al.*, 2006b), baltic cod (Kolodziejska *et al.*, 2006) and tilapia (Pranoto *et al.*, 2007), and tuna (Gomez-Guillen *et al.*, 2007) have been produced by solution casting methods. Recently, molten casting method has been implemented to make films from pectin and other food hydrocolloids using extrusion method (Liu *et al.*, 2008b), soy protein isolate using compression molding (Guerrero *et al.*, 2010), pig skin gelatin resins using single screw extruder (Park *et al.*, 2008) and fish gelatin films using extrusion and compression molding method (Krishna *et al.*, 2012).

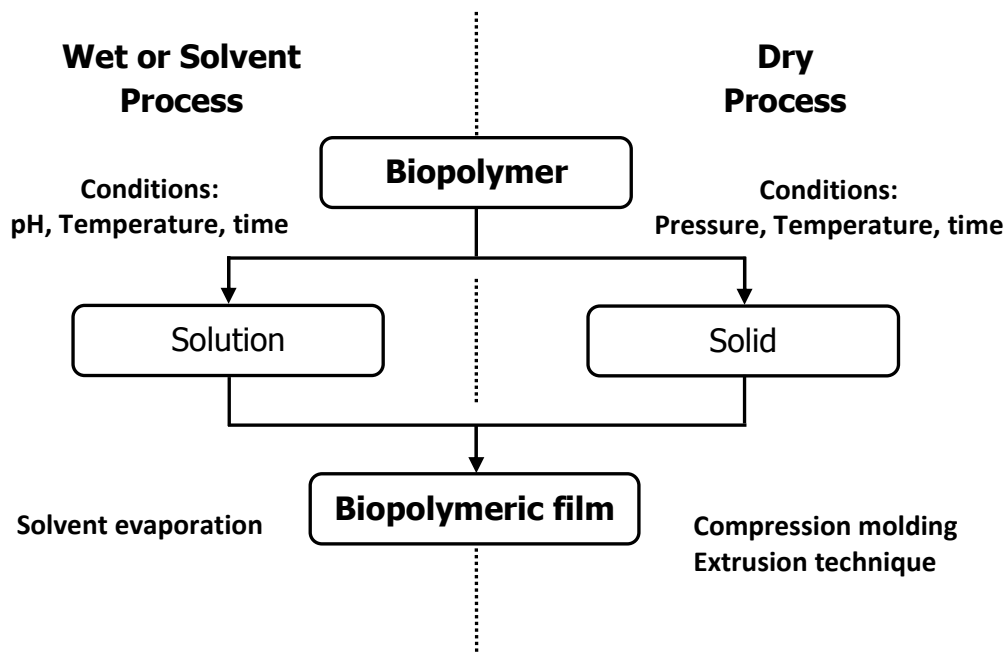


**Figure 2.** Processing methods of film formation: wet (or solvent) and dry process

Source: Guerrero *et al.* (2010)

#### 1.2.3.4 Fish gelatin films

Fish gelatins may be a good alternative to synthetic plastics for making films to preserve foodstuffs because of their good film-forming abilities (Gomez-Guillen *et al.*, 2009). Also, due to the constraints for the use of bovine and porcine gelatin associated with religious prohibition and possible disease transmission, gelatin from aquatic animal has gained increasing attention (Karim and Bhat, 2009). Gelatins from the skin of bigeye snapper and brown stripe red snapper (Jongjareonrak *et al.*, 2008), bigeye snapper (Rattaya *et al.*, 2009), tilapia (Pranoto *et al.*, 2007), cuttle fish (Hoque *et al.*, 2011a) and squid (Gimenez *et al.*, 2009) have been used for film preparation. Gelatin films from different sources with varying properties have been proposed (Table 4). Fish gelatins have been reported to exhibit good film-forming properties, yielding transparent, colourless, and highly extensible films (Jongjareonrak *et al.*, 2006b). Additionally, it can be used as the smart packaging, in which the antioxidants or antimicrobials can be incorporated (Jongjareonrak *et al.*,

2008; Tongnuanchan *et al.*, 2012). Owing to the superior oxygen barrier property, fish gelatin based film could prevent the lipid oxidation in food systems (Jongjareonrak *et al.*, 2006b). Also, gelatins from fish and cuttlefish skin have been demonstrated to render the biodegradable films with the superior UV barrier properties (Houqe *et al.*, 2011a; Jongjareonrak *et al.*, 2008; Rattaya *et al.*, 2009). Gelatin film effectively prevents the lipid oxidation, which is induced by UV light (Limpisophon *et al.*, 2009). However, gelatin film has the relatively poor mechanical properties, in comparison with traditional synthetic polymeric films (McHugh and Krochta, 1994). Gelatins from unicorn leather jacket (Ahmad *et al.*, 2012), Atlantic halibut (Carvalho *et al.*, 2008), Alaska pollock and Alaska pink salmon (Chiou *et al.*, 2008), cod, haddock and pollock (Denavi *et al.*, 2009; Krishna *et al.*, 2012), sole (Gomez-Estaca *et al.*, 2009c), tuna (Gomez-Guillen *et al.*, 2007), cuttlefish (Hoque *et al.*, 2011c), bigeye snapper and brownstripe red snapper (Jongjareonrak *et al.*, 2008), blue shark (Limpisophon *et al.*, 2009), rohu, common carp and grass carp (Ninan *et al.*, 2010), tilapia (Niu *et al.*, 2013; Pranoto *et al.*, 2007; Tongnuanchan *et al.*, 2012), warm water fish gelatin (Nunez-Flores *et al.*, 2013a) and silver carp (Wu *et al.*, 2013) skins have been used to develop films. Furthermore, films from gelatin extracted from tilapia scale have been prepared and characterised (Weng and Zheng, 2015; Weng *et al.*, 2014). Films from different gelatins show the varying properties as shown in Table 4.

Properties of films are mainly dependent the starting gelatin. Pretreatment, extraction and other processing conditions of gelatin play vital role on the resulting film properties. Film prepared from tilapia skin gelatin with pretreatment using 0.03 M citric acid had somewhat better water barrier property than those made from gelatin with pretreatment using HCl or acetic acid (Niu *et al.*, 2013). The films with higher TS were prepared from scale gelatin extracted at pH 5, and the film strength became lower with increasing or decreasing extraction pH (Weng *et al.*, 2014).

**Table 4.** Properties of gelatin-based film from different fish species

Fish Species	Protein Conc. (%)	Plasticiser conc.	Thickness (mm)	Mechanical property		WVP ( $\times 10^{-11} \text{ gmm}^{-2} \text{ s}^{-1} \text{ Pa}^{-1}$ )	References
				TS (MPa)	EAB (%)		
Tilapia ( <i>Tilapia zillii</i> )	2	Glycerol: 20%	NR	18.63-55.17	17.83-44.58	1.56-1.82	Weng <i>et al.</i> (2014)
Tilapia ( <i>Oreochromis niloticus</i> )	1	NR	0.023-0.025	67.06-67.80	3.6-3.9	0.45-0.54 <sup>a</sup>	Niu <i>et al.</i> (2013)
Silver carp	4	Glycerol: 25%	0.031-0.032	25.25-36.63	42.53-49.56	0.92-1.10	Wu <i>et al.</i> (2013)
Warm water tilapia	4	Glycerol, 40%	39.25	3.42	53.05	55.20 <sup>b</sup>	Hanani <i>et al.</i> (2012)
			50.40	3.47	56.07	78.10 <sup>b</sup>	
			63.50	5.85	100.91	110.55 <sup>b</sup>	
Cod/haddock/ pollack	6.67	Glycerol: 20-25%	0.10-0.58	1.51 - 17.8	27.4 - 293.4	1.5 - 2.9 <sup>c</sup>	Krishna <i>et al.</i> (2012)
Tilapia	3.5	Glycerol: 20-30%	0.040-0.049	25.87 - 49.09	9.61 - 69.79	2.81 - 4.07	Tongnuanchan <i>et al.</i> (2012)
Cuttlefish ( <i>Sepia pharaonis</i> )	3	Glycerol: 25%	0.037-0.041	4.99 - 9.66	15.56 – 51.89	0.92 – 1.30	Hoque <i>et al.</i> (2010)
Rohu/ Common carp/ Grass carp	6.67	Glycerol: 1.5g/105g	0.10-0.12	490 - 560 (Kg/cm <sup>2</sup> )	27.00 - 60.89	1.06 - 1.32 <sup>a</sup>	Ninan <i>et al.</i> (2010)

**Table 4.** (Continued)

Fish Species	Protein Conc. (%)	Plasticiser conc.	Thickness (mm)	Mechanical property		WVP ( $\times 10^{-11} \text{gmm}^{-2} \text{s}^{-1} \text{Pa}^{-1}$ )	References
				TS (MPa)	EAB (%)		
Cod ( <i>Gadus morhua</i> )	4	Glycerol:Sorbitol 0.75:0.75 g/g gelatin	0.047-0.086	NR	NR	1.75 - 3.86 <sup>e</sup>	Denavi <i>et al.</i> (2009)
Giant squid ( <i>Dosidicus gigas</i> )	4	Glycerol:Sorbitol-0.15:0.15 (g/g gelatin)	NR	1.57 - 10.51 N	8.35 – 17.60	2.19 - 3.3 <sup>e</sup>	Gimenez <i>et al.</i> (2009a)
Giant squid ( <i>Dosidicus gigas</i> )	4	Glycerol:Sorbitol-0.15:0.15 (g/g gelatin)	NR	4.94	46	1.89 <sup>e</sup>	Gimenez <i>et al.</i> (2009b)
Giant squid ( <i>Dosidicus gigas</i> )	4	Glycerol:Sorbitol- 0.15:0.15	NR	2.63	34.7	1.78 <sup>e</sup>	Giménez <i>et al.</i> (2009c)
Sole (Solea spp.)	4	Glycerol:Sorbitol- 0.15:0.15 (g/g gelatin)	NR	11.4 – 28.5 N	18.1 - 16.8	1.66 – 1.77 <sup>d</sup>	Gomez-Estaca <i>et al.</i> (2009c)
Blue shark ( <i>Prionace glauca</i> )	1 - 3	Glycerol: 0, 25, 50 & 75%	0.011- 0.043	12.58 – 67.78	1.57 – 95.40	0.4 – 2.28	Limpisophon <i>et al.</i> (2009)
Bigeye snapper ( <i>Priacanthus tayenus</i> )	2	Glycerol: 50%	0.029-0.030	10.04 – 11.43	12.11 – 25.98	0.89 – 1.28	Rattaya <i>et al.</i> (2009)
Atlantic halibut ( <i>Hippoglossus hippoglossus</i> )	2	Sorbitol- 30% (w/w) of protein	0.080	3.8	294.5	12.0 <sup>e</sup>	Carvalho <i>et al.</i> (2008)



**Table 4.** (Continued)

Fish Species	Protein Conc.	Plasticiser Conc.	Thickness	Mechanical property		WVP ( $\times 10^{-11} \text{ gmm}^{-2} \text{ s}^{-1} \text{ Pa}^{-1}$ )	References
				TS (MPa)	EAB (%)		
Alaska Pollock ( <i>Theragra chalcogramma</i> )	5	Glutaraldehyde 0.25-0.75%	NR	45.9 – 50.1	3.23. – 3.44	0.73 – 0.86 <sup>f</sup>	Chiou <i>et al.</i> (2008)
Alaska pink salmon ( <i>Oncorhynchus gorbuscha</i> )				49.7 – 60.0	3.36 – 3.8	0.85 – 1.08 <sup>f</sup>	
Tuna ( <i>Thunnus tynnus</i> )	2	Glycerol: 25%	0.097 – 0.10	2.75 – 5.91	3.56 – 13.77	1.83 - 2.87 <sup>d</sup>	Gómez-Guillén <i>et al.</i> (2007)
Tilapia	5	Gellan and <i>k</i> -Carrageenan 1-2%	NR	101.23 – 109.76	5.08 - 6.81	1.75 - 2.4 <sup>f</sup>	Pranoto <i>et al.</i> (2007)
Bigeye snapper ( <i>Priacanthus arcacanthus</i> )	1-4	Glycerol: 25%	0.023-0.035	28.28 - 44.28	2.67 - 7.0	1.22 - 1.37	Jongjareonrak <i>et al.</i> (2006b)
	3	Glycerol: 0, 25, 50 and 75%	NR	7.97 - 57.34	3.04 – 50.30	1.31- 2.73	
Brownstripe red snapper ( <i>Lutjanus vitta</i> )	1-4	Glycerol: 25%	0.024-0.037	41.09 - 58.09	7.02 - 8.20	1.33 - 1.35	Jongjareonrak <i>et al.</i> (2006b)

NR: Not reported

<sup>a</sup>(g mm/m<sup>2</sup> h kPa); <sup>b</sup>(g mm/ kPa d m<sup>2</sup>); <sup>c</sup>(g mm/h cm<sup>2</sup> Pa); <sup>d</sup>(g mm h<sup>-1</sup> cm<sup>-2</sup> Pa<sup>-1</sup>); <sup>e</sup>( $\times 10^{-8}$  g mm h<sup>-1</sup> cm<sup>-2</sup> Pa<sup>-1</sup>); <sup>f</sup>(g mm/m<sup>2</sup> h kPa).

Hoque *et al.* (2011a) reported that films prepared from gelatin with a higher degree of hydrolysis showed a slightly lower thickness than that of the control film (without hydrolysis) and gelatin film was mainly stabilised by the weak bond including hydrogen bond and hydrophobic interaction. Protein content, plasticisers type and concentration have been reported to affect the properties of gelatin films (Vanin *et al.*, 2005). TS of gelatin film from shark (*Prionace glauca*) skin were affected by the protein concentration (1, 2 and 3%) of the film forming solution, FFS. TS of the film from a 2% protein FFS was highest. EAB and water vapour permeability (WVP) increased with increasing FFS protein concentration. The addition of glycerol improved flexibility and enhanced the UV barrier property at 280 nm. However, transparency at the visible range and WVP increased with increasing glycerol content (Limphisophon *et al.*, 2009). TS of gelatin film from the skin of brownstripe red snapper (*Lutjanus vitta*) and bigeye snapper (*Priacanthus macracanthus*) decreased with increasing glycerol concentration from 25 to 75% (Jongjareonrak *et al.*, 2006b). Moreover, at the same plasticiser concentration, fish skin gelatin from the two different species plasticised with glycerol (Gly) showed the greatest EAB, whereas ethylene glycol (EG) plasticised film showed the highest TS (Jongjareonrak *et al.*, 2006b). Gelatin has the hydrophilicity in nature and the film from gelatin generally shows low water vapour barrier property. Film from halibut skin gelatin with higher degraded peptide chains also had the poor water vapour barrier property, compared with that from gelatin having lower degraded chains (Carvalho *et al.*, 2008). This more likely leads to the limitation for commercial uses. Due to the poor water vapour barrier property, gelatin films have gained attention for further improvement.

Gelatin film could be improved by adding some natural extracts or cross-linkers such as aldehyde (Carvalho and Grosso, 2004), phenolic compounds (Nuthong *et al.*, 2009) and plant or herb extracts (Gomez-Estaca *et al.*, 2009a,b; Rattaya *et al.*, 2009), in which the increased mechanical properties can be obtained. Additionally, the preparation of gelatin blend film with other hydrocolloids led to the varying film properties (Yudi *et al.*, 2007). Fish gelatin films from pollock and

salmon skin were cross-linked with glutaraldehyde at the concentration of 0.25%, 0.50%, and 0.75% (w/w). The addition of cross-linkers had little effect on tensile properties and melting temperatures of fish gelatin films (Chiou *et al.*, 2008). The gelatin based films modified with TGase, glyoxal and formaldehyde had 20% reduction in solubility for all modified films (de Carvalho *et al.*, 2004). Fish skin gelatin films incorporated with seaweed extract at pHs 9 and 10 exhibited the higher EAB. However, no differences in TS and transparency between films without and with seaweed extract were observed. WVP and film solubility decreased as seaweed extract was incorporated, regardless of pH. This was associated with the formation of non-disulphide covalent bond in the film matrix, most likely induced by the interaction between oxidised phenols in seaweed extract and gelatin molecules (Rattaya *et al.*, 2009). Kolodziejaska *et al.* (2006) reported that the solubility of fish gelatin films and gelatin chitosan films (4:1, w/v) could be limited by cross-linking of the components with transglutaminase (TGase) or with 1-ethyl-3-(3-dimethylaminopropyl) carbodiimide (EDC). Fish gelatin-chitosan film modified with TGase at a concentration of 0.2 mg/l of the film forming solution decreased the solubility of the films at 25 °C from 65% to 28% at pH 6 and from 96% to 37% at pH 3 (de Carvalho *et al.*, 2004). The fish gelatin-chitosan films were more water resistant and more deformable than the bovine gelatin-chitosan films (Gomez-Estaca *et al.*, 2011).

#### **1.2.4 Nanofilms**

The applications of nanotechnology in the food sector are new emergent. However, the world's largest food companies have been actively exploring the potential of nanotechnology for use in food or food packaging (Cientifica, 2006). Applications in food packaging are considered highly promising because they can improve the safety and quality of food products. This includes intelligent packaging, which is reactive to the environment and active packaging, which is able to interact with the food product. Extensive use of nano-additives to the food is less likely in the near future owing to safety concerns (Sozer and Kokini, 2009). Polymer

nanocomposites have received great interest due to the ability of nanosized material fillers to significantly improve polymer properties when compared with polymer alone or micro-scale composites (Bae *et al.*, 2009a). The potential improvements include enhanced mechanical strength, weight reduction, increased heat-resistance and improved barrier properties (Ray and Okamoto, 2003). The enhanced mechanical and barrier properties of polymer/nanoclay composite films have been reported (Bae *et al.*, 2009a; Farahnaky *et al.*, 2014; Shakila *et al.*, 2012b; Sothornvit *et al.*, 2009). The improved water and gas barrier properties of nanocomposite films is believed to be due to the presence of ordered dispersed silicate layers with large aspect ratios in the polymer matrix and this forces water/gas travelling through the film to follow a tortuous path through the polymer matrix surrounding the silicate particles (Figure 3), thereby increasing the effective path length for diffusion (Ray and Okamoto, 2003; Rhim, 2007).

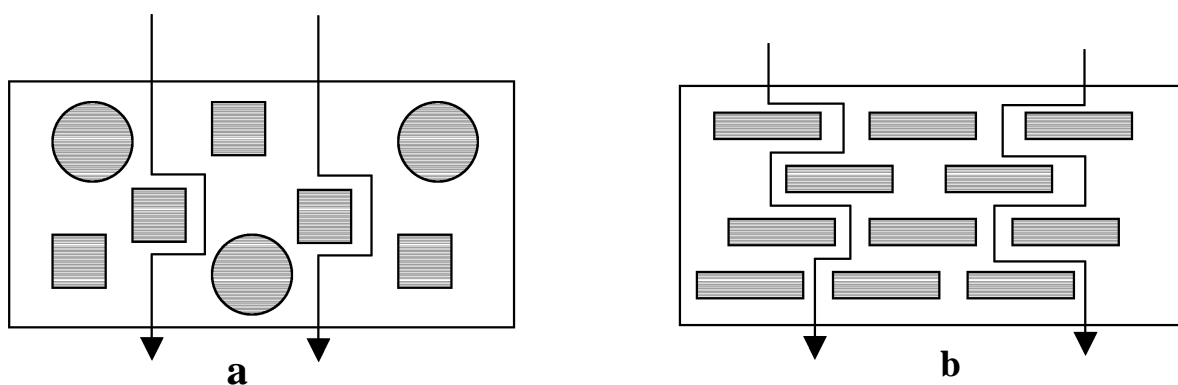


**Figure 3.** Schematic illustration of formation of “tortuous path” in nanocomposite.

(a) conventional filler reinforced composites, (b) polymer/layered silicate nanocomposites

Source: Ray and Okamoto (2003)

Nanotechnology has been applied widely in several fields. Advantages of nanotechnology in food application and packaging are shown in Figure 4. However, most researches on nanotechnology have focused on the electronics, medicine and automation sector (Sozer and Kokini, 2009). The knowledge gained from these sectors has been adapted for the use of food and agriculture products, such

as for applications in food safety (e.g. detecting pesticides and microorganisms), in environmental protection (e.g. water purification) and in delivery of nutrients, etc (Sozer and Kokini, 2009).

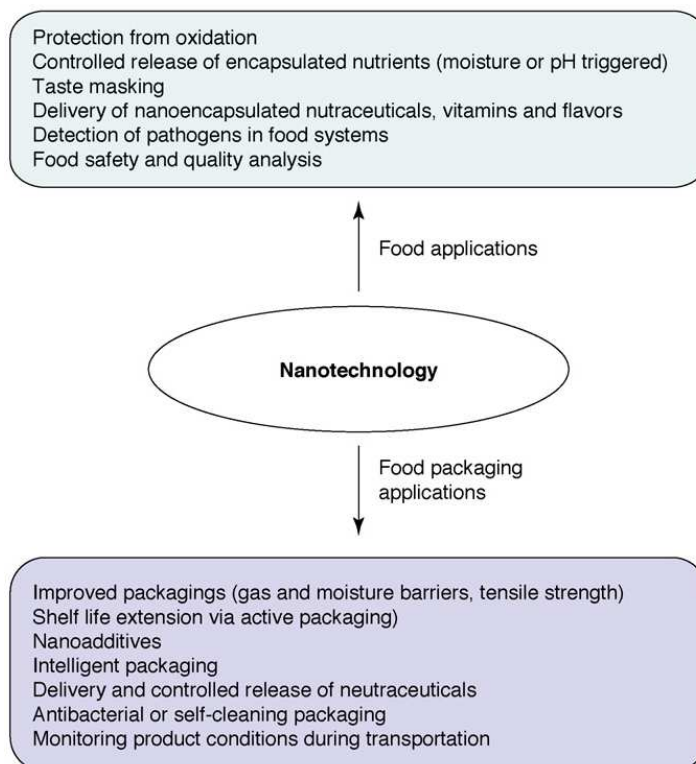


**Figure 4.** Potential applications of nanotechnology in the food and food-packaging industries

Source: Sozer and Kokini (2009)

#### 1.2.4.1 Nanoclay

Nanoclay has been widely used to improve packaging material in many aspects. Layered silicates are commonly known as the cationic clay minerals. Among the most commonly used layered silicates, smectite clays, such as hectorite, montmorillonite (mmt), are naturally occurring 2:1 layered or phyllosilicates (Ray and Okamoto, 2003). In accordance with eCFR (Code of Federal Regulations) § 184.1(b)(1), the ingredient MMT is used in food with no limitation other than current good manufacturing practice known as generally recognized as safe (GRAS).

Layered silicates have two types of structure: tetrahedral-substituted and octahedral substituted. In the case of tetrahedrally substituted layered silicates, the negative charge is located on the surface of silicate layers. Hence the polymer matrices can interact more readily with these than with octahedrally-substituted material. The general formula of layered silicates is presented in Table 5. Its crystal structure (Figure 5) consists of two-dimensional layers formed by fusing two silica tetrahedral sheets to an edge-shared octahedral sheet of either aluminium or magnesium hydroxide (Ray and Okamoto, 2003).

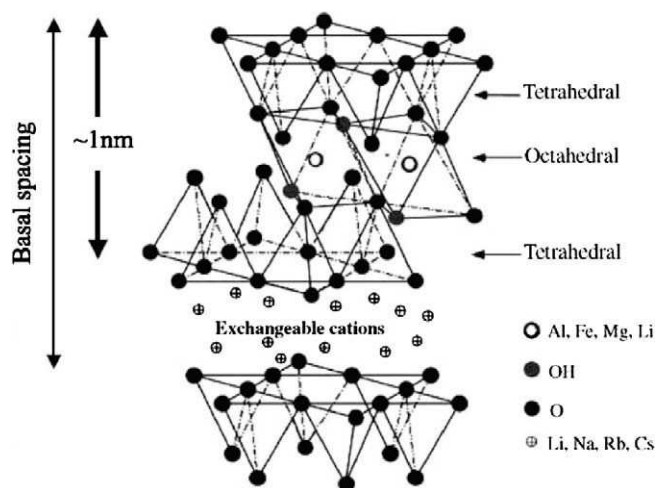


**Figure 5.** The crystal structure of the phyllosilicates

Source: Ray and Okamoto (2003)

**Table 5.** Chemical formula and characteristics of commonly used 2:1 phyllosilicates

2:1 phyllosilicates	Chemical formula <sup>a</sup>	CEC, mequiv/100 g	Particle length/nm
Montmorillonite	$M_x(\text{Al}_{4-x}\text{Mg}_x)\text{Si}_8\text{O}_{20}(\text{OH})_4$	110	100–150
Hectorite	$M_x(\text{Mg}_{6-x}\text{Li}_x)\text{Si}_8\text{O}_{20}(\text{OH})_4$	120	200–300
Saponite	$M_x\text{Mg}_6(\text{Si}_{8-x}\text{Al}_x)\text{Si}_8\text{O}_{20}(\text{OH})_4$	86.6	50–60

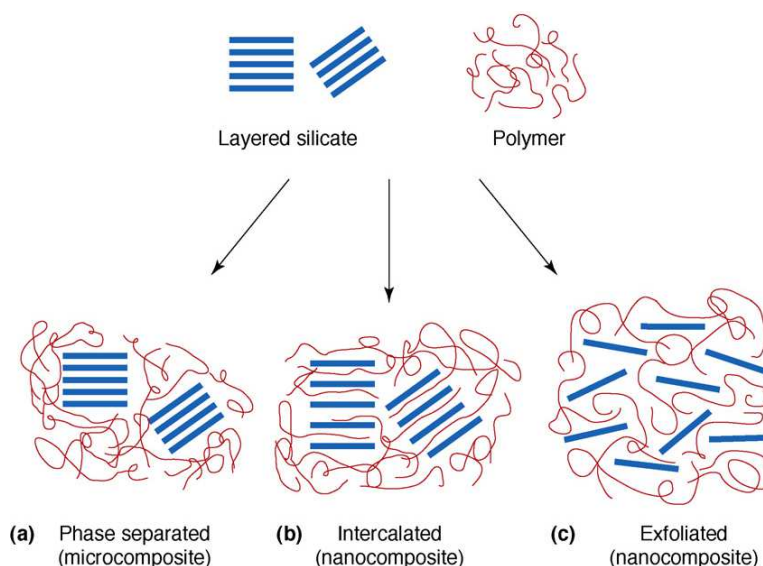
M= monovalent cation; x= degree of isomorphous substitution (between 0.5 and 1.3)<sup>a</sup>

Source: Ray and Okamoto (2003).

The layer thickness is generally about 1 nm, and the lateral dimension of the layers may vary from a few hundred angstroms to a micron scale, depending on the source of clay minerals (Ray and Okamoto, 2003). Parallel stacking of these layers leads to interlayer/galleries. Stacking of the layers is mediated by a regular van der Waals gap between the layers called the interlayer or gallery. Hydrated cations, balance the charge deficiency that is generated by isomorphous substitution within the layers (Pinnavaia, 1983). The degree of this substitution is expressed as cation exchange capacity (CEC), in terms of mequiv/100 g clay. This refers to total negative charges present from isomorphous substitution within the structure, the broken bond at edges, the external surfaces, and the dissociation of accessible hydroxyl groups (Auerbach *et al.*, 2004). Characteristics of different nanoclays are shown in Table 6.

#### 1.2.4.2 Formation and morphology of polymer/clay nanocomposites

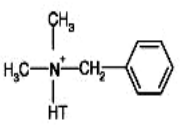
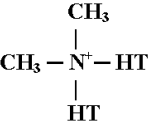
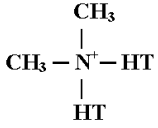
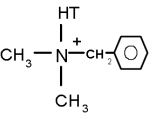
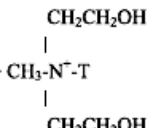
Depending on the compatibility of polymer and clay, three polymer hybrids are possibly formed, namely, conventionally phase separated, intercalated, and delaminated/exfoliated, as schematically shown in Figure 6 (Sozer and Kokini, 2009). Those three hybrids are shown below:



**Figure 6.** Types of composite derived from the interaction between clays and polymers.

Source: Sozer and Kokini (2009).

**Table 6.** Characteristics of nanoclays and organoclays

Name	Cloisite Na	Cloisite Ca	Cloisite 5	Cloisite 10A	Cloisite 15A	Cloisite 20A	Cloisite 11B	Cloisite 30B
<b>Chemical name</b>	Natural bentonite	Natural bentonite	Bis (hydrogenated tallow alkyl) dimethyl, salt with bentonite	Benzyl (hydrogenated tallow alkyl) dimethyl, salt with bentonite	Bis (hydrogenated tallow alkyl) dimethyl, salt with bentonite	Bis (hydrogenated tallow alkyl) dimethyl, salt with bentonite	Benzyl (hydrogenated tallow alkyl) dimethyl, salt with bentonite	Alkyl quaternary ammonium salt bentonite
<b>Modifier structure</b>	-	-	-					
<b>Moisture</b>	4-9%	4-9%	<3%	<3%	<3%	<3%	<3%	<3%
<b>Particle size</b>	<25 μm (d <sub>50</sub> )	<10 μm (d <sub>50</sub> )	<40 μm (d <sub>50</sub> )	<10 μm (d <sub>50</sub> )	<10 μm (d <sub>50</sub> )	<10 μm (d <sub>50</sub> )	<40 μm (d <sub>50</sub> )	<10 μm (d <sub>50</sub> )
<b>Colour</b>	Off White	Off White	Off White	Off White	Off White	Off White	Off White	Off White
<b>Bulk density</b>	568 g/l	625 g/l	480 g/l	265 g/l	165 g/l	175 g/l	265 g/l	365 g/l
<b>Density</b>	2.86 g/cc	2.8 g/cc	1.77 g/cc	1.9 g/cc	1.66 g/cc	1.77 g/cc	2.0 g/cc	1.98 g/cc
<b>X-ray results</b>	d <sub>001</sub> =1.17 nm	d <sub>001</sub> =1.55 nm	d <sub>001</sub> = 3.27 nm	d <sub>001</sub> = 1.92 nm	d <sub>001</sub> = 3.15 nm	d <sub>001</sub> = 2.42 nm	d <sub>001</sub> = 1.8 nm	d <sub>001</sub> = 1.85 nm

Source: Southern clay products Inc. (Gonzlaes, TX, USA).



1) Typically, the phase separated hybrids correspond to the conventionally filled polymers, in which the clay particles agglomerate, and lead to poor mechanical properties (LeBaron, 1999).

2) The intercalated hybrids result from the insertion of extended polymer chains into the clay layers occurring in regular multi-layers with a repeat distance of a few nanometers (Burnside and Giannelis, 1995).

3) The delaminated/exfoliated hybrids, in which the clay platelets (1 nm thick) are expected to be individually dispersed in the polymer matrix, resulting in high aspect ratio of about 1000 (fully dispersed), compared to that value of 10 found in phase separated systems. The interlayer expansion of these delaminated/exfoliated hybrids is comparable to the radius of gyration of the polymers (Burnside and Giannelis, 1995).

Two particular characteristics of layered silicates are generally considered for polymer/layered silicate nanocomposites. The first is the ability of the silicate particles to disperse into individual layers. The second characteristic is the ability to fine-tune their surface chemistry through ion exchange reactions with organic and inorganic cations (Ray and Okamoto, 2003).

Besides their improved material properties, biodegradability makes them an eco-friendly and alternative to traditional packaging (Figure 7) (Sozer and Kokini, 2009).

Property enhancement of mmt/polysaccharide nanocomposites has been reported (Abdollahi *et al.*, 2012; Jang *et al.*, 2011; Lim *et al.*, 2010; Cyrus *et al.*, 2008). Wheat and maize starch (McGlashan and Halley, 2003), thermoplastic starch (Park *et al.*, 2003), and chitosan (Rhim *et al.*, 2006) films added with nanoclays have been prepared. A few studies on protein based nanocomposites have been published, including whey, soy protein isolate and wheat gluten (Kumar *et al.*, 2010; Sothornvit *et al.*, 2010, 2009; Tunc *et al.*, 2007; Olabarrieta *et al.*, 2006; Rhim *et al.*, 2005). Also,

mmt/bovine gelatin nanocomposites (Martucci and Ruseckaite, 2010a) and fish gelatin nanocomposites (Bae *et al.*, 2009a, 2009b) have been reported. Most of biopolymer-based nanocomposites have shown appreciable improvements in mechanical and barrier properties, compared to biopolymer films.

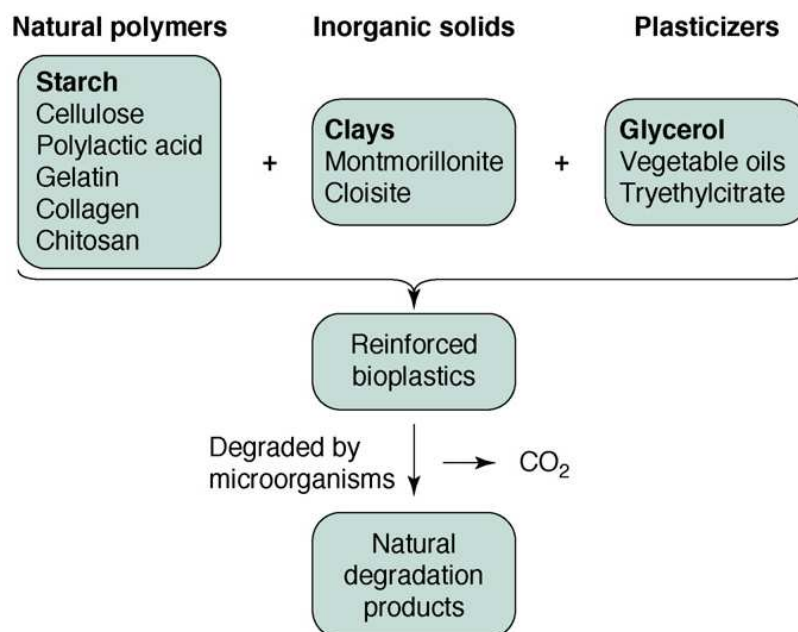


**Figure 7.** Formation of bio-nanocomposites and bio-degradation

Source: Sozer and Kokini (2009)

The mechanical properties, such as TS or young's modulus of biopolymer-based nanocomposite films such as corn starch/Cloisite Na<sup>+</sup> (Pandey and Singh, 2005), thermoplastic starch (TPS)/Cloisite 30B (Park *et al.*, 2003), wheat or maize starch/MMT nanocomposites (McGlashan and Halley, 2003), and chitosan-based nanocomposite films (Rhim *et al.*, 2006) were reported to be improved by the formation of the nanocomposite. In contrast, Sothornvit *et al.* (2009) reported the decreased TS and young's modulus for whey protein/nanoclay composite films. A decrease in WVP of clay/nanocomposite films has been frequently observed with various biopolymer films such as whey protein isolate/organo-clay composites (Sothornvit *et al.*, 2009), TPS/Cloisite Na<sup>+</sup> (Park *et al.*, 2002), chitosan/Cloisite Na<sup>+</sup> nanocomposites (Rhim *et al.*, 2006), and soy protein isolate (SPI)/clays (Rhim *et al.*,

**Table 7.** Properties of nanocomposite films from different sources

Biopolymer and concentration	Clay and concentration	Plasticiser	Thickness (mm)	Mechanical property			WVP ( $\times 10^{-11} \text{ gmm}^{-2} \text{ s}^{-1} \text{ Pa}^{-1}$ )	References
				TS (MPa)	EAB (%)	YM (MPa)		
Carrageenan-2%	CNF	Glycerol	0.053-0.066	29.8-44.7	3.9-21.8	1070-1770	1.54-1.91 <sup>a</sup>	Shankar <i>et al.</i> (2015)
Chicken feather protein- 5%	MMT Na <sup>+</sup> : 1, 3, 5 and 7%	Glycerol-Sorbitol: 40%	NR	4.18-5.95	9.61-16.50	NR	19.6-31.1	Song <i>et al.</i> (2013)
Chitosan: 2%	MMT: 0-5%	Tween 80	0.049-0.052	60.8-83.0	3.01-5.47	NR	0.30-0.71	Abdollahi <i>et al.</i> (2012)
Agar/ $\kappa$ -Carrageenan-4%	MMT Na <sup>+</sup> : 5%	Glycerol: 50%	0.058-0.067	31-44	16-45	NR	16.1-19.5	Rhim <i>et al.</i> (2012)
Starch- 20%	MMT: 1-10%	Glycerol: 20%	NR	NR	NR	NR	2.3-6.3	Slavutsky <i>et al.</i> (2012)
Red Algae: 2%	MMT: 0-5%	Glycerol, Sorbitol, Sucrose, Fructose, PPG	0.029-0.031	9.10-10.89	34.65-41.29	NR	1.13-1.29 <sup>b</sup>	Jang <i>et al.</i> (2011)
	Cloisite 30B: 0-5%	As above: 1.5%	0.029-0.032	9.10-10.85	34.65-40.49	NR	1.14-1.29 <sup>b</sup>	
Soy protein isolate: 70-85%	MMT: 0-15%	Glycerol: 15%	NR	2.26-15.60	11.85-64.60	NR	NR	Kumar <i>et al.</i> (2010)

**Table 7.** (Continued)

Biopolymer and concentration	Clay and concentration	Plasticiser	Thickness (mm)	Mechanical property			WVP ( $\times 10^{-11} \text{ gmm}^{-2} \text{ s}^{-1} \text{ Pa}^{-1}$ )	References
				TS (MPa)	EAB (%)	YM (MPa)		
Algae ( <i>G.corneum</i> ): 2%	MMT: 0-7%	Sorbitol: 1.5%	0.028	19.59-27.37	11.56-24.2	NR	1.07-1.59 <sup>b</sup>	Lim <i>et al.</i> (2010)
Wheat gluten (40%)	MMT: 0-7.5%	Glycerol: 10%	NR	3.73-11.44	15.2-58.4	1.86-4.70	NR	Tunc <i>et al.</i> (2010)
Whey protein isolate: 10%	Control: 0%	Glycerol: 5%	NR	3.40	29.1	171.8	66.0 <sup>c</sup>	Sothornvit <i>et al.</i> (2009)
	MMT: 5%	Glycerol: 5%	NR	2.98	42.4	109.3	47.1 <sup>c</sup>	
	Cloisite 30B: 5%	Glycerol: 5%	NR	3.29	51.7	162.6	55.6 <sup>c</sup>	
	Cloisite 20A: 5%	Glycerol: 5%	NR	1.55	29.1	115.5	64.8 <sup>c</sup>	
Potato starch	MMT: 0-5%	Glycerol: 30%)	NR	3.1-5.2	34.8-60.5	29.6-195.6	NR	Cyras <i>et al.</i> (2008)

NR: Not reported

<sup>a</sup> ( $\times 10^{-9} \text{ g m m}^{-2} \text{ s}^{-1} \text{ Pa}^{-1}$ ); <sup>b</sup>(ng m/m<sup>2</sup> s Pa); <sup>c</sup> ( $\times 10^9 \text{ g m m}^{-2} \text{ s}^{-1} \text{ Pa}^{-1}$ ).

2005). Properties of nano-composite films from different polymer sources are presented in Table 7.

#### **1.2.4.3 Gelatin/nanoclay composites**

Nanoclays have been used to improve physical and thermo-mechanical properties of gelatin-based biopolymers (Bae *et al.*, 2009a,b; Farahnaky *et al.*, 2014; Lim *et al.*, 2010). Jang *et al.* (2011) found that both thermal and mechanical properties were significantly improved by intercalation of montmorillonite (mmt) in gelatin matrix. The intercalation of mmt also reduced the maximum thermal decomposed rate of gelatin up to 45% (Zheng, 2002). Li *et al.* (2003) studied swelling property of gelatin/mmt nanocomposites and reported that the swelling rate and solvent uptake decreased with increasing mmt level. The morphological study related to thermal property of gelatin/mmt was presented by Martucci *et al.* (2007). The exfoliation and exfoliation/intercalation were found at the mmt level of 3-10%wt, which were the optimum levels enhancing thermal property of gelatin.

MMT has been used for property improvement of gelatin based films. Farahnaky *et al.* (2014) reported that Young's Modulus (YM) and TS of bovine gelatin films increased with clay content. However, EAB, WVP and swelling rate were decreased. TS of grouper and redsnapper bone gelatin films were 17–21% lower than that of the mammalian gelatin films. Nevertheless, TS of fish gelatin films increased considerably than that of the mammalian gelatin films when MMT was incorporated (Shakila *et al.*, 2012b). EAB of fish gelatin films were in general 2–3 folds higher than that of MMT added gelatin films. YM of grouper gelatin films increased with the addition of MMT (Shakila *et al.*, 2012b). The mechanical properties increased with MMT concentration, indicating that reinforcement of the biopolymer matrix by the nanoparticle load. Similar behavior was observed for the elastic modulus. These results suggested that the nanoparticles were well dispersed in the pig skin gelatin matrix (Jorge *et al.*, 2011). Rao (2007) observed that at a loading of 5% of MMT, the Young's modulus was increased by 75%, and the tensile strength

was increased by 25%. Martucci and Ruseckaite (2010a) reported that bovine gelatin/MMT nanocomposite films with more uniform thickness were more water resistant than the unfilled counterpart. Additionally, gelatin/MMT films had the good optical transparency as well as lowered surface hydrophilicity and WVP with MMT loading, indicating that filler was mostly distributed at the nanoscale. The presence of strong hydrogen interactions between gelatin and clay combined with the inherent barrier properties of the impermeable clay platelets was proposed (Martucci and Ruseckaite, 2010a).

Additionally, Bae *et al.* (2009a) reported that the addition of 5% nanoclay (w/w) increased TS from 30.31 to 40.71 MPa for tilapia gelatin films. The 9 g clay/100 g fish gelatin film exhibited the largest improvements in oxygen and water barrier properties. Oxygen permeability decreased from  $402.8 \times 10^{-6}$  to  $114.4 \times 10^{-6}$  g m/m<sup>2</sup> day atm and the water vapor permeability decreased from  $31.2 \times 10^{-3}$  to  $8.1 \times 10^{-3}$  ng m/m<sup>2</sup> s Pa (Bae *et al.*, 2009a). TS of microbial transglutaminase (MTGase) treated fish gelatin nanofilms decreased but EAB was increased. This was coincidental increases in molecular weight and viscosity of gelatin solutions (Bae *et al.*, 2009b). Nanocomposite films from different gelatins show the varying properties as shown in Table 8.

### **1.2.5 Improvement of the properties of gelatin films**

Gelatin film properties have been improved by chemicals, physical treatments, enzyme, phenols/plant extracts, hydrophobic substances and biopolymers (Hoque *et al.*, 2011b; Jo *et al.*, 2005; Limpisophon *et al.*, 2010; Rattaya *et al.*, 2009; Tongnuanchan *et al.*, 2012; Wang *et al.*, 2015; Weng and Zheng, 2015). These treatments can be applied to modify the gelatin film network through the cross-linking of gelatin chains to enhance the properties of films. Generally, reactive groups of natural or synthetic cross-linking agents are able to form a covalent inter- and/or intra molecular links between gelatin chains. Cross-linking agents strengthen the films through the formation of new bonds, while reducing film elasticity and solubility in water (Gomez-Estaca *et al.*, 2011).

**Table 8.** Properties of gelatin nanocomposite films from different sources

Biopolymer and conc. (%)	Clay and conc. (%)	Plasticiser	Thickness (mm)	Mechanical property			WVP ( $\times 10^{-11}$ gmm <sup>-2</sup> s <sup>-1</sup> Pa <sup>-1</sup> )	References
				TS (MPa)	EAB (%)	YM (MPa)		
Bovine gelatin: 10%	Cloisite 20A: 0, 2, 6, 10, 14, 18	Glycerol- 20%	0.170	2.2-2.9	16-25	17-32	0.44-0.84 <sup>a</sup>	Farahnaky <i>et al.</i> (2014)
Pig skin gelatin: 5 and 8	MMT: 0, 5, 10 and 15	Glycerol- 30%	NR	NR	NR	NR	NR	Jorge <i>et al.</i> (2014)
Pig skin gelatin: 6	MMT- 5	Glycerol- 25%	NR	30.3	36.0	569.8	28.2 <sup>b</sup>	Vanin <i>et al.</i> (2014)
Red snapper and grouper skin gelatins- 3%	MMT Na <sup>+</sup> - 0.5	Sorbitol- 30%	0.065 0.076	~ 20 ~ 40	~ 32 ~ 29	~ 100 ~ 400	872 <sup>c</sup> 841 <sup>c</sup>	Shakila <i>et al.</i> (2012b)
Tilapia skin gelatin	MMT Na <sup>+</sup> : 0, 1, 3, 5, 7 and 9	Glycerol- 20%	NR	~ 30-40	~ 20-38	NR	0.006-0.028 <sup>b</sup>	Bae <i>et al.</i> (2009a)
Gelatin	MMT Na <sup>+</sup> : 0, 1, 3, 5 and 10	NR	NR	88.1-110.8	0.9-9.6	3.3-8.3 (GPa)	NR	Rao (2007)

NR: Not reported

<sup>a</sup>(g mm/m<sup>2</sup> h kPa); <sup>b</sup>(ng mm/h cm<sup>2</sup> Pa); <sup>c</sup>(g/m<sup>2</sup>/day @ 90% RH at 25 °C).

To improve the properties of bovine hide/bone, pig skin and fish/cuttlefish skin gelatin films, chemicals have been used as cross-linking agents including aldehydes (Carvalho and Grosso, 2004), glutaraldehydes (Bigi *et al.*, 2001), carbodiimide (Kołodziejska *et al.*, 2006), genipin (Bigi *et al.*, 2002), ferulic acid, tannin acid (Cao *et al.*, 2007a), free radical mediated modification through hydrogen peroxide/fenton's reagent (Hoque *et al.*, 2011b), and others. Hydrophobic substances such as oils, fatty acids (Limpisophon *et al.*, 2010) and essential oils (Tongnuanchan *et al.*, 2012) can be used to improve water vapor barrier property of fish gelatin films. However, it may yield films with different properties. Additionally, essential oils are able to extend shelf-life of foods by lowering lipid oxidation (Oussalah *et al.*, 2004). Therefore, the incorporation of essential oils into the films could provide antioxidant activity for resulting films (Tongnuanchan *et al.*, 2013). Properties of fish gelatin films can be modified by addition of other biopolymers (Hoque *et al.*, 2011d; Weng and Zheng, 2015). Gelatin does not have ideal water vapor barrier properties. Thus, some biopolymers can be incorporated to modify the gelatin network through cross-linking of the biopolymer chains (Arvanitoyannis *et al.*, 1997; Cao *et al.*, 2007b).

Polyphenols of plant extracts can interact effectively with gelatin molecules. Under non-oxidising conditions, non-covalent interactions including hydrogen bond and hydrophobic forces stabilise polyphenol-protein complexes (Papadopoulou and Frazier, 2004). The non-covalent interaction may occur between polyphenols and proteins by hydrogen bonding and by hydrophobic bonding (Fig. 8). Principally, five potential types of interaction of phenolics and protein can be proposed: hydrogen bonding,  $\pi$ -bond and hydrophobic, ionic and covalent linkages (Hagermen, 1992; Bianco *et al.*, 1997). The interaction may occur via multi-site interaction (several phenolic compounds bound to one protein molecule) or multi-dentate interaction (one phenolic compound bound to several protein molecules). The type of interaction depends on the type and the molar ratio of both phenolic compound and protein (Prigent *et al.*, 2003).



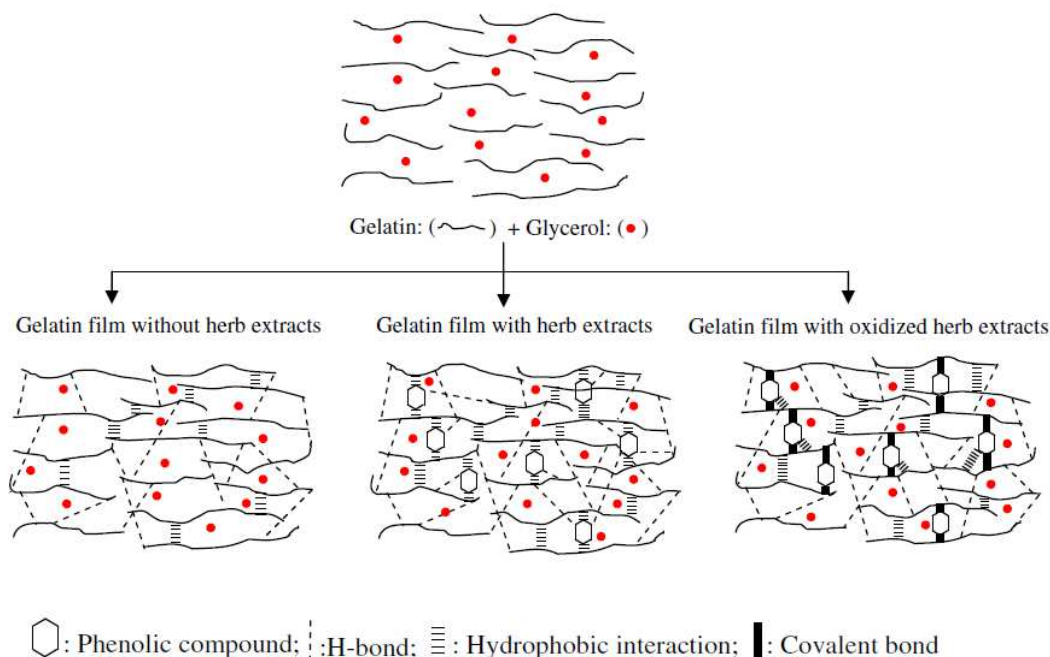


**Figure 8.** A scheme illustrating the impact of herb extracts without and with oxidation on the cross-linking of gelatin molecules in the film matrix

Source: Hoque *et al.* (2011c).

In addition to polyphenolic plant extracts, there has also been growing interest in using other natural extracts as protein cross-linker and antioxidant in food systems. TS of gelatin film from silver carp skin increased with increasing GTE (green tea extract) concentrations (Wu *et al.*, 2013). It is well known that polyphenolic compounds contain many hydrophobic groups, which can form hydrophobic interaction with hydrophobic region of gelatin molecule. Hydroxyl groups of polyphenolic compounds were able to combine with hydrogen acceptors of gelatin molecule by hydrogen bonds. Films obtained from cuttlefish skin gelatin incorporated with CME (cinnamon extract), CLE (clove extract) and SAE (star anise extract) showed higher TS, but lower EAB, as compared with the control film (without addition of herb extracts) (Hoque *et al.*, 2011c). Water vapor permeability (WVP), and film solubility of bigeye snapper skin gelatin films incorporated with seaweed extract at pHs 9 and 10 decreased, regardless of pH (Rattaya *et al.*, 2009). This was associated with the formation of non-disulfide covalent bond in the film

matrix, most likely induced by the interaction between oxidized phenols in seaweed extract and gelatin molecules. Ferulic acid and tannin acid extracted from plant were able to cross-link bovine bone gelatin films (Cao *et al.*, 2007a). The addition of murta extracts increased protection of UV light as well as antioxidant activity of tuna gelatin film (Gómez-Guillén *et al.*, 2007). Gelatin films incorporated with different plant extracts showed the varying properties as shown in Table 9.

Apart from chemicals or plant extracts, cross-linking enzymes have been used for improving film properties. Transglutaminase (Bae *et al.*, 2009b; Chambi and Grosso, 2006; Wang *et al.*, 2015; Weng and Zheng, 2015) and lysozyme (Bower *et al.*, 2006) have been used to enhance the functional properties. Furthermore, physical crosslinking for film improvement can be conducted using several methods including ultraviolet (UV),  $\gamma$ - irradiation and dehydrothermal (DHT) treatment (Bigi *et al.*, 1998).

### **1.2.6 Applications of protein based films**

Films from gelatin can be used as smart/active packaging, in which antioxidants/antimicrobials can be incorporated (Gomez-Estaca *et al.*, 2014). Active packaging is an innovative packaging which can be used to delay oxidation, inhibit microbial growth and control respiration rate, not just providing a barrier property (Ahvenainen, 2003). Antioxidant/antimicrobial packaging is an important kind of active packaging and very promising food preservation technique for extending the shelf life of foods (Lopez-De-Dicastillo *et al.*, 2012). The direct addition of antioxidants/antimicrobials to food results in some loss of activity due to leaching into the bulk of the food (Vojdani and Torres, 1989), or enzymatic activity, and reaction with other food components such as lipids, carbohydrates and proteins (Henning *et al.*, 1986; Jung *et al.*, 1992). If an antioxidant/antimicrobial could be released from the film for an extended period, its activity could be extended during transportation and storage. An ideal solution for the food industry to insure food safety and overcome environmental problems is to incorporate antioxidants/antimicrobials into edible films

**Table 9.** Properties of gelatin films incorporated with plant extracts

Sources of gelatin and concentration	Sources of plant extract and concentration	Thickness ( $\mu\text{m}$ )	Mechanical properties			WVP ( $\times 10^{-11} \text{ gmm}^{-2} \text{ s}^{-1} \text{ Pa}^{-1}$ )	References
			YM (MPa)	TS (MPa)	EAB (%)		
Silver carp skin gelatin- 3%	Green tea extract, Grape seed extracts, Ginkgo leaf extract and Ginger extract- 0.01, 1 and 5 mg/ml	123.80-156.67	NR	14.64-23.42	30.86-62.86	1.81-2.63 <sup>a</sup>	Li <i>et al.</i> , 2014
Cat fish skin gelatin- 3%	Longan seed extract- 50, 100, 300 and 500 ppm	35.93-37.60	NR	49.53-52.84	16.48-18.62	1.04-1.45 <sup>b</sup>	Vichasilp <i>et al.</i> , 2014
Fish gelatin- 3.4%	Lignins- 0.6% of gelatin	96-124	NR	7.51-16.44	136.60-362.83	2.06-4.58 <sup>c</sup>	Nunez-Flores <i>et al.</i> , 2013a
Silver carp skin gelatin- 4%	Green tea extract- 0, 0.3 and 0.7% of gelatin	31.05-32.17	NR	25.25-36.63	42.53-49.56	0.92-1.10	Wu <i>et al.</i> , 2013
Fish gelatin-4%	Lignin:Gelatin at the ratio of 0:100, 15:85, 20:80 and 25:75	NR	NR	4.23-5.39	375-546	2.21-5.56 <sup>c</sup>	Nunez-Flores <i>et al.</i> , 2012

**Table 9.** (Continued)

Sources of gelatin and concentration	Sources of plant extract and concentration	Thickness ( $\mu\text{m}$ )	Mechanical properties			WVP ( $\times 10^{-11} \text{gmm}^{-2} \text{s}^{-1} \text{Pa}^{-1}$ )	References
			YM (MPa)	TS (MPa)	EAB (%)		
Cuttlefish skin gelatin- 3%	Cinnamon, Clove and Star anise extracts- 1% of gelatin	29-32	NR	32.78-46.96	4.28-5.92	0.77-0.96	Hoque <i>et al.</i> , 2011c
Sole skin gelatin- 4%	Borage extract and gelatin solution at the ratio of 1:1	100 105	NR	NR	NR	1.77 <sup>c</sup> 1.60 <sup>c</sup>	Gomez-Estaca <i>et al.</i> , 2009c
Catfish skin gelatin- 4%							
Bigeye snapper skin gelatin- 2%	Brown seaweed extract- 6% of gelatin	29.51-30.62	NR	10.04-11.43	12.51-25.98	0.89-1.28	Rattaya <i>et al.</i> , 2009
Tuna skin gelatin- 2%	Murta leaves extract and gelatin solution at the ratio of 1:1	97-101	NR	NR	NR	1.83-2.87 <sup>c</sup>	Gomez-Guillen <i>et al.</i> , 2007

Note: <sup>a</sup>( $\text{g}\cdot\text{m}/\text{m}^2\cdot\text{d}\cdot\text{KPa}$ ); <sup>b</sup>( $10^{-8}\cdot\text{g}\cdot\text{mm}\cdot\text{h}^{-1}\cdot\text{cm}^{-2}\cdot\text{Pa}^{-1}$ ); <sup>c</sup>( $10^{-8}\cdot\text{g}\cdot\text{mm}/\text{h}\cdot\text{Pa}\cdot\text{cm}^2$ ). NR: Not reported.

such as zein, whey, gelatin, gums, and starch (Dawson *et al.*, 2002; Padgett *et al.*, 1998). According to Papadokostaki *et al.* (1997), polymer structure is related to the release of active components, related with their efficacy in food or food products.

Incorporation of antioxidants into packaging film as an antioxidant packaging has become very popular since oxidation is one of the main causes of food spoilage (Byun *et al.*, 2010). Butylated hydroxyanisole (BHA) and butylated hydroxytoluene (BHT) have been used as antioxidant in active packaging. However, many consumers do not prefer these synthetic antioxidants due to their toxicity and suspect carcinogenic potential (Bonilla *et al.*, 2012; Gomez-Estaca *et al.*, 2014). Thus, natural antioxidants/antimicrobials, such as plant extracts, are more attractive (Byun *et al.*, 2010). Numerous essential oils, such as tea, rosemary, clove, ginger, lemongrass, cinnamon, citrus, etc. (Wu *et al.*, 2013) and aromatic oily liquids obtained from plant material such as flowers, buds, seeds, leaves, twigs, bark, herbs, wood, fruits, and roots (Guenther, 1948) have been used in a broad range of applications. Active packaging to eliminate food-borne pathogen, as well as to delay the rate of oxidation in foods containing lipids has gained increasing attention. Grape seed extract, ginger extract, ginkgo leaf extract, green tea extract, borage extract, longan seed extract, murta ecotypes leaves extracts, spices, lignin, BHT and  $\alpha$ -Tocopherol were incorporated into gelatin films (Gomez-Estaca *et al.*, 2009a,b; Gomez-Guillen *et al.*, 2007; Hoque *et al.*, 2011c; Jongjareonark *et al.*, 2008; Li *et al.*, 2014; Nunez-Flores *et al.*, 2012; Vichasilp *et al.*, 2014; Wu *et al.*, 2013). Incorporation of antioxidants/antimicrobials with the protein matrix may not only affect the release of active components to the food but may also alter the physicochemical properties of the films, thereby altering the film solubility and their barrier properties (Gomez-Guillen *et al.*, 2007).

Recently, active nanofilms have been prepared by incorporating with natural extracts. Antioxidant activity and properties of nanocomposite films from carboxymethylcellulose-MMT/murta leaves extract (Gutierrez *et al.*, 2012), gelatin/tea polyphenol-loaded chitosan nanoparticles (Bao *et al.*, 2009) and chitosan-MMT/rosemary essential oil (Abdollahi *et al.*, 2012) have been studied. Antimicrobial

properties of whey protein isolate/clay composite films (Sothornvit *et al.*, 2010; 2009) and antimicrobial properties of *Gelidium corneum*/nano-clay composite films (Lim *et al.*, 2010) have been reported. WPI/Cloisite 30B composite films showed a beneficially bacteriostatic effect against *Listeria monocytogenes* (Sothornvit *et al.*, 2010, 2009). These activities play an important role in reducing the risk of food-borne pathogenic contamination, and extending the shelf-life of food products (Appendini and Hotchkiss, 2002; Pereira *et al.*, 2011). Antimicrobial films based on gelatin-chitosan composite incorporated with essential oil and bi-layer gelatin-chitosan films (Gomez-Estaca *et al.*, 2010; Pereda *et al.*, 2011) have been prepared.

#### **1.2.6.1 Protection and gas/water barrier for food storage**

All barrier properties of edible films are affected greatly by film composition and environmental conditions (relative humidity and temperature) (Gontard *et al.*, 1996). Protein based film exhibit the excellent barrier to gas especially, oxygen, etc. (Jongjareonrak *et al.*, 2008). They can be used for protection of foods against lipid oxidation by lowering the amount of O<sub>2</sub> involved in oxidation process. Film based on protein had the lowest oxygen permeability ( $<10 \text{ cm}^3 \mu\text{m m}^{-2} \text{ d}^{-1} \text{ kPa}^{-1}$ ) (Han *et al.*, 2005). Tongnuanchan *et al.* (2011) reported that film from fish muscle protein was able to reduce lipid oxidation of dried fish powder during storage at 25 °C up to 20 days, in comparison with control. Artharn *et al.* (2009) found that film from round scad muscle was able to retard the lipid oxidation of dried fish powder during storage at 28-30 °C for 21 days.

#### **1.2.6.2 Active packaging for shelf-life extension of foods**

Active packaging is an innovative concept that can be defined as a type of packaging that changes the condition of the packaging to extend shelf-life or improve safety or sensory properties while maintaining the quality of the food (Barbosa-Pereira *et al.*, 2014; Vermeiren *et al.*, 1999). Films could improve storage, mainly as a result of their ability to act as barriers to water, preventing dehydration, and to oxygen and light, reducing lipid oxidation (Gennadios *et al.*, 1997). Recently,

active nanocomposite films with antimicrobial/antioxidant activities have been produced as the smart packaging (Figure 9).

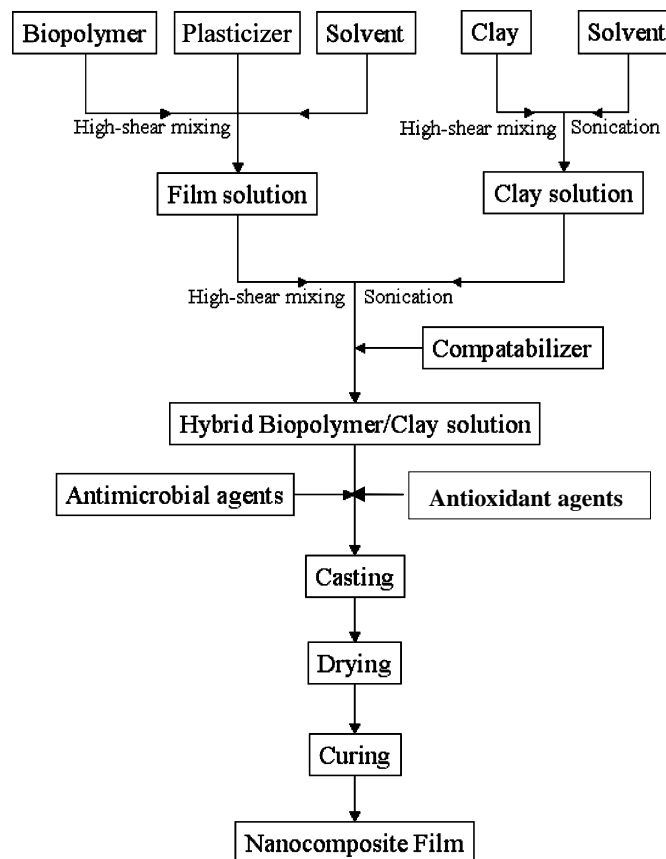


**Figure 9.** Preparation of antioxidant/antimicrobial nanocomposite films using a solvent casting method

Source: Rhim and Ng (2007)

Delayed time-release of antioxidants of this type from films maintains high concentrations on the surface of the food, thereby improving the efficacy of the films (Gomez-Estaca *et al.*, 2007). Recently, a fish gelatin-lignin film was shown to improve the appearance, protein quality and oxidative stability of salmon fillets subjected to high pressure processing (Ojagh *et al.*, 2011). Nunez-Flores *et al.* (2013b) studied the feasibility of using bovine hide gelatin-lignosulphonate (GLS) film to improve the quality of sardine fillets during chilled storage, alone or in combination with high pressure treatment (300 MPa/10 min/7 °C). The combined use

of GLS film with high pressure reduced microbial growth, total volatile basic compounds (TVB) and thiobarbituric acid reactive substances (TBARS) during chilled storage (7 °C) of 17 days (Nunez-Flores *et al.*, 2013b). Films incorporated with cinnamon essential oil, were able to extend the shelf-life of rainbow trout stored at 4 °C for 16 days, mainly by retarding the microbial growth and lowering the lipid oxidation (Ojagh *et al.*, 2010). Milk protein-based edible film incorporated with essential oil could reduce microbial load and increase antioxidative stability of beef during 7 days of storage at 4 °C (Oussalah *et al.*, 2004). The complex gelatin-chitosan film incorporated with clove essential oil was applied to fish during chilled storage (2±1 °C), the growth of gram-negative bacteria, especially enterobacteria, was reduced while lactic acid bacteria remained practically constant during the storage of 11 days (Gomez-Estaca *et al.*, 2010). Gimenez *et al.* (2011) investigated the lipid oxidation of horse mackerel (*Trachurus trachurus*) patties covered with fish gelatin-based films containing a borage seed extract during 240 days of frozen storage and subsequent thawing and 4 day-chilling. Film had protective effects on lipid oxidation of horse mackerel patties throughout frozen storage and particularly after thawing and chilled storage. Furthermore, when compared to vacuum packaging, film showed similar effect until advanced stages of oxidation were reached and exerted the enhanced protection once samples were thawed and exposed to air oxygen during chilled storage. Fish gelatin films without and with BHT or  $\alpha$ -tocopherol incorporated showed a preventive effect on lard oxidation as evidenced by the retardation of thiobarbituric acid reactive substances (TBARS) and peroxide formation (Jongjareonrak *et al.*, 2008). Gomez-Estaca *et al.* (2007) reported that the stability of cold-smoked sardine muscle was improved by coating the muscle with functional gelatin based edible films. Films enriched with an oregano or a rosemary extract were able to retard lipid oxidation, but they failed to inhibit the microbial growth. Nevertheless, gelatin-chitosan films were most effective in reducing microbial growth (Gomez-Estaca *et al.*, 2007).



### **1.3 Objectives**

1. To investigate the effect of extraction condition on the characteristics and functional properties of squid skin gelatin.
2. To study the impact of bleaching on properties and film forming ability of gelatin from squid skin.
3. To prepare and characterise fish skin gelatin/nanoclay composite films as affected by types of clay and some processing factors.
4. To examine the properties of fish skin gelatin/nanoclay composite films incorporated with ethanolic extract from coconut husk.
5. To study the application of fish and squid skin gelatins/nanoclay composite film containing ethanolic extract from coconut husk for shelf-life extension of fish meat powder.

## CHAPTER 2

### CHARACTERISTICS AND FUNCTIONAL PROPERTIES OF GELATIN FROM SPLENDID SQUID (*LOLIGO FORMOSANA*) SKIN AS AFFECTED BY EXTRACTION TEMPERATURES

#### 2.1 Abstract

Gelatin was extracted from the skin of splendid squid (*Loligo formosana*) at different temperatures (50, 60, 70 and 80 °C) with gelatin yield of 8.8%, 21.8%, 28.2%, and 45.3% (dry weight basis) for G50, G60, G70 and G80, respectively. Gelatin from the skin of splendid squid had a high protein content (~90%) with low moisture (8.63-11.09%), fat (0.22-0.31%) and ash contents (0.17-0.68%). Gelatin extracted at higher temperature (G80) had a relatively higher free amino group content than gelatin extracted at lower temperatures (G50, G60 and G70) ( $P < 0.05$ ). All gelatins contained  $\alpha$ - and  $\beta$ -chains as the predominant components. Amino acid patterns of gelatin revealed the high proline and hydroxyproline contents for G50 and G60. FTIR spectra of obtained gelatins revealed the significant loss of molecular order of the triple-helix. The gel strength of gelatin extracted at lower temperature (G50) was higher than that of gelatins extracted at higher temperatures including G60, G70 and G80, respectively. The net charge of G50, G60, G70 and G80 became zero at pHs of 6.84, 5.94, 5.49, and 4.86, respectively, as determined by  $\zeta$ -potential titration. Gelatin extracted at higher temperature (G80) had the lower  $L^*$  value but higher  $a^*$  and  $b^*$  values, compared with those extracted at lower temperatures ( $P < 0.05$ ). Emulsion activity index decreased, whilst emulsion stability index, foam expansion and stability increased as the concentration (1-3%) increased ( $P < 0.05$ ). Those properties were governed by extraction temperatures of gelatin. Thus gelatin can be successfully extracted from splendid squid skin using the appropriate pretreatment and extraction temperature.

## 2.2. Introduction

Fish gelatin, partially hydrolysed form of collagen, has been given increasing attention as the alternative of land animal gelatin due to religious constraint. Both Judaism and Islam forbid the consumption of any pork-related products, while Hindus do not consume cow-related products (Karim and Bhat, 2009). In addition, there is increasing concern whether land animal tissue-derived collagens and gelatins are capable of transmitting pathogenic vectors such as prions (Wilesmith *et al.*, 1991). As a consequence, fish gelatin has gained increasing interest as the potential alternative for land animal counterpart. Due to the abundance of skin, fin, scale and bones, etc., which are the by-product from the fish processing industry, it would be of full benefit to fully utilize those resources as promising raw material for gelatin production (Ahmad and Benjakul, 2011; Gomez-Guillen *et al.*, 2002; Muyonga *et al.*, 2004b).

Squid and cuttlefish have become an important fishery products in Thailand as well as other Southeast Asian countries, and are mainly exported worldwide (Hoque *et al.*, 2010). During processing, skin is generated as a by-product with the low market value and it can create serious ecological problems and environmental pollution without appropriate management. Squid wastes and by-products are rich in collagen (Brinckmann, 2005). Cuttlefish skin was used for gelatin extraction (Aewsiri *et al.*, 2011). Additionally, gelatin was extracted from skin of giant squid, *Dosidicus gigas* (Gimenez *et al.*, 2009c, Uriarte-Montoya *et al.*, 2011).

Gelatin can be used as a foaming, emulsifying and wetting agent in food, pharmaceutical, medical and technical applications due to its surface-active properties (Balti *et al.*, 2011). Gelatins from fish and cuttlefish skin have been demonstrated to render the biodegradable films with the superior UV barrier properties (Hoque *et al.*, 2011c, Rattaya *et al.*, 2009). Gelatin from cuttlefish skin had the improved emulsifying property when modified by oxidised fatty acids (Aewsiri *et al.*, 2011). Functional properties of gelatin and other food proteins are governed by many factors such as chain length or molecular weight, amino acid composition and hydrophobicity, etc (Gomez-Guillen *et al.*, 2002).

Owing to the abundance of squid skin in Thailand, it can be used for gelatin extraction. However, very low yield of gelatin (2.6%) was obtained from skin of giant squid, *Dosidicus gigas* (Gomez-Guillen *et al.*, 2002). Increasing extraction temperatures might be an effective means to increase the yield; however, the functional properties can be affected differently. Therefore, this study aimed to investigate the impact of extraction temperatures on yield, characteristics and functional properties of gelatin extracted from the skin of splendid squid (*Loligo formosana*) caught in Thailand.

## **2.3 Materials and methods**

### **2.3.1 Chemicals**

$\beta$ -Mercaptoethanol ( $\beta$ -ME) and bovine serum albumin were obtained from Sigma Chemical Co. (St. Louis, MO, USA). High molecular weight protein marker was purchased from GE Healthcare UK (Buckinghamshire, UK). Foline Ciocalteu's phenol reagent, acetic acid and phosphoric acid were purchased from Merck (Darmstadt, Germany). Sodium dodecyl sulfate (SDS), Coomassie Blue R-250 and *N,N,N',N'*-tetramethyl ethylene diamine (TEMED) were procured from Bio-Rad Laboratories (Hercules, CA, USA).

### **2.3.2 Collection and preparation of squid skin**

The outer skin of fresh squid (*Loligo formosana*) was obtained from Sea Wealth Frozen Food Co., Ltd., Songkhla, Thailand and stored in ice using skin/ice ratio of 1:2 (w/w). Upon arrival to the Department of Food Technology, Prince of Songkla University, Hat Yai, Thailand, the skin was cleaned and washed with iced tap water (0-2 °C). Skin contained 83% of moisture, 14% of protein, 1.1% of ash and 1.5% of fat as determined by the method of AOAC (2000). The skin was then cut into small pieces (0.5x0.5 cm<sup>2</sup>), placed in polyethylene bags and stored at -20 °C until use. The storage time was not more than 2 months.

### 2.3.3 Extraction of gelatin from squid skin

Gelatin extraction was performed following the method of Ahmad and Benjakul (2011) with slight modification. Before gelatin extraction, the prepared skin was soaked in 0.05 M NaOH with a skin/solution ratio of 1:10 (w/v). The mixture was stirred continuously for 6 h at room temperature at a speed of 150 rpm using an overhead stirrer equipped with a propeller (RW 20.n, IKA-Werke GmbH & CO.KG, Staufen, Germany). The alkaline solution was changed every 90 min to remove non collagenous proteins and pigments. Alkaline-treated skin was then washed with tap water until the neutral or faintly basic pH of wash water was obtained. The skin was then soaked in 0.05 M phosphoric acid with a skin/solution ratio of 1:10 (w/v) for 24 h with gentle stirring at 4 °C. The acidic solution was changed every 12 h to swell the collagenous material in the skin matrix. Acid-pretreated skin was washed thoroughly with tap water until wash water became neutral or faintly basic. To extract gelatin, the swollen skin was soaked in distilled water with different temperatures (50, 60, 70 and 80 °C) using a skin/water ratio of 1:10 (w/v) in a temperature-controlled water bath (W350, Memmert, Schwabach, Germany) for 12 h with a continuous stirring at a speed of 150 rpm. The mixture was then filtered using two layers of cheese cloth. The filtrate was further filtered using a Whatman No. 4 filter paper (Whatman International, Ltd., Maidstone, England) with the aid of JEIO Model VE-11 electric aspirator (JEIO TECH, Seoul, Korea). The resultant filtrate was freeze-dried using a Scanvac Model Coolsafe 55 freeze dryer (Coolsafe, Lynge, Denmark). The dry matter extracted from skin at different temperatures was referred to as ‘G50’, ‘G60’, ‘G70’ and ‘G80’, respectively. All gelatin samples were weighed, calculated for extraction yield and subjected to analyses. The yield of gelatin was calculated based on dry weight of skin.

$$\text{Yield (\%)} = \frac{\text{Weight of freeze dried gelatin (g)}}{\text{Weight of dry skin (g)}} \times 100$$

## 2.3.4 Analyses

### 2.3.4.1 Determination of proximate composition

Moisture, protein, ash and fat contents were determined following the methods of AOAC (2000) with the analytical Nos. of 950.46, 928.08, 920.153 and 960.39, respectively.

### 2.3.4.2 Electrophoretic analysis and free amino group content

SDS-polyacrylamide gel electrophoresis (SDS-PAGE) was performed by the method of Laemmli (1970). Gelatin samples were dissolved in 5% SDS and the mixtures were incubated at 85 °C for 1 h. The mixtures were centrifuged at 3,500xg for 5 min at room temperature using a microcentrifuge (MIK-RO20, Hettich Zentrifugan, Tuttlingen, Germany) to remove undissolved debris. Gelatin samples were mixed at a 1:1 (v/v) ratio with the sample buffer (0.5 M Tris-HCl, pH 6.8, containing 4% SDS and 20% glycerol). Samples (15 µg protein) were loaded onto polyacrylamide gels comprising a 7.5% running gel and a 4% stacking gel and subjected to electrophoresis at a constant current of 15 mA/gel using a Mini Protein II unit (Bio-Rad Laboratories, Inc., Richmond, CA, USA). After electrophoresis, the gel was stained with 0.05% (w/v) Coomassie Blue R- 250 in 15% (v/v) methanol and 5% (v/v) acetic acid and destained with 30% (v/v) methanol and 10% (v/v) acetic acid. High molecular weight marker at the range of 53 kDa to 212 kDa (GE Healthcare UK, Buckinghamshire, UK) was used. Relative mobility ( $R_f$ ) of protein band was calculated and the molecular weight of the protein was calculated from the plot between  $R_f$  and log (MW) of standards.

Free amino group content was determined following the method of Benjakul and Morrissey (1997). Properly diluted samples (125 µl) were mixed thoroughly with 2.0 ml of 0.2 M phosphate buffer, pH 8.2, followed by the addition of 1.0 ml of 0.01% 2,4,6-trinitrobenzenesulfonic acid (TNBS) solution. The mixtures were then placed in a temperature controlled water bath at 50 °C for 30 min in the dark. The reaction was terminated by adding 2.0 ml of 0.1 M sodium sulphite. The mixtures were cooled down at room temperature for 15 min. The absorbance was

measured at 420 nm using a double beam spectrophotometer (Model UV-1800, Shimadzu, Kyoto, Japan) and the free amino group content was expressed in terms of L-leucine.

#### **2.3.4.3 Amino acid analysis**

Amino acid composition of gelatin samples was analysed according to the method of Ganno *et al.* (1985) with a slight modification. Gelatin samples were hydrolysed under reduced pressure in 4 M methanesulphonic acid containing 0.2% (v/v) 3-(2-aminoethyl) indole at 115 °C for 24 h. For analyzing the tryptophan content, gelatin samples were hydrolysed by 3 N mercaptoethanesulphonic acid to avoid the decomposition of tryptophans (Penke, Ferenczi & Kovacs, 1974). The hydrolysates were neutralised with 3.5 M NaOH and diluted with 0.2 M citrate buffer (pH 2.2). An aliquot of 0.04 ml was applied to an amino acid analyser (MLC- 703; Atto Co., Tokyo, Japan).

#### **2.3.4.4 Fourier transform infrared (FTIR) spectroscopic analysis**

Gelatin samples were subjected to FTIR analysis using Bruker Model EQUINOX 55 FTIR spectrometer (Bruker, Ettlingen, Germany) equipped with a deuterated L-alanine triglycine sulphate (DLATGS) detector. The horizontal attenuated total reflectance (HATR) accessory was mounted in the sample compartment. The internal reflection crystal (Pike Technologies, Madison, WI, USA), made of zinc selenide, had a 45° angle of incidence of the IR beam. Spectra were acquired in the IR range of 4000–650  $\text{cm}^{-1}$  (mid-IR region) at 25°C. Automatic signals were collected in 32 scans at a resolution of 4  $\text{cm}^{-1}$  and were ratioed against a background spectrum recorded from the clean and empty cell at 25 °C. Analysis of spectral data was carried out using the OPUS 3.0 data collection software programme (Bruker, Ettlingen, Germany). Prior to data analysis, the spectra were baseline corrected and normalised.

#### 2.3.4.5 Measurement of $\zeta$ -potential

Gelatin samples were dissolved in distilled water at a concentration of 0.5 mg/ml. The mixture was stirred at room temperature for 6 h. The  $\zeta$ -potential of each sample (20 ml) was measured using a zeta potential analyser (ZetaPALS, Brookhaven Instruments Co., Holtsville, NY, USA).  $\zeta$ -Potential of samples adjusted to different pHs with 1.0 M nitric acid or 1.0 M KOH using an autotitrator (BI-ZTU, Brookhaven Instruments Co., Holtsville, New York, USA) was determined. The pI was estimated from pH rendering  $\zeta$ -potential of zero.

#### 2.3.4.6 Colour measurement

The colour of gelatin solutions (6.67% w/v) was measured using a CIE colourimeter (Color Flex, Hunter Lab Inc., Reston, VA, USA).  $L^*$ ,  $a^*$  and  $b^*$  parameters, indicating lightness or brightness, redness or greenness and yellowness or blueness, respectively, were recorded. The colourimeter was calibrated with a white standard.

#### 2.3.4.7 Determination of gel strength

Gels of gelatin were prepared by the method of Fernandez-Diaz *et al.* (2001) with a slight modification. Gelatin samples were dissolved in distilled water at 60 °C to obtain the final concentration of 6.67% (w/v). The solution was stirred until the gelatin was solubilised completely and cooled in a refrigerator at 10 °C for 16-18 h for gel maturation. The pH values of gelatin solutions were 5.64, 4.98, 4.74 and 4.68 for G50, G60, G70 and G80, respectively. The dimensions of the sample were 3 cm in diameter and 2.5 cm in height. The gel strength of the sample gels prepared at 10 °C was determined using a Model TA-XT2 Texture Analyser (Stable Micro System, Surrey, UK) with a load cell of 5 kN and equipped with a 1.27 cm diameter flat faced cylindrical Teflon<sup>®</sup> plunger. The maximum force (in grams) was recorded when the penetration distance reached 4 mm. The speed of the plunger was 0.5 mm/s.



### 2.3.4.8 Determination of emulsifying properties

Emulsion activity index (EAI) and emulsion stability index (ESI) of gelatin samples were determined according to the method of Pearce and Kinsella (1978) with a slight modification. Soy bean oil (2 ml) and gelatin solution (1, 2 or 3% gelatin, 6 ml) were homogenised using a homogeniser (Model T25 basic; IKA Labortechnik, Selangor, Malaysia) at a speed of 20,000 rpm for 1 min. Emulsions were pipette out at 0 and 10 min and 100-fold diluted with 0.1% SDS. The mixture was mixed thoroughly for 10 s using a vortex mixer (Scientific Industries, Inc., Bohemia, NY, USA).  $A_{500}$  of the resulting dispersion was measured using a spectrophotometer (Model UV-1800, Shimadzu, Kyoto, Japan). EAI and ESI were calculated by the following formulae (Ahmad & Benjakul, 2011):

$$EAI (m^2/g) = (2 \times 2.303 \times A \times DF) / l\phi C$$

where,  $A = A_{500}$ , DF = dilution factor (100),  $l$  = path length of cuvette (m),  $\phi$  = oil volume fraction and  $C$  = gelatin concentration in aqueous phase ( $g/m^3$ )

$$ESI (min) = A_0 / (A_0 - A_{10}) \times \Delta t$$

where,  $A_0 = A_{500}$  at time of 0 min;  $A_{10} = A_{500}$  at time of 10 min and  $\Delta t = 10$  min.

### 2.3.4.9 Determination of foaming properties

Foam expansion (FE) and foam stability (FS) of gelatin sample solutions were determined as described by Shahidi *et al.* (1995) with a slight modification. Gelatin solution (1, 2 or 3%) was transferred into 100 ml cylinders. The solution was homogenised at a speed of 13,400 rpm for 1 min at room temperature. The sample was allowed to stand for 0 and 60 min. FE and FS were then calculated using the following equations:

$$FE (\%) = (V_T/V_0) \times 100$$

$$FS (\%) = (V_t/V_0) \times 100$$

where,  $V_T$  = total volume after whipping;  $V_0$  = the original volume before whipping and  $V_l$  = total volume after leaving at room temperature for 60 min.

### **2.3.5 Statistical analyses**

All experiments were performed in triplicates (n=3) and a completely randomised design (CRD) was used. Analysis of variance (ANOVA) was performed and the mean comparisons were done by Duncan's multiple range tests (Steel and Torrie, 1980). Data are presented as mean  $\pm$  standard deviation and the probability value of  $P < 0.05$  was considered as significant. Statistical analysis was performed using the Statistical Package for Social Sciences (SPSS 17.0 for windows, SPSS Inc., Chicago, IL, USA).

## **2.4 Results and discussion**

### **2.4.1 Yield and proximate composition**

Yield of gelatin extracted at different temperatures from the skin of splendid squid is shown in Table 10. Increasing yield was obtained when extraction temperatures increased ( $P < 0.05$ ). Yield of 8.8%, 21.8%, 28.2%, and 45.3% (on dry weight basis) was found for G50, G60, G70, and G80, respectively. Yield of gelatin from the skin of giant squid was 7.5% (Uriarte-Montoya *et al.*, 2011). Gomez-Guillen *et al.* (2002) reported that the extraction of gelatin from the skin of squid, *D. gigas* at 45 °C was not possible. Even at high temperature (80 °C), very low yield was gained (2.6%). Jamilah and Harvinder (2002) stated that the difference in gelatin recovery from different species could be attributed to the intrinsic characteristics of the skin and collagen molecules, the collagen content, the amount of soluble components in the skins, the loss of extracted collagen through leaching during the series of washing steps or to an incomplete collagen hydrolysis. The degree of conversion of collagen into gelatin depends on the processing parameters (temperature, extraction time and pH), the pretreatment conditions, and the properties and the preservation method of the starting raw material (Karim and Bhat, 2009). The increasing temperature directly provided more energy to disrupt bondings stabilising the collagen structures as well as

peptide bonds of  $\alpha$ -chains. As a result, a larger amount of gelatin could be extracted as the temperature was elevated.

**Table 10.** Extraction yield, proximate composition, colour and gel strength of gelatin from the skin of splendid squid extracted at different temperatures

Parameters	G50	G60	G70	G80
Yield (%)	8.8±0.53d	21.8±0.94c	28.2±0.70b	45.3±1.35a
Moisture (%)	10.50±0.14a	11.09±0.16a	8.84±0.84b	8.63±1.16b
Protein (%)	89.05±0.11a	87.57±0.56b	89.52±0.52a	89.03±0.36a
Fat (%)	0.22±0.01c	0.31±0.02a	0.27±0.01b	0.24±0.01bc
Ash (%)	0.17±0.01c	0.54±0.02b	0.68±0.01a	0.54±0.03b
<i>L</i> *	1.70±0.14a	1.28±0.04b	0.93±0.02c	0.10±0.14d
<i>a</i> *	5.06±0.12d	6.40±0.06c	8.58±0.45b	9.03±0.00a
<i>b</i> *	1.53±0.07d	2.27±0.17c	2.78±0.03b	3.05±0.07a
Gel strength (g)	132±3.32a	122±0.99b	116±8.75c	85±3.75d

g: Maximum force in grams

Mean±SD (n=3). Different lower case letters in the same row indicate significant differences (P<0.05).

Gelatin from splendid squid skin had high protein content (~90%) with low fat (0.22-0.31%) and ash (0.17-0.68%) contents. Similar results were observed for cuttlefish (*Sepia officinalis*) skin gelatin (6.48% moisture, 91.35% protein, 0.28% fat and 0.046% ash) (Balti *et al.*, 2011) and giant squid (*D. gigas*) skin gelatin (10.2% moisture, 88% protein and 0.9% ash) (Uriarte-Montoya *et al.*, 2011). In general, recommended moisture content of edible gelatin is less than 15% (GME, 2005). Moisture content of freeze-dried gelatin from the skin of splendid squid ranged from 8.6 to 11%. In addition, gelatins from splendid squid skin contained lower ash content than the recommended maximum value (2.6%) (Jones, 1977) and the limit given for

edible gelatin (2%) (GME, 2005). Therefore, gelatin extracted was rich in protein with low content of ash and fat, revealing the efficient process in gelatin extraction.

#### **2.4.2 Protein patterns and free amino group content**

Protein patterns of gelatin extracted at different temperatures from the skin of splendid squid are shown in Figure 10a. Gelatin had  $\alpha$ -chain with a MW of 123 kDa as the major protein. The  $\alpha$ -chain was predominant in G50 and G60. The decreasing  $\alpha$ -chain band intensity was observed in G70 and G80. Among all gelatin samples, G80 possessed the lowest  $\alpha$ -chain band intensity. Slightly higher band intensity of  $\beta$ -chain was also found in G50 and G60, compared with that of G70 and G80. Therefore, sufficiently high temperature used in gelatin extraction more likely caused the hydrolysis of  $\alpha$ - and  $\beta$ -chains. A strong decrease in the percentage of  $\beta$ -chain was observed for giant squid skin gelatin extracted at higher temperature (80 °C) (Gomez-Guillen *et al.*, 2002). Extraction temperatures played a major role in protein components of resulting gelatin. Nevertheless, very high molecular-weight polymers, plausibly residual heat-stable cross-links, were present in all gelatins. Gelatin from the skin of cuttlefish (Balti *et al.*, 2011) and squid (Gimenez *et al.*, 2009c) had the higher content of hydroxylysine residues (14-17 residues/1000 residues) than fish skin gelatin (5-6 residues/1000 residues) (Jongjareonrak *et al.*, 2010; Kittiphattanabawon *et al.*, 2010b). Gelatins with higher content of  $\alpha$ -chain were reported to possess better functional properties including gel strength, emulsifying and foaming properties (Gomez-Guillen *et al.*, 2002). In general, the formation of peptide fragments is associated with lower viscosity, low melting point, low setting point, high setting time, as well as decreased bloom strength of gelatin (Muyonga *et al.*, 2004b). Result revealed that G70 and G80, which were extracted at higher temperature, had the shorter chains as indicated by lower content of  $\alpha$ -chain and  $\beta$ -chain. This molecular characteristic contributed to their functional properties.

The thermal degradation of gelatin extracted at different temperatures from the skin of splendid squid expressed as free amino group is depicted in Fig. 10b.

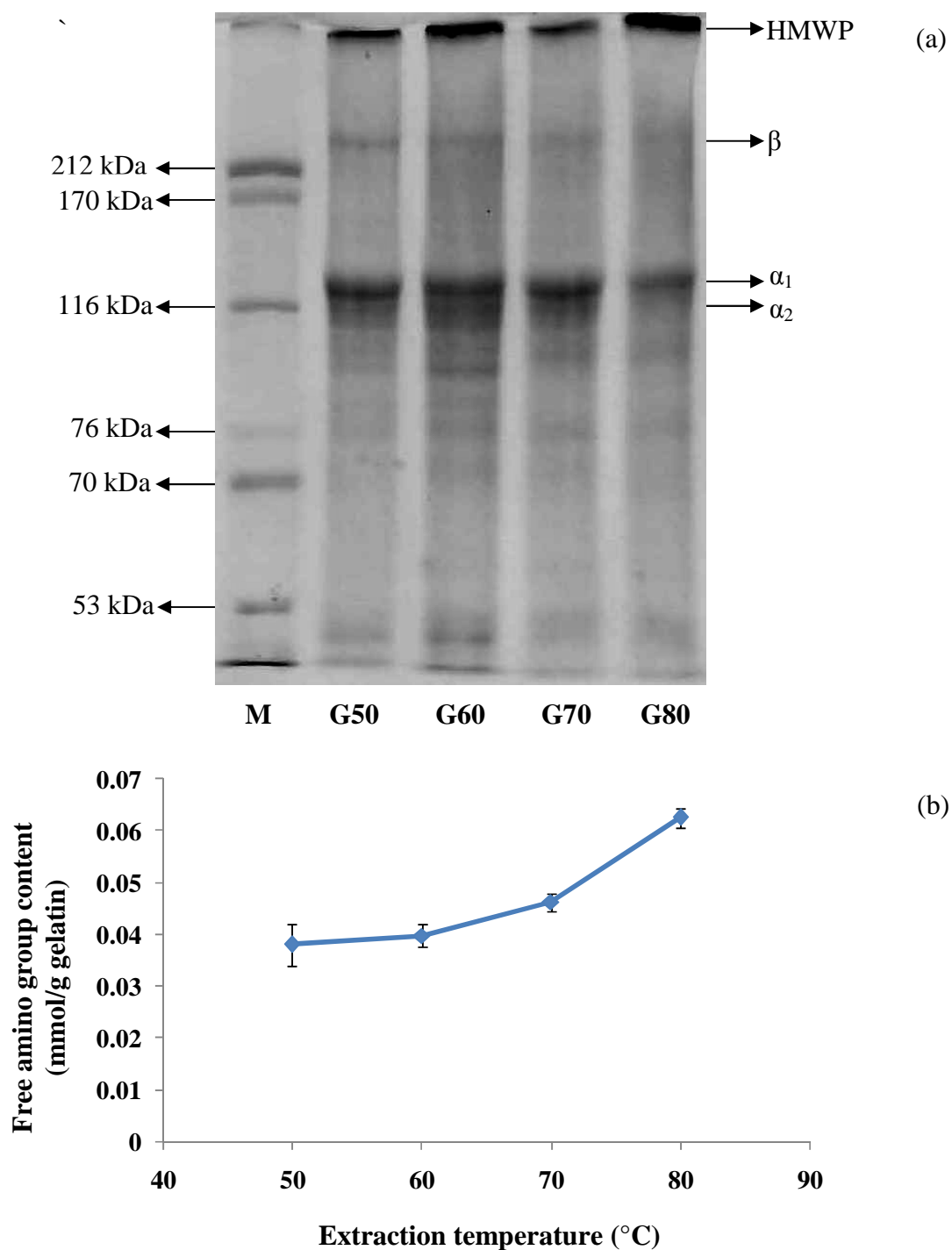


**Figure 10.** Protein patterns (a) and free amino group content (b) of gelatins from the skin of splendid squid extracted at different temperatures. M: High molecular weight markers. G50, G60, G70 and G80 denote the gelatins extracted at 50, 60, 70 and 80 °C, respectively. HMWP: High molecular weight proteins. Bars represent the standard deviation (n=3).

Thermal degradation of gelatins increased with increasing extraction temperatures ( $P < 0.05$ ). The highest degradation of gelatin was observed at  $80^{\circ}\text{C}$  ( $P < 0.05$ ). The result was in agreement with the highest degradation of  $\beta$ -chain and  $\alpha$ -chain in G80 (Figure 10a). The result reconfirmed that high temperature caused the hydrolysis of collagenous proteins, leading to the increasing free amino group (Figure 10b) with the decrease in major proteinaceous compound ( $\alpha$ -chain and  $\beta$ -chain) in the extracted gelatin. As a result, shorter chains were formed (Figure 11).

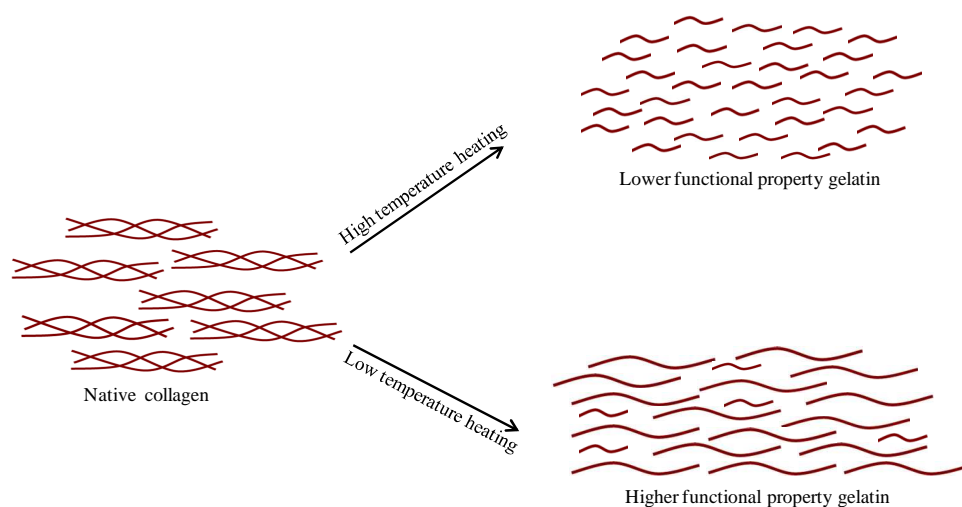


**Figure 11.** Proposed scheme for gelatin extraction from squid skin at low and high temperatures.

### 2.4.3 Amino acid composition

Amino acid composition of gelatins extracted at different temperatures from the skin of splendid squid is shown in Table 11. The properties of gelatin are largely influenced by the amino acid composition and their molecular weight distribution (Gomez-Guillen *et al.*, 2009). Glycine was the predominant amino acid in all gelatin samples, ranging from 339 to 367 residues/1000 residues. This implied that gelatin obtained was derived from its mother collagen. Collagen consists of one-third glycine in its molecule (Balti *et al.*, 2011). It was noted that G70 and G80 had the higher glycine content than G50 and G60. The higher glycine in G70 and G80 might be caused by free glycine, which was released to a high extent during extraction at high temperatures. Hydrolysis was taken place at a high degree at high temperature

(Figure 10b.) Proline and hydroxyproline constituted 96-99 and 58-86 residues/1000 residues, respectively. Imino acids (proline and hydroxyproline) play a role in gelation of gelatin (Ahmad and Benjakul, 2011). For hydroxyproline, G70 and G80 (58 residues/1000residues) had much lower content than G50 and G60 (82-86

**Table 11.** Amino acid composition of gelatin from the skin of splendid squid extracted at different temperatures

Amino acids	Number of residues/ 1000 residues			
	G50	G60	G70	G80
Hydroxyproline	82	86	58	58
Aspartic acid/asparagine	61	60	62	61
Threonine	23	23	23	24
Serine	37	33	34	34
Glutamic acid/glutamine	82	82	83	82
Proline	97	98	99	96
Glycine	339	339	360	367
Alanine	92	89	87	86
Cysteine	1	0	0	0
Valine	24	25	24	24
Methionine	14	14	14	14
Isoleucine	18	19	18	17
Leucine	27	28	28	28
Tyrosine	6	5	6	6
Phenylalanine	10	10	10	11
Hydroxylysine	17	18	18	17
Histidine	5	5	6	6
Arginine	53	54	57	56
Lysine	12	12	12	12
<b>Total</b>	<b>1000</b>	<b>1000</b>	<b>1000</b>	<b>1000</b>
Imino acids	179	184	157	154

residues/1000 residues). In general, Gly-X-Y sequence has been found in collagen molecule, where hydroxyproline is located at only Y position. Hydroxyproline content was generally lower in gelatin extracted at 70 and 80 °C. Gelatin from giant squid (*D. gigas*) contained 16-17% imino acid (Gimenez *et al.*, 2009c; Gomez-Guillen *et al.*, 2002). The stability of the triple helical structure in renatured gelatins has been reported to be proportional to the total content of imino acids. Hydroxyproline plays a key role in the stabilisation of the triple-stranded collagen helix due to its hydrogen bonding ability through its hydroxyl group.

Alanine (86-92 residues/1000 residues) was found at high content. Alanine plays a role in viscoelastic property of gelatin (Gimenez *et al.*, 2005b). Glutamic acid/glutamine and aspartic acid/asparagine were also found at high level. Tyrosine, phenylalanine, histidine and lysine were present in all gelatins at low levels. No cysteine or negligible amount of cysteine was found in all gelatins. The cysteine (1 residue/1000 residues) in G50 might be contaminated from other proteins containing cysteine in skin. Cysteine does not take part in the structure of type I collagen (Morales *et al.*, 2000). The presence of cysteine in the amino acid composition could indicate that gelatin might contain a small quantity of stroma protein, such as elastin, which is highly insoluble and unusually stable in salt (Kim and Park, 2005). Therefore, amino acid composition of gelatin was governed by extraction temperature. The amino acid composition could have the impact on functional properties of gelatin extracted.

#### **2.4.4 ATR-FTIR spectra**

FTIR spectra of gelatin extracted at different temperatures from the skin of splendid squid are depicted in Figure 12. FTIR spectroscopy has been used to monitor the functional groups and secondary structure of gelatin (Muyonga *et al.*, 2004c). All gelatin samples had the major peaks in amide region. G50, G60, G70 and G80 exhibited the amide-I bands at the wavenumber of 1632.88, 1634.24, 1635.30, and 1633.49  $\text{cm}^{-1}$ , respectively. Amide-I represent C=O stretching/hydrogen bonding coupled with COO. The absorption in the amide-I region is probably the most useful for infrared spectroscopic analysis of the secondary structure of proteins (Bandekar,



1992; Benjakul *et al.*, 2009; Surewich and Mantsch, 1988). Its exact location depends on the hydrogen bonding and the conformation of protein structure (Uriarte-Montoya *et al.*, 2011). In the present study, the amide-I peak was observed in the range of 1632-1635  $\text{cm}^{-1}$ , which was in agreement with Yakimets *et al.* (2005) who stated that the absorption peak at 1633  $\text{cm}^{-1}$  was characteristic of the coiled structure of gelatin.

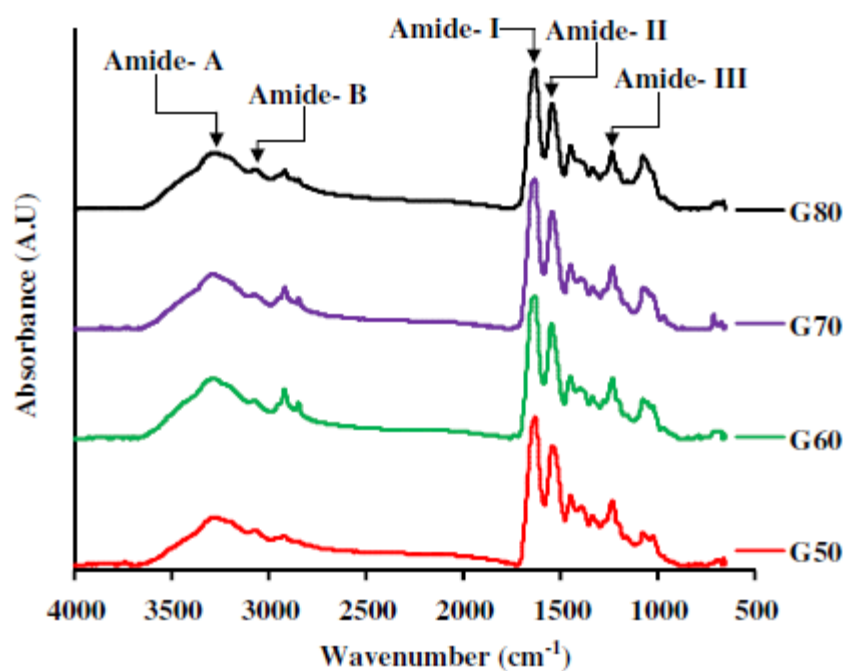


**Figure 12.** ATR-FTIR spectra of gelatins from the skin of splendid squid extracted at different temperatures.

The characteristic absorption bands of G50, G60, G70 and G80 in amide-II region was noticeable at the wavenumber of 1541.57, 1551.38, 1545.93 and 1547.21  $\text{cm}^{-1}$ , respectively. Amide-II arises from bending vibration of N–H groups and stretching vibrations of C–N groups. In addition, amide-III was detected around the wavenumber of 1235.79, 1236.67, 1236.17 and 1236.86  $\text{cm}^{-1}$  for G50, G60, G70 and G80, respectively. The amide-III represents the combination peaks between C–N stretching vibrations and N–H deformation from amide linkages as well as absorptions arising from wagging vibrations from  $\text{CH}_2$  groups from the glycine backbone and proline side-chains (Jackson *et al.*, 1995). G80 had the lowest amplitude, whereas G50 exhibited the highest amplitude at amide-III region. This

indicated that the greater disorder of molecular structure due to transformation of an  $\alpha$ -helical to a random coil structure occurred during heating and these changes were associated with loss of triple-helix state as a result of denaturation of collagen to gelatin (Muyonga *et al.*, 2004c). G70 had higher amplitudes at wave numbers of 1204.73, 1079.45, 1060.63, 1036.46, 970.78 and 713.04  $\text{cm}^{-1}$  (Figure 12). These bands were associated with the C-O stretching vibrations of the short peptide chains (Jackson *et al.*, 1995). The result reconfirmed the higher degradation of gelatin extracted at higher temperatures.

Amide-A band, arising from the stretching vibrations of the N-H group, appeared at 3274.68, 3293.56, 3292.76 and 3275.87  $\text{cm}^{-1}$  for G50, G60, G70 and G80, respectively. Amide-A represents NH-stretching coupled with hydrogen bonding. Normally, a free N-H stretching vibration is found in the range of 3400–3440 $\text{cm}^{-1}$  (Muyonga *et al.*, 2004c). When the N-H group of a peptide is involved in a hydrogen bond, the position shifts to lower frequencies (Doyle *et al.*, 1975). In amide-A region, the lower wavenumber was found in G50 suggesting the hydrogen bonding involvement of an N-H group in  $\alpha$ -chain. In addition, the lower wavenumber with the concomitantly higher amplitude of amide-A observed in G80 would associate with the degradation of gelatin, providing greater free amino groups. These degraded gelatins might undergo hydrogen bonding interaction, resulting in decreased wavenumber of amide-A. The amide-B was observed in 3087.81, 3082.07, 3080.07 and 3078.07  $\text{cm}^{-1}$  for G50, G60, G70 and G80, respectively, corresponding to the asymmetric stretching vibration of  $=\text{C}-\text{H}$  as well as  $-\text{NH}_3^+$ . Among all samples, G70 and G80 showed the lowest wavenumber of amide-B peak, suggesting the interaction of  $-\text{NH}_3$  group between peptide chains (Ahmad and Benjakul, 2011). For G50, G60, G70 and G80, the peaks were observed at the wavenumber of 2848.93, 2850.85, 2850.73 and 2850.96 (symmetrical) or 2919.42, 2920.87, 2920.95 and 2921.52 (asymmetrical), respectively. It represents C-H stretching vibrations of the  $-\text{CH}_2$  groups (D' Souza *et al.*, 2008). Thus, it can be concluded that the secondary structure and functional group of gelatins obtained from the skin of splendid squid was affected by extraction temperature.

### 2.4.5 $\zeta$ -potential

The  $\zeta$ -potential values of gelatin extracted at different temperatures from the skin of splendid squid (G50, G60, G70, and G80) were measured as a function of pH as shown in Figure 13. All gelatin samples were positively charged at acidic pH ranges and become negatively charged under alkaline conditions. At the same pH tested, varying  $\zeta$ -potential values were observed, suggesting the differences in amino acid composition among the samples (Table 11). The net charge of zero was obtained at pH 6.84, 5.94, 5.49 and 4.86 for G50, G60, G70 and G80, respectively.

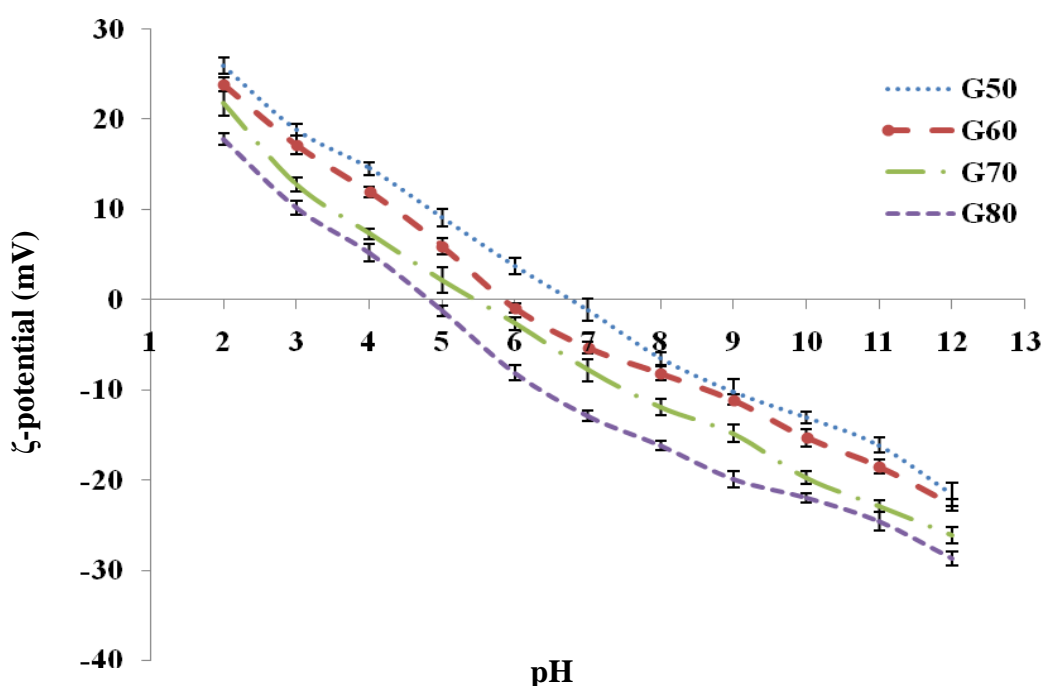


**Figure 13.**  $\zeta$ -potential of gelatins from the skin of splendid squid extracted at different temperatures. Bars represent the standard deviation (n=3).

Protein molecules in an aqueous system have zero net charge at their isoelectric points (pI), in which the positive charges are balanced out by the negative charges (Bonner, 2007). In general, the amount of acidic amino acids (glutamic acid and aspartic acid) was higher than that of basic amino acids (lysine and arginine) (Table 11). With increasing temperature, deamidation might take place, in which glutamic and aspartic acid could be formed. High contents of glutamic and aspartic acid were also reported

for gelatin from cuttlefish (*S. officinalis*) skin and giant squid (*D. gigas*) skin (Balti *et al.*, 2011; Gimenez *et al.*, 2009c). Differences in charge characteristics/distributions more likely determined functional properties of different gelatin extracted with varying temperatures.

#### **2.4.6 Colour**

Differences in colour were observed between the solutions (6.67%) of gelatins extracted at different temperatures (Table 10). Gelatin extracted at lower temperatures (G50 and G60) showed the higher  $L^*$  - value (lightness) than others (G70 and G80). The higher redness ( $a^*$ - value) and yellowness ( $b^*$ - value) were found in the latter ( $P < 0.05$ ). The changes in colour of gelatin increased with increasing temperatures. It indicated that lightness of gelatin decreased with concomitant increases in redness and yellowness when the extraction temperature increased. Higher temperatures more likely induced non-enzymatic browning reaction to a higher extent (Ajandouz and Puigserver, 1999). Since higher temperature extractions yielded the resulting gelatin with higher free amino group caused by higher hydrolysis, those amino groups could undergo browning reaction along with carbonyl compounds in the skin. As a result, the increases in yellowness and redness were found in gelatin extracted at higher temperatures. Furthermore, the higher temperature could lead to the higher extraction efficiency as indicated by higher extraction yield. Simultaneously, pigments retained after bleaching of skins could be co-extracted into gelatin. As a consequence, gelatin turned to be darker with higher yellowness or redness in colour. The result indicated that extraction temperature directly had the impact on colour of gelatin extracted from the skin of splendid squid.

#### **2.4.7 Gel strength**

Gel strength is one of the most important functional properties of gelatin. Gel strength of gelatin extracted at different temperatures from the skin of splendid squid, after 16-18 h maturation at 10 °C, is presented in Table 10. G50, G60, G70 and G80 had the gel strength of 132, 122, 116 and 85 g, respectively. G80 showed the lowest gel strength ( $P < 0.05$ ). The difference in gel strength between the

samples could be due to the differences in intrinsic characteristics, such as molecular-weight distribution and amino acid composition. Protein degradation fragments may reduce the ability of  $\alpha$ -chains to anneal correctly by hindering the growth of the existing nucleation sites (Ledward, 1986). The longer chains in G50 and G60 could undergo aggregation to form gel network more effectively than G70 and G80.  $\alpha$ -chain and  $\beta$ -chain at the higher amount in G50 and G60 might form the stronger gel network than  $\alpha$ -chain at the lower amount found in G70 and G80. Additionally, it was noted that G70 and G80 had the lower imino acid content, especially hydroxyproline content (Table 11). Proline and hydroxyproline are thought to be responsible for the stability of the triple-helix of collagen structure through hydrogen bonding between free water molecules and the hydroxyl group of the hydroxyproline in gelatin (Fernandez-Diaz *et al.*, 2001).

The lower content of proline and hydroxyproline generally gives fish gelatin a low gel modulus, and low gelling and melting temperatures (Balti *et al.*, 2011). Lower hydroxyproline content in gelatin extracted at higher temperature (G70 and G80) might result in the lower gel strength, compared to gelatin extracted at lower temperatures (G50 and G60) (Table 10). The super-helix structure of the gelatin gel, which is critical for the gel properties, is stabilised by steric restrictions. These restrictions are imposed by both the pyrrolidine rings of the imino acids in addition to the hydrogen bonds formed between amino acid residues (Sikorski, 2001).

Squid skin gelatin which was extracted at higher temperature (80 °C) also had the lower gel strength than sole, megrim, cod and hake gelatins which were extracted at lower temperature (45 °C) (Gomez-Guillen *et al.*, 2002). The gelling strength of commercial gelatins ranges from 100 to 300, but gelatins with bloom values of 250-260 are the most desirable (Holzer, 1996). Different gel strength was reported for gelatin from skin of different species including cuttlefish (181 g) (Balti *et al.*, 2011), Atlantic salmon (108 g), cod (71 g) (Arnesen and Gildberg, 2007), sin croaker (125 g), shortfin scad (177 g) (Cheow *et al.*, 2007), bigeye snapper (105.7 g), brownstripe red snapper (218.6 g) (Jongjareonrak *et al.*, 2006a), young and adult Nile perch (217 g and 240 g, respectively) (Muyonga *et al.*, 2004b).

#### 2.4.8 Emulsifying properties

Emulsion activity index (EAI) and emulsion stability index (ESI) of gelatin extracted at different temperatures from the skin of splendid squid are shown in Table 12. EAI of all gelatin samples decreased as the concentration of gelatin increased ( $P < 0.05$ ). Ahmad and Benjakul (2011) also reported that EAI of unicorn leather jacket skin gelatin decreased when the concentration increased. A decrease in emulsifying ability with increasing protein concentration has been reported for gelatin hydrolysates of sole and squid (Gimenez *et al.*, 2009c) and other fish proteins such as round scad protein hydrolysates (Thiansilakul *et al.*, 2007). At a level of 1%, EAI decreased when the extraction temperatures increased ( $P < 0.05$ ). However, no difference was found between G60 and G70 ( $P > 0.05$ ). Gelatins extracted at lower temperatures (G50 and G60) had higher EAI than those extracted at higher temperatures (G70 and G80) when tested at a level of 2%. G70 showed the lowest EAI when the concentration of 3% was used ( $P < 0.05$ ). At high concentration, gelatin with higher hydrophilicity in nature might interact with each other, thus lesser amount of gelatin were available to be localised at the oil-water interface. Properties of protein-stabilised emulsions are affected by temperature. Heat denaturation that is sufficient to cause insolubilisation impairs emulsifying properties of proteins (Damodaran, 1997). With increasing degradation, peptides with the shorter chain possessing more hydrophilicity were preferably localised in aqueous phase. As a result, oil droplets were less stabilised by gelatin films (Ahmad and Benjakul, 2011). This led to the lower EAI of gelatin extracted at higher temperature with the shorter chain length. ESI of all gelatin samples increased with increasing concentration ( $P < 0.05$ ). Protein at high concentrations facilitated more protein adsorption at interfaces (Yamauchi *et al.*, 1980). At the same concentration tested, the decrease in ESI was found ( $P < 0.05$ ) when the extraction temperature increased. Long chains were able to form the stronger and stiffer films surrounding oil droplets, thereby increasing the stability toward emulsion collapse.

**Table 12.** Emulsifying and foaming properties of gelatin from the skin of splendid squid extracted at different temperatures

Samples	Gelatin Conc. (%)	EAI (m <sup>2</sup> /g)	ESI (%)	FE (%)	FS (%)
G50	1	35.10±0.44Aa	14.46±0.14Ac	131.66±2.88Ac	116.77±2.90Ac
	2	16.85±0.03Bb	18.35±0.58Ab	158.33±2.88Ab	145.0±5.0Ab
	3	12.59±0.58Ac	26.55±2.06Aa	206.66±5.77Aa	161.66±2.90Aa
G60	1	32.95±0.07Ba	14.34±0.41Ac	130.0±5.0Ac	115.0±5.0Ac
	2	17.59±0.08Ab	17.22±0.43Bb	158.33±7.63Ab	140.0±10.0Ab
	3	13.15±0.96Ac	24.26±1.05Ba	188.33±7.63Ba	160.0±0.0Aa
G70	1	32.21±0.09Ba	13.80±0.04Bc	125.0±5.0Ac	106.66±5.77ABc
	2	15.40±0.11Cb	14.86±0.37Cb	156.66±5.77Ab	138.33±2.88Ab
	3	11.52±0.24BCc	23.60±0.18Ba	173.33±5.77Ca	151.66±2.88ABa
G80	1	29.77±1.22Ca	12.67±0.26Cb	116.66±5.77Bc	100.0±10.0Bb
	2	15.55±0.27Cb	13.25±0.18Db	138.33±2.88Bb	118.33±2.88Bb
	3	12.23±0.25ABc	16.10±0.49Ca	175.0±5.0Ca	146.66±14.43Ba

Mean ± SD (n=3).

Different uppercase letters in the same column within the same concentration indicate significant differences (P<0.05).

Different lowercase letters in the same column within the same gelatin sample indicate significant differences (P<0.05).

EAI: Emulsion activity index; ESI: Emulsion stability index.

FE: Foam expansion; FS: Foam stability.

#### 2.4.9 Foaming properties

Foam expansion (FE) and foam stability (FS) of gelatin extracted at different temperatures from the skin of splendid squid are shown in Table 12. Foam formation is generally controlled by transportation, penetration and reorganisation of protein molecules at the air–water interface (Halling, 1981). A protein must be capable of migrating rapidly to the air–water interface, unfolding and rearranging at the interface to express good foaming ability (Halling, 1981). FE and FS of all gelatin samples generally increased with increasing gelatin concentrations ( $P < 0.05$ ). Foams with higher concentration of proteins were denser and more stable because of an increase in the thickness of interfacial films (Zayas, 1997). The foam forming ability of proteins is related to their film-forming ability at air–water interface. In general, proteins, which rapidly adsorb at the newly-created air–liquid interface during bubbling and undergo unfolding and molecular rearrangement at the interface, exhibit better foaming ability than proteins that adsorb slowly and resist unfolding at the interface (Damodaran, 1997). FS is directly affected by protein concentration, which influences the thickness, mechanical strength and cohesiveness of the film (Zayas, 1997). The stability of foams depends on various parameters, such as the rate of attaining equilibrium surface tension, bulk and surface viscosities, steric stabilisation, and electrical repulsion between the two sides of the foam lamella (Liu *et al.*, 2003). At the same concentrations used, gelatin extracted at higher temperature had the lower foam expansion and foam stability than those extracted at lower temperature. Ahmad and Benjakul (2011) reported that low molecular weight peptides could not form a well-ordered film at the interface, resulting in poor foaming properties. Foaming properties of protein solutions were generally positively correlated with MW of peptides (Balti *et al.*, 2011; Van der Ven *et al.*, 2002). When the gelatin at levels of 1 and 2% was used, G80 showed the lowest foam expansion ( $P < 0.05$ ). However, G50 had the highest foam expansion when tested at a level of 3% ( $P < 0.05$ ). Gelatin with the less degradation and longer chain length more likely formed the stronger films surrounding the air bubbles, especially when the sufficient concentration was used. Similar result was found for foam stability. Thus, extraction temperature played a crucial role in foaming properties of gelatin from the skin of splendid squid.



## **2.5 Conclusion**

Gelatin from the skin of splendid squid extracted at different temperatures had different characteristics and functional properties. Although higher temperature resulted in the increasing yield, it lowered functional properties of resulting gelatin, mostly governed by the chain length, amino acid composition as well as molecular conformation and interaction. Additionally, higher extraction temperature resulted in the darker colour of gelatin. Therefore, the skin of squid could serve as raw material for gelatin extraction when the extraction at appropriate temperature was implemented.

## CHAPTER 3

### PROPERTIES OF FILM FROM SPLENDID SQUID (*LOLIGO FORMOSANA*) SKIN GELATIN WITH VARIOUS EXTRACTION TEMPERATURES

#### 3.1 Abstract

Properties of film from splendid squid (*Loligo formosana*) skin gelatin extracted at different temperatures (50-80 °C) were investigated. Tensile strength (TS) and elongation at break (EAB) of films decreased, but water vapour permeability (WVP) increased ( $P < 0.05$ ) as the extraction temperature increased. Increase in transparency value with coincidental decrease in lightness was observed with increasing extraction temperatures. Electrophoretic study revealed that degradation of gelatin became more pronounced with increasing extraction temperatures. As a consequence, their corresponding films had the lower mechanical properties. FTIR spectra of obtained gelatin films revealed the significant loss of molecular order of the triple helix. Thermogravimetric analysis indicated that F80 exhibited the higher heat susceptibility and weight loss. Loosen structure was observed in film prepared from gelatin with increasing extraction temperatures. Thus, the temperature used for gelatin extraction from splendid squid skin directly affected the properties of corresponding films.

#### 3.2 Introduction

Nowadays, biodegradable films have known as important eco-friendly packaging materials to reduce plastic wastes (Hoque *et al.*, 2010; Gomez-Guillen *et al.*, 2009). Most synthetic films are non-biodegradable and may cause environmental pollution and serious ecological problems. Biodegradable films were made from renewable biopolymers such as proteins, lipids and polysaccharides (Tharanathan, 2003). Gelatin has been proven as the potential biopolymer and has been extensively studied for its film-forming capacity and applicability as an outer covering to protect

foods (Gomez-Guillen *et al.*, 2009). Gelatins from aquatic animals are gaining increasing attention due to health issues and religious constraints of mammalian counterpart (Hoque *et al.*, 2011a). Because of their good film-forming abilities, fish gelatins may be a good alternative to synthetic plastics for making films to preserve foodstuffs (Gomez-Guillen *et al.*, 2009). Owing to the superior oxygen barrier property, fish gelatin based film could prevent the lipid oxidation in food systems. Additionally, it can be used as the smart packaging, in which the antioxidants or antimicrobials can be incorporated (Jongjareonrak *et al.*, 2008). However, gelatin has the hydrophilicity in nature and the film from gelatin generally shows low water vapour barrier property. Also, the gelatin film has the relatively poor mechanical properties, in comparison with traditional synthetic polymeric films (McHugh and Krochta, 1994). This more likely leads to the limitation for commercial uses.

Squid and cuttlefish have become the important fishery products in Thailand as well as other Southeast Asian countries, and are mainly exported worldwide (Hoque *et al.*, 2011d). During processing, skin is generated as a by-product with the low market value and it can create serious ecological problems and environmental pollution. Squid and cuttlefish skins are rich in collagen and can be used for gelatin extraction (Brinckmann, 2005; Aewsiri *et al.*, 2011; Uriarte-Montoya *et al.*, 2011; Gimenez *et al.*, 2009a). Gelatins from fish and cuttlefish skin have been demonstrated to render the biodegradable films with the superior UV barrier properties (Houque *et al.*, 2011a; Rattaya *et al.*, 2009).

Owing to the abundance of squid skin in Thailand, it can be used for gelatin extraction and film formation. However, very low yield of gelatin (2.6%) was obtained from skin of giant squid, *Dosidicus gigas* (Gomez-Guillen *et al.*, 2002). Increasing extraction temperatures might be an effective means to increase the yield, mainly due to the enhanced energy for disruption of bonds stabilising the mother collagen in skin matrix. Nevertheless, the functional properties and film-forming ability can be affected differently. Therefore, this study aimed to investigate film-forming ability and film properties of gelatin extracted at different temperatures from the skin of splendid squid (*Loligo formosana*).

### **3.3 Materials and methods**

#### **3.3.1 Chemicals**

2,4,6-Trinitrobenzenesulphonic acid (TNBS), sodium sulphite, L-leucine, bovine serum albumin (BSA) and  $\beta$ -mercaptoethanol ( $\beta$ -ME) were obtained from Sigma Chemical Co. (St. Louis, MO, USA). High molecular weight protein marker (53 kDa to 220 kDa) was purchased from GE Healthcare UK (Buckinghamshire, UK). Glycerol, acetic acid and phosphoric acid were procured from Merck (Darmstadt, Germany). Sodium dodecyl sulphate (SDS), Coomassie Blue R-250 and *N,N,N',N'*-tetramethyl ethylene diamine (TEMED) were obtained from Bio-Rad Laboratories (Hercules, CA, USA).

#### **3.3.2 Collection and preparation of squid skin**

The outer skin of fresh squid (*Loligo formosana*) was obtained from Sea Wealth Frozen Food Co., Ltd., Songkhla, Thailand and stored in ice using a skin/ice ratio of 1:2 (w/w). Upon arrival to the Department of Food Technology, Prince of Songkla University, Hat Yai, Thailand, the skin was cleaned and washed with iced tap water (0-2 °C). Skin contained 83% of moisture, 14% of protein, 1.1% of ash and 1.5% of fat as determined by the method of AOAC (2000). The skin was then cut into small pieces (0.5x0.5 cm<sup>2</sup>), placed in polyethylene bags and stored at -20 °C until use. The skin was stored for not more than 2 months.

#### **3.3.3 Extraction of gelatin from squid skin**

Gelatin extraction was performed following the method of Ahmad and Benjakul (2011) with a slight modification. Prior to gelatin extraction, the prepared skin was soaked in 0.05 M NaOH with a skin/solution ratio of 1:10 (w/v). The mixture was stirred continuously for 6 h at room temperature at a speed of 150 rpm using an overhead stirrer equipped with a propeller (RW 20.n, IKA-Werke GmbH & CO.KG, Staufen, Germany). The alkaline solution was changed every 90 min to remove non collagenous proteins and pigments. Alkaline-treated skin was then washed with tap water until the neutral or faintly basic pH of wash water was

obtained. The skin was then soaked in 0.05 M phosphoric acid with a skin/solution ratio of 1:10 (w/v) for 24 h with gentle stirring at 4 °C. The acidic solution was changed every 12 h to swell the collagenous material in the skin matrix. Acid-treated skin was washed thoroughly with tap water until wash water became neutral or faintly basic. To extract gelatin, the swollen skin was soaked in distilled water at different temperatures (50, 60, 70 and 80 °C) using a pretreated skin/water ratio of 1:10 (w/v) in a temperature-controlled water bath (W350, Memmert, Schwabach, Germany) for 12 h with a continuous stirring at a speed of 150 rpm. The mixture was then filtered using two layers of cheese cloth. The filtrate was further filtered using a Whatman No. 4 filter paper (Whatman International, Ltd., Maidstone, England) with the aid of JEIO Model VE-11 electric aspirator (JEIO TECH, Seoul, Korea). The resultant filtrate was freeze-dried using a Scanvac Model Coolsafe 55 freeze dryer (Coolsafe, Lyngø, Denmark). The dry gelatins extracted from skin at different temperatures were referred to as 'G50', 'G60', 'G70' and 'G80', respectively. G50, G60, G70 and G80 contained 89.05, 87.57, 89.52, and 89.03% protein, respectively as analysed by the Kjeldhal method (AOAC, 2000).

### 3.3.4 Preparation of films

Gelatin films were prepared as per the method of Jongjareonrak *et al.* (2006b) with a slight modification. Firstly, film forming solution (FFS) was prepared by mixing the freeze-dried gelatin with distilled water to obtain the protein concentration of 3% (w/v). Thereafter, glycerol (25% of protein) was added into FFS as a plasticiser. FFS was degassed using the sonicating bath (Elmasonic S 30 H, Singen, Germany) for 10 min. FFS ( $4 \pm 0.01$  g) was then cast onto a rimmed silicone resin plate ( $5 \times 5$  cm<sup>2</sup>), air-blown for 12 h at room temperature, followed by drying in an environmental chamber (Binder GmbH, Tuttlingen, Germany) at  $25 \pm 0.5$  °C and  $50 \pm 5\%$  relative humidity (RH) for 24 h. Dried film samples were manually peeled off and referred to as 'F50', 'F60', 'F70' and 'F80', respectively. All films were subjected to the analyses.

### 3.3.5 Analyses

Prior to testing, film samples were conditioned for 48 h at  $50 \pm 5\%$  relative humidity (RH) and  $25 \pm 0.5$  °C. For ATR-FTIR, SEM and TGA studies, films were conditioned in a desiccator containing dried silica gel for 3 weeks to minimise the plasticising effect of water at room temperature (28-30 °C) to obtain the most dehydrated films.

#### 3.3.5.1 Thickness

The thickness of ten film samples of each treatment was measured using a digital micrometer (Mitutoyo, Model ID-C112PM, Serial No. 00320, Mituyoto Corp., Kawasaki-shi, Japan). Ten random locations around each film sample were used for determination of thickness.

#### 3.3.5.2 Mechanical properties

Tensile strength (TS) and elongation at break (EAB) of film samples were determined as described by Iwata *et al.* (2000) using the Universal Testing Machine (Lloyd Instrument, Hampshire, UK). The test was performed in the controlled room at 25°C and  $\sim 50 \pm 5\%$  RH. Ten film samples ( $2 \times 5$  cm<sup>2</sup>) with the initial grip length of 3 cm were used for testing. The film samples were clamped and deformed under tensile loading using a 100 N load cell with the cross head speed of 30 mm/min until the samples were broken. The maximum load and the final extension at break were used for calculation of TS and EAB, respectively.

#### 3.3.5.3 Water Vapour Permeability

WVP was measured using a modified ASTM (American Society for Testing and Materials, 1989) method as described by Shiku *et al.* (2004). The film samples were sealed on an aluminum permeation cup containing dried silica gel (0% RH) with silicone vacuum grease and rubber gasket. The cups were placed at 30 °C in a desiccator containing the distilled water, followed by weighing after every 1 h intervals for up to 8 h. Five film samples were used for WVP testing. WVP of the film was calculated as follows:

$$\text{WVP (gmm}^{-2}\text{s}^{-1}\text{Pa}^{-1}) = w l A^{-1} t^{-1} (P_2 - P_1)^{-1}$$

where,  $w$  is the weight gain of the cup (g);  $l$  is the film thickness (m);  $A$  is the exposed area of film ( $\text{m}^2$ );  $t$  is the time of gain (s);  $(P_2 - P_1)$  is the vapour pressure difference across the film (Pa).

#### 3.3.5.4 Colour, light transmission and transparency

Colour of five film samples was determined using a CIE colourimeter (Hunter associates laboratory, Inc., Reston, VA, USA). Colour of the film was expressed as  $L^*$ - (lightness or brightness),  $a^*$ - (redness or greenness) and  $b^*$ - (yellowness or blueness) values. Total difference in colour ( $\Delta E^*$ ) was calculated according to the following equation (Gennadios *et al.*, 1996).

$$\Delta E^* = \sqrt{(\Delta L^*)^2 + (\Delta a^*)^2 + (\Delta b^*)^2}$$

where,  $\Delta L^*$ ,  $\Delta a^*$  and  $\Delta b^*$  are the differences between the corresponding colour parameter of the sample and that of white standard ( $L^* = 92.84$ ,  $a^* = -1.25$  and  $b^* = 0.49$ ).

Light transmission in ultraviolet (UV) and visible ranges of five film samples was measured at selected wavelengths between 200 and 800 nm, using a UV-Visible spectrophotometer (Model UV-1800, Shimadzu, Kyoto, Japan) according to the method of Jongjareonrak *et al.* (2008). The transparency value of film was calculated by the following equation (Han and Floros, 1997).

$$\text{Transparency value} = (-\log T_{600})/x$$

where,  $T_{600}$  is the fractional transmittance at 600 nm and  $x$  is the film thickness (mm). The higher transparency value represents the lower transparency of films (Hoque *et al.*, 2011d).

### 3.3.5.5 Electrophoretic analysis

SDS-polyacrylamide gel electrophoresis (SDS-PAGE) was performed by the method of Laemmli (1970). Gelatin film samples were dissolved in 5% SDS and the mixtures were incubated at 85 °C for 1 h. The mixtures were centrifuged at 3,500 xg for 5 min at room temperature using a microcentrifuge (MIK-RO20, Hettich Zentrifugan, Tuttlingen, Germany) to remove undissolved debris. Protein content in the supernatant of all samples was determined using the Biuret method (Robinson and Hogden, 1940). Gelatin film samples were mixed at a 1:1 (v/v) ratio with the sample buffer (0.5 M Tris-HCl, pH 6.8, containing 4% SDS and 20% glycerol). Samples (20 µg protein) were loaded onto polyacrylamide gels comprising a 7.5% running gel and a 4% stacking gel and subjected to electrophoresis at a constant current of 15 mA/gel using a Mini Protein II unit (Bio-Rad Laboratories, Inc., Richmond, CA, USA). After electrophoresis, the gel was stained with 0.05% (w/v) Coomassie Blue R- 250 in 15% (v/v) methanol and 5% (v/v) acetic acid and destained with 30% (v/v) methanol and 10% (v/v) acetic acid. Relative mobility ( $R_f$ ) of protein band was calculated and the molecular weight of the protein was calculated from the plot between  $R_f$  and log (MW) of standards.

### 3.3.5.6. Free amino group content

Prior to analysis, film samples were solubilised as described previously. Free amino group content in film solution was determined following the method of Benjakul and Morrissey (1997). Properly diluted samples (125 µl) were mixed thoroughly with 2.0 ml of 0.2 M phosphate buffer, pH 8.2, followed by the addition of 1.0 ml of 0.01% 2,4,6-trinitrobenzenesulfonic acid (TNBS) solution. The mixtures were then placed in a temperature controlled water bath at 50 °C for 30 min in the dark. The reaction was terminated by adding 2.0 ml of 0.1 M sodium sulphite. The mixtures were cooled down at room temperature for 15 min. The absorbance was measured at 420 nm using a spectrophotometer and the free amino group content was expressed in terms of L-leucine.



### **3.3.5.7 Attenuated total reflectance-Fourier transform infrared (ATR-FTIR) spectroscopic analysis**

Gelatin film samples were subjected to FTIR analysis using a Bruker Model EQUINOX 55 FTIR spectrometer (Bruker, Ettlingen, Germany) equipped with a deuterated L-alanine triglycine sulphate (DLATGS) detector as described by Nuthong *et al.* (2009). The Horizontal Attenuated Total Reflectance (HATR) accessory was mounted in the sample compartment. The internal reflection crystal (Pike Technologies, Madison, WI, USA), made of zinc selenide, had a 45° angle of incidence of the IR beam. Spectra were acquired in the IR range of 4000–650 cm<sup>-1</sup> (mid-IR region) at 25 °C. Automatic signals were collected in 32 scans at a resolution of 4 cm<sup>-1</sup> and were ratioed against a background spectrum recorded from the clean and empty cell at 25 °C. Analysis of spectral data was carried out using the OPUS 3.0 data collection software programme (Bruker, Ettlingen, Germany). Prior to data analysis, the spectra were baseline corrected and normalised.

### **3.3.5.8 Thermo-gravimetric analysis (TGA)**

Dried film samples were scanned using a thermogravimetric analyser (TGA-7, Perkin Elmer, Norwalk, CT, USA) from 50 to 600 °C at a rate of 10 °C/min (Nuthong *et al.*, 2009). Nitrogen was used as the purge gas at a flow rate of 20 ml/min.

### **3.3.5.9 Microstructure**

Microstructure of upper surface and cryo-fractured cross-section of the gelatin film samples was visualised using a scanning electron microscope (SEM) (Quanta 400, FEI, Praha, Czech Republic) at an accelerating voltage of 15 kV as described by Hoque *et al.* (2011d). The gelatin film samples were cryo-fractured by immersion in liquid nitrogen. Prior to visualisation, the film samples were mounted on brass stub and sputtered with gold in order to make the sample conductive, and photographs were taken at 8000x magnification for surface. For cross-section, cryo-fractured films were mounted around stubs perpendicularly using double sided adhesive tape, coated with gold and observed at the 4000x magnification.

### 3.3.6 Statistical analyses

All experiments were performed in triplicates ( $n=3$ ) and a completely randomised design (CRD) was used. Analysis of variance (ANOVA) was performed and the mean comparisons were done by Duncan's multiple range tests (Steel and Torrie, 1980). Data are presented as mean  $\pm$  standard deviation and the probability value of  $P<0.05$  was considered as significant. Statistical analysis was performed using the Statistical Package for Social Sciences (SPSS 17.0 for windows, SPSS Inc., Chicago, IL, USA).

## 3.4 Results and Discussion

### 3.4.1 Thickness

Films prepared from squid skin gelatin extracted at different temperatures showed different thickness ( $P<0.05$ ) (Table 13). F50 had the higher thickness, compared with F70 and F80 ( $P<0.05$ ). No differences in thickness were found between F60, F70 and F80 ( $P>0.05$ ). Hoque *et al.* (2011a) reported that films prepared from gelatin with higher degree of hydrolysis showed a slightly lower thickness than that of the control film (without hydrolysis) ( $P<0.05$ ). Gelatin with the shorter chain might align themselves to form the ordered network with the less protrusion. This most likely resulted in the lower thickness of obtained film (Ahmad *et al.*, 2012). In general, gelatin extracted at higher temperature yielded the film with lower thickness. Therefore, thickness of gelatin films was affected by extraction temperatures of gelatin.

### 3.4.2 Mechanical properties

Mechanical properties of gelatin film from squid skin extracted at different temperatures are shown in Table 13. Film obtained from the gelatin extracted at lower temperature (F50) had higher TS and EAB than F70 and F80 ( $P<0.05$ ). Nevertheless, TS and EAB of F50 were not different from those of F60 ( $P>0.05$ ). From our previous study, gelatin extracted at higher temperature had the shorter chain peptides or proteins (Nagarajan *et al.*, 2012a). Longer peptide chains of

gelatin might result in a higher aggregation of protein with higher number of inter-junction zones. Hoque *et al.* (2010) reported that gelatin film was mainly stabilised by the weak bond including hydrogen bond and hydrophobic interaction. It was noted that TS and EAB decreased as the extraction temperature increased ( $P < 0.05$ ). F80 showed the lowest TS and EAB, compared with films prepared from gelatins extracted at lower temperatures (F50, F60 and F70) ( $P < 0.05$ ). Higher content of low molecular weight fragments might impair the formation of junction zones. Furthermore, the renaturation of gelatin chains into helix coil structure could not occur effectively during the conditioning of the gelatin films. This led to a decrease in the mechanical properties of films (Arvanitoyannis *et al.*, 1998). Bigi *et al.* (2004) reported that mechanical properties of pig skin gelatin film increased as the triple-helix content increased. Films prepared from cuttlefish skin gelatin with higher degree of hydrolysis showed a lower TS and EAB than the control film without hydrolysis (Hoque *et al.*, 2011a). Gelatin molecules with the shorter chain most likely established the weaker chain-to-chain interaction mainly via hydrogen bond (Gomez-Guillen *et al.*, 2009). Furthermore, the increasing number of chain ends of shorter chain gelatin extracted at higher temperature directly enhanced the mobility of chains and the weaker film network was formed (Gontard *et al.*, 1993). The result indicated that the chain length of gelatin molecules mostly related to extracting temperature, directly contributed to the formation of film network, thereby affecting the mechanical properties of films.

### **3.4.3 Water vapour permeability (WVP)**

WVP of films prepared from squid skin gelatin extracted at different temperatures is presented in Table 13. Film from the gelatin extracted at the lowest temperature (F50) had the lowest WVP, compared with others ( $P < 0.05$ ). F80 showed the highest WVP ( $P < 0.05$ ). The lowered permeation of water vapour through F50 was probably determined by the stronger interaction of protein molecules in the film network with the high compactness (Tongnuanchan *et al.*, 2011). Furthermore, the higher extraction temperature resulted in the formation of smaller peptide chains. Smaller peptides could be easily inserted in the protein network, thereby decreasing the density of intermolecular interactions between gelatin chains and increasing the

free volume of the film matrix. Additionally, the more hydrolysed gelatin, especially G80, more likely had the increased hydrophilicity caused by the increases in N- or C-termini. Hoque *et al.* (2011a) stated that the hydrolysis could expose more carboxylic group and amino group, which could form hydrogen bond with the water molecules. This resulted in the increased hydrophilicity of the resulting films. Film from halibut skin gelatin with higher degraded peptide chains also had the higher WVP, compared with that from gelatin having lower degraded chains (Carvalho *et al.*, 2008). Thus, gelatin film was varying WVP, depending on the extraction temperature used for gelatin production.

**Table 13.** Tensile strength (TS), elongation at break (EAB), water vapour permeability (WVP) and thickness of films from squid skin gelatin extracted at different temperatures

<b>Film samples</b>	<b>TS (MPa)</b>	<b>EAB (%)</b>	<b>WVP (<math>\times 10^{-11} \text{ gmm}^{-2} \text{ s}^{-1} \text{ Pa}^{-1}</math>)</b>	<b>Thickness (mm)</b>
<b>F50</b>	29.30±3.41a	14.16±1.03a	3.34±0.02c	0.038±0.001a
<b>F60</b>	26.50±1.39ab	12.56±0.94ab	3.63±0.02b	0.035±0.002ab
<b>F70</b>	24.52±3.98b	11.88±1.08b	3.64±0.09b	0.034±0.002b
<b>F80</b>	16.46±0.86c	9.32±0.39c	3.86±0.03a	0.033±0.001b

Mean ± SD (n=3).

Different letters in the same column indicate significant differences ( $P < 0.05$ ).

### 3.4.4 Colour

Colour of films prepared from squid skin gelatin extracted at different temperatures is shown in Table 14. F50 had higher  $L^*$  value (lightness), but lower  $a^*$ ,  $b^*$  and  $\Delta E^*$  values than other samples ( $P < 0.05$ ). Lightness ( $L^*$  value) of films generally decreased with increasing extraction temperatures ( $P < 0.05$ ). This coincided with the increases in  $a^*$  (redness) and  $b^*$  (yellowness) values. Gelatins extracted at higher temperatures contained higher free amino group ( $-\text{NH}_2$ ) content, due to higher hydrolysis (Nagarajan *et al.*, 2012a). Those amino groups could undergo browning reaction along with carbonyl compounds in gelatin (Ajandouz and Puigserver, 1999).

As a result, the increases in yellowness and redness were found in films prepared from gelatin extracted at higher temperatures. Among all film samples, the highest  $a^*$  and  $\Delta E^*$ - values were obtained in F80 ( $P < 0.05$ ). The result indicated that extraction temperature of gelatin had the direct impact on colour of the corresponding films.

**Table 14.** Colour of films from squid skin gelatin extracted at different temperatures

Film samples	$L^*$	$a^*$	$b^*$	$\Delta E^*$
<b>F50</b>	76.92±0.83a	7.23±0.01c	10.7±0.03c	21.61±0.85c
<b>F60</b>	74.27±0.06b	9.32±0.04b	11.88±0.05b	25.22±2.90b
<b>F70</b>	71.91±0.58c	9.41±0.04b	15.38±0.05a	28.19±0.25ab
<b>F80</b>	68.30±1.11d	11.85±0.02a	10.49±0.04c	29.81±1.25a

Mean ± SD (n=3).

Different letters in the same column indicate significant differences ( $P < 0.05$ ).

### 3.4.5 Light transmission and transparency values

Transmission of UV and visible light at selected wavelengths in the range of 200-800 nm of films prepared from squid skin gelatin extracted at different temperatures is shown in Table 15. The transmission of UV light was very low at 200 and 280 nm for all films. Generally, gelatin films exhibited low light transmission in the UV range (Jongjareonrak *et al.*, 2008). Squid skin gelatin film effectively prevents the lipid oxidation, which is induced by UV light (Limpisophon *et al.*, 2009). Light transmission in visible range (350-800 nm) of films was from 19.33 to 82.00%. Light transmission in visible range of gelatin film decreased when gelatin extracted at higher temperatures was used for film preparation. However, F60 shows higher light transmission at 350 and 400 nm than other films (F50, F70 and F80). Decreasing light transmission of film with increasing extraction temperatures was in agreement with the increases in  $a^*$  and  $b^*$ - values of gelatin films (Table 14). Browning products formed might prevent light transmission through films to some extent. F80 also had

**Table 15.** Light transmittance (%) and transparency values of films from squid skin gelatin extracted at different temperatures

Film samples	Wavelength (nm)								Transparency values
	200	280	350	400	500	600	700	800	
<b>F50</b>	0.00	1.46	29.52	44.22	56.36	69.57	78.72	82.00	4.66±0.00c
<b>F60</b>	0.00	2.52	33.18	46.90	56.03	68.56	78.04	81.33	5.23±0.00c
<b>F70</b>	0.00	1.89	26.17	39.12	51.52	63.22	70.93	74.44	6.67±1.08b
<b>F80</b>	0.00	1.31	19.33	29.26	39.79	49.48	55.67	58.08	10.64±0.01a

Mean ± SD (n=3).

Different letters in the same column indicate significant differences (P<0.05).

the highest transparency value (10.64), compared with other films (F50, F60 and F70) ( $P < 0.05$ ). Higher transparency value represents the lower transparency of films (Ahmad *et al.*, 2012). Differences in light transmission and transparency of films obtained from gelatin extracted at different temperatures might be due to the differences in browning reaction products formed as well as the alignment of proteins or thin fragments in the film matrix. Therefore, the extraction temperatures of squid skin gelatin had an impact on light transmission and transparency value of resulting films, apart from mechanical properties and WVP (Table 13).

### 3.4.6 Protein patterns

Protein patterns of films prepared from squid skin gelatin extracted at different temperatures are shown in Figure 14a. Films had the proteins with MW of 121-124 kDa as the major proteins. This protein band, more likely representing  $\alpha$ -chain, was predominant in F50 sample. The decreasing  $\alpha$ -chain band intensity was observed in other films (F60, F70 and F80). Among all film samples, F80 had higher degraded proteins, as evidenced by the formation of peptide/protein bands with the lower MW, especially with MW lower than 70 kDa. Hoque *et al.* (2011a) reported that cuttlefish skin gelatin with the shorter chain molecules yielded the weaker film network with low TS and EAB. In the presence of sodium dodecyl sulphate as well as  $\beta$ -mercaptoethanol used for electrophoresis, hydrogen bond, hydrophobic interaction as well as disulfide bond in the film network was destroyed. Nevertheless, no disulfide bond was present in gelatin film (Hoque *et al.*, 2011d). Gelatin from squid skin contained no cysteine (Nagarajan *et al.*, 2012a) and the formation of disulfide bond was negligible. Therefore, differences in protein compositions and chain length more likely governed the properties of film (Table 13).

To confirm the degree of degradation of gelatin in films,  $\alpha$ -amino group content was determined (Figure 14b). The highest  $\alpha$ -amino group content was found in film prepared from gelatin extracted at 80°C. It indicated that higher cleavage of peptides occurred at higher temperature (Gimenez *et al.*, 2009a). The result was in agreement with the highest degradation of protein chains in F80 (Figure

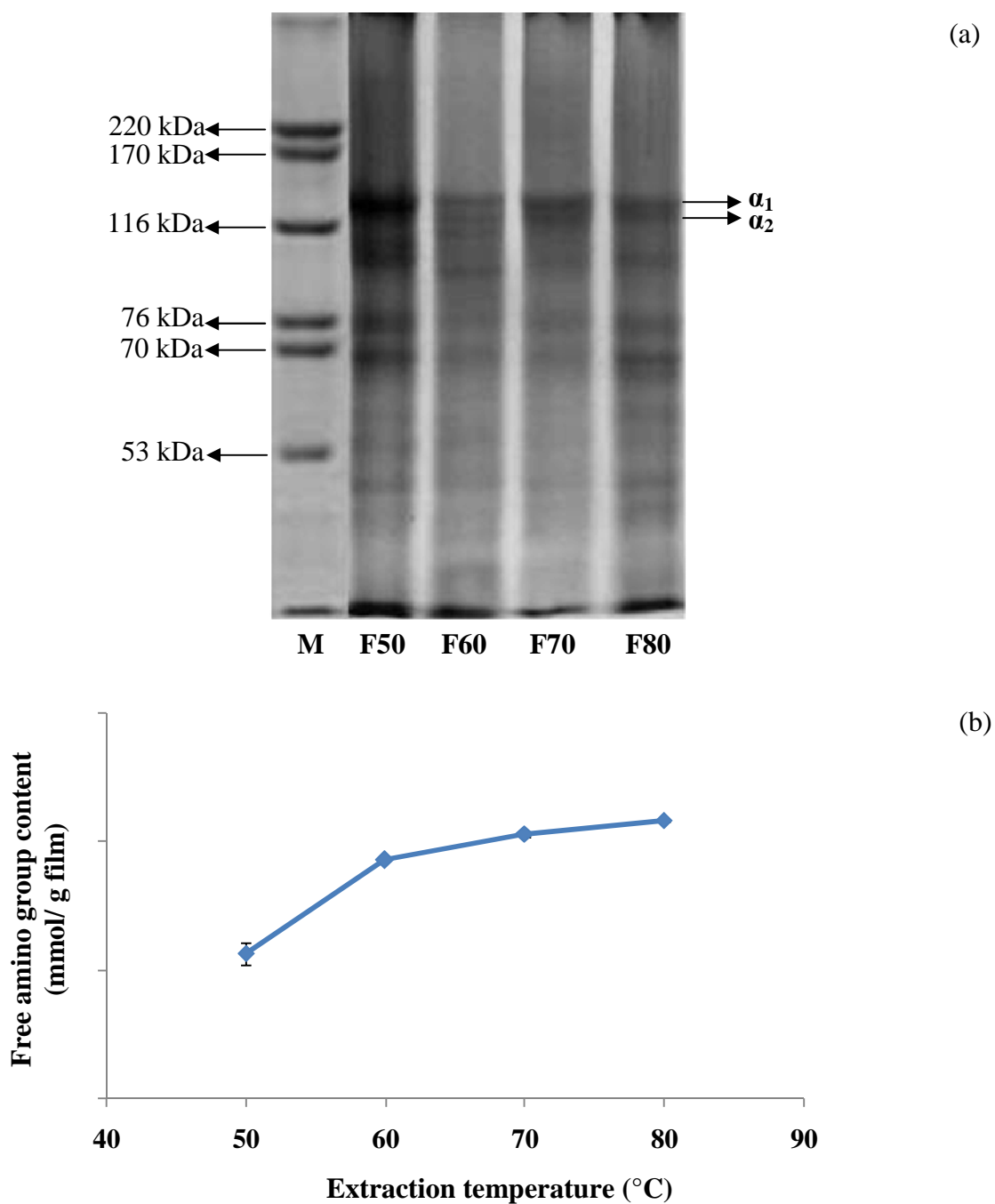


**Figure 14.** Protein patterns (a) and free amino group content (b) of films from splendid squid skin gelatin extracted at different temperatures. M: High molecular weight markers. F50, F60, F70 and F80 denote the films prepared from gelatins extracted at 50, 60, 70 and 80 °C, respectively. Bars represent the standard deviation (n=3).



14a). Therefore, high temperature caused the hydrolysis of collagenous proteins as indicated by the increase in free amino group content. The differences in degradation more likely determined film formation of those gelatin molecules.

### 3.4.7 FTIR spectra analysis

FTIR spectra of films from the squid skin gelatin extracted at various temperatures are depicted in Figure 15. FTIR spectroscopy has been used to monitor the functional groups and secondary structure of gelatin (Muyonga *et al.*, 2004c) and interaction of gelatins in the film (Jongjareonrak *et al.*, 2008). All gelatin film samples had the major peaks in amide region. F50, F60, F70 and F80 exhibited the amide-I band at the wavenumber of 1631.40, 1631.85, 1631.44, and 1631.26  $\text{cm}^{-1}$ , respectively. The amide-I vibration mode is primarily a C=O stretching vibration coupled with the C-N stretch, CCN deformation and in plane N-H bending modes (Muyonga *et al.*, 2004c). The absorption in the amide-I region is probably the most useful for infrared spectroscopic analysis of the secondary structure of proteins (Bandeekar, 1992; Surewich and Mantsch, 1988). Its exact location depends on the hydrogen bonding and the conformation of protein structure (Uriarte-Montoya *et al.*, 2011). In the present study, the amide-I peak was observed in the range of 1631  $\text{cm}^{-1}$ , which was in agreement with Hoque *et al.* (2011a) who stated that the absorption peak at 1631  $\text{cm}^{-1}$  was the characteristic of coiled structure of gelatin for cuttlefish skin gelatin films. The characteristic absorption bands of F50, F60, F70 and F80 in amide-II region was noticeable at the wavenumber of 1541.00, 1544.36, 1540.44 and 1538.39  $\text{cm}^{-1}$ , respectively. The amide-II vibration modes are attributed to out-of-plane combination of the N-H in plane bend and the C-N stretching vibration with smaller contributions from the C-O in plane bend and the C-C and N-C stretching vibrations (Jackson *et al.*, 1995). In addition, amide-III was detected around the wavenumber of 1234.36, 1235.86, 1235.99 and 1235.35  $\text{cm}^{-1}$  for F50, F60, F70 and F80, respectively. The amide-III represents the combination peaks between C-N stretching vibrations and N-H deformation from amide linkages as well as absorptions arising from wagging vibrations from  $\text{CH}_2$  groups from the glycine backbone and proline side-chains (Jackson *et al.*, 1995). F50, F60, F70 and F80 showed the peak at the wavenumber of 1032.26, 1033.89, 1033.95, and 1033.07  $\text{cm}^{-1}$ ,

respectively. This might be related to the interactions arising between plasticiser (OH-group of glycerol) and film structure (Bergo and Sobral, 2007).

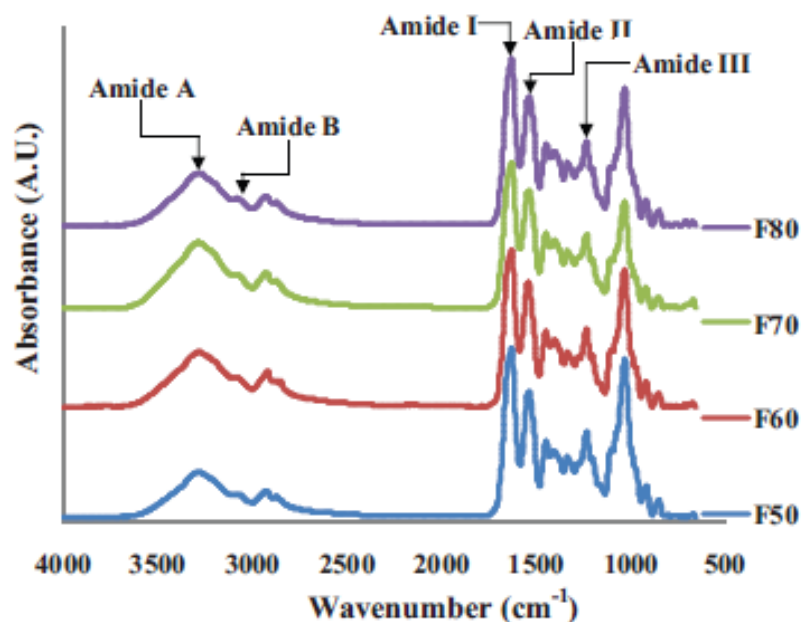


**Figure 15.** ATR-FTIR spectra of films from splendid squid skin gelatin extracted at different temperatures.

Amide-A band, arising from the stretching vibrations of the N-H group, appeared at 3291.45, 3290.36, 3287.87 and 3285.54  $\text{cm}^{-1}$  for F50, F60, F70 and F80, respectively. Amide-A represents NH-stretching coupled with hydrogen bonding (Muyonga *et al.*, 2004c). When the N-H group of a peptide is involved in a hydrogen bond, the position shifts to lower frequencies (Doyle *et al.*, 1975). In amide-A region, the lower wavenumber with the concomitantly higher amplitude of amide-A was observed for F70 and F80, suggesting the higher degradation of gelatin with a higher content of free amino groups (Figure 14b). These degraded gelatins might undergo hydrogen bonding, resulting in the decreased wavenumber of amide-A. The amide-B was observed in 3083.22, 3087.99, 3083.41 and 3081.04  $\text{cm}^{-1}$  for F50, F60, F70 and F80, respectively, corresponding to the asymmetric stretching vibration of =C-H as well as  $-\text{NH}_3^+$ . For F50, F60, F70 and F80, the peaks with the wavenumber of 2875.32, 2876.13, 2877.22 and 2876.22 (symmetrical) or 2925.29, 2921.05, 2927.35 and 2927.54 (asymmetrical) were observed, respectively. It represents C-H

stretching vibrations of the  $-CH_2$  groups (D' Souza *et al.*, 2008). Thus, the secondary structure, functional group and interaction of gelatins in films were affected by extraction temperature used for gelatin production.

### 3.4.8 Thermogravimetric analysis (TGA)

TGA thermograms revealing thermal degradation behaviour of films obtained from squid skin gelatin extracted at different temperatures are shown in Figure 16. Their corresponding degradation temperatures ( $T_d$ ) and weight loss ( $\Delta w$ ) are presented in Table 16. Three stages of weight loss were observed in all films. For all films, the first stage of weight loss ( $\Delta w_1 = 3.19\text{-}6.20\%$ ) was observed approximately at temperature ( $T_{d1}$ ) of  $42.47\text{-}51.90^\circ\text{C}$ , mostly associated with the loss of free water absorbed on the film. Similar result was observed for films from unicorn

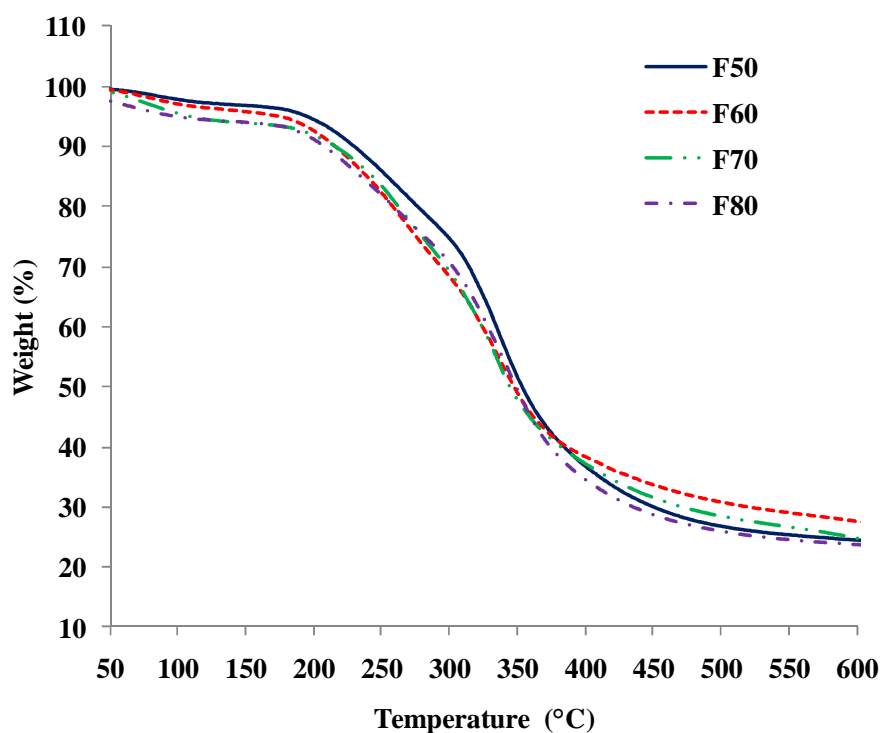


**Figure 16.** Thermogravimetric curves of films from splendid squid skin gelatin extracted at different temperatures.

leather jacket and cuttlefish skin gelatin (Ahmad *et al.*, 2012; Hoque *et al.*, 2011d). The second stage of weight loss ( $\Delta w_2 = 19.09\text{-}25.50\%$ ) was observed approximately at

**Table 16.** Thermal degradation temperature ( $T_d$ , °C) and weight loss ( $\Delta w$ , %) of films from squid skin gelatin extracted at different temperatures

<b>Film samples</b>	$\Delta_1$		$\Delta_2$		$\Delta_3$		<b>Residue (%)</b>
	<b>Td<sub>1</sub>, onset</b>	<b><math>\Delta w_1</math></b>	<b>Td<sub>2</sub>, onset</b>	<b><math>\Delta w_2</math></b>	<b>Td<sub>3</sub>, onset</b>	<b><math>\Delta w_3</math></b>	
<b>F50</b>	51.90	3.19	210.46	19.09	315.16	52.38	25.34
<b>F60</b>	51.28	3.94	211.52	25.50	311.05	41.38	29.18
<b>F70</b>	42.47	6.20	205.77	20.17	309.13	46.19	27.44
<b>F80</b>	46.31	5.30	191.58	19.10	306.45	50.87	24.73

$\Delta_1$ ,  $\Delta_2$  and  $\Delta_3$  denote the first, second and third stage weight loss, respectively of film during TGA heating scan.

temperature ( $Td_2$ ) of 191.58-211.52 °C, mostly associated with the loss of low molecular weight protein fractions, glycerol compounds and also structurally bound water. The third stage of weight loss ( $\Delta w_3 = 41.38-52.38\%$ ) was observed approximately at temperature ( $Td_3$ ) of 306.45-315.16 °C. This was most likely caused by the loss of high molecular weight protein fractions.

At the first stage, F50 and F60 showed the lower weight loss (3.19 and 3.94%, respectively) with the higher  $Td_1$  (51.90 and 51.28 °C, respectively) than F70 and F80 (6.20 and 5.30% of weight loss with  $Td_1$  of 42.47 and 46.31 °C, respectively). At the second and the third stages, decomposition of films from gelatins extracted at higher temperature exhibited lower  $Td_2$  and  $Td_3$ . The result suggested that weak film network prepared from the gelatin with the shorter gelatin molecules (F80) underwent easier thermal degradation, compared with F50. The result revealed that films prepared from gelatin extracted at higher temperatures (F70 and F80) showed the higher heat susceptibility, compared with gelatin extracted at lower temperatures (F50 and F60). Additionally, all films had residual mass (representing char content) at 600 °C in the range of 24.73-29.18%. The lowest char content observed in F80 was most likely due to the lowest thermal stability of film, which was in accordance with the lowest mechanical properties (Table 13). TGA curves showed clearly that different extraction temperatures of gelatin contributed to different thermal stability of resulting gelatin films.

### 3.4.9 Microstructure

SEM micrographs of the surface (A) and cryo-fractured cross-section (B) of films prepared from gelatin extracted at various temperatures are illustrated in Figure 17. F50 had compact, smooth and homogenous surface, indicating an ordered film matrix. However, F60 and F70 had slightly coarser surface than F50. F80 had the rough surface with some cracks. These differences in microstructure of different films were caused by the varying arrangements of protein molecules during film formation (Ahmad *et al.*, 2012; Hoque *et al.*, 2011d). In addition, the low MW gelatin found in F80 might not undergo the inter-connection effectively. This might lead to the formation of crack or void. Longer gelatin chains more likely underwent the network

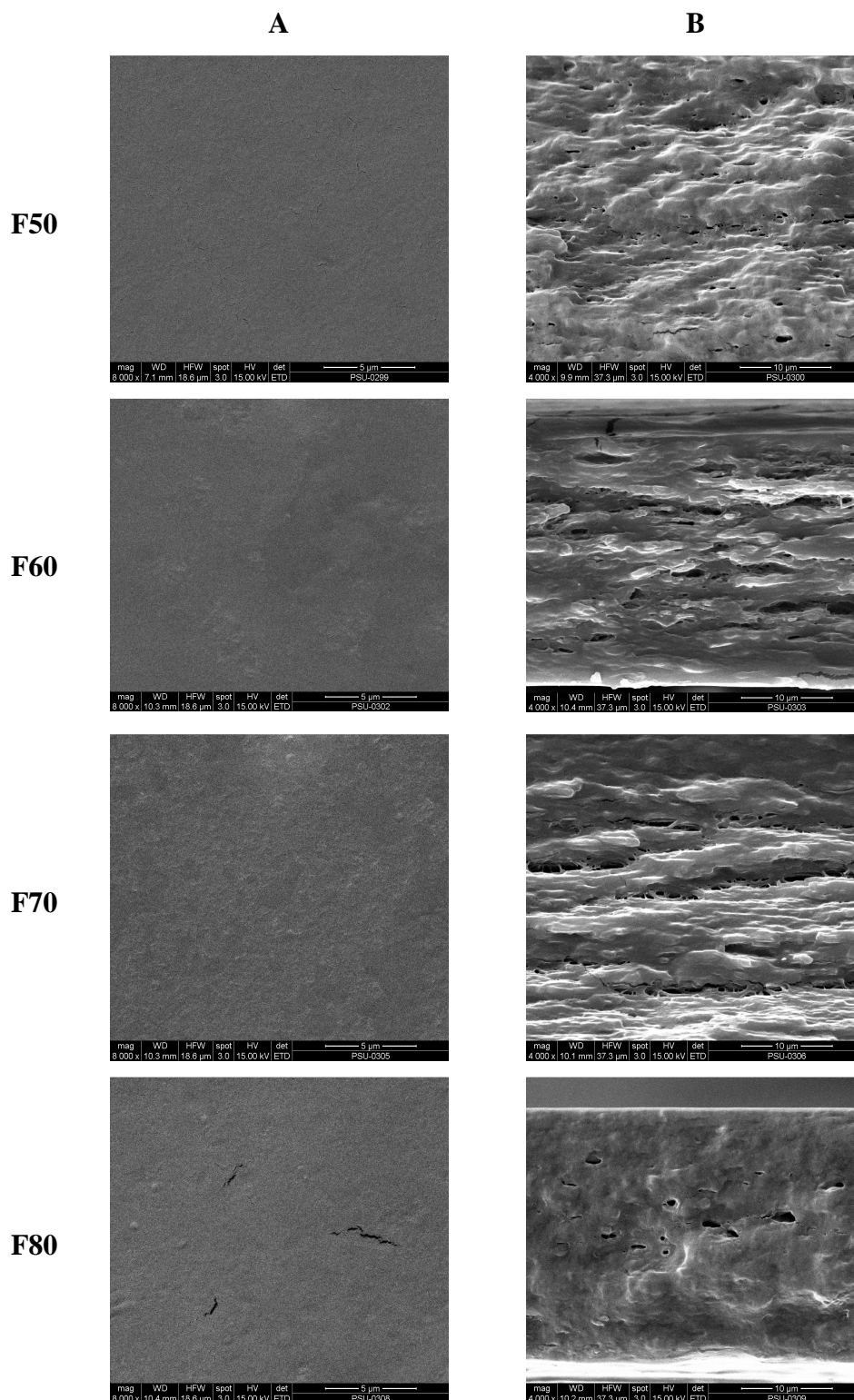


**Figure 17.** SEM micrographs of surface (A) and cryo-fractured cross-section (B) of films from splendid squid skin gelatin extracted at different temperatures. Magnification: 8000x and 4000x for surface and cross-section, respectively.

formation with a great number of junction zones, where the continuous matrix could developed. On the other hand, the shorter chains could not strongly intertwine, thereby forming the weaker network. As a result, the separated network could be easily formed. The looser network in F80 was in accordance with the lower mechanical properties, but higher WVP (Table 13).

For cross-section, film prepared from gelatin extracted at low temperature (F50) showed a more compact structure, compared with other films. Gelatin extracted at lower temperature might contribute to the formation of compact film, due to the longer chain length of proteins. However, films (F60, F70 and F80) from gelatin extracted at higher temperatures had the larger amount of voids and loosen structure. It might be owing to less interaction of protein molecules, in which disconnection of film matrix could occur. Increasing free spaces and loosen structure of films (F60, F70 and F80) were in agreement with higher WVP (Table 13), compared with F50. Thus, the microstructures of films were governed by molecular organisation in the film network, which depended on chain length of proteins and the interaction of proteins in film matrix.

### **3.5 Conclusion**

Squid skin gelatin prepared from different extraction temperatures possessed different molecular size and distribution. This molecular characteristic significantly contributed to interaction and organisation of gelatin molecules upon the formation of film network, which directly governed over properties of the resulting gelatin films. Gelatin extracted at higher temperature yielded the weaker film network, mainly caused by the higher degraded peptide chains. This led to the lower mechanical properties and thermal stability of their resulting films. Increased voids and loosen structure formed in films prepared from gelatin extracted at higher temperature resulted in the increased WVP. Gelatin with higher extraction temperature also rendered films with darker colour. Therefore, squid skin gelatin could serve as raw material for film formation when gelatin extraction at an appropriate temperature was implemented.

## CHAPTER 4

### EFFECTS OF BLEACHING ON CHARACTERISTICS AND GELLING PROPERTY OF GELATIN FROM SPLENDID SQUID (*LOLIGO FORMOSANA*) SKIN

#### 4.1 Abstract

Gelatins obtained from splendid squid (*Loligo formosana*) skin subjected to bleaching using hydrogen peroxide ( $H_2O_2$ ) at various concentrations were characterised. Yield of gelatin increased with increasing  $H_2O_2$  concentration used. Gelatin from skin bleached with higher  $H_2O_2$  concentrations had the lower free amino group and carbonyl group contents than the control gelatin (without bleaching). Gelatins had  $\alpha$ -chains with MW of 123-129 kDa as the major components. FTIR spectra of all gelatins revealed the significant loss of triple-helix. Gel strength of gelatin generally decreased as  $H_2O_2$  concentrations increased. Varying pHs rendering net charge of zero (5.18-6.34) were found among samples, as determined by  $\zeta$ -potential titration. Gelatin prepared from skin bleached with 2%  $H_2O_2$  showed the highest  $L^*$ , but lowest  $\Delta E^*$ -values, compared with others.  $H_2O_2$  at higher concentrations yielded gelatin with increasing  $b^*$ -value. Thus, the properties of gelatin were governed by bleaching process, particularly  $H_2O_2$  concentration.

#### 4.2 Introduction

Gelatin is a water soluble protein obtained by partial hydrolysis of collagen, the main fibrous protein constituent in bones, cartilages and skins (Johnston-Banks, 1990). Gelatin from pig skins is not acceptable for Judaism and Islam and beef gelatin is prohibited for Hindu (Karim and Bhat, 2009). Due to the outbreak of Foot and Mouth Disease (FMD) or Bovine Spongiform Encephalopathy (BSE), land animal tissue-derived collagens and gelatins are questionable for transmitting pathogenic vectors such processing discards such as prions (Wilesmith *et al.*, 1991). As a consequence, fish gelatin has gained increasing interest as the potential alternative for land animal counterpart. Fish processing discards such as skin, fin, scale



and bones, etc., accounts for 70–85% of the total weight of catch (Shahidi, 1994). Disposal of these wastes poses serious environmental problem. Those resources have been reported as promising raw material for gelatin production (Gomez-Guillen *et al.*, 2002).

Nowadays, Thailand and other Southeast Asian countries are consuming a large amount of squid and cuttlefish (Hoque *et al.*, 2011b). During processing, skin is generated as a by-product and it can create serious ecological problems and environmental pollution without appropriate management. Skin has a low market value and is generally used as animal feed. Gelatin from cuttlefish skin was extracted by Aewsiri *et al.* (2009). Squid processing by-products are rich in collagen (Brinckmann, 2005), which can be used for gelatin production. Gelatin has been extracted from skins of splendid and giant squid (Gimenez *et al.*, 2009c; Nagarajan *et al.*, 2012a; Uriarte-Montoya *et al.*, 2011). Nevertheless, the pigments in squid skin pose a colour problem in the resulting gelatin. To tackle such a limitation, H<sub>2</sub>O<sub>2</sub> can be used as bleaching agent. H<sub>2</sub>O<sub>2</sub> has been used widely to improve the whiteness of seafoods (Kolodziejska *et al.*, 1999; Thanonkaew *et al.*, 2008). Aewsiri *et al.* (2009) reported that soaking cuttlefish skin in 5% H<sub>2</sub>O<sub>2</sub> for 48 h at 4 °C could improve the colour of the resulting gelatin. Currently, no information regarding the use of H<sub>2</sub>O<sub>2</sub> as a bleaching agent in squid skin prior to gelatin extraction and its effect on yield and properties of gelatin has been reported. The objective of this work was to study the effects of bleaching the skin using H<sub>2</sub>O<sub>2</sub> at different levels on yield, colour and properties of resulting gelatin from splendid squid skin.

### **4.3 Materials and methods**

#### **4.3.1 Chemicals**

2,4-dinitrophenylhydrazine (DNPH) was purchased from Wako Pure Chemical Industries Ltd. (Chuo-Ku, Osaka, Japan). Guanidine hydrochloride, 2,4,6-trinitrobenzenesulphonic acid (TNBS), sodium sulphite, L-leucine, bovine serum albumin (BSA) and  $\beta$ -mercaptoethanol ( $\beta$ -ME) were obtained from Sigma Chemical Co. (St. Louis, MO, USA). High molecular weight protein marker (53 kDa to 220

kDa) was purchased from GE Healthcare UK (Buckinghamshire, UK). Trichloroacetic acid (TCA), hydrogen peroxide (H<sub>2</sub>O<sub>2</sub>) (30.96%, w/v), glycerol and acetic acid were procured from Merck (Darmstadt, Germany). Sodium dodecyl sulphate (SDS), Coomassie Blue R-250 and *N,N,N',N'*-tetramethyl ethylene diamine (TEMED) were obtained from Bio-Rad Laboratories (Hercules, CA, USA).

#### **4.3.2 Collection and preparation of squid skin**

The skin of fresh splendid squid (*Loligo formosana*) was obtained from Sea Wealth Frozen Food Co., Ltd., Songkhla, Thailand and stored in ice using a skin/ice ratio of 1:2 (w/w). Upon arrival to the Department of Food Technology, Prince of Songkla University, Hat Yai, Thailand, the skin was cleaned and washed with iced tap water (0-2 °C). Skin contained 83% moisture, 14% protein, 1.1% ash and 1.5% fat as determined by the method of AOAC (2000). The skin was then cut into small pieces (0.5x0.5 cm<sup>2</sup>), placed in polyethylene bags and stored at -20 °C until use. The skin was stored for not more than 2 months.

#### **4.3.3 Extraction of gelatin from squid skin bleached with H<sub>2</sub>O<sub>2</sub> at various concentrations**

Gelatin extraction was performed following the method of Aewsiri *et al.* (2009) with a slight modification. Prior to gelatin extraction, the prepared skin was soaked in 0.05 M NaOH with a skin/solution ratio of 1:10 (w/v). The mixture was stirred continuously for 6 h at room temperature at a speed of 150 rpm using an overhead stirrer equipped with a propeller (RW 20.n, IKA-Werke GmbH & CO.KG, Staufen, Germany). The alkaline solution was changed every 90 min for totally four times to remove non collagenous proteins and pigments. Alkaline-treated skin was separated using two layers of cheese cloth (40x40 threads per inch<sup>2</sup>). The obtained skin was then washed with tap water with a skin/water ratio of 1:20 (w/v) until the pH of wash water became neutral or faintly basic. To bleach the skin, the prepared skin was then soaked in 0, 1, 2, 4, 6 and 8% H<sub>2</sub>O<sub>2</sub> (w/v) with a skin/solution ratio of 1:10 (w/v) for 24 h with gentle stirring at a speed of 150 rpm using an overhead stirrer at 4

°C. H<sub>2</sub>O<sub>2</sub> solution was changed every 12 h for totally two times. Bleached skin was washed thoroughly with a running tap water.

To extract gelatin, the bleached skin was soaked in distilled water at 60 °C using a bleached skin/water ratio of 1:10 (w/v) in a temperature-controlled water bath (W350, Memmert, Schwabach, Germany) for 12 h with a continuous stirring using an overhead stirrer at a speed of 150 rpm (Nagarajan *et al.*, 2012a). The mixture was then filtered using two layers of cheese cloth. The filtrate was further filtered using a Whatman No. 4 filter paper (Whatman International Ltd., Maidstone, England) with the aid of JEIO Model VE-11 electric aspirator (JEIO TECH, Seoul, Korea). The resultant filtrate was freeze-dried using a Scanvac Model CoolSafe 55 freeze dryer (CoolSafe, Lyngø, Denmark). The freeze-dried gelatins extracted from the bleached squid skin using 0, 1, 2, 4, 6 and 8% H<sub>2</sub>O<sub>2</sub> were referred to as 'G0', 'G1', 'G2', 'G4', 'G6' and 'G8', respectively. All gelatin samples were calculated for extraction yield and subjected to analyses.

#### 4.3.4 Yield and Characterisation of gelatin

##### 4.3.4.1 Yield of gelatin

Yield of gelatin was calculated based on dry weight of initial skin according to the method of Nagarajan *et al.* (2012a).

$$\text{Yield (\%)} = \frac{\text{Weight of freeze dried gelatin (g)}}{\text{Weight of dry skin (g)}} \times 100$$

##### 4.3.4.2 Determination of carbonyl content

Carbonyl content of gelatin was determined according to the method of Liu and Xiong (2000a) with a slight modification. Aqueous gelatin solution (0.5 ml, 3 mg protein/ml) was added with 2.0 ml of 10 mM 2,4-dinitrophenylhydrazine (DNPH) in 2 N HCl. The mixture was allowed to stand for 1 h at room temperature. Thereafter, 2 ml of 20% (w/v) TCA was added to precipitate the protein. The pellet

was washed twice with 4 ml of ethanol:ethyl acetate (1:1, v/v) mixture, to remove unreacted DNPH, blow-dried, and dissolved in 1.5 ml of 0.6 M guanidine hydrochloride in 20 mM potassium phosphate buffer (pH 2.3). The absorbance of solution was measured at 370 nm using a spectrophotometer (UV-1800, Shimadzu, Kyoto, Japan). A molar absorptivity of  $22,400 \text{ M}^{-1} \text{ cm}^{-1}$  was used to calculate carbonyl content (Levine *et al.*, 1990). Carbonyl content was expressed as  $\mu\text{mol/g}$ .

#### **4.3.4.3 Determination of free amino group content**

Free amino group content of aqueous gelatin solution ( $15 \mu\text{g}$  protein/ $\mu\text{l}$ , w/v) was determined following the method of Benjakul and Morrissey (1997). Properly diluted samples ( $125 \mu\text{l}$ ) were mixed thoroughly with 2.0 ml of 0.2 M phosphate buffer, pH 8.2, followed by the addition of 1.0 ml of 0.01% 2,4,6-trinitrobenzenesulphonic acid (TNBS) solution. The mixture was then placed in a temperature controlled water bath at  $50 \text{ }^\circ\text{C}$  for 30 min in the dark. The reaction was terminated by adding 2.0 ml of 0.1 M sodium sulphite. The mixtures were cooled down at room temperature for 15 min. The absorbance was measured at 420 nm using a spectrophotometer (Model UV-1800, Shimadzu, Kyoto, Japan). Free amino group content was expressed in terms of L-leucine as  $\mu\text{mol/g}$ .

#### **4.3.4.4 Electrophoretic analysis**

SDS-polyacrylamide gel electrophoresis (SDS-PAGE) was performed by the method of Laemmli (1970). Gelatin samples were dissolved in 5% SDS and the mixtures were incubated at  $85 \text{ }^\circ\text{C}$  for 1 h. The mixtures were centrifuged at  $3,500 \times g$  for 5 min at room temperature using a microcentrifuge (MIK-RO20, Hettich Zentrifugan, Tuttlingen, Germany) to remove undissolved debris. Protein content in the supernatant of all samples was determined using the Biuret method (Robinson and Hogden, 1940). Gelatin samples were mixed at a 1:1 (v/v) ratio with the sample buffer (0.5 M Tris-HCl, pH 6.8, containing 4% SDS and 20% glycerol). Samples ( $15 \mu\text{g}$  protein) were loaded onto polyacrylamide gels comprising a 7.5% running gel and a 4% stacking gel and subjected to electrophoresis at a constant current of 15 mA/gel using a MINI PROTEAN II unit (Bio-Rad Laboratories, Inc., Richmond, CA, USA).

After electrophoresis, the gel was stained with 0.05% (w/v) Coomassie Blue R- 250 in 15% (v/v) methanol and 5% (v/v) acetic acid and destained with 30% (v/v) methanol and 10% (v/v) acetic acid. High molecular weight marker (53 kDa to 220 kDa) was used. Relative mobility ( $R_f$ ) of protein band was manually calculated and the molecular weight of proteins was calculated from the plot between  $R_f$  and  $\log$  (MW) of standards.

#### **4.3.4.5 Attenuated total reflectance-Fourier transform infrared (ATR-FTIR) spectroscopic analysis**

Gelatin samples were subjected to FTIR analysis using Bruker Model EQUINOX 55 FTIR spectrometer (Bruker, Ettlingen, Germany) equipped with a deuterated L-alanine triglycine sulphate (DLATGS) detector. The horizontal attenuated total reflectance (HATR) accessory was mounted in the sample compartment. The internal reflection crystal (Pike Technologies, Madison, WI, USA), made of zinc selenide, had a  $45^\circ$  angle of incidence of the IR beam. Spectra were acquired in the IR range of  $4000\text{--}650\text{ cm}^{-1}$  (mid-IR region) at  $25^\circ\text{C}$ . Automatic signals were collected in 32 scans at a resolution of  $4\text{ cm}^{-1}$  and were ratioed against a background spectrum recorded from the clean and empty cell at  $25^\circ\text{C}$ . Analysis of spectral data was carried out using the OPUS 3.0 data collection software programme (Bruker, Ettlingen, Germany). Prior to data analysis, the spectra were baseline corrected and normalised.

#### **4.3.4.6 Measurement of $\zeta$ -potential**

Gelatin samples were dissolved in distilled water to obtain a concentration of 0.5 mg/ml. The mixture was stirred at room temperature for 6 h. The  $\zeta$ -potential of each sample (20 ml) was measured using a zeta potential analyser (ZetaPALS, Brookhaven Instruments Corp., Holtsville, NY, USA).  $\zeta$ -Potential of samples adjusted to different pHs with 1.0 M nitric acid or 1.0 M KOH using an autotitrator (BI-ZTU, Brookhaven Instruments Co., Holtsville, New York, USA) was determined. The pI of gelatin samples was estimated from pH rendering  $\zeta$ -potential of zero.

#### 4.3.4.7 Colour measurement

Colour of freeze-dried gelatin was measured using a CIE colourimeter (Color Flex, Hunter Lab Inc., Reston, VA, USA). Samples were spread over the white plate and  $L^*$ ,  $a^*$  and  $b^*$  parameters, indicating lightness or brightness, redness or greenness and yellowness or blueness, respectively, were recorded. The colourimeter was calibrated with a white standard. Total difference in colour ( $\Delta E^*$ ) was calculated according to the following equation (Gennadios *et al.*, 1996).

$$\Delta E^* = \sqrt{(\Delta L^*)^2 + (\Delta a^*)^2 + (\Delta b^*)^2}$$

where,  $\Delta L^*$ ,  $\Delta a^*$  and  $\Delta b^*$  are the differences between the corresponding colour parameter of the sample and that of white standard ( $L^*= 93.63$  ,  $a^*= -0.94$  and  $b^*= 0.40$ ).

#### 4.3.4.8 Determination of gel strength

Gelatin gels were prepared by the method of Fernandez-Diaz, Montero, and Gomez-Guillen (2001) with a slight modification. Gelatin samples were dissolved in distilled water at 60 °C to obtain the final concentration of 6.67% (w/v). The solution was stirred until the gelatin was solubilised completely and cooled in a refrigerator at 10 °C for 16-18 h for gel maturation. The dimensions of the sample were 3 cm in diameter and 2.5 cm in height. Samples (10 °C) were taken from refrigerator and gel strength was determined immediately using a Model TA-XT2 Texture Analyser (Stable Micro System, Surrey, UK) with a load cell of 5 kN and equipped with a 1.27 cm diameter flat faced cylindrical Teflon<sup>®</sup> plunger. The maximum force (in grams) was recorded when the penetration distance reached 4 mm. The speed of the plunger was 0.5 mm/s.

#### 4.3.5 Statistical analyses

All experiments were performed in triplicates (n=3) and a completely randomised design (CRD) was used. Analysis of variance (ANOVA) was performed and the mean comparisons were done by Duncan's multiple range tests (Steel and

Torrie, 1980). Data are presented as mean  $\pm$  standard deviation and the probability value of  $P < 0.05$  was considered as significant. Statistical analysis was performed using the Statistical Package for Social Sciences (SPSS 17.0 for windows, SPSS Inc., Chicago, IL, USA).

## 4.4 Results and discussion

### 4.4.1 Extraction yield

Extraction yield of gelatins from the splendid squid skin subjected to bleaching with  $H_2O_2$  at various concentrations is shown in Table 17. Increasing yield was obtained when the concentration of  $H_2O_2$  increased ( $P < 0.05$ ). Yield of 8.09, 14.48, 19.19, 22.82, 22.20 and 29.09% (on dry weight basis) was found for G0, G1, G2, G4, G6 and G8, respectively. However, no differences in yield were observed between G4 and G6 ( $P > 0.05$ ). Aewsiri *et al.* (2009) reported a similar result for cuttlefish skin gelatin, in which pretreatment of skin using  $H_2O_2$  at higher concentrations resulted in the increased yield ( $P < 0.05$ ).  $H_2O_2$  was found to break the hydrogen bond of collagen (Courts, 1961). Donnelly and McGinnis (1977) reported that tissue containing collagen was liquefied through agitation with  $H_2O_2$  (4–20%  $H_2O_2$ ) for 4–24 h. Therefore,  $H_2O_2$  more likely destroyed H-bond of collagen molecules in splendid squid skin, resulting in an increased efficiency in gelatin extraction. Furthermore, radicals generated from  $H_2O_2$  related reactions might cleave the peptide chain of collagen, thereby reducing chain length. The decomposition of  $H_2O_2$  in aqueous solution occurs by dissociation and homolytic cleavage of O–H or O–O bonds, with the formation of highly reactive products: hydroperoxyl anion ( $HOO^-$ ), and hydroperoxyl ( $HOO\cdot$ ) and hydroxyl ( $OH\cdot$ ) radicals, which can react to many substances, including chromatophores (Perkins, 1996). As a result, the gelatin could be extracted with ease. The degree of conversion of collagen into gelatin depends on the pretreatment conditions, the processing parameters (temperature, extraction time and pH), and the properties and the preservation method of the starting raw material (Karim and Bhat, 2009). Therefore,  $H_2O_2$  concentration used for bleaching directly affected the extraction yield of gelatin from splendid squid skin.

**Table 17.** Yield, carbonyl content, free amino group content and colour of gelatins from the splendid squid skin bleached with H<sub>2</sub>O<sub>2</sub> at various concentrations

Parameters	G0	G1	G2	G4	G6	G8
<b>Yield</b> (% , on dry weight basis)	8.09±0.53e	14.48±0.94d	19.19±0.70c	22.82±1.35b	22.20±1.54b	29.09±2.01a
<b>Carbonyl content</b> (µmol/g gelatin)	29.85±0.73a	19.25±2.22b	17.57±0.01b	13.58±0.29c	13.32±0.25c	12.56±0.09c
<b>Free amino group content</b> (µmol/g gelatin)	0.42±0.00a	0.26±0.00b	0.25±0.00b	0.18±0.01c	0.18±0.01c	0.14±0.00d
<b>Colour</b>						
<i>L</i> *	66.01±0.10f	80.23±0.08c	83.16±0.24a	78.18±0.08d	77.77±0.01e	82.73±0.01b
<i>a</i> *	8.75±0.06a	4.15±0.04b	3.42±0.06d	3.96±0.01c	2.22±0.04e	1.16±0.07f
<i>b</i> *	5.46±0.07e	8.47±0.02d	8.58±0.18d	9.32±0.04c	11.26±0.02b	12.86±0.14a
$\Delta E^*$	29.70±0.07a	16.45±0.09e	13.99±0.10f	18.50±0.07c	19.90±0.02b	17.33±0.08d

G0, G1, G2, G4, G6 and G8 denote the skin bleached with H<sub>2</sub>O<sub>2</sub> at levels of 0, 1, 2, 4, 6 and 8% (w/v), respectively.

Mean ± SD (n=3).

Different letters in the same row indicate significant differences (P<0.05) according to Duncan's multiple range tests.



#### 4.4.2 Carbonyl content

Carbonyl content of gelatins from the splendid squid skin with different bleaching conditions is shown in Table 17. Decreases in carbonyl content were observed as  $H_2O_2$  concentration used for bleaching increased ( $P < 0.05$ ). However, no differences in carbonyl content between G4, G6 and G8 was observed ( $P > 0.05$ ). Moreover, similar carbonyl contents were found between G1 and G2 ( $P > 0.05$ ). Carbonyl content is one of the most reliable measures of protein oxidation (Levine *et al.*, 1990). In the presence of oxidising agent,  $H_2O_2$ , particularly at high concentration, gelatin was postulated to undergo oxidation to higher extent. The decrease in carbonyl content in gelatin bleached with  $H_2O_2$  at high concentration might be associated with their reactivity with amino acid groups, especially via Schiff's base process (Stadtman, 1997). As a consequence, the remaining carbonyl group was decreased. Baron *et al.* (2007) suggested that interactions between protein carbonyl and other cell constituents may decrease carbonyl content.

#### 4.4.3 Free amino group content

Free amino group content of gelatins from the splendid squid skin subjected to bleaching using  $H_2O_2$  at various concentrations is shown in Table 17. Free amino group content of gelatins decreased with increasing  $H_2O_2$  concentrations used for bleaching ( $P < 0.05$ ). The highest free amino group content was observed for unbleached squid skin gelatin ( $P < 0.05$ ).  $H_2O_2$  might cause both protein fragmentation and aggregation (Decker *et al.*, 1993). Due to the marked increases in extraction yield, the degradation of gelatin might take place. Nevertheless, those  $\alpha$ -amino groups generated were postulated to react with carbonyl group. Liu and Xiong (2000a) also reported that carbonyls may react with the free amino groups to form amide bond. Thus, the residual free amino groups were lowered. The decreases in free amino group contents were in accordance with the lowered carbonyl content. The result suggested that  $H_2O_2$  with increasing concentration might induce the aggregation and oxidation of proteins more effectively.

#### 4.4.4 Protein patterns

Protein patterns of gelatins from the splendid squid skin bleached with  $H_2O_2$  at different concentrations are depicted in Figure 18. Gelatin extracted from splendid squid skin was composed mainly of  $\alpha$ -chains (MW of 123-129 kDa). Dimer ( $\beta$ -components) and higher MW aggregates ( $\gamma$ -components and others) were found at a low content. Among all samples, G0 had the highest band intensity of  $\alpha$ -chains as well as proteins with MW of 70 and 76 kDa. The decreasing  $\alpha$ -chain band intensity was observed in gelatins extracted from skin bleached with  $H_2O_2$  (G1, G2, G4, G6 and G8). High MW protein bands appeared in the stacking gel. Aewsiri *et al.* (2009) and Hoque *et al.* (2011b) also reported the similar results for cuttlefish skin gelatin. It

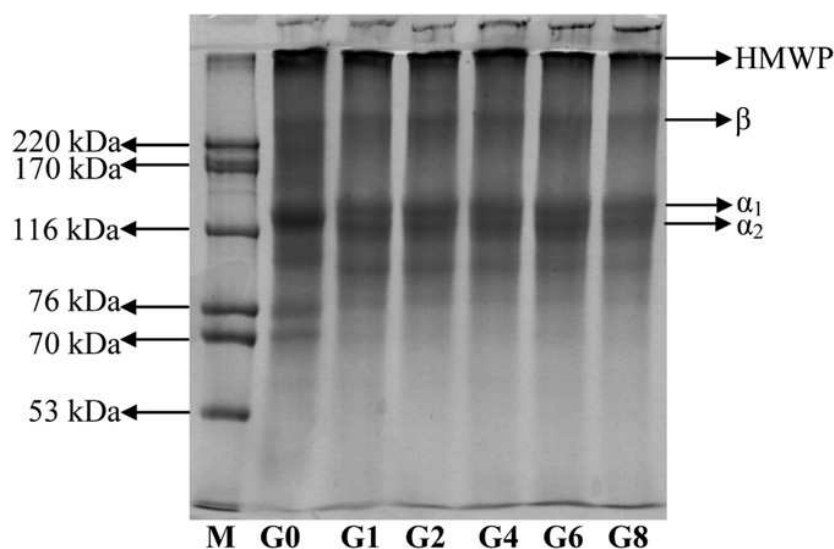


**Figure 18.** Protein patterns of gelatins from the splendid squid skin bleached with  $H_2O_2$  at various concentrations. M: High molecular weight markers. G0, G1, G2, G4, G6 and G8 denote the skin bleached with  $H_2O_2$  at levels of 0, 1, 2, 4, 6 and 8% (w/v), respectively. HMWP: High molecular weight proteins.

was noted that no proteins with MW of 70 and 76 kDa were retained in gelatin extracted from skin bleached with  $H_2O_2$ , regardless of concentration used. It was postulated that those proteins might be susceptible to either degradation or

polymerisation induced by  $\text{H}_2\text{O}_2$ . Additionally, less protein band intensity was observed in G8, compared with others. Therefore,  $\text{H}_2\text{O}_2$  used for bleaching caused the disappearance of  $\alpha$ -chains and some low MW proteins of gelatin.

#### 4.4.5 ATR-FTIR spectra

FTIR spectra of gelatins from the splendid squid skin subjected to bleaching with  $\text{H}_2\text{O}_2$  at various concentrations are shown in Figure 19. FTIR spectroscopy has been used to monitor the functional groups and secondary structure of gelatin (Muyonga *et al.*, 2004c). All gelatin samples had the major peaks in amide region. G0, G1, G2, G4, G6 and G8 exhibited the amide-I band at the wavenumber of 1632.71, 1633.98, 1635.28, 1641.12, 1640.45 and 1640.49  $\text{cm}^{-1}$ , respectively. Amide-I vibration mode is primarily a C=O stretching vibration coupled with the C-N stretch and CCN deformation (Bandekar, 1992). Its exact location depends on the hydrogen bonding and the conformation of protein structure (Uriarte-Montoya *et al.*, 2011). In the present study, the amide-I peak was observed in the range of 1632-1641  $\text{cm}^{-1}$ , which was in accordance with that reported for gelatin from cephalopod skin (Aewsiri *et al.*, 2009; Hoque *et al.*, 2011b). The characteristic absorption bands of G0, G1, G2, G4, G6 and G8 in amide-II region was noticeable at the wavenumber of 1538.76, 1547.06, 1548.84, 1547.46, 1543.81 and 1544.36  $\text{cm}^{-1}$ , respectively. The amide-II vibration mode is attributed to combination of the N-H in plane bend and the C-N stretching vibration with smaller contributions from the C-O in plane bend and the C-C and N-C stretching vibrations (Jackson, Choo, Watson, Halliday, & Mantsch, 1995). In addition, amide-III was detected around the wavenumber of 1234.03, 1236.50, 1236.71, 1237.25, 1236.21 and 1236.59  $\text{cm}^{-1}$  for G0, G1, G2, G4, G6 and G8, respectively. The amide-III represents the combination peaks between C-N stretching vibrations and N-H deformation from amide linkages as well as absorptions arising from wagging vibrations from  $\text{CH}_2$  groups from the glycine backbone and proline side-chains (Jackson *et al.*, 1995). The wavenumbers of amide-I, amide-II and amide-III peaks were lower for unbleached skin (G0), compared to

other gelatins extracted from skin bleached with  $H_2O_2$  (G1, G2, G4, G6 and G8). Higher wavenumbers were more likely related to the changes in carbonyl and amino group contents during bleaching, caused by protein oxidation and fragmentation, respectively. Those reactive groups were able to undergo glycation process, as indicated by the decreasing in carbonyl and free amino group (Table 17). Hydrogen bond between molecules of gelatin with bleaching could be plausibly impeded since H-donor or H-acceptor residues or domains were masked via aggregation mediated by glycation. Conversely, G0 could have higher H-bond between adjacent molecules as indicated by the lower wavenumbers.

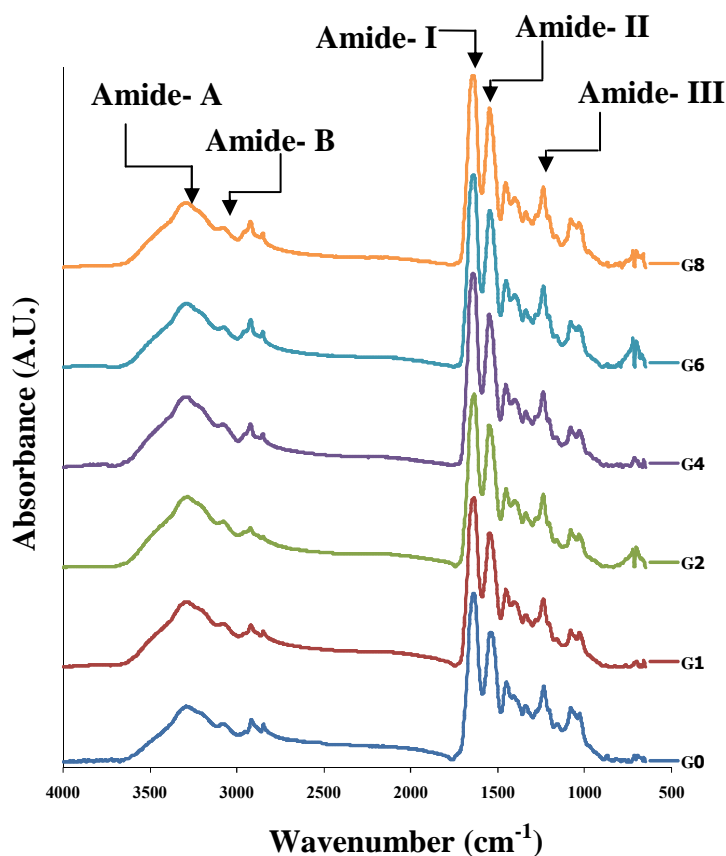


**Figure 19.** ATR-FTIR spectra of gelatins from the splendid squid skin bleached with  $H_2O_2$  at various concentrations. G0, G1, G2, G4, G6 and G8 denote the skin bleached with  $H_2O_2$  at levels of 0, 1, 2, 4, 6 and 8% (w/v), respectively.

Amide-A band, arising from the stretching vibrations of the N-H group, appeared at 3290.80, 3287.65, 3282.33, 3290.64, 3287.90 and 3289.12  $\text{cm}^{-1}$  for G0, G1, G2, G4, G6 and G8, respectively. Amide-A represents NH-stretching coupled with hydrogen bonding (Muyonga *et al.*, 2004c). When the N-H group of a peptide is involved in a H-bond, the position shifts to lower wavenumbers (Doyle *et al.*, 1975). This shift of amide-A to lower wavenumbers was more likely associated with the reactivity of free amino acid towards glycation. The amide-B was observed at wavenumber of 3085.38, 3084.59, 3077.88, 3079.46, 3077.93 and 3082.00  $\text{cm}^{-1}$  for G0, G1, G2, G4, G6 and G8, respectively, corresponding to the asymmetric stretching vibration of  $=\text{C}-\text{H}$  as well as  $-\text{NH}_3^+$ . For G0, G1, G2, G4, G6 and G8, the peaks with the wavenumber of 2846.34, 2847.19, 2848.14, 2849.69, 2849.69, and 2849.96 (symmetrical) or 2915.11, 2918.04, 2920.98, 2920.14, 2919.11 and 2919.30 (asymmetrical) were observed, respectively. It represents C-H stretching vibrations of the  $-\text{CH}_2$  groups (D'Souza *et al.*, 2008). Thus, the secondary structure and functional group of gelatins from squid skin bleached with  $\text{H}_2\text{O}_2$  was affected to some extent and  $\text{H}_2\text{O}_2$  concentration was a factor governing those changes.

#### 4.4.6 $\zeta$ -potential analysis

$\zeta$ -potential values of gelatin from the splendid squid skin bleached with  $\text{H}_2\text{O}_2$  at various concentrations were measured as a function of pH as illustrated in Figure 20. All gelatin samples were positively charged at acidic pH ranges and became negatively charged under alkaline conditions. Net charge of zero was obtained at pH 5.56, 5.42, 5.18, 5.66, 5.95 and 6.34 for G0, G1, G2, G4, G6 and G8, respectively. Those pHs were presumably pI of those gelatin samples. Protein molecules in an aqueous system have zero net charge at their isoelectric points (pI), in which the positive charges are balanced out by the negative charges (Bonner, 2007). Lower pI value was observed for G2 and higher values were noticeable for G6 and G8 ( $P < 0.05$ ). Squid skin gelatin had higher amount of acidic amino acids (glutamic acid and aspartic acid) than that of basic amino acids (lysine and arginine) (Nagarajan *et*

*al.*, 2012a). High glutamic acid and aspartic acid contents were also reported for gelatin from cuttlefish (*Sepia officinalis*) skin and giant squid (*Dosidicus gigas*) skin (Balti *et al.*, 2011; Gimenez *et al.*, 2009c). Deamidation might take place and glutamic acid and aspartic acid could be formed in gelatins, obtained from squid skin bleached with H<sub>2</sub>O<sub>2</sub> at low concentrations (G1 and G2). Glycation process found in gelatin extracted from skin bleached with H<sub>2</sub>O<sub>2</sub> at high concentrations (G6 and G8) might contribute to the alteration of charged residues of those gelatins. Differences in charge characteristics or distributions more likely determined functional properties of gelatins obtained from splendid squid skin subjected to bleaching using H<sub>2</sub>O<sub>2</sub> at various concentrations.

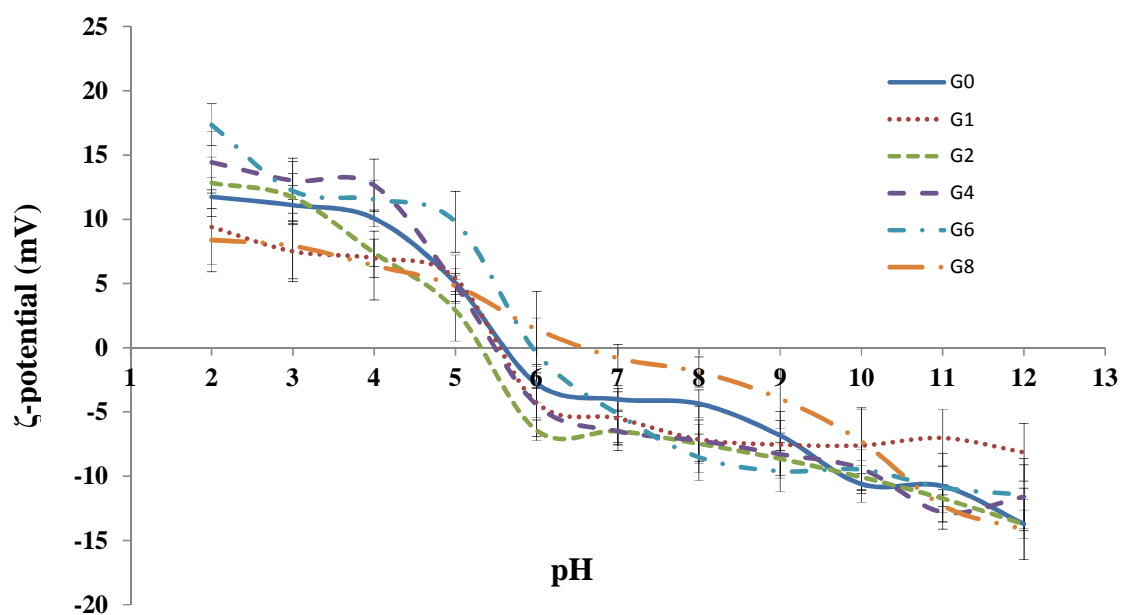


**Figure 20.**  $\zeta$ -potential of gelatins from the splendid squid skin bleached with H<sub>2</sub>O<sub>2</sub> at various concentrations. G0, G1, G2, G4, G6 and G8 denote the skin bleached with H<sub>2</sub>O<sub>2</sub> at levels of 0, 1, 2, 4, 6 and 8% (w/v), respectively. Bars represent the standard deviation (n=3).

#### 4.4.7 Colour

Differences in colour were observed between the gelatins from splendid squid skin bleached with H<sub>2</sub>O<sub>2</sub> at various concentrations (P<0.05) (Table 17). G2 showed the higher L\*-value (lightness) than others (P<0.05). The a\*-value (redness) of gelatin decreased with increasing H<sub>2</sub>O<sub>2</sub> concentrations. On the other hand, b\*-value (yellowness) of gelatin increased as the concentration of H<sub>2</sub>O<sub>2</sub> increased (P<0.05). The increase in b\*-value was coincidental with both decreases in carbonyl and free amino group contents (Table 17). The result suggested that those free amino groups could undergo browning reaction along with carbonyl compounds in gelatin during extraction. Among all gelatin samples, G2 showed the lowest ΔE\* (13.99). This was concomitant with the highest lightness (L\*-value). Perkins (1996) stated that hydroperoxyl anion is a strong nucleophile which, during bleaching, is able to break the chemical bonds that make up the chromophore. This might lead to the formation of different substances, which either did not contain a chromophore, or contained a chromophore that did not absorb visible light. Therefore, H<sub>2</sub>O<sub>2</sub> at a concentration of 2% was able to improve the colour of gelatin from splendid squid skin.

#### 4.4.8 Gel strength

Gel strength of gelatins from the splendid squid skin with various bleaching conditions is shown in Figure 21. Gel strength is one of the most important functional properties of gelatin. Gel strength of gelatin decreased with increasing H<sub>2</sub>O<sub>2</sub> concentrations used for bleaching. G0 showed the highest gel strength (234 g) (P<0.05). The difference in gel strength between the samples could be due to the differences in intrinsic characteristics, such as molecular-weight distribution and amino acid composition (Nagarajan *et al.*, 2012a). Protein fragments caused by degradation may reduce the ability of α-chains to anneal correctly by hindering the growth of the existing nucleation sites (Ledward, 1986). However, large protein aggregates also possess poor gel forming ability, in which the binding sites with adjacent protein molecules became lowered. When H<sub>2</sub>O<sub>2</sub> at high concentration was

used, it might induce both fragmentation and aggregation of gelatin molecules. As a result, gel forming ability turned to be inferior as evidenced by the lowered gel strength. Gelatins with higher content of  $\alpha$ -chain were reported to possess better functional properties including gelation, emulsifying and foaming properties (Gomez-Guillen *et al.*, 2002). In general, the formation of peptide fragments is associated with lower viscosity, low melting point, low setting point, high setting time, as well as decreased bloom strength of gelatin (Karim and Bhat, 2009).  $H_2O_2$  concentration used for bleaching directly determined gel forming ability of gelatin from squid skin.

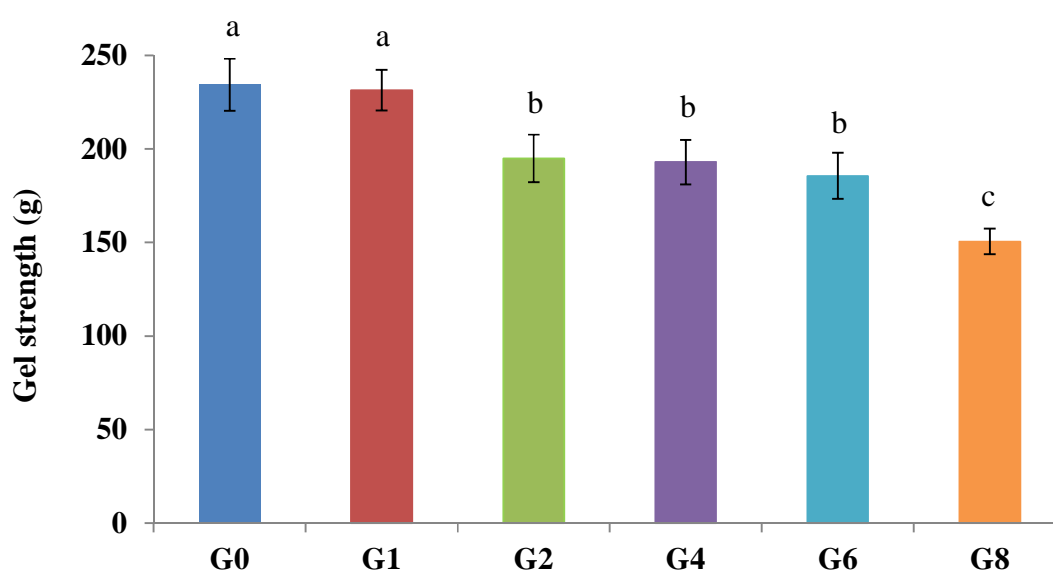


**Figure 21.** Gel strength of gelatins from the splendid squid skin bleached with  $H_2O_2$  at various concentrations. G0, G1, G2, G4, G6 and G8 denote the skin bleached with  $H_2O_2$  at levels of 0, 1, 2, 4, 6 and 8% (w/v), respectively. Bars represent the standard deviation (n=3). Different letters indicate significant differences ( $P < 0.05$ ) according to Duncan's multiple range tests. g: Maximum force in grams.



## **4.5 Conclusion**

Gelatin from splendid squid skin bleached with  $\text{H}_2\text{O}_2$  at a concentration of 2% had the improved colour.  $\text{H}_2\text{O}_2$  at higher concentration resulted in the increasing yield however negatively affected gelling property and colour. Therefore, bleaching of squid skin using 2%  $\text{H}_2\text{O}_2$  was recommended prior to gelatin extraction.

## CHAPTER 5

### FILM FORMING ABILITY OF GELATINS FROM SPLENDID SQUID (*LOLIGO FORMOSANA*) SKIN BLEACHED WITH HYDROGEN PEROXIDE

#### 5.1 Abstract

Properties of gelatin films from splendid squid (*Loligo formosana*) skin bleached with hydrogen peroxide ( $H_2O_2$ ) at various concentrations (0-8% w/v) were investigated. Tensile strength (TS) and water vapour permeability (WVP) of films decreased, but elongation at break (EAB) increased ( $P < 0.05$ ) as the concentration of  $H_2O_2$  increased. Among all films, that prepared from gelatin with 2%  $H_2O_2$  bleaching showed the lowest  $\Delta E^*$ -value (total colour difference), which was concomitant with the highest  $L^*$ -value (lightness). Generally, higher concentration of  $H_2O_2$  resulted in the increased  $b^*$ -value (yellowness) of resulting films. Electrophoretic study revealed that  $\alpha$ -chains of gelatin in films became lowered with increasing  $H_2O_2$  concentrations used for bleaching. Thermogravimetric analysis indicated that heat susceptibility and weight loss of different films varied with  $H_2O_2$  concentrations. Rougher surface was obtained in gelatin films prepared from skin bleached with  $H_2O_2$  concentrations above 4%. Thus, the concentrations of  $H_2O_2$  used for bleaching of squid skin prior to gelatin extraction directly affected the properties of corresponding gelatin films.

#### 5.2 Introduction

Nowadays, biodegradable films are gaining increasing attention as important non-toxic and eco-friendly packaging materials over synthetic thermoplastic films (Tongnuanchan *et al.*, 2012). Moreover, biodegradable materials have several desirable physico-chemical characteristics over synthetic counterpart.

Renewable biopolymers such as proteins, lipids and polysaccharides have been used as potential film-forming material (Tharanathan, 2003). Gelatin is a

well known biopolymer among the animal proteins for its film-forming ability and applicability for food packaging and storage (Gomez-Guillen *et al.*, 2009). Due to the constraints for the use of bovine and porcine gelatin associated with religious prohibition and possible disease transmission, gelatin from aquatic animal has gained increasing attention (Karim and Bhat, 2009). Gelatins from the skin of unicorn leatherjacket (Ahmad *et al.*, 2012), bigeye snapper (Rattaya *et al.*, 2009), and tilapia (Pranoto *et al.*, 2007) have been used for film preparation. Fish gelatins have been reported to exhibit good film-forming properties, yielding transparent, colourless, and highly extensible films (Jongjareonrak *et al.*, 2006b). Additionally, it can be used as the smart packaging, in which the antioxidants or antimicrobials can be incorporated (Jongjareonrak *et al.*, 2008; Tongnuanchan *et al.*, 2012). Owing to the superior oxygen barrier property, fish gelatin based film could prevent the lipid oxidation in food systems (Jongjareonrak *et al.*, 2006b). However, gelatin has the hydrophilicity in nature and the film from gelatin generally shows low water vapour barrier property. Furthermore, gelatin film has the relatively poor mechanical properties, in comparison with traditional synthetic polymeric films (McHugh and Krochta, 1994), which may limit its commercial use. To tackle this problem, several approaches have been developed to improve the barrier property, e.g. the incorporation of essential oils (Tongnuanchan *et al.*, 2012) and fatty acid (Limpisophon *et al.*, 2010). The mechanical properties of fish gelatin film were improved by the incorporation of nanoclays (Shakila *et al.*, 2012b).

Squid and cuttlefish have become the important fishery products in Thailand as well as other Southeast Asian countries, and are mainly exported worldwide (Hoque *et al.*, 2011b). During processing, skin is generated as a by-product with the low market value. Skin generally constitutes around 3-5% of total weight. Nevertheless, it can be used as alternative raw material for gelatin production. Gelatin has been extracted from the skins of splendid and giant squid (Gimenez *et al.*, 2009c; Nagarajan *et al.*, 2012a; Uriarte-Montoya *et al.*, 2011). Nevertheless, the pigments in squid skin pose a colour problem in the resulting gelatin. To tackle such a limitation, H<sub>2</sub>O<sub>2</sub> has been recently used for bleaching squid skin prior to extraction of gelatin (Nagarajan *et al.*, 2013a). However, no information regarding properties of gelatin

film from squid skin as affected by bleaching has been reported. Therefore, this study aimed to investigate the effects of H<sub>2</sub>O<sub>2</sub> at various concentrations for squid skin bleaching prior to gelatin extraction on properties of corresponding gelatin films.

## **5.3 Materials and methods**

### **5.3.1 Chemicals**

Bovine serum albumin (BSA) and  $\beta$ -mercaptoethanol ( $\beta$ -ME) were obtained from Sigma Chemical Co. (St. Louis, MO, USA). High molecular weight protein marker was purchased from GE Healthcare UK (Little Chalfont, UK). Hydrogen peroxide (H<sub>2</sub>O<sub>2</sub>) (30.96% w/v), glycerol and acetic acid were procured from Merck (Darmstadt, Germany). Sodium dodecyl sulphate (SDS), Coomassie Blue R-250 and *N,N,N',N'*-tetramethyl ethylene diamine (TEMED) were obtained from Bio-Rad Laboratories (Hercules, CA).

### **5.3.2 Collection and preparation of squid skin**

The skin of fresh splendid squid (*Loligo formosana*) was obtained from Sea Wealth Frozen Food Co., Ltd., Songkhla, Thailand and stored in ice using a skin/ice ratio of 1:2 (w/w). The sample was transported to the Department of Food Technology, Prince of Songkla University, Hat Yai, Thailand within 2 h. Upon arrival, the skin was cleaned and washed with iced tap water (0-2 °C). The skin was then cut into small pieces (0.5x0.5 cm<sup>2</sup>), placed in polyethylene bags and stored at -20 °C until use. The skin was stored for not more than 2 months.

### **5.3.3 Extraction of gelatin from squid skin**

Gelatin extraction was performed following the method of Aewsiri *et al.* (2009) and Nagarajan *et al.* (2013a) with a slight modification. Prior to gelatin extraction, the prepared skin was soaked in 0.05 M NaOH with a skin/solution ratio of 1:10 (w/v). The mixture was stirred continuously for 6 h at room temperature at a speed of 150 rpm using an overhead stirrer equipped with a propeller (RW 20.n, IKA-Werke GmbH & CO.KG, Staufen, Germany). The alkaline solution was changed

every 90 min to remove non collagenous proteins and pigments. Alkaline-treated skin was then washed with tap water until the neutral or faintly basic pH of wash water was obtained. The skin was then soaked in 0, 1, 2, 4, 6 and 8% H<sub>2</sub>O<sub>2</sub> (w/v) solution with a skin/solution ratio of 1:10 (w/v) for 24 h with an occasional stirring at 4 °C. H<sub>2</sub>O<sub>2</sub> solution was changed every 12 h to bleach the skin. Bleached skin was washed thoroughly with a running tap water.

To extract gelatin, the bleached skin was soaked in distilled water at 60 °C using a bleached skin/water ratio of 1:10 (w/v) in a temperature-controlled water bath (W350, Memmert, Schwabach, Germany) for 12 h with a continuous stirring at a speed of 150 rpm. The mixture was then filtered using two layers of cheese cloth. The filtrate was further filtered using a Whatman No. 4 filter paper (Whatman International, Ltd., Maidstone, UK) with the aid of JEIO Model VE-11 electric aspirator (JEIO TECH, Seoul, Korea). The resultant filtrate was freeze-dried using a Scanvac Model CoolSafe 55 freeze dryer (CoolSafe, Lyngø, Denmark). The freeze-dried gelatins extracted from the skin bleached at various concentrations of H<sub>2</sub>O<sub>2</sub> were referred to as 'G0', 'G1', 'G2', 'G4', 'G6' and 'G8', respectively. 'G0', 'G1', 'G2', 'G4', 'G6' and 'G8' contained 94.93, 97.94, 97.58, 96.95, 94.98 and 94.53% protein (dry weight basis), respectively as analysed by the Kjeldhal method (AOAC, 2000).

#### 5.3.4 Preparation of gelatin films

Gelatin films were prepared as per the method of Nagarajan *et al.* (2012b) with a slight modification. The freeze-dried gelatins extracted from the skin bleached at various concentrations of H<sub>2</sub>O<sub>2</sub> were used for film preparation. Firstly, film forming solutions (FFS) were prepared by mixing the freeze-dried gelatins with distilled water to obtain the protein concentration of 3% (w/v). Thereafter, glycerol (25% of protein) was added into FFS as a plasticiser. FFS was degassed using the sonicating bath (S 30 H; Elmasonic, Singen, Germany) for 10 min. FFS (4 ± 0.01 g) was then cast onto a rimmed silicone resin plate (5 × 5 cm<sup>2</sup>), air-blown for 12 h at 25 °C, followed by drying in an environmental chamber (Binder GmbH, Tuttlingen, Germany) at 25 ± 0.5 °C and 50 ± 5% relative humidity (RH) for 24 h. Dried film

samples were manually peeled off and referred to as 'F0', 'F1', 'F2', 'F4', 'F6' and 'F8', respectively. All films were analysed.

### **5.3.5 Analyses**

Prior to testing, film samples were conditioned for 48 h at  $50 \pm 5\%$  relative humidity (RH) and  $25 \pm 0.5$  °C. For ATR-FTIR, SEM and TGA studies, films were conditioned in a desiccator containing dried silica gel for 3 weeks to minimise the plasticising effect of water at room temperature (28-30 °C) to obtain the most dehydrated films.

#### **5.3.5.1 Thickness**

The thickness of ten film samples of each treatment was measured using a digital micrometer (Mitutoyo, Model ID-C112PM, Serial No. 00320, Mituyoto Corp., Kawasaki-shi, Japan). Ten random locations around each film sample were used for determination of thickness.

#### **5.3.5.2 Mechanical properties**

Tensile strength (TS) and elongation at break (EAB) of film samples were determined as described by Iwata *et al.* (2000) using the Universal Testing Machine (Lloyd Instrument, Hampshire, UK). The test was performed in the controlled room at 25°C and  $50 \pm 5\%$  RH. Ten film samples ( $2 \times 5$  cm<sup>2</sup>) with the initial grip length of 3 cm were used for testing. The film samples were clamped and deformed under tensile loading using a 100 N load cell with the cross head speed of 30 mm/min until the samples were broken. The maximum load and the final extension at break were used for calculation of TS and EAB, respectively.

#### **5.3.5.3 Water Vapour Permeability**

Water vapour permeability (WVP) was measured using a modified ASTM (American Society for Testing and Materials, 1989) method as described by Shiku *et al.* (2004). The film samples were sealed on an aluminium permeation cup containing dried silica gel (0% RH) with silicone vacuum grease and rubber gasket.

The cups were placed at 30 °C in a desiccator containing the distilled water, followed by weighing after every 1 h intervals for up to 8 h. Five film samples were used for WVP testing. WVP of the film was calculated as follows:

$$\text{WVP (gmm}^{-2}\text{s}^{-1}\text{Pa}^{-1}) = w/lA^{-1} t^{-1} (P_2 - P_1)^{-1}$$

where,  $w$  is the weight gain of the cup (g);  $l$  is the film thickness (m);  $A$  is the exposed area of film (m<sup>2</sup>);  $t$  is the time of gain (s);  $(P_2 - P_1)$  is the vapour pressure difference across the film (Pa).

#### 5.3.5.4 Colour

Colour of five film samples was determined using a CIE colourimeter (Hunter associates laboratory, Inc., Reston, VA, USA). Colour of the film was expressed as  $L^*$ - (lightness or brightness),  $a^*$ - (redness or greenness) and  $b^*$ - (yellowness or blueness) values. Total difference in colour ( $\Delta E^*$ ) was calculated according to the following equation (Gennadios *et al.*, 1996).

$$\Delta E^* = \sqrt{(\Delta L^*)^2 + (\Delta a^*)^2 + (\Delta b^*)^2}$$

where,  $\Delta L^*$ ,  $\Delta a^*$  and  $\Delta b^*$  are the differences between the corresponding colour parameter of the sample and that of white standard ( $L^*= 92.83$ ,  $a^*= -1.28$  and  $b^*= 0.52$ ).

#### 5.3.5.5 Light transmission and transparency

Light transmission in ultraviolet (UV) and visible ranges of five films was measured at selected wavelengths between 200 and 800 nm, using a UV-Visible spectrophotometer (Model UV-1800, Shimadzu, Kyoto, Japan) according to the method of Jongjareonrak *et al.* (2008). The transparency value of film was calculated by the following equation (Han and Floros, 1997).

$$\text{Transparency value} = (-\log T_{600})/x$$

where,  $T_{600}$  is the fractional transmittance at 600 nm and  $x$  is the film thickness (mm). The higher transparency value represents the lower transparency of films.

#### **5.3.5.6 Electrophoretic analysis**

SDS-polyacrylamide gel electrophoresis (SDS-PAGE) was performed by the method of Laemmli (1970). Gelatin film samples were dissolved in 5% SDS and the mixtures were incubated at 85 °C for 1 h. The mixtures were centrifuged at 3,500xg for 5 min at room temperature using a microcentrifuge (MIK-RO20, Hettich Zentrifugan, Tuttlingen, Germany) to remove undissolved debris. Protein content in the supernatant of all samples was determined using the Biuret method (Robinson & Hogden, 1940). Gelatin film samples were mixed at a 1:1 (v/v) ratio with the sample buffer (0.5 M Tris-HCl, pH 6.8, containing 4% SDS and 20% glycerol). Samples (20 µg protein) were loaded onto polyacrylamide gels comprising a 7.5% running gel and a 4% stacking gel and subjected to electrophoresis at a constant current of 15 mA/gel using a Mini Protean II unit (Bio-Rad Laboratories, Inc., Richmond, CA, USA). After electrophoresis, the gel was stained with 0.05% (w/v) Coomassie Blue R- 250 in 15% (v/v) methanol and 5% (v/v) acetic acid and destained with 30% (v/v) methanol and 10% (v/v) acetic acid. Relative mobility ( $R_f$ ) of protein band was calculated and the molecular weight of the protein was calculated from the plot between  $R_f$  and log (MW) of standards.

#### **5.3.5.7 Attenuated total reflectance-Fourier transform infrared (ATR-FTIR) spectroscopic analysis**

Gelatin film samples were subjected to FTIR analysis using a Bruker Model EQUINOX 55 FTIR spectrometer (Bruker, Ettlingen, Germany) equipped with a deuterated L-alanine triglycine sulphate (DLATGS) detector as described by Nuthong, Benjakul, and Prodpran (2009). The horizontal attenuated total reflectance (HATR) accessory was mounted in the sample compartment. The internal reflection crystal (Pike Technologies, Madison, WI, USA), made of zinc selenide, had a 45° angle of incidence of the IR beam. Spectra were acquired in the IR range of 4000–650  $\text{cm}^{-1}$  (mid-IR region) at 25 °C. Automatic signals were collected in 32 scans at a



resolution of  $4\text{ cm}^{-1}$  and were ratioed against a background spectrum recorded from the clean and empty cell at  $25\text{ }^{\circ}\text{C}$ . Analysis of spectral data was carried out using the OPUS 3.0 data collection software programme (Bruker, Ettlingen, Germany). Prior to data analysis, the spectra were baseline corrected and normalised.

#### **5.3.5.8 Thermo-gravimetric analysis (TGA)**

Dried film samples were scanned using a thermogravimetric analyser (TGA-7, Perkin Elmer, Norwalk, CT, USA) from  $50$  to  $600\text{ }^{\circ}\text{C}$  using a heating rate of  $10\text{ }^{\circ}\text{C}/\text{min}$  (Nuthong *et al.*, 2009). Nitrogen was used as the purge gas at a flow rate of  $20\text{ ml}/\text{min}$ .

#### **5.3.5.9 Microstructure analysis**

Microstructure of upper surface and cryo-fractured cross-section of the gelatin film samples was visualised using a scanning electron microscope (SEM) (Quanta 400, FEI, Praha, Czech Republic) at an accelerating voltage of  $15\text{ kV}$  as described by Hoque *et al.* (2011b). The gelatin film samples were cryo-fractured by immersion in liquid nitrogen. Prior to visualisation, the film samples were mounted on brass stub and sputtered with gold in order to make the sample conductive, and photographs were taken at  $5000\times$  magnification for surface. For cross-section, cryo-fractured films were mounted around stubs perpendicularly using double sided adhesive tape, coated with gold and observed at the  $4000\times$  magnification.

#### **5.3.6 Statistical analyses**

All experiments were performed in triplicates ( $n=3$ ) and a completely randomised design (CRD) was used. Analysis of variance (ANOVA) was performed and the mean comparisons were done by Duncan's multiple range tests (Steel and Torrie, 1980). Data are presented as mean  $\pm$  standard deviation and the probability value of  $P<0.05$  was considered as significant. Statistical analysis was performed using the Statistical Package for Social Sciences (SPSS 17.0 for windows, SPSS Inc., Chicago, IL, USA).

## 5.4 Results and discussion

### 5.4.1 Thickness

Thickness of gelatin films from the splendid squid skin subjected to bleaching with  $H_2O_2$  at various concentrations is shown in Table 18. Thickness of gelatin films prepared from skin bleached with  $H_2O_2$  above 1% was higher than that of control gelatin film (F0), prepared from skin without bleaching ( $P < 0.05$ ). It was noted that F4, F6 and F8 showed the similar thickness ( $P > 0.05$ ). Increased thickness with increasing concentration of  $H_2O_2$  might be due to protrusion of the resulting films.  $H_2O_2$  plausibly induced the oxidation of proteins, in which the aggregation of proteins took place to some extent. Those aggregates were not able to align themselves into the compact network, as indicated by the increased thickness (Ahmad *et al.*, 2012). Therefore, the thickness of gelatin films was affected by the levels of  $H_2O_2$  used for bleaching of skin prior to gelatin extraction.

### 5.4.2 Mechanical properties

Mechanical properties of gelatin films from the splendid squid skin with different bleaching conditions are shown in Table 18. Tensile strength (TS) of gelatin films decreased with increasing concentration of  $H_2O_2$ . On the other hand, elongation at break (EAB) of gelatin films increased as  $H_2O_2$  concentration used for skin bleaching increased ( $P < 0.05$ ). However, the use of  $H_2O_2$  at low concentration (1 or 2%) for skin bleaching had no impact on TS of resulting film. An increase in EAB was observed in F6 and F8 samples, compared with the control ( $P < 0.05$ ). Of all films, F8 showed the highest EAB ( $P < 0.05$ ). No difference in EAB between F4 and F6 was observed.  $H_2O_2$  is the powerful oxidising agent, which is able to produce the  $HO\cdot$  radicals and those radicals can oxidise most organic compounds including proteins (Kocha *et al.*, 1997). Several proteins including myosin (Liu and Xiong, 2000b), collagen and related substrates (Hawkins and Davies, 1997) and albumin (Kocha *et al.*, 1997) were reported to undergo oxidation in the presence of  $H_2O_2$ .  $H_2O_2$  caused the formation of highly reactive products, such as hydroperoxyl anion ( $HOO^-$ ), hydroperoxyl ( $HOO\cdot$ ) and hydroxyl ( $HO\cdot$ ) radicals, which are reactive toward proteins

(Perkins, 1996). Stadtman (2001) reported that high concentration of H<sub>2</sub>O<sub>2</sub> might contribute to the production of excessive amounts of the HO· radical, which most likely caused peptide cleavage of the glutamyl side chain and proline residue of the protein. In the present study, shorter chain peptides found in gelatin caused by fragmentation induced by H<sub>2</sub>O<sub>2</sub> at high levels might be associated with lower intermolecular interaction in the film matrix. This was more likely attributable to the weaker film network, as evidenced by the decreased TS and simultaneously increased EAB of films prepared from gelatin bleached with H<sub>2</sub>O<sub>2</sub> at high concentrations (F6 and F8). The results suggested that the mechanical properties of gelatin films were largely affected by the concentration of H<sub>2</sub>O<sub>2</sub> used for skin bleaching.

**Table 18.** Tensile strength (TS), elongation at break (EAB), water vapour permeability (WVP) and thickness of gelatin films from the splendid squid skin bleached with H<sub>2</sub>O<sub>2</sub> at various concentrations

<b>Film Samples</b>	<b>TS (MPa)</b>	<b>EAB (%)</b>	<b>WVP (X10<sup>-11</sup> gmm<sup>-2</sup>s<sup>-1</sup>Pa<sup>-1</sup>)</b>	<b>Thickness (mm)</b>
<b>F0</b>	33.51±3.46a	5.74±0.76c	4.01±0.04a	0.025±0.0033c
<b>F1</b>	31.09±2.74a	5.39±0.95c	3.75±0.01ab	0.031±0.0038b
<b>F2</b>	28.14±1.48a	7.33±0.96c	3.33±0.04abc	0.032±0.0049b
<b>F4</b>	22.06±3.31b	10.52±5.88bc	3.13±0.05bc	0.040±0.0040a
<b>F6</b>	21.33±1.01b	14.6±4.31b	2.72±0.05c	0.042±0.0035a
<b>F8</b>	12.20±1.74c	21.86±2.85a	2.81±0.04c	0.040±0.0042a

Mean ± SD (n=3).

Different letters in the same column indicate significant differences (P<0.05).

### 5.4.3 Water Vapour Permeability (WVP)

WVP of gelatin films from the splendid squid skin subjected to bleaching using  $H_2O_2$  at various concentrations is shown in Table 18. Gelatin film from unbleached skin (F0) had similar WVP to those of F1 and F2 ( $P>0.05$ ). It was found that F6 and F8 had the lower WVP than F0 and F1 ( $P<0.05$ ), but their WVP was not different from those of F2 and F4. This result suggested that films of gelatin extracted from skin bleached with  $H_2O_2$  at high concentration had the lower hydrophilicity. From our previous study, the highest free amino group and carbonyl group contents were observed for unbleached squid skin gelatin (Nagarajan *et al.*, 2013a). The decreases in free amino group and carbonyl group contents were found in gelatin prepared from squid skin bleached with  $H_2O_2$  at high concentrations. Hoque *et al.* (2011a) stated that carbonyl and amino groups with increasing numbers could form hydrogen bonds with the water molecules to a higher degree. This resulted in the increased hydrophilicity of the resulting films.  $OH^\cdot$  radicals, generated from  $H_2O_2$  might cause a wide variety of reactions on protein molecules, including modification of amino acids, fragmentation and polymerisation of peptide chains (Liu and Xiong, 2000b). Those changes might be associated with the lowering of hydrophilic domains of gelatins extracted from skin bleached with high concentration of  $H_2O_2$ . As a result, the migration of water molecules in those gelatin films could be lowered, thus decreasing WVP. Therefore, gelatin films had varied WVP, depending on the concentrations of  $H_2O_2$  used for skin bleaching prior to gelatin extraction.

### 5.4.4 Colour

Differences in colour were observed amongst gelatin films from the splendid squid skin bleached with  $H_2O_2$  at various concentrations ( $P<0.05$ ) (Table 19). Gelatin films from squid skin bleached with 2%  $H_2O_2$  (F2) showed higher  $L^*$ - value (lightness) than F0 and F1 ( $P<0.05$ ), but had no differences in  $L^*$ - value, in comparison with F4, F6 and F8. The  $a^*$ - value (redness) of gelatin films decreased when skin was bleached with  $H_2O_2$ .  $H_2O_2$  in the range of 2-8% gave similar  $a^*$ - value for films ( $P>0.05$ ), while  $b^*$ - value (yellowness) of gelatin films increased as the

concentration of H<sub>2</sub>O<sub>2</sub> increased (P<0.05). The highest *b*\*- value was obtained in F8 (P<0.05). Among all gelatin samples, F2 showed the lowest  $\Delta E^*$  (17.70) (P<0.05). H<sub>2</sub>O<sub>2</sub> at high concentration was able to oxidise the pigments as shown by the lower *a*\*- value. However, H<sub>2</sub>O<sub>2</sub> at high level induced the formation of yellow films. Free amino group and carbonyl group in F8 sample more likely undergo browning reaction during film casting and drying (Ajandouz and Puigserver, 1999). Therefore, H<sub>2</sub>O<sub>2</sub> at an appropriate concentration was able to improve the colour of gelatin films from splendid squid skin, whereas H<sub>2</sub>O<sub>2</sub> at high level caused the yellowish colour in gelatin films.

#### 5.4.5 Light transmission and transparency values

Transmission of UV and visible light at selected wavelengths in the range of 200-800 nm of gelatin films from the splendid squid skin bleached with H<sub>2</sub>O<sub>2</sub> at various concentrations is shown in Table 19. Low UV light transmission was observed at 200 and 280 nm for all films. However, slightly higher transmission at 280 nm was found for F0, compared with those from gelatin with bleaching. Generally, gelatin films exhibited low light transmission in the UV range (Jongjareonrak *et al.*, 2008). Gelatin film effectively prevents the lipid oxidation, which is induced by UV light (Limpisophon *et al.*, 2009). Light transmission in visible range (350-800 nm) of films ranged from 11.21 to 86.44%. Similar light transmission in visible range of 400-800 nm was found between F0 and F2. However, at 350 and 400 nm, the former showed the high transmission. Decreasing light transmission of films prepared from gelatin bleached with increasing concentration of H<sub>2</sub>O<sub>2</sub> was in agreement with the increased *b*\*- values of gelatin films (Table 19). The increased yellowness and opaqueness of those films might contribute to lowering light transmission of those films. The results suggested that the concentration of H<sub>2</sub>O<sub>2</sub> used for skin bleaching prior to gelatin extraction had an impact on light transmission and transparency of resulting films.

**Table 19.** Colour, light transmittance and transparency values of gelatin films from the splendid squid skin bleached with H<sub>2</sub>O<sub>2</sub> at various concentrations

Film samples	Colour				Transmittance (%)								Transparency values
	L*	a*	b*	ΔE*	200	280	350	400	500	600	700	800	
<b>F0</b>	76.77±2.75c	6.26±1.44a	11.49±1.92d	20.86±3.66cd	0.00	8.19	45.86	58.79	69.66	78.64	84.07	86.05	4.60±0.47a
<b>F1</b>	78.41±0.95bc	2.90±0.42b	14.46±1.20d	22.63±1.58bc	0.02	0.07	12.28	30.29	56.72	70.91	80.30	83.72	3.72±0.52b
<b>F2</b>	82.03±1.30a	1.28±0.52c	17.32±1.51c	17.70±2.03d	0.00	3.24	35.24	53.78	72.20	80.01	84.58	86.44	3.54±0.03b
<b>F4</b>	79.81±1.85ab	1.47±0.71c	21.73±1.31b	25.04±3.84ab	0.00	0.42	16.93	35.83	59.85	70.22	76.02	78.87	3.95±0.14b
<b>F6</b>	79.75±1.89ab	1.74±0.81c	21.04±1.91b	24.53±2.71abc	0.00	0.41	18.38	37.91	61.90	72.13	77.89	80.60	3.99±0.30ab
<b>F8</b>	80.0±1.50ab	1.17±0.60c	24.55±2.81a	27.34±3.22a	0.01	0.10	11.21	30.03	57.96	69.94	76.22	79.25	4.11±0.23ab

Mean ± SD (n=3).

Different letters in the same column indicate significant differences (P<0.05).

### 5.4.6 Protein patterns

Protein patterns of gelatin films from the splendid squid skin bleached with  $H_2O_2$  at different concentrations are illustrated in Figure 22. Gelatin films were composed of  $\alpha$ -chains with the MW of 121-128 kDa. Amongst all samples, F0 had the highest band intensity of  $\alpha$ -chains as well as proteins with MW of 76 and 70 kDa. No proteins with MW of 76 and 70 kDa were retained in gelatin films prepared from squid skin bleached with  $H_2O_2$ , regardless of concentration used. It was postulated that those proteins might be susceptible to either degradation or polymerisation induced by  $H_2O_2$ . When  $H_2O_2$  was used for bleaching, it might induce both fragmentation and polymerisation (Liu and Xiong, 2000b; Stadtman, 2001). Molecular distribution as affected by  $H_2O_2$  used for skin bleaching was an important factor determining the properties of resulting films.

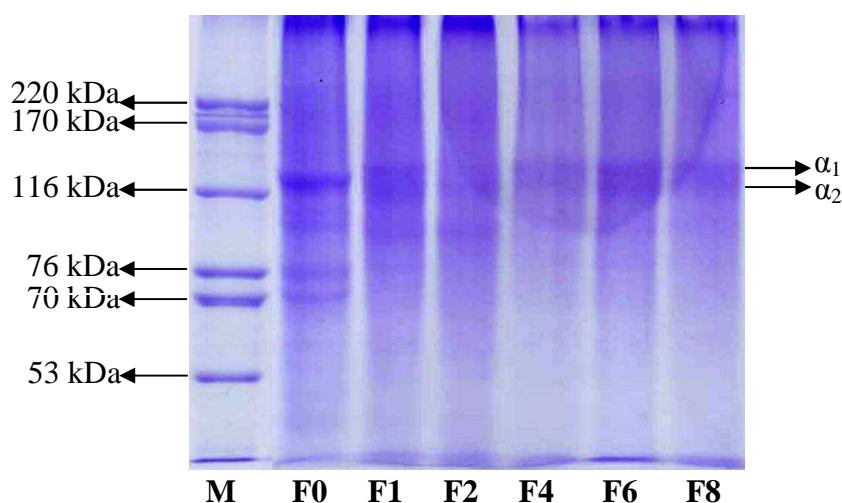


**Figure 22.** Protein patterns of gelatin films from the splendid squid skin bleached using  $H_2O_2$  at various concentrations. M: High molecular weight markers. F0, F1, F2, F4, F6 and F8 denote the gelatin films from splendid squid skin bleached with  $H_2O_2$  at levels of 0, 1, 2, 4, 6 and 8%, respectively.

### 5.4.7 FT-IR spectra analysis

FTIR spectra of gelatin films from the splendid squid skin subjected to bleaching with H<sub>2</sub>O<sub>2</sub> at various concentrations are depicted in Figure 23a. FTIR spectroscopy has been used to monitor the functional groups and secondary structure of gelatin (Muyonga *et al.*, 2004c) and interaction of gelatins in the film (Jongjareonrak *et al.*, 2008). All gelatin samples had the major peaks in amide region. Amide-I peak (C=O stretching vibration coupled with the C-N stretch and CCN deformation) was found for F0, F1, F2, F4, F6 and F8 at the wavenumber of 1642.95, 1647.71, 1641.51, 1642.74, 1642.00 and 1644.47 cm<sup>-1</sup>, respectively. The result suggested that the hydrogen bonding and the conformation of protein structure might be slightly different (Bandekar, 1992; Uriarte-Montoya *et al.*, 2011). The amide I is the most useful peak for infrared analysis of the secondary structure of protein including gelatin (Surewicz and Mantsch, 1988). The characteristic absorption peaks of F0, F1, F2, F4, F6 and F8 in amide-II region was noticeable at the wavenumber of 1548.40, 1553.07, 1546.71, 1551.04, 1550.92 and 1549.20 cm<sup>-1</sup>, respectively. The amide-II vibration mode is attributed to combination of the N-H in plane bend and the C-N stretching vibration with smaller contributions from the C-O in plane bend and the C-C and N-C stretching vibrations (Jackson *et al.*, 1995). In addition, amide-III peak (the combination peaks between C-N stretching vibrations and N-H deformation from amide linkages as well as absorptions arising from wagging vibrations from CH<sub>2</sub> groups from the glycine backbone and proline side-chains) was detected at the wavenumber of 1239.57, 1240.89, 1242.05, 1240.06, 1241.23 and 1238.40 cm<sup>-1</sup> for F0, F1, F2, F4, F6 and F8, respectively. Film obtained from cuttlefish skin gelatin treated with H<sub>2</sub>O<sub>2</sub> at all levels showed similar spectra for amide-I, amide-II and amide-III at their corresponding wavenumbers (Hoque *et al.*, 2011b). Pranoto *et al.* (2007) also reported that amide-I, amide-II and amide-III peaks were found at the wavenumbers of 1650, 1550 and 1240 cm<sup>-1</sup>, respectively. The peak situated around 1033 cm<sup>-1</sup> might be related to the interactions arising between plasticiser (OH group of glycerol) and film structure (Bergo and Sobral, 2007).



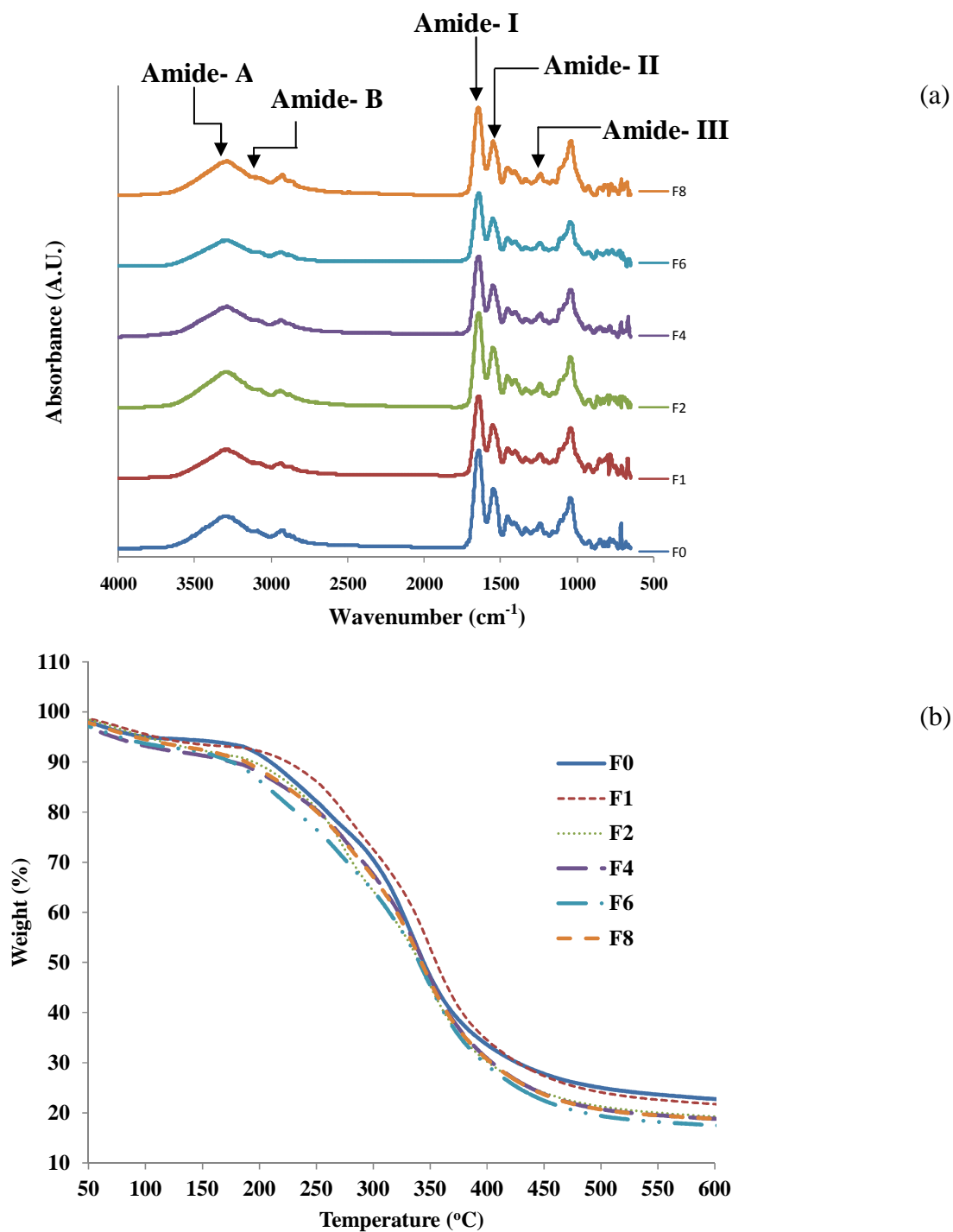


**Figure 23.** ATR-FTIR spectra (a) and TGA curves (b) of gelatin films from splendid squid skin bleached with  $\text{H}_2\text{O}_2$  at various concentrations. F0, F1, F2, F4, F6 and F8 denote the gelatin films from splendid squid skin bleached with  $\text{H}_2\text{O}_2$  at levels of 0, 1, 2, 4, 6 and 8%, respectively.

Amide-A peak (NH-stretching coupled with hydrogen bonding) appeared at the wavenumber of 3298.27, 3294.20, 3297.07, 3290.48, 3297.00 and 3286.34  $\text{cm}^{-1}$  for F0, F1, F2, F4, F6 and F8, respectively. When the N–H group of a peptide is involved in H-bond, the position shifts to lower wavenumbers (Doyle *et al.*, 1975). Amide-B was observed at the wavenumber of 3129.58, 3115.94, 3096.20, 3097.46, 3097.33 and 3090.18  $\text{cm}^{-1}$  for F0, F1, F2, F4, F6 and F8, respectively, corresponding to the asymmetric stretching vibration of =C–H as well as  $-\text{NH}_3^+$ . The amplitude of amide-A and amide-B peak was higher for F0 than others. These results suggested that  $\text{NH}_2$  group of gelatin prepared from skin bleached with  $\text{H}_2\text{O}_2$  at high level could undergo glycation with carbonyl group formed via protein oxidation (Nagarajan *et al.*, 2013a). This was confirmed by the increase in  $b^*$ -value of those films. Similar result was observed for gelatin films from the cuttlefish skin as affected by  $\text{H}_2\text{O}_2$  and Fenton's reagent added in FFS (Hoque *et al.*, 2011b). Liu and Xiong (2000b) reported that the hydroxyl radical can modify the primary structure of proteins. For F0, F1, F2, F4, F6 and F8, the peaks with the wavenumber of 2853.01, 2878.09, 2878.63, 2880.60, 2887.10 and 2855.86  $\text{cm}^{-1}$  (symmetrical) or 2927.27, 2940.23, 2937.62, 2933.33, 2933.88 and 2924.82  $\text{cm}^{-1}$  (asymmetrical) were observed, respectively. It represents C–H stretching vibrations of the  $-\text{CH}_2$  groups (D'Souza *et al.*, 2008). The lower wavenumber of F0 suggested that gelatin from skin without  $\text{H}_2\text{O}_2$  bleaching more likely underwent association between protein molecules more effectively. This was in agreement with the higher TS of F0 (Table 18). Thus, the secondary structure and functional group as elucidated by the changes in FTIR spectra, especially for the amide-A and amide-B regions of gelatin films from squid skin were influenced to some extent by  $\text{H}_2\text{O}_2$  concentration used for skin bleaching before gelatin extraction.

#### 5.4.8 Thermogravimetric analysis

TGA thermograms revealing thermal degradation behaviour of gelatin films obtained from the splendid squid skin subjected to bleaching using  $\text{H}_2\text{O}_2$  at various concentrations is illustrated in Figure 23b. Their corresponding degradation temperatures ( $T_d$ ) and weight loss ( $\Delta w$ ) are presented in Table 20. Three stages of

weight loss were observed in all films. First stage of weight loss ( $\Delta w_1 = 5.40\text{-}8.38\%$ ) was observed for all films approximately at temperature ( $T_{d1}$ ) of  $64.28\text{-}80.01\text{ }^\circ\text{C}$ , mostly associated with the continuous loss of free water absorbed in the film. Similar results were observed for films from unicorn leather jacket skin gelatin (Ahmad *et al.*, 2012). F0 showed the lower weight loss (5.40%) with the higher  $T_{d1}$  ( $70.02\text{ }^\circ\text{C}$ ) than F8 (7.01% of weight loss with  $T_{d1}$  of  $66.66\text{ }^\circ\text{C}$ ). Alteration of proteins induced by  $\text{H}_2\text{O}_2$  might lower water binding sites or domains via H-bond. For all films, the second stage of weight loss ( $\Delta w_2 = 17.92\text{-}27.76\%$ ) was observed approximately at temperature ( $T_{d2}$ ) of  $188.10\text{-}231.10\text{ }^\circ\text{C}$ . The result was in agreement with Tongnuanchan *et al.* (2012) who reported the degradation temperature of fish gelatin film in the range of  $200\text{-}240\text{ }^\circ\text{C}$ . This change was mostly associated with the loss of glycerol compound (plasticiser) and smaller size protein fraction, as well as structurally bound water. The third stage of weight loss ( $\Delta w_3 = 44.77\text{-}54.06\%$ ) was observed approximately at temperature ( $T_{d3}$ ) of  $306.00\text{-}330.18\text{ }^\circ\text{C}$ , mostly associated with the loss of high molecular weight protein fractions. A similar result was observed in cuttlefish skin gelatin films (Hoque *et al.*, 2011b). F0 showed higher weight loss (54.06%) with lower  $T_{d3}$  ( $306.0\text{ }^\circ\text{C}$ ) than others. The result revealed that gelatin film from skin bleached with  $\text{H}_2\text{O}_2$  showed higher heat resistance than did the control film (F0). It was implied that  $\text{H}_2\text{O}_2$  could in part induce the polymerisation of protein chains via radicals formed or glycation. However, a lower  $\Delta w_3$  was observed for gelatin films from skin bleached with  $\text{H}_2\text{O}_2$ , compared to that of the control film. Additionally, all films had residual mass (representing char content) at  $600\text{ }^\circ\text{C}$  in the range of  $17.70\text{-}22.62\%$ . Furthermore, it was plausible that  $\text{H}_2\text{O}_2$  also contributed to fragmentation, in which those small fragments had lower thermal stability. Liu and Xiong (2000b) and Stadtman (2001) have been reported that  $\text{H}_2\text{O}_2$  could induce both fragmentation and polymerisation. TGA study clearly showed that  $\text{H}_2\text{O}_2$  at various concentrations led to different thermal stability of resulting gelatin films.

**Table 20.** Thermal degradation temperature (Td, °C) and weight loss ( $\Delta w$ , %) of gelatin films from the splendid squid skin bleached with H<sub>2</sub>O<sub>2</sub> at various concentrations

Film samples	$\Delta_1$		$\Delta_2$		$\Delta_3$		Residue (%)
	Td <sub>1, onset</sub>	$\Delta w_1$	Td <sub>2, onset</sub>	$\Delta w_2$	Td <sub>3, onset</sub>	$\Delta w_3$	
<b>F0</b>	70.02	5.40	189.20	17.92	306.00	54.06	22.62
<b>F1</b>	79.75	6.70	227.37	20.07	330.18	51.64	21.59
<b>F2</b>	80.01	8.38	231.10	27.76	328.27	44.77	19.09
<b>F4</b>	64.28	7.63	221.40	20.99	319.21	52.37	19.01
<b>F6</b>	73.80	6.71	188.10	27.54	319.68	48.05	17.70
<b>F8</b>	66.66	7.01	205.45	21.26	320.14	52.90	18.83

$\Delta_1$ ,  $\Delta_2$  and  $\Delta_3$  denote the first, second and third stage weight loss, respectively of film during TGA heating scan.

#### 5.4.9 Microstructure

SEM micrographs of the surface (A) and cryo-fractured cross-section (B) of gelatin films prepared from the splendid squid skin subjected to bleaching with  $H_2O_2$  at various concentrations are shown in Figure 24. F0 had slightly coarser surface than other films. F1 and F2 had the compact, smooth and homogeneous surface, indicating an ordered film matrix. These differences in microstructure of different films were caused by the varying arrangements of protein molecules during film formation (Ahmad *et al.*, 2012). These results suggested that the matrix of film was governed by  $H_2O_2$  used for skin bleaching to some degree. An oxidising agent or radicals at proper concentration could render an ordered and fine film matrix (Hoque *et al.*, 2011b). Gelatin films prepared from squid skin bleached with  $H_2O_2$  at higher concentrations (F4, F6 and F8) showed protein aggregates on film surface. The excessive cross-linking induced by  $H_2O_2$  might lead to the formation of protein agglomerates.

For cross-section, gelatin film prepared from unbleached squid skin showed coarser film matrix with micro-voids and micro-cracks. A smoother and more compact structure was observed for F1 and F2 samples. This result suggested that  $HO\cdot$  radicals at appropriate level might induce cross-linking of gelatin molecules, in which the ordered matrix could be formed to a greater extent compared to others (Hoque *et al.*, 2011a). For F6 and F8, slightly coarser matrix was noticeable. Stadtman (2001) stated that  $HO\cdot$  radicals formed from  $H_2O_2$  caused both polymerisation and fragmentation of gelatin molecules. These carbonyl groups generated during protein oxidation might undergo Schiff base formation with the amino groups, in which protein crosslinks were most likely formed as the protein bundles or aggregates. The  $HO\cdot$  radical can abstract H atoms from amino acid residues to form carbon-centred radical derivatives, which can react with one another, to form C-C protein crosslinked products (Stadtman, 2001). Those aggregates likely yielded the film with a coarser and non-uniform network. Shakila *et al.* (2012b) also reported that protrusion of polymerised chains yields granular and coarser fish gelatin films. The microstructures

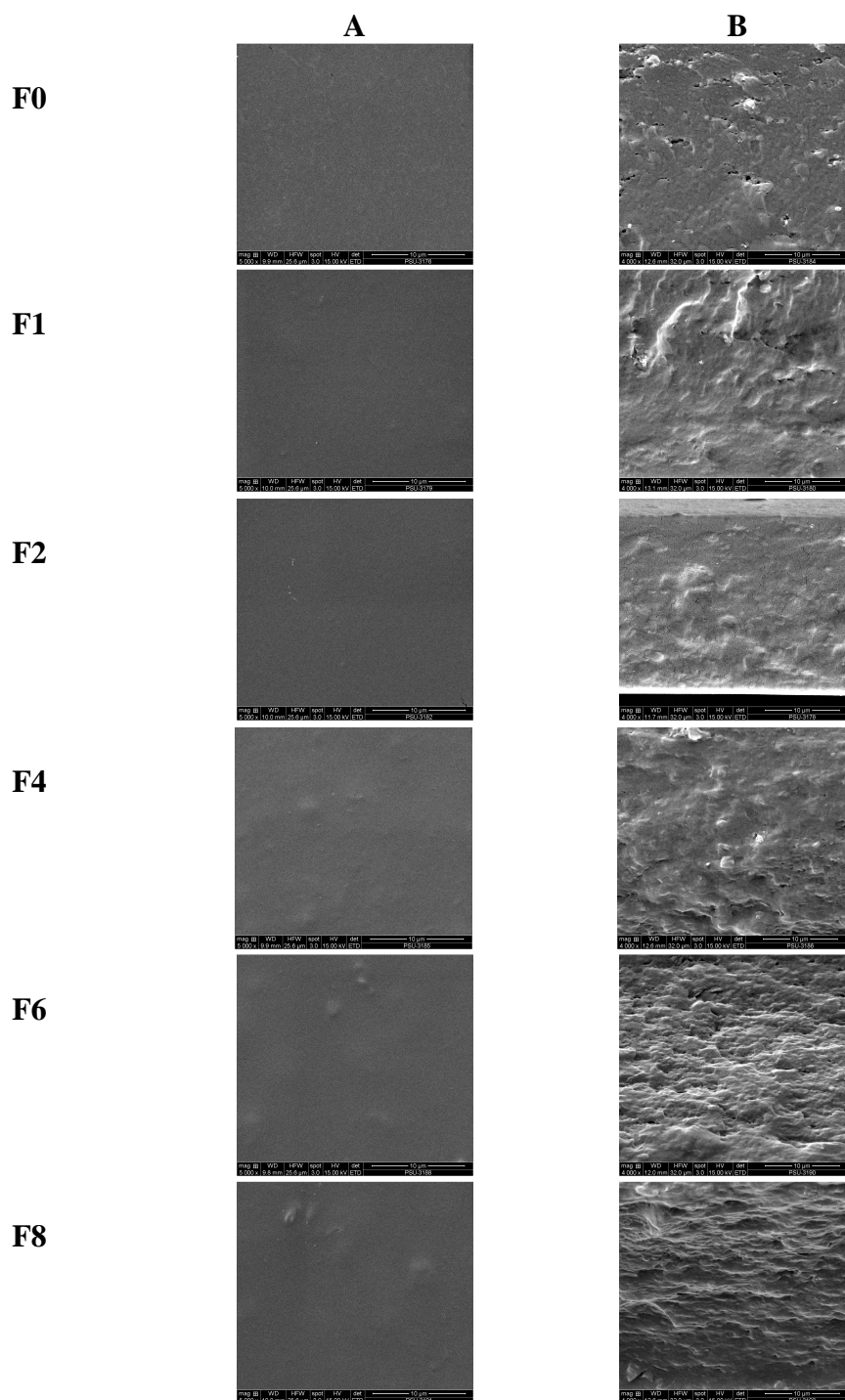


**Figure 24.** SEM micrographs of surface (A) and cryo-fractured cross-section (B) of gelatin films from the splendid squid skin bleached with H<sub>2</sub>O<sub>2</sub> at various concentrations. Magnification: 5000x and 4000x for surface and cross-section, respectively. F0, F1, F2, F4, F6 and F8 denote the gelatin films from splendid squid skin bleached with H<sub>2</sub>O<sub>2</sub> at levels of 0, 1, 2, 4, 6 and 8%, respectively.

of films were thus governed by molecular organisation in the film network, which depended on chain length of proteins and the interaction of proteins in film matrix.

## **5.5 Conclusion**

Gelatins from squid skin bleached using  $H_2O_2$  at various concentrations yielded the films with different properties. The colour of films from gelatin of splendid squid skin bleached with  $H_2O_2$  at an appropriate concentration was improved markedly. However, an excessive concentration of  $H_2O_2$  could cause the yellowish colour of the resulting films. Gelatin from squid skin bleached with  $H_2O_2$  at higher concentrations yielded the films with lower WVP but higher extensibility. Therefore, squid skin gelatin could serve as raw material for film formation when skin was bleached at 2%  $H_2O_2$  prior to gelatin extraction.

## CHAPTER 6

### CHARACTERISTICS OF BIO-NANOCOMPOSITE FILMS FROM TILAPIA SKIN GELATIN INCORPORATED WITH HYDROPHILIC AND HYDROPHOBIC NANOCCLAYS

#### 6.1 Abstract

Properties of films from tilapia skin gelatin incorporated with hydrophilic and hydrophobic montmorillonite (MMT) nanoclays at various levels (0-10%, w/w) were investigated. Generally, mechanical properties were improved by the addition of hydrophilic nanoclay (i.e., Cloisite Na<sup>+</sup>) in the range of 0.5-5% (w/w). The lowest water vapour permeability was observed for films incorporated with Cloisite Na<sup>+</sup> and Cloisite 20A at a level of 1% (w/w) (P<0.05). The lowest  $L^*$  and the highest  $\Delta E^*$  values were observed (P<0.05) when the film was incorporated with Cloisite 15A at 10% (w/w). Generally,  $b^*$  value (yellowness) of resulting films increased with increasing amount of all nanoclays (P<0.05). All films became less transparent with increasing levels of nanoclay incorporated (P<0.05). Wide angle X-ray diffraction and scanning electron microscopic analyses revealed the intercalated/exfoliated structure of nanocomposite gelatin-based films incorporated with hydrophilic and hydrophobic nanoclays. Homogeneity and smoothness of film surface decreased with the addition of both nanoclays as revealed by SEM micrographs. Thermogravimetric and differential scanning calorimetric analyses indicated that the incorporation of nanoclays enhanced the rigidity and heat stability of the gelatin-based films differently, depending on the types of MMT-nanoclay used. Thus, the types and levels of nanoclay incorporated directly affected the properties of tilapia skin gelatin films.

#### 6.2 Introduction

Gelatin is a biopolymer, commonly being known for its film-forming ability and applicability for food packaging (Gomez-Guillen *et al.*, 2009). Gelatins from aquatic animals are gaining attention due to health issues and religious constraints on gelatin from mammals (Karim and Baht, 2009). Because of its good



film-forming abilities, fish gelatin may be a good alternative to synthetic plastics for making packaging films to preserve food stuffs (Gomez-Guillen *et al.*, 2009). Owing to the superior oxygen barrier property, fish gelatin-based film could prevent lipid oxidation in food systems (Bigi *et al.*, 2000; Jongjareonrak *et al.*, 2008). Additionally, it can be used as a smart packaging material, in which antioxidants or antimicrobials can be incorporated (Gomez-Guillen *et al.*, 2007; Jongjareonrak *et al.*, 2006b). Although gelatin films have good mechanical properties, it could swell at high humid conditions, due to their hydrophilic nature. This is associated with loss in mechanical and barrier properties, thereby limiting their applications in food packaging (Martucci and Ruseckaite, 2009). To tackle this problem, gelatin-based films must be modified. Over the years, several approaches have been developed to improve the barrier properties such as, incorporation of essential oils (Gomez-Estaca *et al.*, 2010; Tongnuanchan *et al.*, 2013) and fatty acid (Bertan *et al.*, 2005; Limpisophon *et al.*, 2010). Recently, the properties of gelatin based film were improved by the incorporation of nano-clays (Bae *et al.*, 2009a; Farahnaky *et al.*, 2014; Shakila *et al.*, 2012b). As a consequence, gelatin films can compete with petroleum-based polymers as a biodegradable packaging material (Martucci and Ruseckaite, 2010b).

Polymer nanocomposites have received great interest because nanosized material fillers significantly improve polymer properties when compared with polymer alone or micro-scale composites (Bae *et al.*, 2009a). Nanocomposite films developed from biopolymers known as 'bio-nanocomposites' showed improved mechanical properties, thermal stability and barrier properties (Martucci and Ruseckaite, 2010a; Ray and Okamoto, 2003), due to the enhanced polymer-filler interfacial interaction. The improved water and gas barrier properties of nanocomposite films are believed to be due to the presence of dispersed silicate layers in organised manner with large aspect ratios in the polymer matrix. This forces water/gas travelling through the film via. an increased 'tortuous path' of the polymer matrix surrounding the nano-fillers, thereby increasing the effective path length for diffusion (Ray and Okamoto, 2003; Rhim, 2007). Amongst various nano-fillers,

layered silicates commonly known as the cationic clay minerals, especially the naturally occurring smectite clays, such as hectorite and montmorillonite (MMT) are widely used (Ray and Okamoto, 2003; Rhim *et al.*, 2009; Sothornvit *et al.*, 2009).

Nanoclays, Cloisite Na<sup>+</sup> (hydrophilic) and Cloisite 20A (hydrophobic) have been used to improve mechanical and barrier properties of gelatin-based biopolymers (Bae *et al.*, 2009a; Farahnaky *et al.*, 2014; Shakila *et al.*, 2012b). Rhim *et al.* (2009) reported that, hydrophobicity of organically modified nanoclays (Cloisite 20A and Cloisite 30B) and hydrophilicity of unmodified nanoclay (Cloisite Na<sup>+</sup>) have different impact on barrier properties of PLA-based films. Therefore, the relative hydrophobicity of nanoclays would have different impacts on the properties of resulting nanocomposite films. However, little information is available regarding the influence of hydrophobic nanoclays such as Cloisite 15A (highly hydrophobic), Cloisite 20A (moderately hydrophobic) and Cloisite 30B (least hydrophobic) on barrier properties of gelatin-based films, particularly for those from fish gelatin. Therefore, this study aimed to investigate the effects of different MMT-nanoclays at various inclusion levels on the barrier and mechanical properties of fish gelatin-based films.

## 6.3 Materials and methods

### 6.3.1 Chemicals

Fish skin gelatin from tilapia (~240 bloom) was purchased from Lapi Gelatine (Empoli, Italy). MMT-nanoclays including, Cloisite<sup>®</sup> Na<sup>+</sup>, Cloisite<sup>®</sup> 15A, Cloisite<sup>®</sup> 20A and Cloisite<sup>®</sup> 30B were purchased from Southern clay products Inc. (Gonzlaes, TX, USA). Glycerol was procured from Merck (Darmstadt, Germany). All chemicals were of analytical grade. The general characteristics of these Cloisite<sup>®</sup> nanoclays are presented in Table 21.

**Table 21.** Characteristics of hydrophilic and hydrophobic nanoclays

Nanoclays	Cloisite® Na <sup>+</sup>	Cloisite® 15A	Cloisite® 20A	Cloisite® 30B
<b>Chemical name</b>	Natural bentonite	Bis (hydrogenated tallow alkyl) dimethyl, salt with bentonite	Bis (hydrogenated tallow alkyl) dimethyl, salt with bentonite	Alkyl quaternary ammonium salt bentonite
<b>Chemical structure</b>	$\text{Na}_{0.33}(\text{Al}_{1.67}\text{Mg}_{0.33})\text{Si}_4\text{O}_{10}(\text{OH})_2$	$\text{MMT} + \text{CH}_3 - \overset{\text{CH}_3}{\underset{\text{HT}}{\text{N}^+}} - \text{HT}$	$\text{MMT} + \text{CH}_3 - \overset{\text{CH}_3}{\underset{\text{HT}}{\text{N}^+}} - \text{HT}$	$\text{MMT} + \text{CH}_3 - \overset{\text{CH}_2\text{CH}_2\text{OH}}{\underset{\text{CH}_2\text{CH}_2\text{OH}}{\text{N}^+}} - \text{T}$
<b>Organic modifier</b>	None	Dimethyl dihydrogenated tallow, quaternary ammonium (2M2HT)	Dimethyl dihydrogenated tallow, quaternary ammonium (2M2HT)	Methyl tallow, bis-2-hydroxyethyl, quaternary ammonium (MT2EtOH)
<b>Modifier concentration</b>	-	125 meq/100 g clay	95 meq/100 g clay	90 meq/100 g clay
<b>Relative hydrophobicity</b>	Hydrophilic	Highest hydrophobic	Moderately hydrophobic	Lowest hydrophobic
<b>Moisture content</b>	4-9%	<3%	<3%	<3%
<b>Particle size</b>	<25 μm (d <sub>50</sub> )	<10 μm (d <sub>50</sub> )	<10 μm (d <sub>50</sub> )	<10 μm (d <sub>50</sub> )
<b>Bulk density</b>	568 g/l	165 g/l	175 g/l	365 g/l
<b>Density</b>	2.86 g/cc	1.66 g/cc	1.77 g/cc	1.98 g/cc
<b>X-ray results</b>	d <sub>001</sub> =1.17 nm	d <sub>001</sub> = 3.15 nm	d <sub>001</sub> = 2.42 nm	d <sub>001</sub> = 1.85 nm

**Source:** Southern clay products Inc. (Gonzlaes, TX, USA).

### 6.3.2 Preparation of gelatin nanocomposite films

Gelatin films were prepared as per the method of Bae *et al.* (2009a) with a modification. Firstly, gelatin solution was prepared by mixing the gelatin powder with distilled water to obtain protein concentration of 3% (w/v) as determined by the Kjeldhal method (AOAC, 2000). Thereafter, glycerol (25% of protein, w/w) was added into the gelatin solution as a plasticiser. Nanoclays including Cloisite Na<sup>+</sup>, Cloisite 15A, Cloisite 20A and Cloisite 30B were mixed with distilled water to obtain a final concentration of 0, 0.5, 1, 2.5, 5 and 10% (w/w, on dry protein basis). The mixtures were stirred at 1000 rpm (IKA Labortechnik stirrer, Selangor, Malaysia) for 5 min at room temperature. Nanoclay suspensions were then incubated at 60 °C for 1 h to delaminate the nanoclays in a temperature controlled water bath (W350; Memmert, Schwabach, Germany) with occasional stirring. Nanoclay suspensions were cooled down to room temperature and homogenised for 1 min at 5000 rpm (IKA Labortechnik homogeniser, Selangor, Malaysia). Gradually, nanoclay suspensions were dropped into the gelatin solution and the mixtures were homogenised for 30 sec at 5000 rpm. The mixtures were degassed using a desiccator equipped with JEIO Model VE-11 electric aspirator (JEIO TECH, Seoul, Korea). The final volume was made up to 100 ml and referred to as film-forming suspension, FFS. FFSs were sonicated for intercalation/exfoliation of the gelatin and nanoclay for 30 min using the sonicating bath (Elmasonic S 30 H, Singen, Germany) and then the FFSs were gently stirred for 24 h at room temperature to obtain a homogenous suspension. Prior to casting, FFS were degassed for 10 min using the sonicating bath. FFS (4 ± 0.01 ml) were then cast onto a rimmed silicone resin plate (5×5 cm<sup>2</sup>), air-blown for 12 h at 25 °C, followed by drying in an environmental chamber (Binder GmbH, Tuttlingen, Germany) at 25 ± 0.5 °C and 50 ± 5% relative humidity (RH) for 24 h. Films obtained were manually peeled off and further subjected to analyses. Gelatin film without nanoclay was named as C (control) and those incorporated with Cloisite Na<sup>+</sup>, Cloisite 15A, Cloisite 20A and Cloisite 30B were referred to as Na<sup>+</sup>, 15A, 20A and 30B, respectively, followed by numbers representing the level of nanoclay used (0.5, 1, 2.5, 5 and 10%, w/w).

### 6.3.3 Analyses

Prior to testing, samples were conditioned in an environmental chamber for 48 h at  $50 \pm 5\%$  relative humidity (RH) and  $25 \pm 0.5$  °C. For WAXD, SEM, TGA and DSC studies, films were conditioned in a desiccator containing dried silica gel for 3 weeks at room temperature (28-30 °C) to obtain the most dehydrated films.

#### 6.3.3.1 Thickness

The thickness of ten film samples of each condition was measured using a digital micrometer (Mitutoyo, Model ID-C112PM, Serial No. 00320, Mituyoto Corp., Kawasaki-shi, Japan). Ten random locations around each film sample were used for determination of thickness.

#### 6.3.3.2 Mechanical properties

Young's Modulus (YM), tensile strength (TS) and elongation at break (EAB) of film samples were determined as described by Iwata *et al.* (2000) using the Universal Testing Machine (Lloyd Instruments, Hampshire, UK). The test was performed in the controlled room at 25 °C and  $50 \pm 5\%$  RH. Ten film samples ( $2 \times 5$  cm<sup>2</sup>) with the initial grip length of 3 cm were used for testing. The film samples were clamped and deformed under tensile loading using a 100 N load cell with the cross head speed of 30 mm/min until the samples were broken. The initial slope of the stress-strain curve, the maximum load and final extension at break of the film samples were used to calculate YM, TS and EAB respectively.

#### 6.3.3.3 Water Vapour Permeability

Water vapour permeability (WVP) was measured using a modified ASTM (American Society for Testing and Materials, 1989) method as described by Shiku *et al.* (2004). Film samples were sealed on an aluminium permeation cup containing dried silica gel (0% RH) with silicone vacuum grease and rubber gasket. The cups were placed at 30 °C in a desiccator containing distilled water, followed by

weighing at every 1 h intervals for up to 8 h. Five film samples were used for WVP testing. WVP of the film was calculated as follows:

$$\text{WVP (gmm}^{-2}\text{s}^{-1}\text{Pa}^{-1}) = w l A^{-1} t^{-1} (P_2 - P_1)^{-1}$$

where,  $w$  is the weight gain of the cup (g);  $l$  is the film thickness (m);  $A$  is the exposed area of film ( $\text{m}^2$ );  $t$  is the time of gain (s);  $(P_2 - P_1)$  is the vapour pressure difference across the film (Pa).

#### 6.3.3.4 Colour

Colour of five film samples was determined using a CIE colourimeter (Hunter associates laboratory, Inc., Reston, VA, USA). Colour of the film was expressed as  $L^*$ - (lightness or brightness),  $a^*$ - (redness or greenness) and  $b^*$ - (yellowness or blueness) values. Total difference in colour ( $\Delta E^*$ ) was calculated according to the equation of Gennadios *et al.* (1996).

$$\Delta E^* = \sqrt{(\Delta L^*)^2 + (\Delta a^*)^2 + (\Delta b^*)^2}$$

where,  $\Delta L^*$ ,  $\Delta a^*$  and  $\Delta b^*$  are the difference between the colour parameter of corresponding film samples and that of white standard ( $L^* = 92.82$ ,  $a^* = -1.29$  and  $b^* = 0.51$ ).

#### 6.3.3.5 Light transmission and transparency

Light transmission of the films in ultraviolet (UV) and visible range were measured at selected wavelengths between 200 and 800 nm, using a UV-Visible spectrophotometer (model UV-1800, Shimadzu, Kyoto, Japan) according to the method of Jongjareonrak *et al.* (2008). The transparency value of five film samples was calculated by following the equation of Shiku *et al.* (2004).

$$\text{Transparency value} = (-\log T_{600})/x$$

where,  $T_{600}$  is the fractional transmittance at 600 nm and  $x$  is the film thickness (mm). The higher transparency value represents the lower transparency of films.

### 6.3.4 Characterisation of selected gelatin films

Gelatin films incorporated with Cloisite Na<sup>+</sup> (1 and 2.5%, w/w) and Cloisite 20A (1%, w/w) were further characterised, in comparison with the control film (without nanoclays).

#### 6.3.4.1 Wide angle x-ray diffraction (WAXD) analysis

WAXD analysis of the film samples was conducted in reflection mode, with an incident wavelength ( $\lambda$ ) at 0.154 nm of CuK $\alpha$  radiation (Martucci and Ruseckaite, 2010a). Measurements were performed for  $2\theta$  from 1° to 10° at a scan rate of 1.0°/min. The layer spacing of the clay was calculated from Bragg's law:

$$n\lambda = 2d \sin\theta$$

where  $\lambda$  is the wavelength of the radiation;  $d$  is the c-dimension distance or the interlayer spacing; and  $\theta$  is the diffraction angle (Bae *et al.*, 2009a).

#### 6.3.4.2 Scanning electron microscopic (SEM) analysis

Microstructure of the upper surface and cryo-fractured cross-section of the gelatin film samples was visualised using a scanning electron microscope (Quanta 400; FEI, Praha, Czech Republic) at an accelerating voltage of 15 kV, as described by Farahnaky *et al.* (2014). The gelatin film samples were cryo-fractured by immersion in liquid nitrogen. Prior to visualisation, the film samples were mounted on a brass stub and sputtered with gold in order to make the sample conductive, and photographs were taken at 300x and 5000x magnification for surface analysis. For cross-sectional analysis, cryo-fractured films were mounted around stubs perpendicularly using double sided adhesive tape, coated with gold and observed at the 3000x magnification.

#### 6.3.4.3 Thermo-gravimetric analysis (TGA)

Dried film samples were scanned using a thermogravimetric analyser (TGA-7, Perkin Elmer, Norwalk, CT, USA) from 30 to 600 °C using a heating rate of

10 °C/min (Nuthong *et al.*, 2009). Nitrogen was used as the purge gas at a flow rate of 20 ml/min.

#### **6.3.4.4. Differential Scanning Calorimetry (DSC)**

Thermal properties of film samples were determined using a differential scanning calorimeter (DSC-7, Perkin Elmer, Norwalk, CT, USA) as per the method of Hoque *et al.* (2011d). Temperature calibration was performed using the Indium thermogram. Film samples (2–5 mg) were accurately weighed into aluminium pans, hermetically sealed, and scanned over the temperature range of –30 to 150 °C with a heating rate of 10 °C/min. Dry ice was used as the cooling medium and the system was equilibrated at –30 °C for 5 min prior to scanning. The empty aluminium pan was used as a reference.

#### **6.3.5 Statistical analyses**

All experiments were performed in triplicates (n=3) and a completely randomised design (CRD) was used. Analysis of variance (ANOVA) was performed and the mean comparisons were done by Duncan's multiple range tests (Steel and Torrie, 1980). Data are presented as mean  $\pm$  standard deviation and the probability value of  $P < 0.05$  was considered as significant. Statistical analysis was performed using the Statistical Package for Social Sciences (SPSS 17.0 for windows, SPSS Inc., Chicago, IL, USA).

### **6.4 Results and discussion**

#### **6.4.1 Thickness**

Thickness of films from tilapia skin gelatin incorporated with different MMT-nanoclays at various levels is shown in Table 22. In general, thickness of the films increased when nanoclays were incorporated, especially at higher inclusion levels ( $P < 0.05$ ), regardless of the type of nanoclay. Increased thickness was observed for gelatin films incorporated with hydrophilic and hydrophobic nanoclays at higher levels (Zheng *et al.*, 2002). When the amount of nanoclay increased, the clay particles



more likely distributed as a thicker layer between gelatin particles. As a result, thickness of the film increased. Shakila *et al.* (2012b) reported that the changes in the thickness with the addition of Cloisite Na<sup>+</sup> and chitosan were determined by varying molecular size of the molecules inserted between fish gelatin structures. However, films from bovine gelatin had no difference in thickness when incorporated with Cloisite Na<sup>+</sup> at various levels (Martucci and Ruseckaite, 2010a; Martucci *et al.*, 2007).

#### 6.4.2 Mechanical properties

Mechanical properties of films added with nanoclays at various levels such as Young's Modulus (YM), tensile strength (TS) and elongation at break (EAB) are presented in Table 22. Differences in mechanical properties were observed for gelatin films added with different nanoclays. This was plausibly governed by the structural change of the original gelatin network in the presence of MMT-nanoclays. Generally, YM of the films increased when hydrophilic nanoclay (Cloisite Na<sup>+</sup>) at levels of 1-5% (w/w) was incorporated and further increase in levels decreased the YM (P<0.05). MMT is a clay mineral consisting of stacked silicate sheets and plate like structure. The interlayer of Cloisite Na<sup>+</sup> consists of hydrated Na<sup>+</sup>, K<sup>+</sup> ions and the silicates are miscible only with hydrophilic natural polymer. The gelatin–Cloisite Na<sup>+</sup> interaction was mainly due to an exchange between cationic NH<sub>3</sub><sup>+</sup> group of the amino acid side chain and Na<sup>+</sup> ions at the surface of Cloisite Na<sup>+</sup> (Theng, 1979). In the present study, pH of gelatin FFS was 5.9. pI of gelatin used was 8.4 (data not shown). High rigidity and aspect ratio of the nano-clay as well as the presence of strong hydrogen interactions between matrix and clay resulted in increased YM or stiffness (Martucci and Ruseckaite, 2008). In addition, strong gelatin-hydrophilic nanoclay interactions at the interface could facilitate the force or load transfer from matrix to nanoclay filler more effectively. This resulted in enhancement of reinforcing effect (i.e. increased YM) of the nanocomposite films. For films incorporated with Cloisite 15A and Cloisite 30B, the continuous decrease in YM was observed with increasing amount of nanoclay (P<0.05). In contrast, an increase in YM was observed for films incorporated with Cloisite 20A up to 2.5-5% (w/w) but decreased with further increasing clay content. Zheng *et al.* (2002) reported similar results for bovine gelatin

**Table 22.** Young's Modulus (YM), tensile strength (TS), elongation at break (EAB), water vapour permeability (WVP) and thickness of films from tilapia skin gelatin incorporated with different types of nanoclays at various levels

<b>Film Samples</b>	<b>YM (MPa)</b>	<b>TS (MPa)</b>	<b>EAB (%)</b>	<b>WVP (<math>\times 10^{-11}</math> gmm<sup>-2</sup>s<sup>-1</sup>Pa<sup>-1</sup>)</b>	<b>Thickness (mm)</b>
<b>C</b>	1148.30±35.25kl	58.30±1.61bc	8.38±0.64bcd	2.70±0.10bcdef	0.039±0.003gh
<b>Na<sup>+</sup>- 0.5%</b>	1196.66±42.57jk	59.21±0.42b	8.47±1.49bcd	2.67±0.11cdefg	0.040±0.003fgh
<b>1%</b>	1224.37±33.22ij	62.48±1.60a	9.32±1.50ab	1.98±0.24j	0.043±0.002de
<b>2.5%</b>	1393.80±44.76g	63.58±2.32a	9.71±0.32a	2.49±0.10ghi	0.042±0.004def
<b>5%</b>	1335.03±8.78h	61.99±0.69a	9.10±0.69ab	2.65±0.07cdefgh	0.043±0.006def
<b>10%</b>	1195.43±68.17jk	51.86±1.19ef	5.30±0.30ij	2.80±0.01bcd	0.045±0.002bcde
<b>15A- 0.5%</b>	1154.50±32.46kl	58.97±0.93b	7.93±0.31cde	2.78±0.04bcde	0.041±0.002efg
<b>1%</b>	1111.73±8.77lm	57.86±0.66bc	8.81±0.17abc	2.77±0.01bcde	0.043±0.004cde
<b>2.5%</b>	1069.50±17.14m	55.58±0.55cd	7.43±0.14def	2.73±0.09bcdef	0.044±0.003bcde
<b>5%</b>	991.79±23.83n	49.32±1.91fgh	7.36±0.21defg	2.68±0.10bcdefg	0.047±0.004ab
<b>10%</b>	1000.97±3.03n	49.69±0.25fg	8.35±0.59bcd	2.58±0.17efgh	0.048±0.004a
<b>20A-0.5%</b>	1266.10±30.76i	35.39±5.28m	5.19±0.71ij	2.53±0.02fghi	0.039±0.002gh
<b>1%</b>	1461.86±26.09f	44.42±1.52ij	6.83±0.19efgh	1.70±0.21k	0.044±0.003bcde
<b>2.5%</b>	1587.93±13.82c	46.81±2.20ghi	6.82±0.30efgh	2.36±0.31i	0.044±0.004bcde
<b>5%</b>	1549.60±28.84cde	46.51±0.06hi	6.26±0.07ghi	2.46±0.10hi	0.044±0.003bcde
<b>10%</b>	1503.76±46.46ef	40.85±1.06kl	5.95±0.37hi	2.87±0.11b	0.047±0.002ab
<b>30B-0.5%</b>	1715.83±19.64a	53.23±0.09de	8.66±0.71abc	3.13±0.16a	0.045±0.001abcd
<b>1%</b>	1650.86±4.57b	46.36±0.29hi	6.83±0.56efgh	2.79±0.03bcde	0.045±0.001abcd
<b>2.5%</b>	1568.96±23.76cd	43.01±1.13jk	6.69±0.07fgh	2.61±0.12defgh	0.046±0.002ab
<b>5%</b>	1515.76±50.86def	40.86±1.22kl	6.44±0.12fgh	2.83±0.05bc	0.046±0.003abc
<b>10%</b>	1464.40±13.09f	38.90±1.28l	4.70±0.26j	2.80±0.04bcd	0.048±0.004a

C: Control gelatin film (without nanoclays). Mean ± SD (n=3). Different letters in the same column indicate significant differences (P<0.05).

nanocomposite films. Decrease in YM might be due to the aggregation of nanoclay particles when the level of nanoclay was high (Zheng *et al.*, 2002). Amongst films incorporated with hydrophobic nanoclays, those added with Cloisite 15A had the lowest YM than others (P<0.05). This is because the effective concentration of

inorganic alumina–silicate platelets is lower for the nanocomposites based on Cloisite 15A than other nanoclays because the organic content of the Cloisite 15A is higher than the Cloisite 20A and Cloisite 30B that 43, 38 and 30 wt%, respectively (Martins, 2009). Moreover, the more hydrophobic Cloisite 15A might tend to aggregate to a greater extent, leading to less effective interfacial interaction between clays and gelatin. As a result, the force transfer at matrix-filler interface would be less effective, thus exhibiting less reinforcing effect. Thus, the nanocomposite gelatin film added with Cloisite 15A had lower YM than did the control gelatin film.

The increase in TS was observed for films incorporated with hydrophilic nanoclay (Cloisite Na<sup>+</sup>) at levels above 0.5% (w/w) (P<0.05), in comparison with the control film. However, TS was lowered with the highest level of hydrophilic nanoclay (10%, w/w) was incorporated (P<0.05). Similar result was reported for agar-based nanocomposites (Rhim, 2011). The addition of Cloisite Na<sup>+</sup> was reported to increase the TS of fish and bovine gelatin films (Bae *et al.*, 2009a; Martucci and Ruseckaite, 2010a). The significant improvement in TS was ascribed to the uniform nanodispersion of Cloisite Na<sup>+</sup> layers in gelatin matrix and the strong interaction between gelatin and Cloisite Na<sup>+</sup> (Zheng *et al.*, 2002). However, the incorporation of clay at high level resulted in agglomerated (microcomposite) structures, in which the interactions within each individual component were more favoured over those between components. This led to less reinforcing effect of clay filler on film matrix. TS of gelatin films generally decreased as hydrophobic nanoclays were incorporated (P<0.05). Amongst films added with hydrophobic MMT clays, those incorporated with Cloisite 20A exhibited 40-20% lower TS than films added with hydrophilic MMT clay, when the same amount of clay was used (P<0.05). Cloisite 20A is an organoclay with no polar groups on its organic salt while the Cloisite Na<sup>+</sup> does have polar hydroxyl groups. It was expected that the Cloisite Na<sup>+</sup> might have better interaction with the gelatin (Martins, 2009). The present results suggested that the hydrophobic nanoclays could not interact well with the hydrophilic gelatin molecules and the degree of interaction varied with hydrophobicity of the clays being used.

EAB of films increased when the level of hydrophilic nanoclay (Cloisite Na<sup>+</sup>) incorporated up to 2.5% (w/w) (P<0.05). The result suggested that Cloisite Na<sup>+</sup> at an appropriate level could enhance the mechanical properties of the resulting gelatin nanocomposite film. This was possibly due to sufficiently strong interfacial interaction between gelatin and this particular nanoclay, resulting in better transfer of load or force from gelatin matrix to the nanoclay filler without the ease of disruption at the gelatin-nanoclay interface upon tensile deformation. However, films added with Cloisite Na<sup>+</sup> at 10% (w/w) as well as those added with hydrophobic nanoclays at all levels showed decreased EAB, when compared to the control gelatin film (without nanoclay) (P<0.05). For films incorporated with hydrophobic nanoclays, those containing Cloisite 20A and Cloisite 30B showed decreased EAB to a greater extent when compared to those added with Cloisite 15A. This was most likely ascribed to the large aggregation of nanoclays, particularly when the hydrophobic nanoclays were used at high levels. The larger clay agglomerates could result in lower interfacial interaction between gelatin matrix and nanoclay filler causing interfacial failure. As a result, the decrease in tensile resistant performance (lower TS and EAB) of the resulted composite film was obtained. Thus, the types and levels of nanoclay directly affected mechanical properties of resulting films.

#### **6.4.3 Water Vapour Permeability (WVP)**

WVP of films from tilapia skin gelatin incorporated with various nanoclays at different levels is shown in Table 22. WVP of films decreased with increasing levels of Cloisite Na<sup>+</sup> up to 2.5% (w/w) and film with 1% (w/w) clay showed the lowest WVP (P<0.05). For film incorporated with Cloisite 20A, the lowest WVP was observed when clay was incorporated at 1% level (w/w) (P<0.05). However, the incorporation of Cloisite 15A or Cloisite 30B generally caused no changes in WVP but WVP could be decreased or increased at some extent. Layered structure of the nanoclays delayed the diffusing of water vapor through the film matrix due to diffusion path tortuosity (Ray and Okamoto, 2003; Rhim, 2007). Li *et al.* (2003) stated that Cloisite Na<sup>+</sup> serves as a physical cross linking site, which could enhance the stability of the network. The strong interaction between gelatin chains

and Cloisite Na<sup>+</sup> sheets consumes some hydrophilic groups and reduces the water uptake through capillary action at the interface. Nanodispersion of Cloisite Na<sup>+</sup> sheets in the composite impeded the diffusion of water molecules (Li *et al.*, 2003). Bae *et al.* (2009a) also reported that fish gelatin–MMT films had lower water vapour transmission rate (WVTR) than that of control gelatin film. This was due to the decrease in free volume of polymer matrix, leading to the reduction in the permeability of films. The reduction in WVTR by MMT was attributed to the increase in effective path length for the diffusion of water vapour (Zeng *et al.*, 2005). Higher aggregation of hydrophobic nanoclays lowered the effective diffusion path length and tortuosity, thus decreasing the water vapour barrier ability of nanoclay filler, as compared to the hydrophilic nanoclay. However, WVP of films was affected by different nanoclays ( $P < 0.05$ ). Among the hydrophobic nanoclays used, Cloisite 20A incorporation resulted in lowest WVP of the gelatin films. The moisture repulsion characteristic of Cloisite 20A was also responsible for the decreased WVP (Rhim *et al.*, 2009). Films incorporated with Cloisite 15A and Cloisite 30B showed more or less similar or higher WVP than the control film. In contrast, lowered WVP was observed for films incorporated with Cloisite Na<sup>+</sup> and Cloisite 20A when compared to control film ( $P < 0.05$ ), except for the highest level (10% w/w) incorporation. This suggested that the interaction between the clays and gelatin in film matrix could be different, resulting in varying WVP. The permeability of film is also dependent on membrane porosity, surface absorption relative humidity, nature of macromolecules, type of nanoclays and degree of cross-linking (Carvalho and Grosso, 2004; Kim, 2005).

#### 6.4.4 Colour

Differences in colour were observed amongst films from tilapia skin gelatin incorporated with hydrophilic and hydrophobic nanoclays at different levels ( $P < 0.05$ ) (Table 23). Generally,  $L^*$ - values (lightness) of films added with Cloisite Na<sup>+</sup> and Cloisite 15A clays were not much different from that of the control film. However, the incorporation of Cloisite 20A and Cloisite 30B clays into films, particularly at 5 or 10% (w/w), increased  $L^*$ - value of the corresponding films

( $P < 0.05$ ). This was in agreement with the decreases in  $a^*$ - value. However, the increased  $b^*$ - value (yellowness) was observed for films incorporated with nanoclays at higher levels ( $P < 0.05$ ). Amongst all the clay types tested, Cloisite 30B rendered the

**Table 23.** Colour of films from tilapia skin gelatin incorporated with different types of nanoclays at various levels

Film samples	$L^*$	$a^*$	$b^*$	$\Delta E^*$
<b>C</b>	90.70±0.07fg	-1.14±0.03a	1.33±0.11j	2.28±0.10hi
<b>Na<sup>+</sup>- 0.5%</b>	90.58±0.27ghi	-1.11±0.02a	1.46±0.08ij	2.44±0.27efgh
<b>1%</b>	90.65±0.06g	-1.14±0.04a	1.41±0.04ij	2.35±0.07ghi
<b>2.5%</b>	90.69±0.18fg	-1.23±0.05cde	1.75±0.20g	2.49±0.06defg
<b>5%</b>	90.87±0.09de	-1.28±0.03ghi	1.82±0.22fg	2.37±0.20ghi
<b>10%</b>	90.57±0.08ghi	-1.38±0.01j	2.71±0.14c	3.18±0.15b
<b>15A- 0.5%</b>	90.46±0.09ijk	-1.14±0.02a	1.56±0.10hi	2.59±0.12cdef
<b>1%</b>	90.62±0.05gh	-1.18±0.01b	1.50±0.06ij	2.42±0.06fgh
<b>2.5%</b>	90.67±0.06g	-1.25±0.02def	1.93±0.07f	2.60±0.08cdef
<b>5%</b>	90.34±0.08kl	-1.30±0.02i	2.49±0.08d	3.20±0.10b
<b>10%</b>	90.23±0.17l	-1.29±0.08hi	2.86±0.39bc	3.52±0.38a
<b>20A-0.5%</b>	90.39±0.15jk	-1.21±0.02bc	1.56±0.04hi	2.65±0.15cde
<b>1%</b>	90.50±0.12hij	-1.25±0.03efg	1.76±0.05g	2.64±0.13cde
<b>2.5%</b>	90.99±0.11d	-1.26±0.03fgh	1.76±0.18g	2.22±0.16i
<b>5%</b>	91.31±0.07b	-1.37±0.02j	2.32±0.14e	2.37±0.11ghi
<b>10%</b>	91.60±0.11a	-1.45±0.02k	2.98±0.27b	2.76±0.29c
<b>30B-0.5%</b>	90.33±0.15kl	-1.22±0.02cd	1.54±0.15i	2.69±0.19cd
<b>1%</b>	90.49±0.14hij	-1.20±0.02bc	1.48±0.20ij	2.53±0.15defg
<b>2.5%</b>	90.81±0.05ef	-1.25±0.02def	1.73±0.12gh	2.35±0.06ghi
<b>5%</b>	91.15±0.48c	-1.37±0.01j	2.53±0.26d	2.64±0.48cde
<b>10%</b>	91.36±0.30b	-1.39±0.05j	3.19±0.48a	3.06±0.57b

C: Control gelatin film (without nanoclays). Mean ± SD (n=3). Different letters in the same column indicate significant differences ( $P < 0.05$ ).

film with higher  $b^*$ - value ( $P < 0.05$ ). The  $\Delta E^*$  varied depending on type and level of clays incorporated into films. Generally, larger colour difference was observed for films incorporated with nanoclays at higher levels (5 and 10%, w/w). This was plausibly due to the poor dispersion of nanoclays. Additionally, differences in colour of films might also be due to the varying colours of different nanoclays.

#### 6.4.5 Light transmission and transparency

Transmission of UV and visible light at selected wavelengths in the range of 200–800 nm of films from tilapia skin gelatin incorporated with various nanoclays at different levels is shown in Table 24. Decrease in light transmission of films at all wavelengths was observed when incorporated with nanoclays, and the degree of decrease varied with the type of clay used. All films had the excellent barrier property to light in UV at 200 nm. Higher UV light barrier ability was reported for gelatin films from bigeye snapper skin (Jongjareonrak *et al.*, 2006b) and splendid squid skin (Nagarajan *et al.*, 2013b, 2012b). Light transmittance of films at wavelength of 280 nm decreased markedly with all nanoclays incorporated, especially with increasing levels of clay. Amongst all clays, Cloisite 15A and Cloisite 30B clays rendered the film with the highest barrier property in the visible range ( $P < 0.05$ ). Thus, the incorporation of nanoclays to gelatin film could improve the UV-barrier property, regardless of the type of nanoclay. Transmission of visible light range (350–800 nm) of gelatin films also decreased with increasing levels of nanoclays. The decrease in light transmittance might be caused by the light scattering effect of nanoclay particles distributed throughout the protein network. The result indicated that nanoclays were able to impede the light transmission through the film.

Transparency value of films increased as the amount of nanoclay increased ( $P < 0.05$ ). Films added with Cloisite 30B showed the highest transparency value compared with those containing other clays ( $P < 0.05$ ). Higher transparency value indicated that the films had lower transparency. Transparency of protein based films is generally affected by additives, processing conditions, thickness as well as compatibility between polymer and nanoclay (Farahnaky *et al.*, 2014; Hoque *et al.*,

2011d; Martucci and Ruseckaite, 2010a; Nagarajan *et al.*, 2012b; Rhim, 2007; Tongnuanchan *et al.*, 2013). Generally, films with less transparency coincidentally showed higher thickness. The limited compatibility between gelatin and nanoclays,

**Table 24.** Light transmittance and transparency values of films from tilapia skin gelatin incorporated with different types of nanoclays at various levels

Film samples	Transmittance (%)								Transparency values
	200	280	350	400	500	600	700	800	
<b>C</b>	0.01	48.43	81.86	84.34	86.11	87.00	87.57	87.98	1.44±0.001r
<b>Na<sup>+</sup>-0.5%</b>	0.01	38.60	75.20	81.29	84.63	86.30	87.13	87.77	1.44±0.000r
<b>1%</b>	0.01	35.93	68.28	77.29	82.80	84.98	86.09	86.89	1.79±0.001p
<b>2.5%</b>	0.01	21.65	52.65	66.54	76.16	80.05	82.17	83.70	2.10±0.001o
<b>5%</b>	0.00	15.49	45.32	58.21	67.25	72.47	75.58	77.95	2.94±0.000j
<b>10%</b>	0.01	9.16	31.33	40.11	48.40	55.12	60.22	64.44	6.26±0.008g
<b>15A-0.5%</b>	0.02	37.23	74.99	79.68	83.11	84.42	85.20	85.73	1.59±0.001q
<b>1%</b>	0.02	34.43	66.76	71.40	75.19	76.82	77.88	78.72	2.39±0.002m
<b>2.5%</b>	0.02	29.71	62.46	66.94	70.22	72.00	73.32	74.53	3.01±0.001i
<b>5%</b>	0.00	15.72	34.29	37.02	39.69	41.65	43.37	45.07	8.16±0.006e
<b>10%</b>	0.01	8.52	20.98	23.54	25.74	27.34	28.94	30.75	13.53±0.015b
<b>20A-0.5%</b>	0.02	48.55	81.15	82.89	84.39	85.11	85.61	86.04	1.60±0.002q
<b>1%</b>	0.02	36.73	71.02	73.80	76.33	77.68	78.61	79.37	2.46±0.002l
<b>2.5%</b>	0.01	31.83	63.30	66.23	69.14	70.81	72.06	73.12	3.34±0.005h
<b>5%</b>	0.01	26.34	48.03	50.40	52.60	53.90	54.94	55.92	6.72±0.010f
<b>10%</b>	0.00	7.51	22.69	24.82	26.97	28.58	30.24	32.12	10.62±0.005c
<b>30B-0.5%</b>	0.01	40.68	76.24	79.06	81.68	82.96	83.81	84.43	1.80±0.000p
<b>1%</b>	0.02	40.61	71.31	74.03	76.76	78.24	79.25	80.03	2.34±0.001n
<b>2.5%</b>	0.01	36.32	69.09	71.54	74.00	75.51	76.74	77.84	2.68±0.003k
<b>5%</b>	0.01	15.33	33.26	35.59	38.18	40.02	41.62	43.19	8.39±0.009d
<b>10%</b>	0.00	3.10	12.10	13.45	14.65	15.40	16.00	16.61	18.38±0.012a

C: Control gelatin film (without nanoclays). Mean ± SD (n=3). Different letters in the same column indicate significant differences (P<0.05).



especially for hydrophobic nanoclays might result in large agglomerated nanoclay phase. Consequently, the films became develop more internal light scattering property and become turbid (Martucci and Ruseckaite, 2008). In general, nanocomposite films incorporated with hydrophilic nanoclay were more transparent (lower transparency value) than those incorporated with hydrophobic nanoclays ( $P < 0.05$ ). Therefore, the incorporation of nanoclays had an impact on the appearance and light barrier properties of gelatin film, depending upon the type and level of nanoclay used.

#### **6.4.6 Characterisation of selected gelatin nanocomposite films**

Gelatin films incorporated with Cloisite Na<sup>+</sup> (1 and 2.5%, w/w) and Cloisite 20A (1%, w/w) were further subjected to characterisation, in comparison with the control film (without nanoclays). Those films generally showed the lower WVP with improved mechanical properties, compared to other films.

##### **6.4.6.1 Wide angle x-ray diffraction (WAXD) analysis**

The dispersion of the nanoclays in the tilapia skin gelatin–nanocomposite films were determined by using WAXD analysis and the WAXD patterns of selected nanoclays and different films are illustrated in Figure 25. The  $d$ -spacing due to the interlayer spacing of the nanoclay gallery indicated whether the nanoclay was intercalated or exfoliated (Martucci *et al.*, 2007). It was calculated and assigned on each diffraction peak of WAXD diffractograms. WAXD patterns of nanoclays (Figure 25a) exhibited characteristic diffraction peaks at  $2\theta$  of  $7.04^\circ$  ( $d = 1.25$  nm) for Cloisite Na<sup>+</sup> and  $3.10^\circ$  ( $d = 2.85$  nm) for Cloisite 20A. Similar results were previously reported for original Cloisite Na<sup>+</sup> and Cloisite 20A and also close to the claimed value of the manufacturer (Bae *et al.*, 2009a; Koh *et al.*, 2010; Martucci and Ruseckaite, 2010a; Pradhan *et al.*, 2012). The control gelatin film exhibited a broad peak in the  $2\theta$  range of  $6.2$  to  $9.5^\circ$  (Figure 25b), which is the characteristic of amorphous proteins (Grevellec *et al.*, 2001; Martucci and Ruseckaite, 2010b). WAXD patterns of composite gelatin films were changed considerably in comparison with those of Cloisite nanoclays. In the present study, gelatin films incorporated with Cloisite Na<sup>+</sup> at 1 and 2.5% (w/w) had broad diffraction peak. The characteristic peak

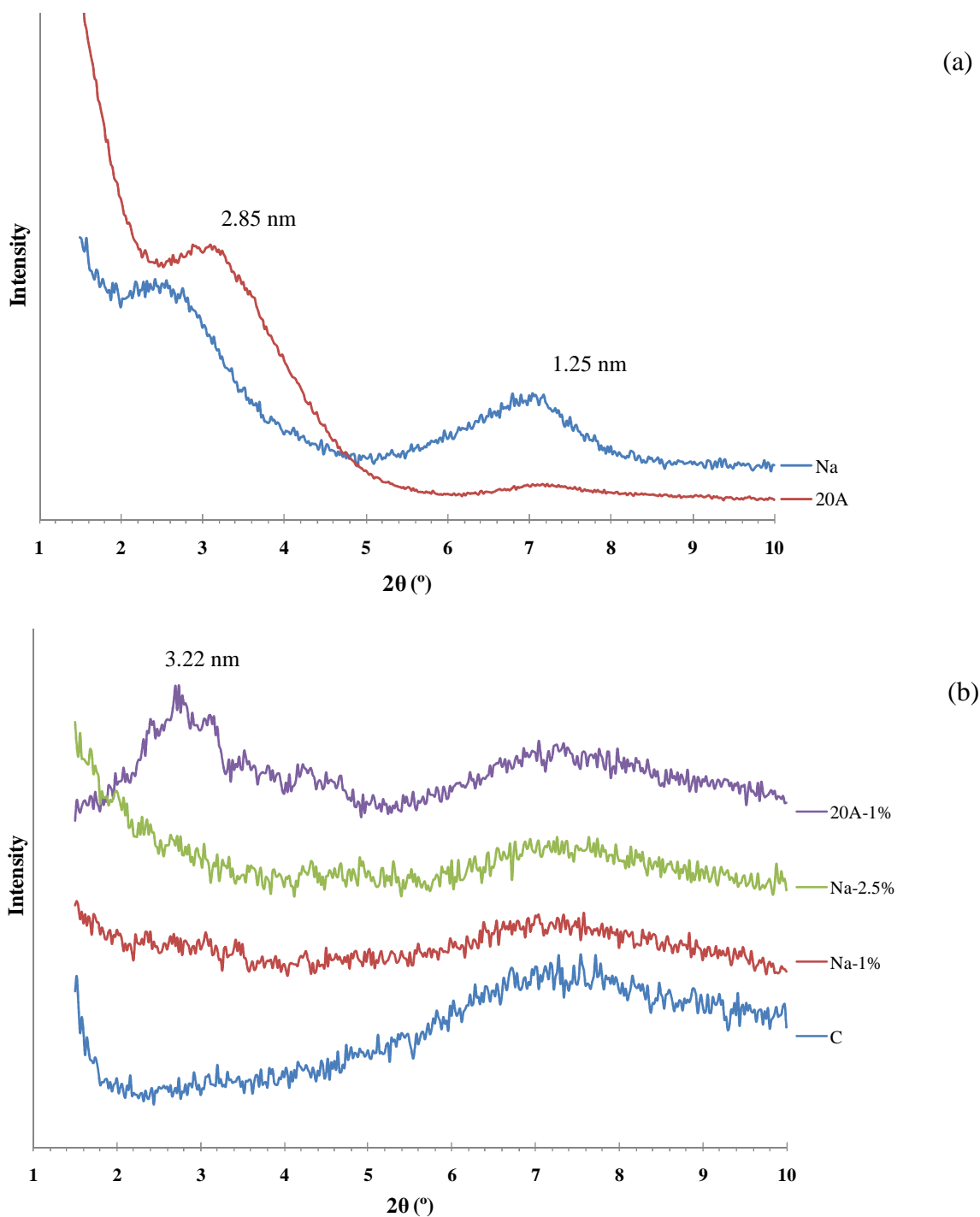


**Figure 25.** WAXD patterns of nanoclays (a) and films from tilapia skin gelatin incorporated with different nanoclays (b). Na: Cloisite Na<sup>+</sup>; 20A: Cloisite 20A; C: Control gelatin film; Na-1%, Na-2.5% and 20A-1% represent the gelatin films incorporated with Cloisite Na<sup>+</sup> and Cloisite 20A at levels of 1 and 2.5% (w/w), respectively. The number assigned on each diffraction peak is *d*-spacing value.

of nanoclay observed in WAXD pattern of nanocomposite films were determined by intercalated/exfoliated structure (Bae *et al.*, 2009a; Martucci and Ruseckaite, 2010a). For film added with Cloisite 20A (hydrophobic nanoclay) at 1% (w/w), diffraction peak ( $2\theta = 3.10^\circ$ ,  $d = 2.85$  nm) shifted to lower angle value ( $2\theta = 2.74^\circ$ ,  $d = 3.22$  nm) and became wider. This more likely suggested that intercalated structure was formed (Zheng *et al.*, 2002). Similar result was reported for film from bovine gelatin incorporated with MMT-nanoclay (Martucci and Ruseckaite, 2010a). The results also indicated that the protein chains effectively entered into the silicate layers of hydrophilic nanoclay, thereby forming intercalated/exfoliated gelatin/Cloisite Na<sup>+</sup> nanocomposites. This was probably due to the presence of strong interaction between the carbonyl groups of gelatin and the hydroxyl groups of the clay galleries via hydrogen bonds, which contributes to a stable nanoclay distribution within the matrix (Martucci and Ruseckaite, 2010a). Nanocomposite structures elucidated by WAXD analysis could be correlated well with the improved mechanical and water vapour barrier properties of intercalated/exfoliated gelatin/Cloisite Na<sup>+</sup> nanocomposite films, compared to those intercalated nanocomposite films based on gelatin and hydrophobic nanoclay. Therefore, the structures of gelatin-based nanocomposite films were dependent on the type of nanoclays.

#### 6.4.6.2 Scanning electron microscopy (SEM)

SEM micrographs of the surface (A, 300x and B, 5000x) and cryo-fractured cross-section (C, 3000x) of the films prepared from tilapia skin gelatin incorporated with Cloisite Na<sup>+</sup> and Cloisite 20A are shown in Figure 26. All films showed crack/void-free surface. Smooth and homogenous surface was obtained for control gelatin film (without nanoclays). However, the homogeneity and smoothness of film surface decreased with the addition of both nanoclays. This might be due to the different dispersion efficiency of nanoclays in gelatin matrix. Different film surface morphologies at higher magnification (5000x) were observed when different levels (1 or 2.5%, w/w) of Cloisite Na<sup>+</sup> clay were incorporated. Gelatin chains more likely underwent the formation of stronger film network with a great number of junction zones by strong interaction between the carbonyl groups of gelatin and the

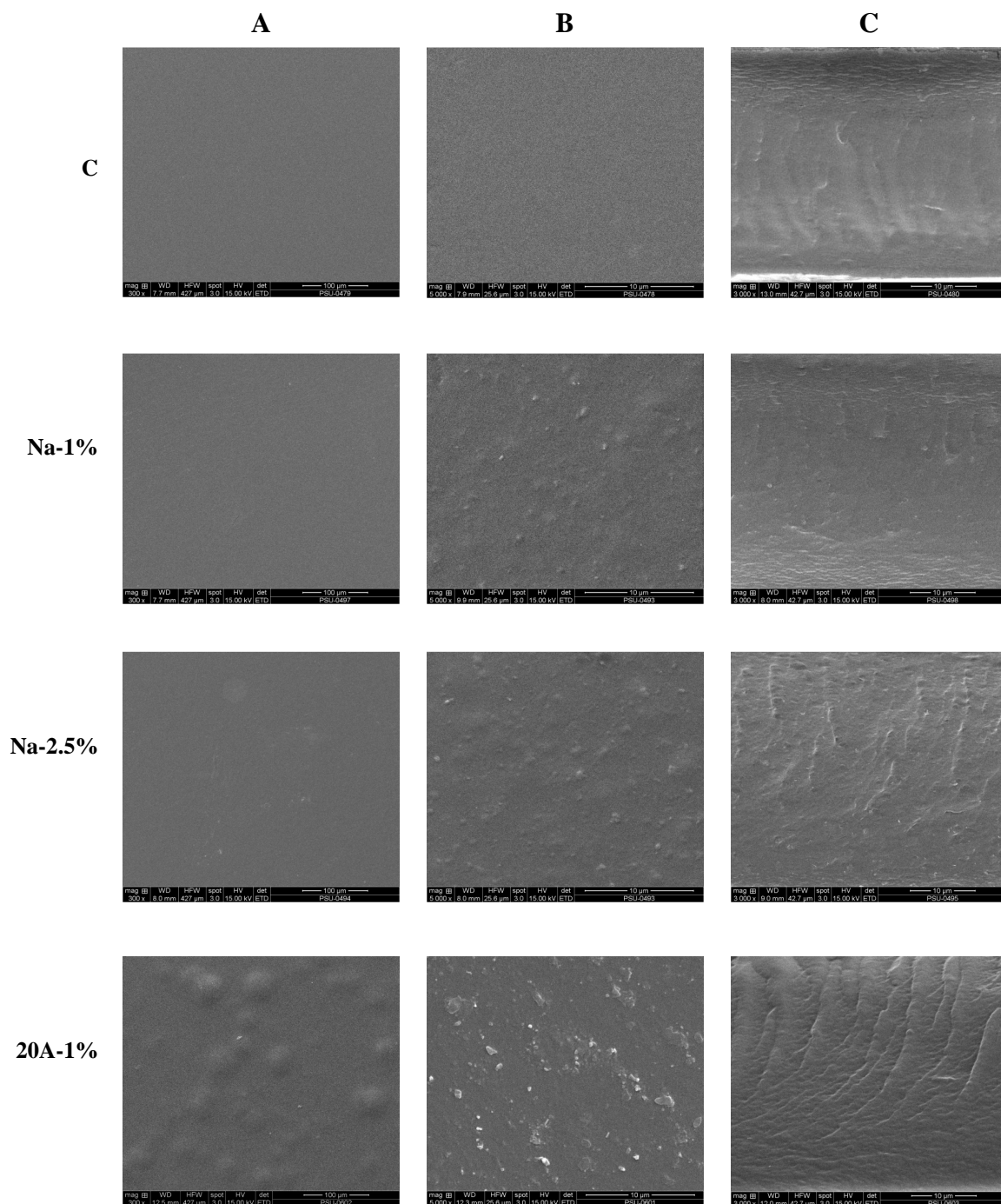


**Figure 26.** SEM micrographs of surface (A and B) and cryo-fractured cross-section (C) of films from tilapia skin gelatin incorporated with different nanoclays. Magnification: 300x and 5000x for surface and 3000x for cross-section. C: Control gelatin film; Na-1%, Na-2.5% and 20A-1% represent the gelatin films incorporated with Cloisite Na<sup>+</sup> and Cloisite 20A at levels of 1 and 2.5% (w/w), respectively.

hydroxyl groups of the clay galleries via hydrogen bonds in films incorporated with Cloisite Na<sup>+</sup> (Theng, 1979). As a result, the continuous strong matrix could be developed. The well dispersion of Cloisite Na<sup>+</sup> in the matrix of gelatin as observed from SEM images could correlate well with the characteristic broader diffraction peak of Cloisite Na<sup>+</sup> as found in WAXD pattern (Figure 25b), suggesting the intercalated/exfoliated structure of gelatin/Cloisite Na<sup>+</sup> nanocomposite films. This result also correlated with the higher mechanical and barrier properties of gelatin/Cloisite Na<sup>+</sup> nanocomposite films (Table 22). Gelatin film incorporated with hydrophobic nanoclay (Cloisite 20A) showed larger aggregates or agglomerates on surface, compared to that with the Cloisite Na<sup>+</sup> incorporation. Hydrophobic nanoclay plausibly could not interact or disperse well with hydrophilic gelatin molecules. This was in accordance with the lower mechanical and water vapour barrier properties of gelatin/Cloisite 20A nanocomposite films. The variations in microstructure of different films were caused by the varying arrangements and interactions of gelatin molecules with nanoclays during film formation.

For cross-section, gelatin films incorporated with Cloisite Na<sup>+</sup> at 1% (w/w) level showed a more compact and smooth structure, when compared to other films. This compact structure of the Cloisite Na<sup>+</sup> incorporated gelatin films was also responsible for the lower WVP (Table 22). This compact structure of gelatin–nanoclay composite films was mainly because of the reduced free volume space within the gelatin due to intermolecular attractive forces and protein chain arrangements with the nanoclays. Films incorporated with Cloisite Na<sup>+</sup> at higher level (2.5%, w/w) and those incorporated with Cloisite 20A did not show smooth cross section, but had the compactness with some undulations. The increase in roughness was associated with an improved toughness. Similar results were reported for different gelatin-based composite films (Hoque *et al.*, 2011d; Shakila *et al.*, 2012b). Thus, the microstructures of nanocomposite films were governed by the dispersion level of nanoclays in the film network, which merely depended on hydrophobicity of the nanoclays.

### 6.4.6.3 Thermogravimetric analysis (TGA)

TGA thermograms revealing thermal degradation behaviour of selected films obtained from tilapia skin gelatin incorporated with Cloisite Na<sup>+</sup> and Cloisite 20A are depicted in Figure 27. Their corresponding degradation temperatures ( $T_d$ ) and weight loss ( $\Delta w$ ) are presented in Table 25. From TGA thermograms, the weight loss ( $\Delta w_1 = 4.50\text{--}7.13\%$ ) observed for all films at onset temperatures of  $47.13\text{--}59.75\text{ }^\circ\text{C}$ , mostly associated with the continuous loss of free moisture absorbed in the films. The weight loss observed at a temperature of approximately  $222.65\text{--}243.58\text{ }^\circ\text{C}$  depending on the film samples, revealed the thermal degradation temperature of the films. This was most likely due to the degradation or decomposition of protein components and glycerol. In general, films incorporated

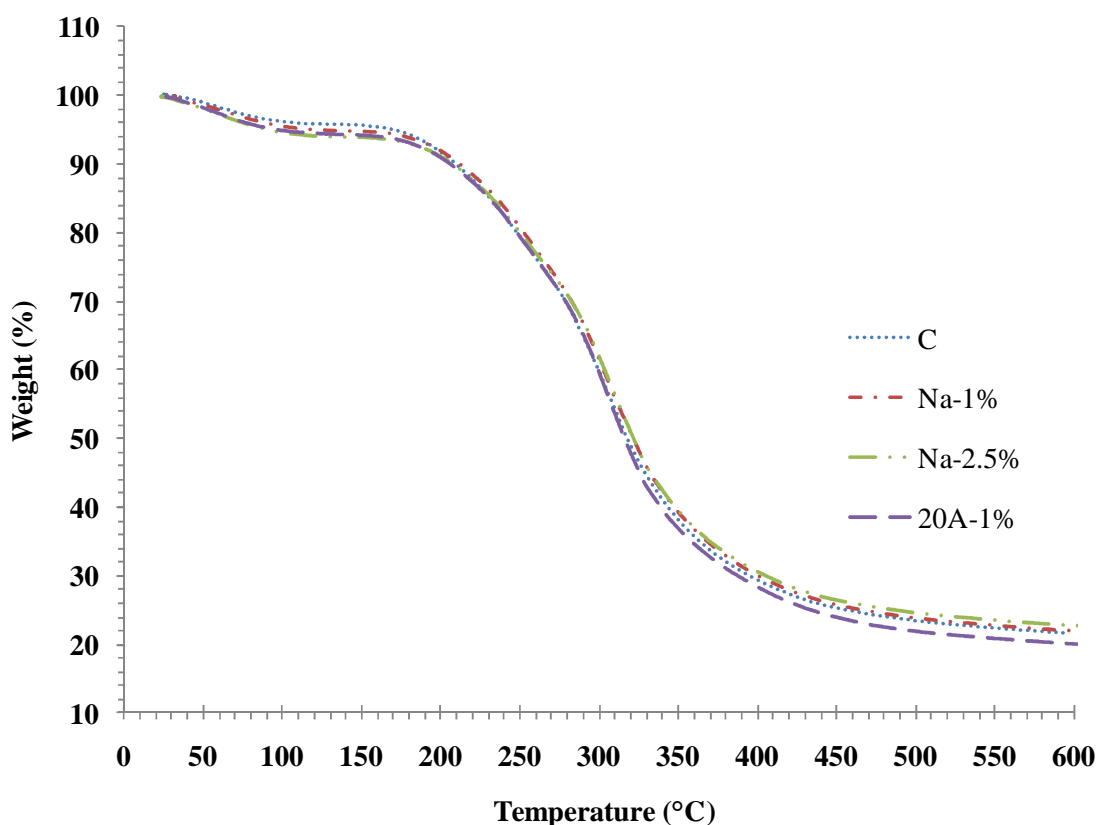


**Figure 27.** Thermogravimetric curves of films from tilapia skin gelatin incorporated with different nanoclays. C: Control gelatin film; Na-1%, Na-2.5% and 20A-1% represent the gelatin films incorporated with Cloisite Na<sup>+</sup> and Cloisite 20A at levels of 1 and 2.5% (w/w), respectively.

**Table 25.** Thermal degradation temperature (Td, °C), weight loss ( $\Delta w$ , %) and glass transition temperature (T<sub>g</sub>, °C) of films from tilapia skin gelatin incorporated with different types of nanoclays

Film samples	$\Delta_1$ (Moisture loss)		$\Delta_2$ (Degradation)		Residue (%)	T <sub>g</sub>
	Td <sub>1</sub> , onset	$\Delta w_1$	Td <sub>2</sub> , onset	$\Delta w_2$		
<b>C</b>	48.53±2.50b	4.58±0.28a	222.65±7.45b	74.50±0.69a	20.93±0.97b	45.36±2.18c
<b>Na<sup>+</sup>-1%</b>	47.13±1.63b	5.46±0.49a	243.58±4.38a	72.87±0.25b	21.67±0.23ab	56.06±2.55a
<b>Na<sup>+</sup>-2.5%</b>	50.95±2.22b	7.13±2.64a	242.06±7.29a	71.79±0.69b	22.59±0.18a	58.35±0.32a
<b>20A-1%</b>	59.75±1.42a	4.50±0.74a	235.92±7.37ab	74.81±0.81a	20.70±0.08b	50.65±2.21b

C: Control gelatin film (without nanoclays).

$\Delta_1$  and  $\Delta_2$  denote the first and second stage weight loss, respectively of films during TGA heating scan.

Mean ± SD (n=3).

Different letters in the same column indicate significant differences (P<0.05).

with nanoclays had increased thermal stability, compared to the control film as indicated by higher  $T_d$  ( $P < 0.05$ ). With the increase in nanoclay level from 1 to 2.5% (w/w) for films incorporated with Cloisite Na<sup>+</sup>,  $T_d$  and weight loss were not significantly different ( $P > 0.05$ ). This might be due to minor differences in the clay content. Additionally, all films had slight difference in residual mass (representing char content) at 600 °C in the range of 20.70–22.59% ( $P < 0.05$ ). Zheng *et al.* (2002) reported that the increased thermal stability of the nanocomposite films was mainly attributed to thermal resistance of MMT and the nanodispersion of MMT sheets in the gelatin matrix. The thermal stabilisation of gelatin/MMT nanocomposites was due to the strong interactions between the carbonyl groups of gelatin and the hydroxyl groups of the clay galleries via hydrogen bonds (Martucci and Ruseckaite, 2010a). TGA study clearly showed that nanoclay incorporation had an impact on the thermal stability of the resulting fish gelatin-based films.

#### 6.4.6.4 Differential Scanning Calorimetry (DSC)

DSC thermograms of films from tilapia skin gelatin are shown in Figure 28. Thermograms of all film samples exhibited step-like or glass transition at temperature ( $T_g$ ) ranging from 45.36 to 58.35 °C (Table 25). It was noted that the film samples had moisture content, as derived from TGA, in the range of 4.50–7.13% ( $P > 0.05$ ). Thermogram of gelatin film incorporated with 2.5% (w/w) Cloisite Na<sup>+</sup> showed the highest  $T_g$  (58.35 °C), whereas the lowest  $T_g$  (45.36 °C) was found for control film ( $P < 0.05$ ).  $T_g$  is generally correlated to the segmental motion of the polymer molecules in the amorphous phase (Slade and Levine, 1991). The results suggested that incorporation of nanoclay decreased the molecular mobility of gelatin as evidenced from the increased  $T_g$ , especially when Cloisite Na<sup>+</sup> was incorporated at higher level (2.5%, w/w). Nanodispersion of Cloisite Na<sup>+</sup> within gelatin matrix might enhance the strong interaction via hydrogen bonds, and thus increasing the rigidity of the gelatin matrix of the film (Martucci *et al.*, 2007). The DSC results were in agreement with the results of the mechanical properties, in which gelatin film added



with Cloisite Na<sup>+</sup> had increased stiffness (i.e. YM value) (Table 22). Smaller difference in T<sub>g</sub> was noticed between the control film (45.36 °C) and that added with 1% (w/w) Cloisite 20A (50.65 °C), as compared to that with Cloisite Na<sup>+</sup>. This might be attributable to the weaker interfacial interaction between gelatin and Cloisite 20A (hydrophobic nanoclay) as also indicated by the lower TS (Table 22). Therefore, thermal properties of films from tilapia skin gelatin were affected by types and levels of nanoclay to some extent.

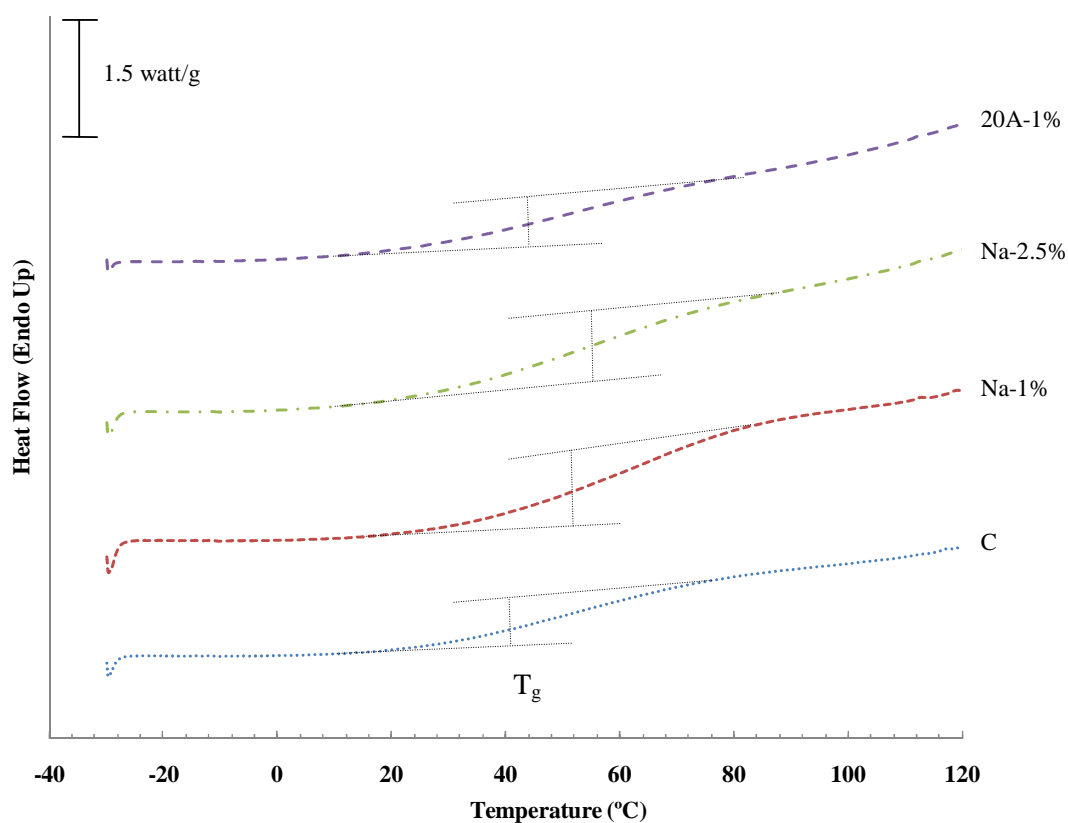


**Figure 28.** DSC thermograms of films from tilapia skin gelatin incorporated with different nanoclays. C: Control gelatin film; Na-1%, Na-2.5% and 20A-1% represent the gelatin films incorporated with Cloisite Na<sup>+</sup> and Cloisite 20A at levels of 1 and 2.5% (w/w), respectively.

## 6.5 Conclusion

Films from tilapia skin gelatin incorporated with hydrophilic or hydrophobic nanoclays at various levels showed different properties and characteristics. Gelatin film incorporated with the hydrophilic nanoclay (i.e. Cloisite Na<sup>+</sup>) resulted in a stronger film network, mainly caused by strong interaction between gelatin and nanoclay molecules as well as better dispersion of nanoclay in the gelatin matrix compared to the hydrophobic nanoclays. Hydrophilic nanoclay particularly Cloisite Na<sup>+</sup>, at a level of 1% (w/w) could effectively improve the water vapour barrier and mechanical properties as well as the thermal stability of fish gelatin films.

## CHAPTER 7

### PROPERTIES OF BIO-NANOCOMPOSITE FILMS FROM TILAPIA SKIN GELATIN AS AFFECTED BY DIFFERENT NANOCCLAYS AND HOMOGENISING CONDITIONS

#### 7.1 Abstract

Fish gelatin films incorporated with hydrophilic and hydrophobic montmorillonite (mmt) nanoclays with the aid of homogenisation using different pressure levels (1000 to 4000 psi) and passes (2 and 4) were characterised. Young's Modulus, tensile strength and elongation at break of films decreased with increasing pressure levels and number of passes. High pressure homogenisation generally lowered the mechanical properties of nanocomposite films. Additionally, water vapour barrier property became poorer, when high pressure homogenisation was implemented. Films incorporated with hydrophobic nanoclay (Cloisite 20A) exhibited the lower WVP than those with hydrophilic nanoclay (Cloisite Na<sup>+</sup>). Colour parameters ( $L^*$ ,  $a^*$ ,  $b^*$  and  $\Delta E^*$ ) of nanocomposite films were affected to some degrees by homogenisation conditions. Transparency of films increased when homogenisation pressure and number of passes increased. As revealed by wide angle x-ray diffraction (WAXD) analysis, nanocomposite films prepared using homogenisation had exfoliated nanostructure, whilst those prepared without homogenisation exhibited intercalated nanostructure. Thermogravimetric (TGA) and differential scanning calorimetric (DSC) analyses indicated that thermal stability of nanocomposite films varied with homogenisation condition, being higher in these films than in those without nanoclay. Thus, homogenisation condition and relative hydrophobicity of nanoclay directly affected the properties of nanocomposite films from fish skin gelatin.

#### 7.2 Introduction

Biodegradable films from agriculture and food industry byproducts are known as an alternative to synthetic thermoplastic counterpart (Vartiainen *et al.*,

2010). Most synthetic films are non-biodegradable and may cause environmental and ecological problems (Gomez-Guillen *et al.*, 2009). Furthermore, biodegradable films as eco-packaging materials have gained interest globally (Vartiainen *et al.*, 2010). Biodegradable films are generally made from renewable biopolymers such as proteins, lipids and polysaccharides (Tharanathan, 2003).

Gelatin is a water soluble protein derived from collagen by thermal extraction. It has been known for its film-forming ability and applicability as an outer covering/wrapping to food products (Hoque *et al.*, 2011d). Nowadays, gelatin from aquatic species is gaining the increasing attention due to health issues and religious constraints of mammalian counterpart (Karim and Baht, 2009). Industrial use of gelatin obtained from non-mammalian source is therefore rising significantly. Films from fish gelatin can be used to preserve food stuffs and extend their shelf-life (Gomez-Guillen *et al.*, 2009).

The incorporation of active compounds such as antioxidants, antimicrobials or other non-active additives (fillers) can make the gelatin film become multi-functional and known as 'active packaging' (Bower *et al.*, 2006; Gomez-Estaca *et al.*, 2010; Jongjareonrak *et al.*, 2008; Li *et al.*, 2014; Limpisophon *et al.*, 2010; Rattaya *et al.*, 2009; Tongnuanchan *et al.*, 2013; Wu *et al.*, 2013). Nevertheless, gelatin film has poor water vapour barrier property due to its hydrophilic nature (Jongjareonrak *et al.*, 2006b). To overcome this drawback, the appropriate modifications of films are required, particularly by the incorporation of nanoclays or nano-fillers.

Polymer nanocomposites usually have much better polymer-nanofiller interaction than conventional composites (Bae *et al.*, 2009a). Nanocomposite films developed from biopolymers known as 'bio-nanocomposites' showed better properties, compared with the polymer alone or micro-scale composites (Martucci and Ruseckaite, 2010b; Sothornvit *et al.*, 2009). The layered silicates, naturally occurring smectite clays, such as hectorite and montmorillonite (mmt), etc have been used to

improve the properties of films based on biopolymers (Ray and Okamoto, 2003; Rhim *et al.*, 2009; Sothornvit *et al.*, 2009). The presence of dispersed silicate layers in organised manner with large aspect ratios in the polymer matrix could enhance the water and gas barrier properties of nanocomposite films (Ray and Okamoto, 2003).

The properties of different types of clays can affect their application when incorporated into films. Hydrophobic nanoclays are hardly dispersed in the film forming solution of hydrophilic polymer and further treatments such as high pressure homogenisation and ultrasonication, etc could be implemented (Alamsi *et al.*, 2010; Rhim, 2011). Gelatin film added with hydrophobic nanoclay, Cloisite 20A with the aid of conventional homogenisation for nanoclay dispersion, had poor mechanical properties (Nagarajan *et al.*, 2014a). It might be due to the poor dispersion of nanoclay and lesser interaction between hydrophilic polymer and hydrophobic nanoclay. However, the film had improved water vapour barrier property, plausibly due to the hydrophobicity of Cloisite 20A nanoclay (Farahnaky *et al.*, 2014; Rhim, 2011). High-pressure homogenisation under the appropriate condition might be a mean to improve the property of nanocomposite films. The method and condition used to disperse the nanoclay in the film forming solution could influence the distribution and morphology of nanocomposite film, and thus, resulting in variation in properties. To the best of our knowledge, there was no information regarding the effect of different homogenisation processes on water vapour barrier and mechanical properties of fish gelatin/mmt nanocomposite films. Therefore, this study aimed to investigate the effect of different homogenising conditions on properties of fish gelatin based films incorporated with different mmt nanoclays.

## **7.3 Materials and methods**

### **7.3.1 Chemicals**

Fish gelatin from tilapia skin (~240 bloom) was purchased from Lapi Gelatine (Empoli, Italy). MMT-nanoclays, including Cloisite<sup>®</sup> Na<sup>+</sup> (hydrophilic mmt)

and Cloisite<sup>®</sup> 20A (hydrophobic mmt) were purchased from Southern clay products Inc. (Gonzales, TX, USA). Glycerol was procured from Merck (Darmstadt, Germany). All chemicals were of analytical grade.

### **7.3.2 Preparation of gelatin films containing nanoclays with different homogenising conditions**

Nanocomposite gelatin films were prepared as per the method of Bae *et al.* (2009a) with a modification as illustrated in Figure 29. Firstly, gelatin solution was prepared by mixing the gelatin with distilled water to obtain the protein concentration of 3% (w/v) as determined by the Kjeldhal method (AOAC, 2000). Thereafter, glycerol (25% of protein, w/w) was added into the gelatin solution as a plasticiser. Nanoclays including Cloisite Na<sup>+</sup> and Cloisite 20A were mixed with distilled water. The mixtures were magnetically stirred at the speed of 1000 rpm for 5 min (IKA Labortechnik stirrer, Selangor, Malaysia). Nanoclay suspensions were then incubated at 60 °C for 1 h in a temperature controlled water bath (W350; Memmert, Schwabach, Germany) with occasional stirring to delaminate the nanoclays. Nanoclay suspensions were cooled down to room temperature and then homogenised for 1 min at the speed of 5000 rpm (IKA Labortechnik homogeniser, Selangor, Malaysia). Nanoclay suspensions were gradually dropped into the gelatin solution to obtain the nanoclay concentration of 1% (w/w) of protein and the mixtures were homogenised for 30 sec at the speed of 5000 rpm. The obtained film forming suspension (FFS) was used for film casting. The resulting film was referred to as the film with conventional homogenising process (CH). The mixture (gelatin solution-nanoclay suspension) was subjected to high pressure homogenisation using a Microfluidics homogeniser (Model HC-5000, Microfluidiser, Newton, MA, USA) at different pressure levels (1000, 2000, 3000 and 4000 psi) with 2 and 4 passes. The obtained films were named as films with high pressure homogenising process (HPH). FFS without homogenisation was used for film preparation and the resulting films were referred to as film without

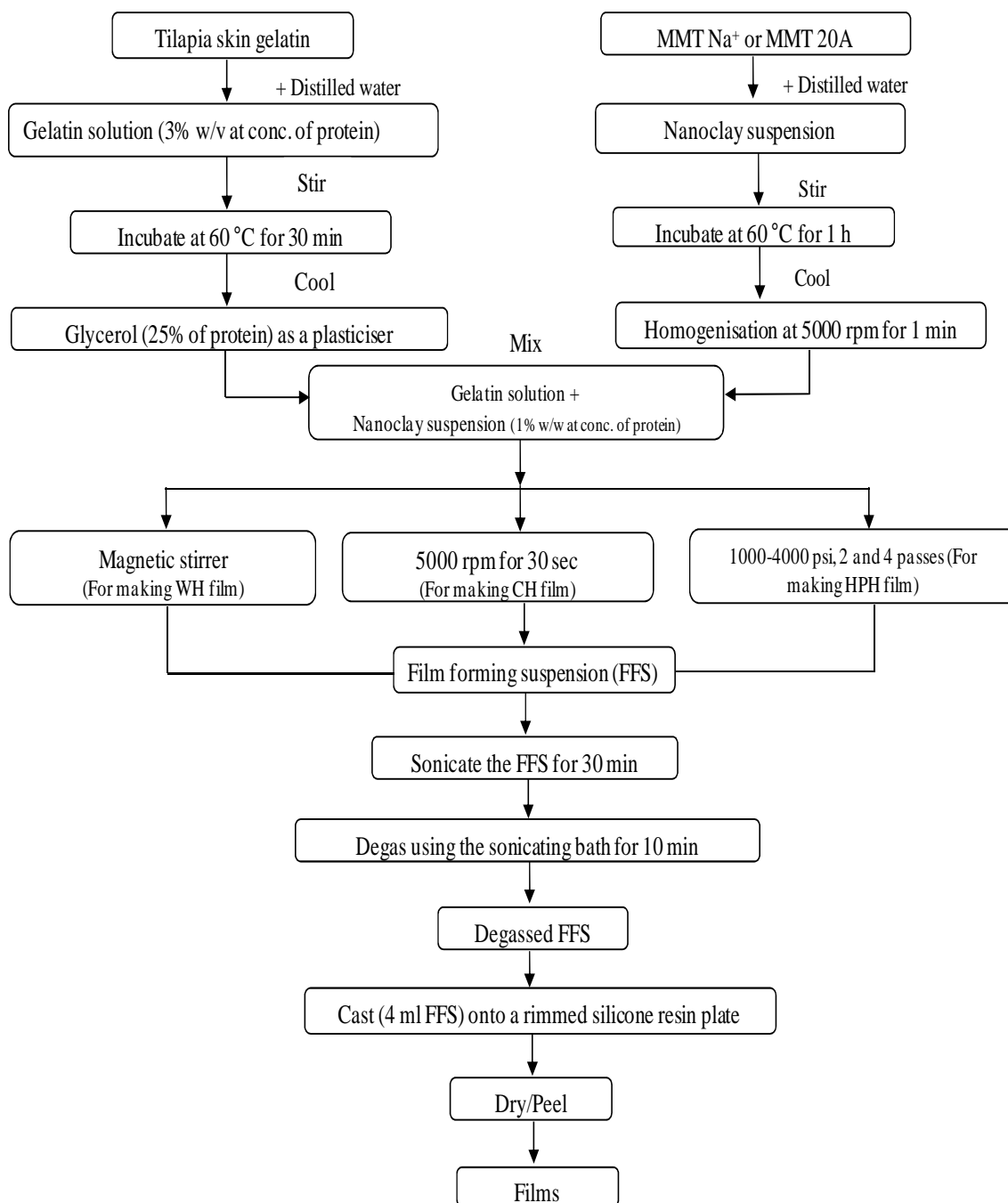


**Figure 29.** Scheme for preparation of film forming suspensions of fish gelatin and MMT nanoclays using different homogenisation conditions

homogenising process (WH). Gelatin solution without nanoclay incorporation was also used for film preparation and the resulting films were referred to as control (C). All FFS samples were sonicated for intercalation/exfoliation of the gelatin and nanoclay for 30 min using the sonicating bath (Elmasonic S 30 H, Singen, Germany). Prior to casting, FFS samples were degassed for 10 min using the sonicating bath. FFS ( $4 \pm 0.01$  ml) were then cast onto a rimmed silicone resin plate ( $5 \times 5$  cm<sup>2</sup>), air-blown for 12 h at 25 °C, followed by drying in an environmental chamber (Binder GmbH, Tuttlingen, Germany) at  $25 \pm 0.5$  °C and  $50 \pm 5\%$  relative humidity (RH) for 24 h. Films obtained were manually peeled off and subjected to analyses.

### **7.3.3 Analyses**

Prior to testing, film samples were conditioned in an environmental chamber for 48 h at  $50 \pm 5\%$  relative humidity (RH) and  $25 \pm 0.5$  °C. For WAXD, TGA and DSC studies all films including WH, CH and HPH films prepared by different homogenising conditions and also the control film (C) were conditioned in a desiccator containing dried silica gel for 3 weeks at room temperature (28-30 °C) to obtain the most dehydrated films.

#### **7.3.3.1 Thickness**

The thickness of ten film samples of each treatment was measured using a digital micrometer (Mitutoyo, Model ID-C112PM, Serial No. 00320, Mituyoto Corp., Kawasaki-shi, Japan). Ten random locations around each film sample were used for determination of thickness.

#### **7.3.3.2 Mechanical properties**

Young's Modulus (YM), tensile strength (TS) and elongation at break (EAB) of ten film samples were determined as described by Iwata *et al.* (2000) using the Universal Testing Machine (Lloyd Instruments, Hampshire, UK). The test was performed in the controlled room at 25 °C and  $50 \pm 5\%$  RH. Ten film samples (2 x 5



cm<sup>2</sup>) with the initial grip length of 3 cm were used for testing. The film samples were clamped and deformed under tensile loading using a 100 N load cell with the cross-head speed of 30 mm/min until the samples were broken. The initial slope of the stress-strain curve, maximum load and final extension at break were used to calculate YM, TS and EAB, respectively.

### 7.3.3.3 Water Vapour Permeability

Water vapour permeability (WVP) was measured using a modified ASTM (American Society for Testing and Materials, 1989) method as described by Shiku *et al.* (2004). Film samples were sealed on an aluminium permeation cup containing dried silica gel (0% RH) with silicone vacuum grease and rubber gasket. The cups were placed at 30 °C in a desiccator containing the distilled water, followed by weighing every 1 h intervals for up to 8 h. Five film samples were used for WVP testing. WVP of the film was calculated as follows:

$$\text{WVP (gmm}^{-2}\text{s}^{-1}\text{Pa}^{-1}) = w/lA^{-1} t^{-1} (P_2 - P_1)^{-1}$$

where,  $w$  is the weight gain of the cup (g);  $l$  is the film thickness (m);  $A$  is the exposed area of film (m<sup>2</sup>);  $t$  is the time of gain (s);  $(P_2 - P_1)$  is the vapour pressure difference across the film (Pa).

### 7.3.3.4 Colour

Colour of five film samples of each treatment was determined using a CIE colourimeter (Hunter associates laboratory, Inc., Reston, VA, USA). The colour of the film was expressed as  $L^*$ - (lightness/brightness),  $a^*$ - (redness/greenness) and  $b^*$ - (yellowness/blueness) values. Total difference in colour ( $\Delta E^*$ ) was calculated according to the following equation (Gennadios *et al.*, 1996):

$$\Delta E^* = \sqrt{(\Delta L^*)^2 + (\Delta a^*)^2 + (\Delta b^*)^2}$$

where,  $\Delta L^*$ ,  $\Delta a^*$  and  $\Delta b^*$  are the differences between the corresponding colour

parameter of film sample and that of white standard ( $L^*= 92.83$ ,  $a^*= -1.27$  and  $b^*= 0.53$ ).

### 7.3.3.5 Light transmission and transparency

Light transmission in ultraviolet (UV) and visible ranges of five films was measured at selected wavelengths between 200 and 800 nm, using a UV-Visible spectrophotometer (model UV-1800, Shimadzu, Kyoto, Japan) according to the method of Jongjareonrak *et al.* (2008). The transparency value of film samples was calculated by the following equation (Shiku *et al.*, 2004):

$$\text{Transparency value} = (-\log T_{600})/x$$

where,  $T_{600}$  is the fractional transmittance at 600 nm and  $x$  is the film thickness (mm). Higher transparency values represent a lower transparency of the films.

## 7.3.4 Characterisation of selected films

Films incorporated with Cloisite Na<sup>+</sup> including WH, CH and HPH (1000/2, 4000/2, 1000/4 and 4000/4; the first number represents pressure level, whilst the second one represents the number of passes) were further subjected to characterisation, in comparison with the control film (without nanoclays).

### 7.3.4.1 Wide angle x-ray diffraction (WAXD) analysis

WAXD analysis of the film samples was conducted in reflection mode with an incident wavelength ( $\lambda$ ) at 0.154 nm of CuK $\alpha$  radiation (Martucci and Ruseckaite, 2010a). Measurements were performed for  $2\theta$  from 1° to 10° at a scan rate of 1.0°/min. The layer spacing of the clay was calculated from Bragg's law:

$$n\lambda = 2d \sin\theta$$

where  $\lambda$  is the wavelength of the radiation;  $d$  is the c-dimension distance or the interlayer spacing; and  $\theta$  is the diffraction angle (Bae *et al.*, 2009a).

#### **7.3.4.2 Thermo-gravimetric analysis (TGA)**

Dried film samples were scanned using a thermogravimetric analyser (TGA-7, Perkin Elmer, Norwalk, CT, USA) from 30 to 600 °C using a heating rate of 10 °C/min (Nuthong *et al.*, 2009). Nitrogen was used as the purge gas at a flow rate of 20 ml/min.

#### **7.3.4.3 Differential scanning calorimetry (DSC)**

Thermal properties of film samples were determined using a differential scanning calorimeter (DSC) (Perkin Elmer, Model DSC-7, Norwalk, CT, USA) as per the method of Hoque *et al.* (2011d). Temperature calibration was performed using the Indium thermogram. Film samples (2–5 mg) were accurately weighed into aluminium pans, hermetically sealed, and scanned over the temperature range of –30 to 150 °C with a heating rate of 10 °C/min. Dry ice was used as a cooling medium and the system was equilibrated at –30 °C for 5 min prior to the scan. The empty aluminium pan was used as a reference.

#### **7.3.5 Statistical analyses**

All experiments were performed in triplicates (n=3) and a completely randomised design (CRD) was used. Analysis of variance (ANOVA) was performed and the mean comparisons were done by Duncan's multiple range tests (Steel and Torrie, 1980). Data are presented as mean  $\pm$  standard deviation and the probability value of  $P < 0.05$  was considered as significant. Statistical analysis was performed using the Statistical Package for Social Sciences (SPSS 17.0 for windows, SPSS Inc., Chicago, IL, USA).

## **7.4 Results and discussion**

### **7.4.1 Properties of films**

#### **7.4.1.1 Thickness**

Films prepared from gelatin incorporated with hydrophilic and hydrophobic nanoclays using different homogenising conditions had varying thickness ( $P < 0.05$ ) (Table 26). The highest thickness was found for WH film prepared without homogenisation ( $P < 0.05$ ). In general, thickness was slightly affected by homogenisation conditions. Nevertheless, higher thickness was generally obtained when HPH films were incorporated with hydrophobic nanoclay (Cloisite 20A) in comparison with hydrophilic nanoclay (Cloisite Na<sup>+</sup>) ( $P < 0.05$ ). Due to its hydrophilic character, sodium montmorillonite was highly compatible and well dispersed in the plasticised-gelatin matrix (Martucci, 2008; Martucci and Ruseckaite 2009). When the HPH films were incorporated with nanoclays, those clay particles were more evenly distributed between gelatin molecules with the aid of high pressure homogenisation. As a result, thickness of HPH films was lower than those of WH and CH films ( $P < 0.05$ ). Therefore, the thickness of gelatin films was affected by types of nanoclay and homogenising conditions.

#### **7.4.1.2 Mechanical properties**

Mechanical properties, including Young's Modulus (YM), tensile strength (TS) and elongation at break (EAB) of films incorporated with hydrophilic and hydrophobic nanoclays by different homogenisation processes are shown in Table 26. YM indicating stiffness of films incorporated with Cloisite 20A was higher when homogenised at a lower pressure (1000 and 2000 psi). Homogenisation at this lower pressure range might result in the increase of distribution or dispersion of hydrophobic nanoclay in the hydrophilic gelatin film matrix. However, pressure higher than 2000 psi resulted in the decrease in YM ( $P < 0.05$ ). This might be due to

the high shear stresses developed in the microchannels of the interaction chamber via intensive microfluidisation. This might cause the partial degradation of gelatin, resulting in weaker film network (Ma *et al.*, 2012). For HPH films containing Cloisite Na<sup>+</sup>, YM decreased with increasing pressure levels. However, numbers of passes tested did not markedly affect YM of HPH films. When comparing different means of nanoclay dispersion, the use of high pressure homogenisation at lower pressure level (1000 psi) yielded the HPH films with higher YM than did the films prepared without homogenisation (WH) and conventional homogenisation (CH). This was plausibly due to the proper distribution and strong interaction of nanoclays with gelatin molecules without causing significant degradation at this lower pressure level. However, WH and CH films showed the similar YM, regardless of types of nanoclay. Gelatin films showed higher YM when incorporated with hydrophobic nanoclay by high pressure homogenisation ( $P < 0.05$ ). Martucci and Ruseckaite (2008) stated that the high rigidity and aspect ratio of the nanoclay as well as the presence of strong hydrogen interactions between matrix and clay resulted in the increased YM or stiffness. Gelatin films incorporated with Cloisite 20A had higher YM than Cloisite Na<sup>+</sup> (Nagarajan *et al.*, 2014a).

TS of films prepared without homogenisation (WH) was lower than the registered on the control film ( $P < 0.05$ ). This might be governed by the improper distribution of nanoclays in gelatin film network. CH films had the higher TS when incorporated with hydrophilic nanoclay, Cloisite Na<sup>+</sup>, in comparison with HPH films ( $P < 0.05$ ). TS of HPH films decreased with increasing pressure levels and number of passes, regardless of types of nanoclay ( $P < 0.05$ ). However, HPH films incorporated with Cloisite 20A at the homogenising condition of 1000 psi and 2 passes had higher TS than the control film ( $P < 0.05$ ). Bae *et al.* (2009a) also reported that TS of gelatin films decreased when the homogenisation speed increased. This might be associated with the fact that the higher shear force generated during high pressure homogenisation might cause partial degradation of gelatin molecules, resulting in less interaction or junction between protein molecules. Additionally, the interaction

between nanoclays and gelatin in FFS might be destroyed to some degree. When the film was formed, those associated complex could not undergo film formation properly. Consequently, the less interaction might contribute to weaker matrix as indicated by the decrease in TS and YM. Ma *et al.* (2012) reported that the high pressure or cycles for homogenisation caused the loss in chain length of dispersed protein molecules with subsequent formation of the less junction zones in the film matrix. Fu *et al.* (2011) found that the TS of films from starch were not improved significantly as the homogenisation pressure and the number of passes increased.

The EAB of films added with both nanoclays by using different dispersing methods was lower than that of control film ( $P < 0.05$ ). Elongation of nanocomposite films was generally lower than that of control film when the free volume between polymer chains decreased due to the incorporation of nanoclays (Farahnaky *et al.*, 2014). Consequently, an increase in intermolecular attractive forces might decrease elasticity of films (Gomez-Estaca *et al.*, 2011). EAB of gelatin/mmt nanocomposite films varied, depending on dispersing methods and conditions used as well as types of nanoclay added. For HPH films, EAB tended to decrease with increasing in pressure and passes used. HPH films incorporated with Cloisite Na<sup>+</sup> exhibited higher EAB than did CH and WH films ( $P < 0.05$ ), respectively, for almost all pressure levels and number of passes applied. For films added with Cloisite 20A, poorer EAB was obtained with increasing pressure level and number of passes ( $P < 0.05$ ). However, HPH film containing Cloisite 20A had lower EAB, compared with WH and CH films, when 4 passes were used. Increasing homogenisation pressure could reduce the molecular weight of polymer, which decreased mechanical properties of the resulting film (Vargas *et al.*, 2011). Thus, homogenisation process and type of nanoclay directly affected the mechanical properties of resulting nanocomposite films.

**Table 26.** Young's Modulus (YM), tensile strength (TS), elongation at break (EAB), water vapour permeability (WVP) and thickness of films from tilapia skin gelatin incorporated with hydrophilic and hydrophobic nanoclays using different homogenisation conditions

Film Samples	YM (MPa)	TS (MPa)	EAB (%)	WVP ( $\times 10^{-11} \text{gmm}^{-2} \text{s}^{-1} \text{Pa}^{-1}$ )	Thickness (mm)
C	1091.70 $\pm$ 33.39d	38.18 $\pm$ 0.51ab	12.08 $\pm$ 1.16a	2.83 $\pm$ 0.37def	0.044 $\pm$ 0.004c
WH-Na <sup>+</sup>	1063.10 $\pm$ 1.65de	35.66 $\pm$ 0.77c	5.84 $\pm$ 0.26h	2.50 $\pm$ 0.06gh	0.053 $\pm$ 0.004a
CH-Na <sup>+</sup>	1057.20 $\pm$ 2.70e	37.18 $\pm$ 0.61b	7.15 $\pm$ 2.04efg	1.92 $\pm$ 0.14jk	0.048 $\pm$ 0.003b
HPH-Na <sup>+</sup> -1000/2	1073.0 $\pm$ 9.15de	35.70 $\pm$ 0.79c	9.59 $\pm$ 0.96b	2.50 $\pm$ 0.24gh	0.039 $\pm$ 0.003efg
2000/2	957.59 $\pm$ 2.01g	32.45 $\pm$ 2.42de	8.64 $\pm$ 0.87bcd	2.77 $\pm$ 0.26efg	0.037 $\pm$ 0.004fg
3000/2	870.08 $\pm$ 10.52ij	31.26 $\pm$ 0.83ef	8.58 $\pm$ 0.10bcd	3.05 $\pm$ 0.15cde	0.037 $\pm$ 0.004fg
4000/2	824.56 $\pm$ 9.01k	28.63 $\pm$ 0.61hi	8.42 $\pm$ 0.20bcde	3.43 $\pm$ 0.18ab	0.038 $\pm$ 0.003fg
1000/4	1008.90 $\pm$ 10.71f	33.30 $\pm$ 1.12d	8.87 $\pm$ 0.87bc	3.08 $\pm$ 0.23cd	0.039 $\pm$ 0.005efg
2000/4	970.83 $\pm$ 10.00g	31.88 $\pm$ 0.68def	7.51 $\pm$ 0.10defg	3.23 $\pm$ 0.13bc	0.038 $\pm$ 0.002fg
3000/4	847.94 $\pm$ 32.30jk	30.44 $\pm$ 1.16fg	7.60 $\pm$ 1.42cdef	3.67 $\pm$ 0.02a	0.036 $\pm$ 0.003g
4000/4	829.28 $\pm$ 9.95k	27.50 $\pm$ 0.90i	7.45 $\pm$ 0.28defg	3.60 $\pm$ 0.12a	0.039 $\pm$ 0.004def
WH-20A	923.19 $\pm$ 27.57h	28.45 $\pm$ 0.81hi	5.40 $\pm$ 0.03h	2.74 $\pm$ 0.06fg	0.052 $\pm$ 0.003a
CH-20A	953.21 $\pm$ 28.48gh	31.34 $\pm$ 0.89ef	6.36 $\pm$ 0.33fgh	1.75 $\pm$ 0.08k	0.044 $\pm$ 0.006c
HPH-20A-1000/2	1271.70 $\pm$ 28.01a	39.16 $\pm$ 0.64a	7.39 $\pm$ 0.37defg	3.50 $\pm$ 0.09ab	0.042 $\pm$ 0.005cde
2000/2	1202.20 $\pm$ 24.21b	37.39 $\pm$ 0.39b	6.23 $\pm$ 0.06gh	2.78 $\pm$ 0.22efg	0.044 $\pm$ 0.001c
3000/2	941.01 $\pm$ 6.50gh	30.42 $\pm$ 2.09fg	5.73 $\pm$ 0.04h	2.31 $\pm$ 0.05hi	0.044 $\pm$ 0.002c
4000/2	886.16 $\pm$ 5.02i	25.45 $\pm$ 0.01j	5.07 $\pm$ 0.07h	3.01 $\pm$ 0.13cde	0.039 $\pm$ 0.002def
1000/4	1142.40 $\pm$ 40.26c	36.71 $\pm$ 0.24bc	5.66 $\pm$ 0.13h	3.26 $\pm$ 0.09bc	0.043 $\pm$ 0.004cd
2000/4	1093.80 $\pm$ 4.26d	35.55 $\pm$ 0.43c	5.50 $\pm$ 0.02h	2.63 $\pm$ 0.01fg	0.040 $\pm$ 0.003def
3000/4	961.84 $\pm$ 4.01g	29.53 $\pm$ 0.32gh	5.04 $\pm$ 0.03h	2.11 $\pm$ 0.72ij	0.039 $\pm$ 0.001efg
4000/4	882.97 $\pm$ 4.00i	25.41 $\pm$ 0.02j	5.00 $\pm$ 0.00h	2.20 $\pm$ 0.01i	0.039 $\pm$ 0.002efg

C: Control gelatin film (without nanoclay).

Mean  $\pm$  SD (n=3).

Different letters in the same column indicate significant differences (P<0.05).

#### 7.4.1.3 Water Vapour Permeability (WVP)

WVP of films incorporated with hydrophilic and hydrophobic nanoclays using different homogenisation conditions is shown in Table 26. WH and CH films added with both nanoclays had lower WVP than the control film (without nanoclay incorporation) ( $P < 0.05$ ). The improved water barrier property of nanocomposite films might be due to the presence of ordering dispersed silicate layers with large aspect ratios in the polymer matrix. This forces water travelling through the film via increased tortuous path of the polymer matrix surrounding the silicate particles, thereby increasing the effective path length for diffusion (Ray and Okamoto, 2003; Rhim, 2007). WH films showed higher WVP than CH films ( $P < 0.05$ ), regardless of types of nanoclay. Higher water vapor permeation of WH films was plausibly due to the presence of large agglomeration and non-uniform distribution of nanoclays in the film matrix, as compared to the CH films (Fu *et al.*, 2011). Amongst films prepared using different mixing conditions, the lowest WVP was obtained for CH films ( $P < 0.05$ ). In general, HPH films showed higher WVP, in comparison with the CH counterpart when the same nanoclay was incorporated ( $P < 0.05$ ). High pressure homogenisation with high shear force might cause partial degradation of gelatin molecules, resulting in shorter gelatin chains and higher amount of hydrophilic moieties. Thus, the increased WVP was observed for HPH films. For films incorporated with Cloisite Na<sup>+</sup>, the WVP increased when the homogenisation pressure and number of passes increased. High pressure homogenisation could modify the functional properties of proteins and caused the aggregation as well as the irreversible disruption of the biopolymer conformation (Vargas *et al.*, 2011). Bae *et al.* (2009a) reported that the increases in homogenisation speed caused no changes or slightly increased WVP of fish gelatin films. WVP of soybean protein isolate-beeswax films was also increased when the homogenisation pressure increased (Zhang *et al.*, 2012). In contrast, the decreased WVP was observed for films incorporated with Cloisite 20A with increasing pressure and number of passes, except for that with 4000 psi and



2 passes, which exhibited the increased WVP. The increase in shear force within the range tested might enhance the dispersion ability of hydrophobic nanoclay layer in the gelatin film matrix. This resulted in more uniform dispersion and thus increased diffusing path tortuosity. Generally, lower WVP was observed for films incorporated with hydrophobic nanoclay (Cloisite 20A) than hydrophilic nanoclay (Cloisite Na<sup>+</sup>) (P<0.05), regardless of homogenisation conditions. The moisture repulsion characteristics of Cloisite 20A could contribute to lower WVP. The modifier (dialkyl ammonium) in Cloisite 20A is responsible for the lower WVP (Rhim *et al.*, 2009). The incorporation of Cloisite 20A nanoclay could reduce the polarity and the surface energy of nanocomposite films, resulting in less hydrophilic surface (Rhim *et al.*, 2009). Thus, gelatin films had varying WVP, depending on the relative hydrophobicity of incorporated nanoclays as well as dispersing methods and conditions used.

#### 7.4.1.4 Colour

Colour of films prepared from tilapia skin gelatin incorporated with hydrophilic and hydrophobic nanoclays using different homogenisation conditions is presented in Table 27. The highest  $L^*$ - value (lightness) was obtained for CH films (P<0.05). This result was in agreement with lowest  $\Delta E^*$ - value (total colour difference) of films. High  $L^*$ - values were also found in films containing Cloisite 20A with 4 passes of homogenisation. However, amongst HPH films, there were no differences in  $L^*$ - value of films incorporated with Cloisite Na<sup>+</sup> when the homogenisation pressure or number of passes increased (P>0.05). On the other hand, the differences in  $L^*$ - value were observed for HPH films incorporated with Cloisite 20A when the passes level increased (P<0.05). Differences in colour of films might be due to the varying colours of nanoclays incorporated (Nagarajan *et al.*, 2014a). The highest  $a^*$ - value (greenness) was observed for the control film (without nanoclay) (P<0.05). Slight or no difference in  $a^*$ - value was noticeable between films prepared with or without homogenisation (P>0.05). The  $b^*$ - value (yellowness) of control film

was lower than other films ( $P < 0.05$ ). In general, no marked difference in  $b^*$ - value was observed for all films incorporated with nanoclays under the study conditions ( $P > 0.05$ ). Thus, colour of nanocomposite gelatin films was not greatly affected by homogenisation conditions.

**Table 27.** Colour of films from tilapia skin gelatin incorporated with hydrophilic and hydrophobic nanoclays using different homogenisation conditions

Film samples	$L^*$	$a^*$	$b^*$	$\Delta E^*$
C	90.42±0.27j	-1.18±0.03a	1.48±0.05c	2.64±0.10a
WH-Na <sup>+</sup>	90.84±0.15defg	-1.25±0.03abc	1.63±0.09abc	2.29±0.16def
CH-Na <sup>+</sup>	91.18±0.27ab	-1.26±0.02bc	1.63±0.10bc	2.00±0.21gh
HPH-Na <sup>+</sup> -1000/2	90.61±0.20ghij	-1.30±0.03cde	1.53±0.10bc	2.44±0.15abcd
2000/2	90.66±0.12ghi	-1.29±0.01cde	1.55±0.09bc	2.40±0.14bcd
3000/2	90.68±0.12ghi	-1.31±0.01cde	1.59±0.08bc	2.40±0.12bcd
4000/2	90.59±0.09hij	-1.34±0.02e	1.67±0.04abc	2.52±0.09abc
1000/4	90.66±0.07ghi	-1.30±0.02cde	1.71±0.02abc	2.47±0.06abcd
2000/4	90.62±0.17ghij	-1.32±0.01cde	1.61±0.04bc	2.46±0.16abcd
3000/4	90.79±0.05efgh	-1.33±0.02de	1.65±0.04abc	2.32±0.03cdef
4000/4	90.55±0.10ij	-1.29±0.03cde	1.55±0.14bc	2.51±0.12abcd
WH-20A	90.83±0.08efg	-1.27±0.04bcd	1.78±0.08ab	2.37±0.07bcde
CH-20A	91.29±0.08a	-1.21±0.02ab	1.57±0.11bc	1.87±0.13h
HPH-20A-1000/2	90.59±0.11hij	-1.27±0.05bcd	1.90±0.18a	2.59±0.27ab
2000/2	90.59±0.25hij	-1.20±0.02ab	1.73±0.10abc	2.55±0.24abc
3000/2	90.66±0.13ghi	-1.25±0.03abc	1.74±0.16abc	2.50±0.09abcd
4000/2	90.73±0.20fghi	-1.21±0.02ab	1.59±0.10bc	2.36±0.16cdef
1000/4	91.00±0.05bcde	-1.21±0.02ab	1.63±0.14bc	2.15±0.12fg
2000/4	91.05±0.07bcd	-1.25±0.02abc	1.76±0.06ab	2.18±0.08efg
3000/4	90.94±0.13cdef	-1.22±0.03ab	1.56±0.06bc	2.16±0.12efg
4000/4	91.13±0.18abc	-1.22±0.05ab	1.57±0.24bc	2.01±0.19gh

C: Control gelatin film (without nanoclay).

Mean ± SD (n=3). Different letters in the same column indicate significant differences ( $P < 0.05$ ).

#### 7.4.1.5 Light transmission and transparency

Transmission of UV and visible light at selected wavelengths in the range of 200-800 nm of gelatin films incorporated with hydrophilic and hydrophobic nanoclays prepared using varying homogenisation conditions is shown in Table 28. Light transmission of nanocomposite films increased when homogenisation was implemented. This was plausibly governed by proper distribution of nanoclays in the original gelatin network. The excellent barrier property to the light in UV at 200 nm was observed for all films. Similar results were reported for gelatin films from bigeye snapper skin (Jongjareonrak *et al.*, 2006b) and splendid squid skin (Nagarajann *et al.*, 2013b; 2012b). For WH films, the lower light transmittance at wavelength of 280 nm was found in comparison with their CH counterparts. In general, light transmittance of films at wavelength of 280 nm increased with increasing homogenising pressures irrespective of types of nanoclay. Nevertheless, transmission of visible light range (350-800 nm) of gelatin films incorporated with Cloisite Na<sup>+</sup> was generally higher, compared to those containing Cloisite 20A. The significant difference in transmission was more likely ascribed to the uniform nanodispersion of hydrophilic nanoclay in the hydrophilic polymer matrix (Zheng *et al.*, 2002). Homogenisation process and hydrophilicity of nanoclays could therefore improve the light transmission of gelatin films in the range of either UV or visible.

Transparency value of gelatin films decreased as the homogenisation pressure increased ( $P < 0.05$ ). Higher transparency of nanocomposite films prepared by using high pressure homogenisation was in agreement with lower thickness (Table 26). However, higher transparency value was observed for WH films ( $P < 0.05$ ). When the compatibility between polymer and nanoclay components is poor, the light transmittance becomes low due to light dispersion or reflection at the two-phase interface (Rhim *et al.*, 2007). Transparency of films is thus an auxiliary criterion to judge the compatibility of the components (Liu and Zhang, 2006). From the results,

**Table 28.** Light transmittance and transparency values of films from tilapia skin gelatin incorporated with hydrophilic and hydrophobic nanoclays using different homogenisation conditions

Film samples	Transmittance (%)								Transparency values
	200	280	350	400	500	600	700	800	
C	0.01	34.64	74	77.93	81.77	83.89	85.33	86.39	1.49±0.00i
WH-Na <sup>+</sup>	0.02	32.19	65.48	69.67	74.40	77.36	79.60	81.37	2.57±0.139de
CH-Na <sup>+</sup>	0.03	41.64	77.74	80.88	83.77	85.28	86.37	87.17	1.37±0.095i
HPH-Na <sup>+</sup> -1000/2	0.01	45.77	71.09	74.58	78.74	81.33	83.18	84.57	2.80±0.262c
2000/2	0.02	41.13	71.42	75.60	80.31	83.05	84.88	86.19	2.51±0.00def
3000/2	0.01	42.06	74.95	78.56	82.35	84.52	85.97	87.03	2.31±0.00fg
4000/2	0.00	53.35	77.13	80.12	83.45	85.37	86.68	87.62	2.07±0.008h
1000/4	0.00	34.81	68.76	73.03	77.89	80.82	82.83	84.31	2.34±0.00fg
2000/4	0.01	41.73	71.86	74.72	78.73	81.17	82.92	84.25	2.19±0.00gh
3000/4	0.01	42.04	71.14	75.68	80.04	82.64	84.50	85.76	2.16±0.00gh
4000/4	0.02	47.31	74.34	77.71	81.51	83.82	85.36	86.54	1.99±0.002h
WH-20A	0.01	40.76	66.08	68.83	71.59	73.24	74.54	75.59	3.47±0.00a
CH-20A	0.02	42.79	70.48	73.05	75.36	76.54	77.37	78.01	2.59±0.00cde
HPH-20A-1000/2	0.01	39.43	65.83	68.04	70.13	71.29	72.12	72.88	3.63±0.358a
2000/2	0.02	40.19	68.04	70.83	73.64	75.25	76.42	77.35	3.14±0.064b
3000/2	0.01	43.19	71.93	74.64	77.24	78.69	79.72	80.52	2.60±0.138cde
4000/2	0.02	47.51	76.14	78.11	79.85	80.78	81.51	82.15	2.48±0.168ef
1000/4	0.02	36.62	63.41	65.97	68.61	70.12	71.36	72.42	3.12±0.00b
2000/4	0.01	38.51	67.87	71.22	74.91	77.17	78.88	80.20	2.72±0.005cd
3000/4	0.02	45.50	74.55	77.34	79.92	81.26	82.20	82.90	2.15±0.048gh
4000/4	0.02	42.54	75.69	78.39	80.70	81.85	82.68	83.32	2.01±0.00h

C: Control gelatin film (without nanoclay).

Mean ± SD (n=3). Different letters in the same column indicate significant differences (P<0.05).

nanocomposite films incorporated with hydrophilic nanoclay were more transparent than those incorporated with hydrophobic nanoclays, regardless of homogenisation conditions ( $P < 0.05$ ). Compatibility between polymer and nanoclay, processing conditions, additives, and thickness are generally play the vital role in the transparency of protein based films (Hoque *et al.*, 2011d; Martucci and Ruseckaite, 2010a; Nagarajan *et al.*, 2012b; Rhim, 2007; Tongnuanchan *et al.*, 2013; 2012). Films incorporated with Cloisite 20A were opaque in appearance and agglomerated clay particles were obviously observed in films. Film transparency is one of the important criterions in packaging industries. Films incorporated with Cloisite 20A were therefore not selected for further characterisation. Therefore, homogenisation conditions and types of nanoclay had the impact on appearance and light transmission of gelatin films.

#### **7.4.2 Characteristics of selected nanocomposite films**

WH, CH and HPH (1000/2, 4000/2, 1000/4 and 4000/4) films incorporated with Cloisite Na<sup>+</sup> were characterised, in comparison with the control film (without nanoclays and homogenisation).

##### **7.4.2.1 WAXD analysis**

WAXD analysis was used to determine the dispersion of the nanoclay in the gelatin–nanocomposite films from tilapia skin. WAXD patterns of nanoclay, Cloisite Na<sup>+</sup>, and films incorporated with Cloisite Na<sup>+</sup> by different homogenisation processes are illustrated in Figure 30. Intercalated or exfoliated structures of nanocomposites were typically revealed by the *d*-spacing due to the interlayer spacing of the nanoclay gallery in polymer matrix (Martucci *et al.*, 2007). Cloisite Na<sup>+</sup> exhibited the sharp peak at  $2\theta$  of  $7.04^\circ$  (*d*-spacing = 1.25 nm, based on Bragg's equation;  $n\lambda = 2d \sin\theta$ ). Similar results were previously reported for original Cloisite Na<sup>+</sup> and also close to the claimed value of manufacturer (Bae *et al.*, 2009a; Koh *et al.*, 2010; Martucci and Ruseckaite, 2010a; Pradhan *et al.*, 2012). WAXD pattern of the

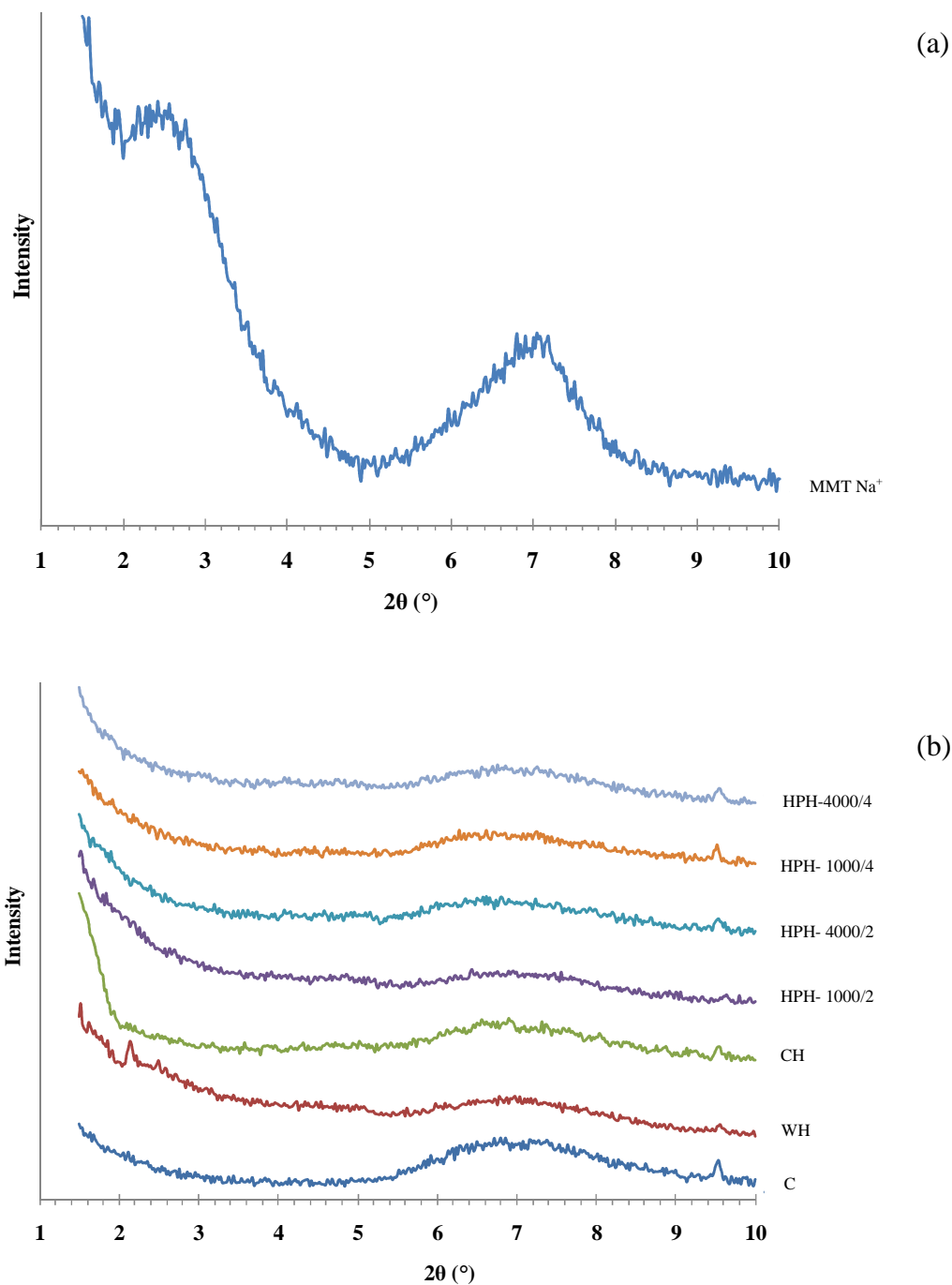


**Figure 30.** WAXD patterns of nanoclay (a) and films from tilapia skin gelatin incorporated with Cloisite Na<sup>+</sup> using different homogenisation conditions (b). Na: Cloisite Na<sup>+</sup>; C: Control gelatin film; WH: film without homogenisation, CH: film with conventional homogenisation and HPH: film prepared with high pressure homogenisation. 1000/2, 4000/2, 1000/4 and 4000/4: The first number represents pressure level, whilst the second number represents the number of passes.

control gelatin film exhibited a broad and low intensity peak in the  $2\theta$  range of 6.2 to 9.5°, which is the characteristic of amorphous proteins (Grevellec *et al.*, 2001; Martucci and Ruseckaite, 2010b). Gelatin-nanocomposite films had significantly different WAXD patterns, compared to nanoclay, Cloisite Na<sup>+</sup>. In the present study, gelatin films incorporated with Cloisite Na<sup>+</sup> by homogenisation process (CH and HPH) had no characteristic diffraction peak of nanoclay; this typically revealed the exfoliation or delaminated structure (Martucci and Ruseckaite, 2010a; Zheng *et al.*, 2002). For WH film (without homogenisation), diffraction peak ( $2\theta = 2.42^\circ$ ,  $d = 3.64$  nm) was shifted to lower angle value ( $2\theta = 2.14^\circ$ ,  $d = 4.12$  nm) and became sharp, indicating that intercalated structure was formed. This was plausibly due to improper distribution of inorganic nanoclay throughout polymeric matrix and thus the sufficient homogeneity together with nano-sized fine structure could not be achieved without sufficient homogenisation. Therefore, the intercalated or exfoliated structures of obtained nanocomposite films were dependent on the homogenisation conditions.

#### 7.4.2.2 TGA analysis

Thermal degradation behaviors of selected gelatin films incorporated with hydrophilic and hydrophobic nanoclays under different homogenisation conditions were revealed with the aid of TGA analysis and their thermograms are depicted in Figure 31. Their corresponding degradation temperatures ( $T_d$ ) and weight loss ( $\Delta w$ ) are presented in Table 29. For all films, the first stage of weight loss ( $\Delta w_1 = 5.56\text{--}7.56\%$ ) observed approximately at onset temperatures ( $T_{d1}$ ) of 42.08–53.47 °C was mostly associated with the continuous loss of free water absorbed in the films. The second stage of weight loss ( $\Delta w_2 = 71.39\text{--}73.66\%$ ) occurred approximately at onset temperatures ( $T_{d2}$ ) of 236.27–255.77 °C, due to the degradation of protein matrix as well as glycerol compounds in the film (Tongnuanchan *et al.*, 2012). WH films incorporated with Cloisite Na<sup>+</sup> had lower thermal degradation temperature ( $T_{d2}$ ) than did the control film. This might be associated with large aggregation with non-

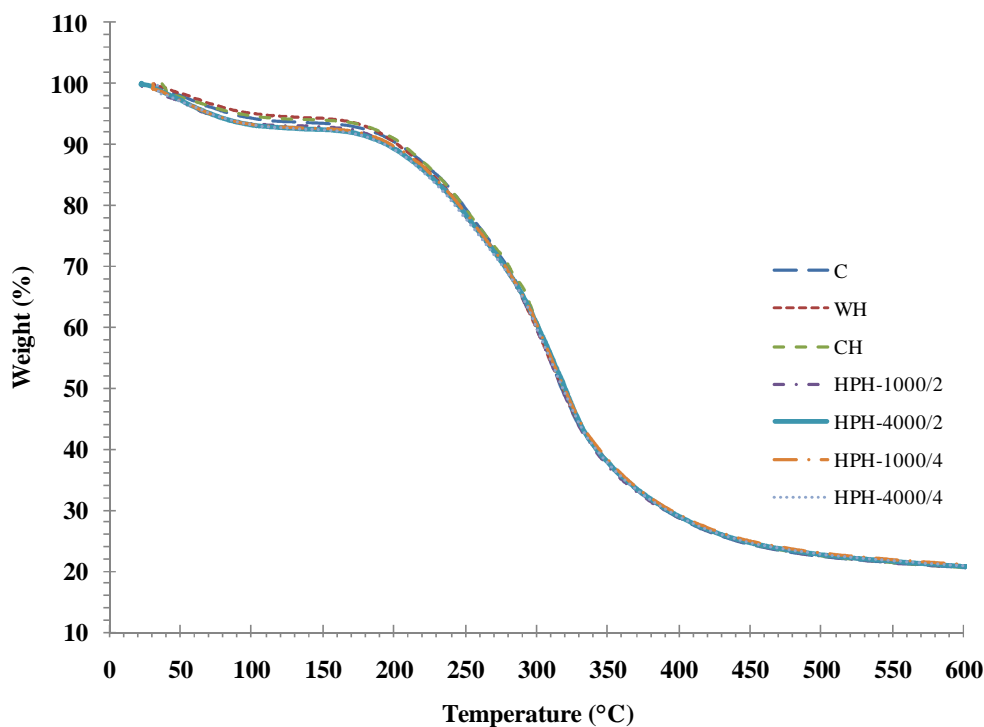


**Figure 31.** Thermogravimetric curves of films from tilapia skin gelatin incorporated with Cloisite Na<sup>+</sup> using different homogenisation conditions.

uniform distribution of nanoclays in protein matrix and less interaction between protein and nanoclay molecules (Ma *et al.*, 2012). This result was in agreement with lower TS of WH films (Table 26). In contrast, nanocomposite film prepared using conventional homogenisation (CH) had higher thermal stability ( $Td_2 = 255.77$  °C) in comparison with the other films ( $Td_2 = 236.27$ - $246.25$  °C) as indicated by higher  $Td_2$ . When high pressure homogenisation (HPH) was used to prepare gelatin/Cloisite Na<sup>+</sup> nanocomposite films, the  $Td_2$  of HPH films seemed to decrease with increasing applied pressure and number of passes. The results showed that HPH nanocomposite films prepared using high pressure of 4000 psi exhibited the lowest thermal stability as suggested by the lowest  $Td_2$  of 236.27 °C in comparison with other films. The lowest thermal stability was in agreement with the lowest mechanical performance observed in these HPH films (Table 26). Partially degraded or shorter protein chains generated by high pressure homogenisation more likely underwent less interaction,



resulting in weaker and more heat susceptible network of film. Therefore, TGA study clearly showed that incorporation of nanoclay and homogenisation methods and conditions determined the thermal stability of resulting gelatin/Cloisite Na<sup>+</sup> nanocomposite films.

**Table 29.** Thermal degradation temperature (Td, °C), weight loss ( $\Delta w$ , %), and glass transition temperature (T<sub>g</sub>, °C) of films from tilapia skin gelatin incorporated with hydrophilic and hydrophobic nanoclays using different homogenisation conditions

Film samples	$\Delta_1$		$\Delta_2$		T <sub>g</sub>
	Td <sub>1</sub>	$\Delta w_1$	Td <sub>2</sub>	$\Delta w_2$	
<b>C</b>	46.21	6.41	241.51	73.11	47.50
<b>WH-Na<sup>+</sup></b>	48.65	5.56	238.80	73.66	54.05
<b>CH-Na<sup>+</sup></b>	53.47	5.87	255.77	73.61	52.01
<b>HPH-Na<sup>+</sup>-1000/2</b>	45.23	6.96	246.25	72.24	50.62
<b>4000/2</b>	47.86	7.56	242.50	71.61	50.33
<b>1000/4</b>	45.10	7.29	237.48	71.39	49.61
<b>4000/4</b>	42.08	7.20	236.27	71.55	48.01

C: Control gelatin film (without nanoclay).  $\Delta_1$  and  $\Delta_2$  denote the first and second stage weight loss, respectively, of films during TGA heating scan.

#### 7.4.2.3 DSC analysis

DSC thermograms of the first (a) and second heating scan (b) of the selected gelatin films are depicted in Figure 32. Glass transition temperature (T<sub>g</sub>) of films is presented in Table 29. Thermograms of all film samples exhibited step-like or glass transition at temperature (T<sub>g</sub>) ranging from 47.50 to 54.05 °C. T<sub>g</sub> is generally correlated to the segmental motion of polymer molecules in the amorphous phase (Slade and Levine, 1991). The glass transition temperature (T<sub>g</sub>) is an important parameter that determines both the mechanical and barrier properties of polymers and

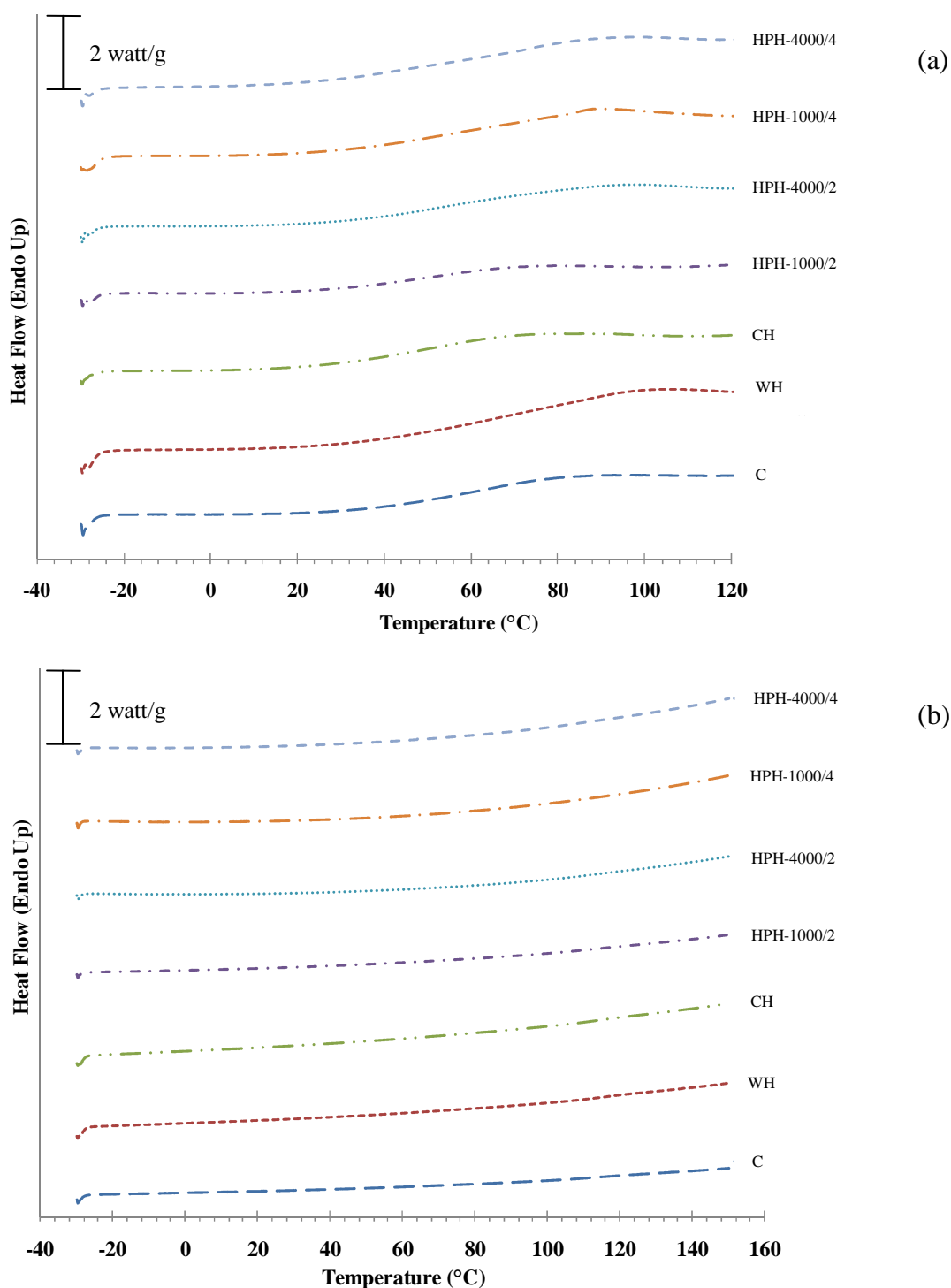


**Figure 32.** DSC thermograms of first (a) and second (b) heating scan of films from tilapia skin gelatin incorporated with Cloisite Na<sup>+</sup> using different homogenisation conditions.

controls the crystallisation kinetics of polymeric materials (Oxford *et al.*, 1989). Gelatin/Cloisite Na<sup>+</sup> nanocomposite films had higher T<sub>g</sub> than did the control gelatin film (without nanoclay incorporation), especially when dispersion with lower shear force was performed. This suggested that adding Cloisite Na<sup>+</sup> nanoclay could decrease gelatin chain mobility, thus increasing chain rigidity, most likely due to the strong interaction between gelatin and Cloisite Na<sup>+</sup> via hydrogen bonds (Martucci *et al.*, 2007). For HPH nanocomposite films, T<sub>g</sub> of films seemed to decrease as the homogenisation pressure and number of passes increased. Gelatin with short chains formed during high pressure homogenisation might not align and build up the strong film network (Figure 33). This could also determine the WVP and transparency of resulting films (Figure 33). The DSC results were generally in agreement with the mechanical properties of films (Table 26).

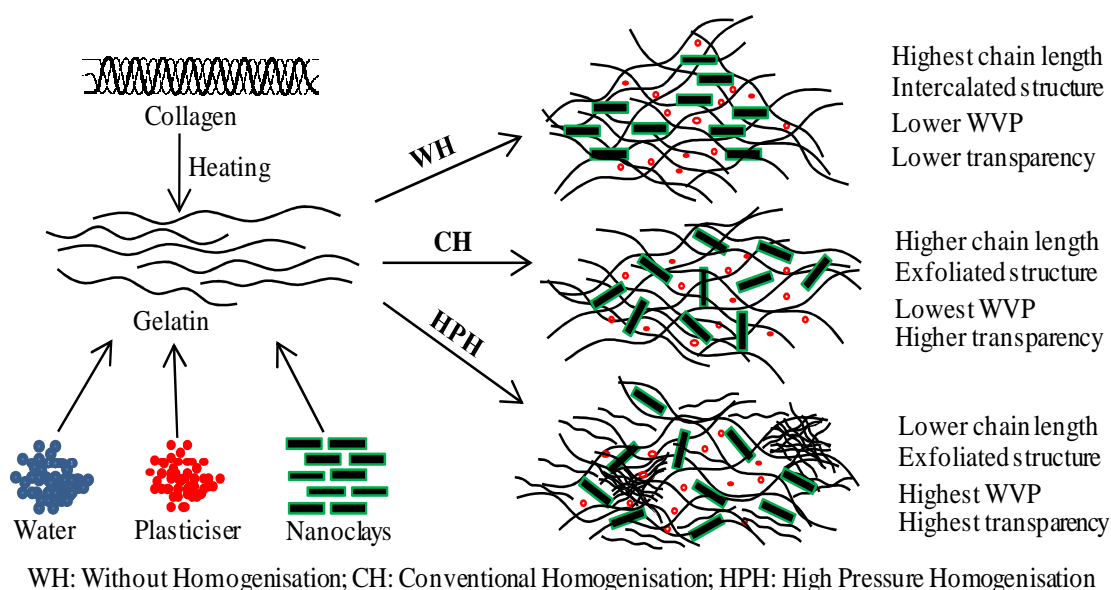


**Figure 33.** Proposed scheme of nanoclay incorporated gelatin film matrix as affected by different homogenisation conditions.

For the second heating scan, no transition was generally observed for both the control film and films incorporated with nanoclays (Figure 32b). The absorbed water, acting as plasticiser, might be removed during the first heating scan.

As a consequence, the interaction between gelatin molecules could be enhanced along with the formation of more rigid film network. As a consequence, the transition temperature of film became too high and could not be detected in the temperature range tested. Therefore, thermal properties of films from skin gelatin were affected by nanoclay incorporation and the homogenisation process to some extent.

## **7.5 Conclusion**

Gelatin films from tilapia skin incorporated with MMT-nanoclays under different homogenisation conditions showed different properties. Exfoliated or delaminated structure of nanocomposite films was obtained by homogenisation via both conventional (CH) and high pressure homogenisation (HPH) processes. In general, homogenisation under appropriate shear force, especially the CH could improve the mechanical resistance, water vapour barrier property, transparency and thermal stability of nanocomposite gelatin films. The decrease in overall properties of the nanocomposite gelatin films was obtained when homogenisation under higher pressures and more than 2 passes was implemented, plausibly caused by partial degradation of gelatin molecules.

## CHAPTER 8

### EFFECTS OF pHs ON PROPERTIES OF BIO-NANOCOMPOSITE BASED ON TILAPIA SKIN GELATIN AND CLOISITE Na<sup>+</sup>

#### 8.1 Abstract

Effects of various pHs (4-8) of film forming suspensions (FFS) on the properties of nanocomposite film based on tilapia skin gelatin and hydrophilic nanoclay (Cloisite Na<sup>+</sup>) were investigated. Intercalated/exfoliated structure of nanocomposite films was revealed by WAXD analysis. Young's Modulus (YM) and tensile strength (TS) of nanocomposite films increased up to pH 6 (P<0.05). Nevertheless, the further increases in pH levels resulted in the decreases in both YM and TS (P<0.05). The highest water vapour barrier property of the film was observed when the pH of FFS was 6 (P<0.05). Lightness ( $L^*$ ) and yellowness ( $b^*$ ) of nanocomposite films generally increased with increasing pH levels. Transparency of nanocomposite films was affected to some extent by pHs. Homogeneity and smoothness of film surface were obtained for nanocomposite films with pH 6 as confirmed by SEM micrographs. Thermogravimetric (TGA) and differential scanning calorimetric (DSC) analyses indicated that thermal stability of nanocomposite films varied with different pH levels. In general, mechanical and water vapour barrier properties of nanocomposite films were improved when FFS having pH 6 was used. Thus, the pH of FFS directly affected the properties of nanocomposite gelatin films incorporated with hydrophilic nanoclay.

#### 8.2 Introduction

Natural biopolymers have the several advantages, especially for being biodegradable, renewable, and edible (Chinabark *et al.*, 2007, Tharanathan, 2003). Films are thin layers, which can be used to protect food stuffs by covering or wrapping the food surface (Shiku *et al.*, 2003). Apart from wrapping, films can be used for making the bag or pouch via sealing (Krochta, 2002). However, biopolymer films exhibited relatively poor mechanical and water vapour barrier properties when compared to traditional synthetic polymeric films, therefore limiting their commercial

use (Gomez-Guillen *et al.*, 2009). Due to their inherent hydrophilic properties, biopolymer films absorb large quantities of water at elevated relative humidity (RH) conditions. This results in the plasticised film matrices that have weakened barrier and mechanical properties (Martucci and Ruseckaite, 2009). Several technologies have been implemented for improvement of film properties (Gomez-Guillen *et al.*, 2009).

Gelatin is a biopolymer derived from collagen via thermal denaturation or partial hydrolysis (Benjakul *et al.*, 2012). It is universally known for its film forming ability and applicability for food packaging (Gomez-Guillen *et al.*, 2009). Gelatin is normally obtained from bovine hides, bones and pig skins. Gelatins from non-mammalian source, especially those from fish processing byproducts, are gaining the increasing attention as packaging or coating materials, due to health issues and religious constraints of mammalian counterpart (Karim and Baht, 2009). Recently, nanotechnology has been introduced for packaging materials as a potential means to bring about the desirable properties (Bae *et al.*, 2009a). Nanocomposite films/coatings developed from biopolymers known as 'bio-nanocomposites' show the better properties, compared with polymer alone or micro-scale composites (Martucci and Ruseckaite, 2010a; Sothornvit *et al.*, 2009). Polymer nanocomposites usually have much better polymer/nanofiller interaction than conventional composites (Bae *et al.*, 2009a; Farahnaky *et al.*, 2014).

Nanoclays were incorporated with gelatin films to improve their mechanical and water vapour barrier properties as well as thermal properties (Bae *et al.*, 2009a; Farahnaky *et al.*, 2014; Martucci and Ruseckaite, 2010b; Nagarajan *et al.*, 2014a). To enhance the nanoclay dispersion in polymer matrix and improve the properties of nanocomposite films, different processing conditions such as shear rate and pH level have been optimised (Bae *et al.*, 2009a; Nagarajan *et al.*, 2014b). Basically, protein has the positive charge when the pH is lower than the pI and has the negative charge when the pH is higher than the pI (Shiku *et al.*, 2003). Electrostatic repulsion between protein molecules occurs at pH values outside of the isoelectric point (pI), and the pH alteration can be also used as an alternative method to improve the functional properties such as film-forming, gelling, emulsifying, and foaming

properties of gelatin (Wihodo and Moraru, 2013). The physical properties of protein based films were highly influenced by the pH of film-forming solution (Avena-Bustillos and Krochta, 1993). The proteins with charged residues more likely undergo interaction with hydrophilic nanoclay at different degrees. Cloisite Na<sup>+</sup>, a hydrophilic nanoclay which is frequently used in bio-based nanocomposites, is the cationic clay mineral with the negative charge on their outer structure (Martucci and Ruseckaite, 2010a). Thus, pH of film forming suspension directly affects the interaction and distribution of nanoclay in gelatin matrix. Nevertheless, the information concerning the effect of pH on the properties of film incorporated with nanoclays is scarce. The present study was therefore undertaken to determine the effects of the pH of film forming suspensions on water vapour permeability and mechanical properties, as well as thermal stability of films from tilapia skin gelatin incorporated with Cloisite Na<sup>+</sup>.

### **8.3 Materials and methods**

#### **8.3.1 Chemicals**

Fish gelatin from tilapia skin (~240 bloom) was obtained from Lapi Gelatine (Empoli, Italy). Montmorillonite (MMT) nanoclay, Cloisite<sup>®</sup> Na<sup>+</sup> (hydrophilic in nature), was purchased from Southern clay products Inc. (Gonzales, TX, USA). Glycerol was procured from Merck (Darmstadt, Germany). All chemicals were of analytical grade.

#### **8.3.2 Study on $\zeta$ -potential of gelatin solution as affected by pHs**

Gelatin from tilapia skin was dissolved in distilled water to obtain a concentration of 0.5 mg/ml. The mixture was stirred at room temperature for 6 h. Solutions were adjusted to different pHs (2 to 12) with 1.0 M nitric acid or 1.0 M KOH using an autotitrator (BI-ZTU, Brookhaven Instruments Co., Holtsville, New York, USA). The  $\zeta$ -potential of gelatin solution (20 ml) was measured using a zeta potential analyser (ZetaPALS, Brookhaven Instruments Corp., Holtsville, NY, USA). The pI of gelatin sample was estimated from pH rendering  $\zeta$ -potential of zero.

### 8.3.3 Characteristics of gelatin films containing nanoclay as influenced by pHs

#### 8.3.3.1 Preparation of nanocomposite films

Gelatin nanocomposite films were prepared as per the method of Bae *et al.* (2009a) with slight modifications. Firstly, gelatin solution was prepared by mixing the gelatin powder with distilled water to obtain the protein concentration of 3% (w/v) as determined by the Kjeldhal method (AOAC, 2000). Thereafter, glycerol (25% of protein, w/w) was added into the gelatin solution as a plasticiser. Nanoclay, Cloisite Na<sup>+</sup> (1% of protein, w/w) was mixed with distilled water. The mixture was stirred at a speed of 1000 rpm (IKA Labortechnik stirrer, Selangor, Malaysia) for 5 min at room temperature. Nanoclay suspension was then incubated at 60 °C for 1 h to delaminate the nanoclay in a temperature controlled water bath (W350; Memmert, Schwabach, Germany) with an occasional stirring. Nanoclay suspension was cooled down to room temperature (27-30 °C) and then homogenised for 1 min at a speed of 5000 rpm (IKA Labortechnik homogeniser, Selangor, Malaysia). Gradually, nanoclay suspension was dropped into the gelatin solution and the mixture was homogenised for 30 sec at the speed of 5000 rpm. The mixtures were degassed using a desiccator equipped with JEIO Model VE-11 electric aspirator (JEIO TECH, Seoul, Korea). Then, the pH of mixtures was adjusted to 4, 5, 6, 7 and 8 with 1 M HCl or 1 M NaOH solution. The final volume was made up to 100 ml using distilled water. The obtained film-forming suspensions (FFS) were further sonicated for intercalation/exfoliation of the gelatin and nanoclay for 30 min using the sonicating bath (Elmasonic S 30 H, Singen, Germany). FFS were then gently stirred for 24 h at room temperature to obtain a homogenous suspension. Prior to casting, FFS were degassed for 10 min using the sonicating bath. FFS (4 ± 0.01 ml) were then cast onto a rimmed silicone resin plate (5×5 cm<sup>2</sup>), air-blown for 12 h at 25 °C, followed by drying in an environmental chamber (Binder GmbH, Tuttlingen, Germany) at 25 ± 0.5 °C and 50 ± 5% relative humidity (RH) for 24 h. Nanocomposite films prepared from FFS with pHs of 4, 5, 6, 7 and 8 were manually peeled off and referred to as NF4, NF5, NF6, NF7 and NF8, respectively. Nanocomposite films were further subjected to analyses.



### 8.3.3.2 Analyses

Prior to testing, samples were conditioned in an environmental chamber for 48 h at  $50 \pm 5\%$  relative humidity (RH) and  $25 \pm 0.5$  °C. For WAXD, SEM, TGA and DSC studies, nanocomposite films were conditioned in a desiccator containing dried silica gel for 3 weeks at room temperature (28-30 °C) to obtain the most dehydrated films.

#### 8.3.3.2.1 Wide angle x-ray diffraction (WAXD) pattern

WAXD analysis of the film samples was conducted in reflection mode, with an incident wavelength ( $\lambda$ ) at 0.154 nm of CuK $\alpha$  radiation (Martucci and Ruseckaite, 2010a). Measurements were performed for  $2\theta$  from 1° to 10° at a scan rate of 1.0°/min. The layer spacing of the clay was calculated from Bragg's law:

$$n\lambda = 2d \sin\theta$$

where  $\lambda$  is the wavelength of the radiation;  $d$  is the c-dimension distance or the interlayer spacing; and  $\theta$  is the diffraction angle (Bae *et al.*, 2009a).

#### 8.3.3.2.2 Thickness

The thickness of ten film samples of each treatment was measured using a digital micrometer (Mitutoyo, Model ID-C112PM, Serial No. 00320, Mituyoto Corp., Kawasaki-shi, Japan). Ten random locations around each film sample were used for determination of thickness.

#### 8.3.3.2.3 Mechanical properties

Young's Modulus (YM), tensile strength (TS) and elongation at break (EAB) of ten film samples for each pH were determined as described by Iwata *et al.* (2000) using the Universal Testing Machine (Lloyd Instruments, Hampshire, UK). The test was performed in the controlled room at 25 °C and  $50 \pm 5\%$  RH. Ten film samples ( $2 \times 5$  cm<sup>2</sup>) with the initial grip length of 3 cm were used for testing. Film samples were clamped and deformed under tensile loading using a 100 N load cell

with the cross head speed of 30 mm/min until the samples were broken. The initial slope of the stress-strain curve, the maximum load and final extension at break, were used to calculate YM, TS and EAB, respectively.

#### 8.3.3.2.4 Water vapour permeability

Water vapour permeability (WVP) was measured using a modified ASTM (American Society for Testing and Materials, 1989) method as described by Shiku *et al.* (2004). Film samples were sealed on an aluminium permeation cup containing dried silica gel (0% RH) with silicone vacuum grease and rubber gasket. The cups were placed at 30 °C in a desiccator containing the distilled water, followed by weighing at every 1 h intervals for up to 8 h. Five film samples were used for WVP testing. WVP of nanocomposite films was calculated as follows:

$$\text{WVP (gmm}^{-2}\text{s}^{-1}\text{Pa}^{-1}) = w/lA^{-1} t^{-1} (P_2 - P_1)^{-1}$$

where,  $w$  is the weight gain of the cup (g);  $l$  is the film thickness (m);  $A$  is the exposed area of film ( $\text{m}^2$ );  $t$  is the time of gain (s);  $(P_2 - P_1)$  is the vapour pressure difference across the film (Pa).

#### 8.3.3.2.5 Colour

Colour of five film samples was determined using a CIE colourimeter (Hunter associates laboratory, Inc., Reston, VA, USA). Colour of the nanocomposite films was expressed as  $L^*$ - (lightness or brightness),  $a^*$ - (redness or greenness) and  $b^*$ - (yellowness or blueness) values. Total difference in colour ( $\Delta E^*$ ) was calculated according to the following equation (Gennadios *et al.*, 1996).

$$\Delta E^* = \sqrt{(\Delta L^*)^2 + (\Delta a^*)^2 + (\Delta b^*)^2}$$

where,  $\Delta L^*$ ,  $\Delta a^*$  and  $\Delta b^*$  are the differences between the corresponding colour parameter of film sample and that of white standard ( $L^* = 95.91$ ,  $a^* = -0.85$  and  $b^* = 0.50$ ).

### 8.3.3.2.6 Light transmission and transparency

Light transmission of five film samples in ultraviolet (UV) and visible range were measured at selected wavelengths between 200 and 800 nm using a UV-Visible spectrophotometer (model UV-1800, Shimadzu, Kyoto, Japan) according to the method of Jongjareonrak *et al.* (2008). The transparency value of film samples were calculated by following the equation (Shiku *et al.*, 2004).

$$\text{Transparency value} = (-\log T_{600})/x$$

where,  $T_{600}$  is the fractional transmittance at 600 nm and  $x$  is the film thickness (mm). The higher transparency value represents the lower transparency of films.

### 8.3.3.2.7 Scanning electron microscopic (SEM) image

Microstructure of the upper surface and cryo-fractured cross-section of the gelatin nanocomposite films was visualised using a scanning electron microscope (SEM) (Quanta 400; FEI, Praha, Czech Republic) at an accelerating voltage of 15 kV, as described by Hoque *et al.* (2011c). The film samples were cryo-fractured by immersion in liquid nitrogen. Prior to visualisation, the film samples were mounted on a brass stub and sputtered with gold in order to make the sample conductive, and photographs were taken at 8000x magnification for surface analysis. For cross-sectional analysis, cryo-fractured nanocomposite films were mounted around stubs perpendicularly using double sided adhesive tape, coated with gold and observed at the 3000x magnification.

### 8.3.3.2.8 Thermo-gravimetric curve

Dried film samples were scanned using a thermogravimetric analyser (TGA-7, Perkin Elmer, Norwalk, CT, USA) from 30 to 600 °C using a heating rate of 10 °C/min (Nuthong *et al.*, 2009). Nitrogen was used as the purge gas at a flow rate of 20 ml/min.

### **8.3.3.2.9 Differential scanning calorimetric (DSC) thermograms**

Thermal properties of film samples were determined using a differential scanning calorimeter (DSC) (Perkin Elmer, Model DSC-7, Norwalk, CT, USA) as per the method of Hoque *et al.* (2011c). Temperature calibration was performed using the Indium thermogram. Film samples (2–5 mg) were accurately weighed into aluminium pans, hermetically sealed, and scanned over the temperature range of –30 to 150 °C with a heating rate of 10 °C/min. Dry ice was used as the cooling medium and the system was equilibrated at –30 °C for 5 min prior to the scan. The empty aluminium pan was used as a reference.

### **8.3.4 Statistical analyses**

Experiments were performed in triplicates (n=3) and a completely randomised design (CRD) was used. Analysis of variance (ANOVA) was performed and the mean comparisons were done by Duncan's multiple range tests (Steel and Torrie, 1980). Data are presented as mean  $\pm$  standard deviation and the probability value of  $P < 0.05$  was considered as significant. Statistical analysis was performed using the Statistical Package for Social Sciences (SPSS 17.0 for windows, SPSS Inc., Chicago, IL, USA).

## **8.4 Results and discussion**

### **8.4.1 Effect of pHs on $\zeta$ -potential of gelatin solution**

$\zeta$ -potential values of tilapia skin gelatin solutions as a function of pH are illustrated in Figure 34. The solution was positively charged at acidic pH ranges and became negatively charged under alkaline conditions. Net charge of zero was obtained at pH 8.38. This pH was most likely the pI of gelatin. Protein molecules in an aqueous system have zero net charge at their isoelectric point (pI), in which the positive charges are balanced out by the negative charges (Bonner, 2007). Gelatins from megrim, tilapia and cod were reported to have the pI of 9.5, 9.1 and 8.9, respectively (Gudmundsson, 2002). However, gelatin from splendid squid skin

showed pI at 5.94 (Nagarajan *et al.*, 2012a). Thus, gelatin possessed varying charge, depending on pH.

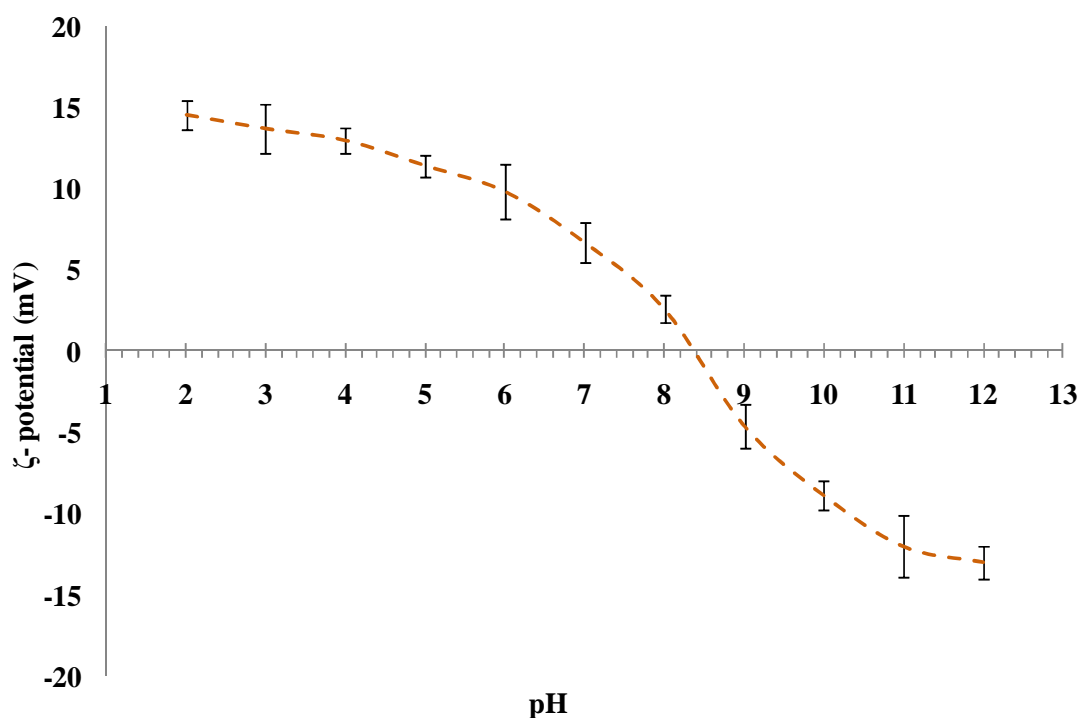


**Figure 34.** ζ-potential value of tilapia skin gelatin.

## 8.4.2 Characteristics of gelatin nanocomposite films as influenced by pH

### 8.4.2.1 Wide angle x-ray diffraction patterns

WAXD patterns of nanocomposite films prepared from FFS with different pH levels are illustrated in Figure 35. WAXD analysis was used to determine the dispersion of the nanoclay in the nanocomposite films prepared from tilapia skin gelatin. The  $d$ -spacing due to the interlayer spacing of the nanoclay gallery indicated whether the nanoclay was intercalated or exfoliated in gelatin matrix (Martucci *et al.*, 2007). Cloisite Na<sup>+</sup> exhibited the sharp peak at  $2\theta$  of  $7.04^\circ$  ( $d$ -spacing = 1.25 nm, based on Bragg's equation;  $n\lambda = 2d \sin\theta$ ) (Figure 35 a). This result was in agreement with the earlier reports of original Cloisite Na<sup>+</sup> and the value provided by the manufacturer (Gutierrez *et al.*, 2012; Koh *et al.*, 2010; Pradhan *et al.*, 2012). Differences in WAXD patterns of nanocomposite films were observed compared with

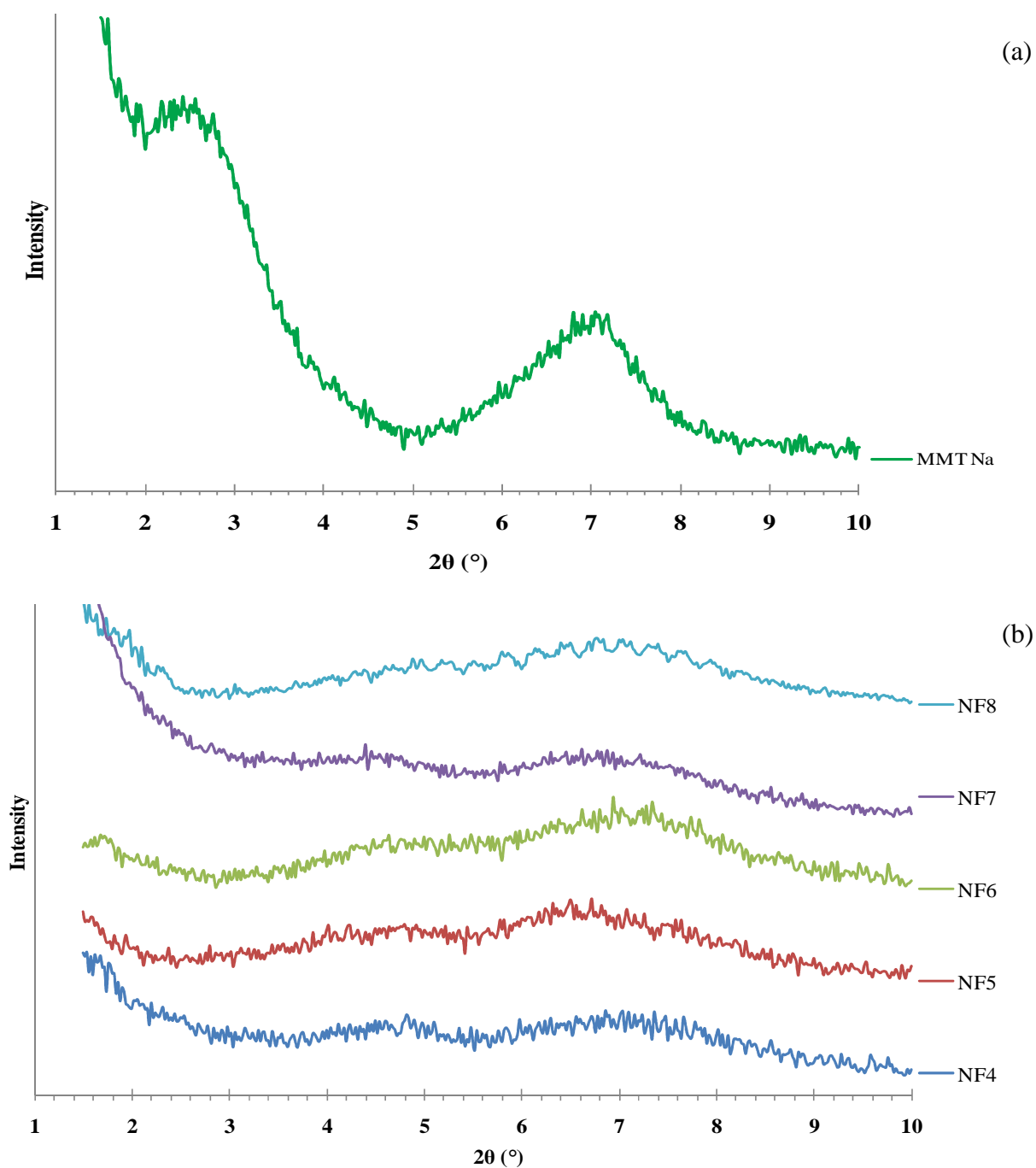


**Figure 35.** WAXD patterns of Cloisite Na<sup>+</sup> (a) and nanocomposite films from tilapia skin gelatin incorporated with Cloisite Na<sup>+</sup> prepared from FFS at different pH levels (b). MMT Na: Cloisite Na<sup>+</sup>; NF4, NF5, NF6, NF7 and NF8 represent gelatin nanocomposite films incorporated with Cloisite Na<sup>+</sup> prepared from FFS at pHs 4, 5, 6, 7 and 8, respectively.

that of Cloisite nanoclay (Figure 35b). In general, the characteristic broad peak of amorphous proteins was obtained in the  $2\theta$  range of 6.2 to 9.5 ° for all nanocomposite films (Grevellec *et al.*, 2001; Martucci and Ruseckaite, 2010a). Gelatin nanocomposite films showed the differences in WAXD patterns. This suggested varying intercalation or exfoliation of nanoclays in gelatin matrix as affected by pHs (Bae *et al.*, 2009a). In general, the WAXD patterns of all nanocomposite films exhibited the halo diffraction peak at  $2\theta$  in the range of 6-9 ° as well as no sharp characteristic diffraction peak of nanoclay was observed. This suggested the intercalated/exfoliated structure of nanocomposites (Bae *et al.*, 2009a; Martucci and Ruseckaite, 2010b). Positively charged protein chains more likely interacted well with the negatively charged hydrophilic nanoclay, thereby forming intercalated/exfoliated gelatin/Cloisite Na<sup>+</sup> nanocomposites to a high extent (Bae *et al.*, 2009a). Moreover, the exchange between the cationic -NH<sub>3</sub><sup>+</sup> groups on the amino acid side chains of the gelatin and the Na<sup>+</sup> ion occupying exchange sites of the montmorillonite surface was reported (Ensminger and Giesecking, 1941). Nevertheless, it was noticed that the halo diffraction peak of NF7 and NF8 films became even broader. This suggested the lost of regularity or homogeneity of the film structures, possibly due to non-homogeneous aggregation of gelatin chains at those particular pH levels which were neutral or close to the pI. Therefore, the intercalated or exfoliated structures of obtained gelatin nanocomposite films were dependent on the pH levels.

#### 8.4.2.2 Thickness

Thickness of nanocomposite films prepared from FFS containing tilapia skin gelatin and Cloisite Na<sup>+</sup> at different pHs is shown in Table 30. Differences in thickness were observed between nanocomposite films prepared from FFS with various pHs ( $P < 0.05$ ). Generally, thickness was increased as the pH of FFS increased ( $P < 0.05$ ). Highest thickness was observed for NF7 ( $P < 0.05$ ). Gelatin might be coagulated rather than dispersed at this pH level since pH was close to the isoelectric point of gelatin (8.38) (Gennadios *et al.*, 1993). Protruded film matrix built up from coagulated proteins was more likely thicker than ordered film. The lowest thickness

was obtained for NF4 ( $P < 0.05$ ). At acidic pH, most of gelatin molecules were plausibly unfolded. These unfolded chains could undergo interaction with fewer grooves. As a result, the thinner films could be obtained. Due to the small level, nanoclays were distributed throughout the film matrix and played a negligible role in thickness of resulting films. Therefore, the thickness of tilapia skin gelatin nanocomposite films was mainly affected by the pH of FFS.

#### 8.4.2.3 Mechanical properties

Mechanical properties, including YM, TS and EAB of nanocomposite films from tilapia skin gelatin and Cloisite Na<sup>+</sup> as influenced by pH of FFS are shown in Table 30. Differences in mechanical properties were observed for nanocomposite films prepared from FFS having different pHs ( $P < 0.05$ ). Generally, YM of the nanocomposite films increased as pH of FFS increased up to 6 ( $P < 0.05$ ). Nevertheless, further increase in pH of FFS (pHs 7 and 8) decreased YM of resulting films ( $P < 0.05$ ). At pH 6, the stronger interaction between positively charged gelatin molecules and negatively charged nanoclay might take place. However, when the pH was too far away from the pI, the protein was more positively charged. As a consequence, the repulsion became dominant, thereby lowering the chain interaction. Amongst all sample, NF4 had the lowest YM ( $P < 0.05$ ). At pH close to pI (8.38), strong electrostatic interaction between of ionised groups occurred, leading to coagulation/aggregation of proteins (Bae *et al.*, 2009a; Gennadios *et al.*, 1993). As a result, charged domains were less available for binding with nanoclays. Thus, strengthening effect caused by nanoclays was lower as indicated by the lower YM of films prepared from FFS at pH 7 and 8. Decrease in YM at alkaline pH level, which can be ascribed to electrostatic repulsion between the protein anion and the negatively charged montmorillonite surface (McClaren *et al.*, 1958).

TS, indicating the maximum stress that the film can withstand while being stretched or pulled before failing or breaking, increased with increasing pH levels of FFS up to 6 and further increase in pH levels decreased the TS ( $P < 0.05$ ). Amongst all films, that prepared from FFS at the pH of 6 showed the highest TS



( $P < 0.05$ ). This result suggested that the mechanism of film formation could be different when film-forming suspensions with various pHs were used. The main associative forces between positively charged gelatin molecules and negatively charged Cloisite  $\text{Na}^+$  could be a major factor determining TS of films. The intercalation or exfoliation of gelatin in Na-homoionic smectites was maximised at a particular pH, which promoted the protonation of amino groups of the gelatin. The positively charged gelatin was able to replace the sodium ions which are mainly located on the interlayer space of the smectites totally or partially (Ruiz-Hitzky *et al.*, 2005). The stronger interaction between gelatin and montmorillonite primarily involved an exchange between the cationic ( $-\text{NH}_3^+$ ) groups on the amino acid side chains of the gelatin and the  $\text{Na}^+$  ion occupying exchange sites at the montmorillonite surface (Theng, 1979). Moreover, their high ability to establish protein-protein interactions via hydrogen bonds, hydrophobic and ionic interactions at pH 6 also contributed to the stronger network (Koli *et al.*, 2013; Shiku *et al.*, 2004). The lowest TS was observed for films prepared from FFS with the acidic pH level (NF4). Similar result was reported earlier for films obtained from tilapia scale gelatin (Weng *et al.*, 2014). Repulsion force between positively charged gelatin molecules at very acidic pH could impede the interaction between chains, thereby lowering the strength of film network.

EAB of nanocomposite films decreased with increasing levels of pH up to 6 ( $P < 0.05$ ) and further increase in pH levels increased the EAB ( $P < 0.05$ ). The highest EAB was observed for NF4 ( $P < 0.05$ ), which was correlated well with the lowest TS of NF4. EAB is determined at the point where the film breaks under tensile testing and is expressed as the percentage of change of the original length of the specimen between the grips of the testing machine (Briston, 1988). The ability of a film to stretch/extend is indicated by EAB. On the other hand, the lowest EAB of NF6 was in accordance with the highest YM and TS. The result suggested that the strengthening effect mediated by pH of nanocomposite films could reduce the extensibility of resulting films. Thus, the pH levels of FFS directly affected the mechanical properties of resulting nanocomposite films.

**Table 30.** Young's Modulus (YM), tensile strength (TS), elongation at break (EAB), water vapour permeability (WVP) and thickness of nanocomposite films from tilapia skin gelatin incorporated with Cloisite Na<sup>+</sup> prepared from FFS at different pH levels

<b>Film samples</b>	<b>YM (MPa)</b>	<b>TS (MPa)</b>	<b>EAB (%)</b>	<b>WVP (X 10<sup>-11</sup> gmm<sup>-2</sup>s<sup>-1</sup>Pa<sup>-1</sup>)</b>	<b>Thickness (mm)</b>
<b>NF4</b>	482.51±14.38c	19.94±0.53d	15.50±3.61a	2.37±0.17a	0.043±0.002d
<b>NF5</b>	689.75±23.70b	25.88±0.58b	10.91±2.64b	2.07±0.21b	0.050±0.005c
<b>NF6</b>	888.90±3.09a	30.59±0.14a	6.46±0.16c	1.27±0.10c	0.055±0.004ab
<b>NF7</b>	674.26±12.52b	23.92±0.47c	8.85±0.38b	1.94±0.21b	0.058±0.002a
<b>NF8</b>	668.97±8.94b	24.56±0.92bc	10.65±2.45b	2.06±0.22b	0.053±0.003bc

Mean ± SD (n=3).

Different letters in the same column indicate significant differences (P<0.05).

#### 8.4.2.4 Water vapour permeability (WVP)

WVP of nanocomposite films from FFS containing tilapia skin gelatin and Cloisite Na<sup>+</sup> at different pH levels is shown in Table 30. WVP of nanocomposite films decreased with increasing pHs of FFS up to 6 ( $P < 0.05$ ). The increase in WVP was found in films prepared from FFS with pHs 7 and 8 ( $P < 0.05$ ). The lowest WVP of film prepared from FFS having pH of 6 was coincidental with the highest TS or YM of film. It could be suggested that the proper interaction between gelatin and Cloisite Na<sup>+</sup> could provide the strong network, which could hinder the migration of water vapour through the films. The distribution of nanoclays throughout the film might also serve as hinder for water vapour migration. High compactness of film can prevent the permeation of water vapour (Heng *et al.*, 2003). It was noted that NF4 film showed the highest WVP, compared with other films prepared from FFS having higher pH ( $P < 0.05$ ). NF4 film probably had less compactness with low ordered network. Weng *et al.* (2014) reported that the WVP of scale gelatin films prepared at mild acidic condition were higher than those of films prepared from gelatin extracted at neutral or alkaline conditions. Less intermolecular protein crosslinking occurred under acidic pH conditions and was caused by the repulsive forces developed amongst positively charged gelatins. As a result, the association of gelatin chains became lower, leading to the decreased strength and less dense structure (Gontard *et al.*, 1993). Therefore, gelatin nanocomposite films had varying WVP, depending on the pH of FFS used for film formation.

#### 8.4.2.5 Colour

Colour of nanocomposite films prepared from FFS containing tilapia skin gelatin and Cloisite Na<sup>+</sup> at different pH levels is shown in Table 31. The highest  $L^*$ - value (lightness) was obtained for NF8 film ( $P < 0.05$ ). However, there was no significant difference in  $L^*$ - value between other nanocomposite films ( $P > 0.05$ ). Similar  $a^*$ - value was observed for nanocomposite films prepared under acidic condition ( $P > 0.05$ ). Films prepared at the pHs of 7 and 8 showed similar  $a^*$ - value ( $P > 0.05$ ) and showed higher  $b^*$ - value than other films ( $P < 0.05$ ). The  $b^*$ - value was

**Table 31.** Colour of nanocomposite films from tilapia skin gelatin incorporated with Cloisite Na<sup>+</sup> prepared from FFS at different pH levels

<b>Film samples</b>	<b><i>L</i>*</b>	<b><i>a</i>*</b>	<b><i>b</i>*</b>	<b><math>\Delta E^*</math></b>
<b>NF4</b>	93.48±0.06b	-0.96±0.01a	0.84±0.01c	2.46±0.06a
<b>NF5</b>	93.52±0.05b	-0.95±0.02a	0.87±0.04bc	2.42±0.05ab
<b>NF6</b>	93.60±0.26ab	-0.97±0.02a	0.95±0.04b	2.36±0.26ab
<b>NF7</b>	93.56±0.07b	-1.07±0.02b	1.14±0.07a	2.44±0.07ab
<b>NF8</b>	93.83±0.07a	-1.07±0.02b	1.15±0.04a	2.19±0.06b

Mean ± SD (n=3).

Different letters in the same column indicate significant differences (P<0.05).

increased as the pH level of FFS increased ( $P < 0.05$ ). This was plausibly due to the formation of yellowish pigment, especially via Maillard reaction. The reductone formation over furfural production from the amadori products could induced at alkaline pH level, leading to colour development in nanocomposite films (Bates *et al.*, 1998). The lowest  $\Delta E^*$ - value (total colour difference) of NF8 film was in agreement with the highest  $L^*$ - value ( $P < 0.05$ ). Thus, colour of nanocomposite gelatin films was affected by different pH levels of FFS.

#### 8.4.2.6 Light transmission and transparency

Transmission of UV and visible light at selected wavelengths in the range of 200–800 nm of films made from FFS containing tilapia skin gelatin and Cloisite Na<sup>+</sup> at different pH levels is shown in Table 32. Light transmission of nanocomposite films at all wavelengths decreased when the pH level of FFS increased ( $P < 0.05$ ). Nevertheless, slight increase in transmission was found in NF8 films. Gelatin nanocomposite films had the excellent barrier property against the light in UV at 200 nm. Gelatin films are commonly known to have the excellent UV barrier property due to the presence of high content of aromatic amino acids, which can absorb UV light (Jongjareonrak *et al.*, 2008; Weng *et al.*, 2014). Higher UV light barrier ability was reported for gelatin films (Arvanitoyannis, 2002; Gomez-Guillen *et al.*, 2009; Hoque *et al.*, 2011c; Jongjareonrak *et al.*, 2006b). Light transmittance of nanocomposite films at wavelength of 280 nm decreased markedly with increasing pH levels of FFS. Light transmission in visible range (350–800 nm) of all nanocomposite films was in the range of 75.77–87.93%. Amongst all films, NF7 had the highest barrier property in the visible range ( $P < 0.05$ ).

Transparency value of nanocomposite films decreased when the pH of FFS increased up to 6 ( $P < 0.05$ ). However, the highest transparency value was obtained for NF7 ( $P < 0.05$ ). Higher transparency value indicated that the films had lower transparency. NF8 had the lowest transparency value ( $P < 0.05$ ), indicating the highest transparency. Transparency of protein based films is generally affected by additives, processing conditions, thickness as well as compatibility between polymer

**Table 32.** Light transmittance (%) and transparency values of nanocomposite films from tilapia skin gelatin incorporated with Cloisite Na<sup>+</sup> prepared from FFS at different pH levels

Film samples	Wavelength (nm)								Transparency values
	200	280	350	400	500	600	700	800	
<b>NF4</b>	0.02	48.20	80.70	83.08	85.26	86.46	87.29	87.93	1.40±0.0001b
<b>NF5</b>	0.03	42.45	78.97	81.65	84.03	85.36	86.27	86.96	1.38±0.0002c
<b>NF6</b>	0.03	40.00	76.60	79.58	82.45	84.05	85.21	86.12	1.37±0.0005d
<b>NF7</b>	0.02	35.65	75.77	79.05	81.99	83.55	84.70	85.59	1.42±0.0010a
<b>NF8</b>	0.03	36.82	76.73	80.11	83.36	85.00	86.12	86.97	1.34±0.0005e

Mean ± SD (n=3).

Different letters in the same column indicate significant differences (P<0.05).

and nanoclay (Farahnaky *et al.*, 2014; Hoque *et al.*, 2011c; Martucci and Ruseckaite, 2010b; Nagarajan *et al.*, 2014a,b; Rhim, 2007). The lowest transparency of NF7 was in agreement with the highest thickness ( $P < 0.05$ ). The results indicated that the pH of FFS had an impact on the appearance and light barrier property of gelatin nanocomposite films.

#### 8.4.2.7 Microstructure

SEM micrographs of the surface (8000x) and cryo-fractured cross-section (3000x) of nanocomposite films from tilapia skin gelatin incorporated with Cloisite Na<sup>+</sup> as affected by pHs of FFS are shown in Figure 36. Nanocomposite films prepared from FFS with different pH levels had no crack on the surface. It was noted that, homogeneity and smoothness of film surface varied, upon the pH levels of FFS. This might be due to different interaction between nanoclay and gelatin in film matrix. NF6 had the smooth surface in comparison with other gelatin nanocomposite films. At pH 6, the continuous and ordered matrix might be developed (Theng, 1979), due to the positively charged gelatin molecules interacted well with negatively charged nanoclay particles. SEM images correlated well with the WAXD pattern of NF6 film as demonstrated in Figure 35b, suggesting the intercalated/exfoliated structure. Gelatin film incorporated with nanoclay at pH 4 (NF4) showed rougher surface, compared to other nanocomposite films. Nanoclay plausibly could not interact or disperse well within NF4 film, in which the electrostatic repulsive force at this acidic pH was dominant. This was in accordance with the lowest mechanical and water vapour barrier properties of NF4 films.

For cross-section, gelatin films incorporated with Cloisite Na<sup>+</sup> prepared from FFS with pH 6 showed a more compact structure, compared to other films. The compact structure of NF6 film was also responsible for the lowest WVP and the highest YM and TS (Table 30). The compactness of gelatin–nanoclay composite films was mainly because of the reduced free volume space within the gelatin matrix, probably owing to intermolecular attractive forces and protein chains arrangement with nanoclays. For NF7 and NF8 films, their cross-sectional images showed rougher

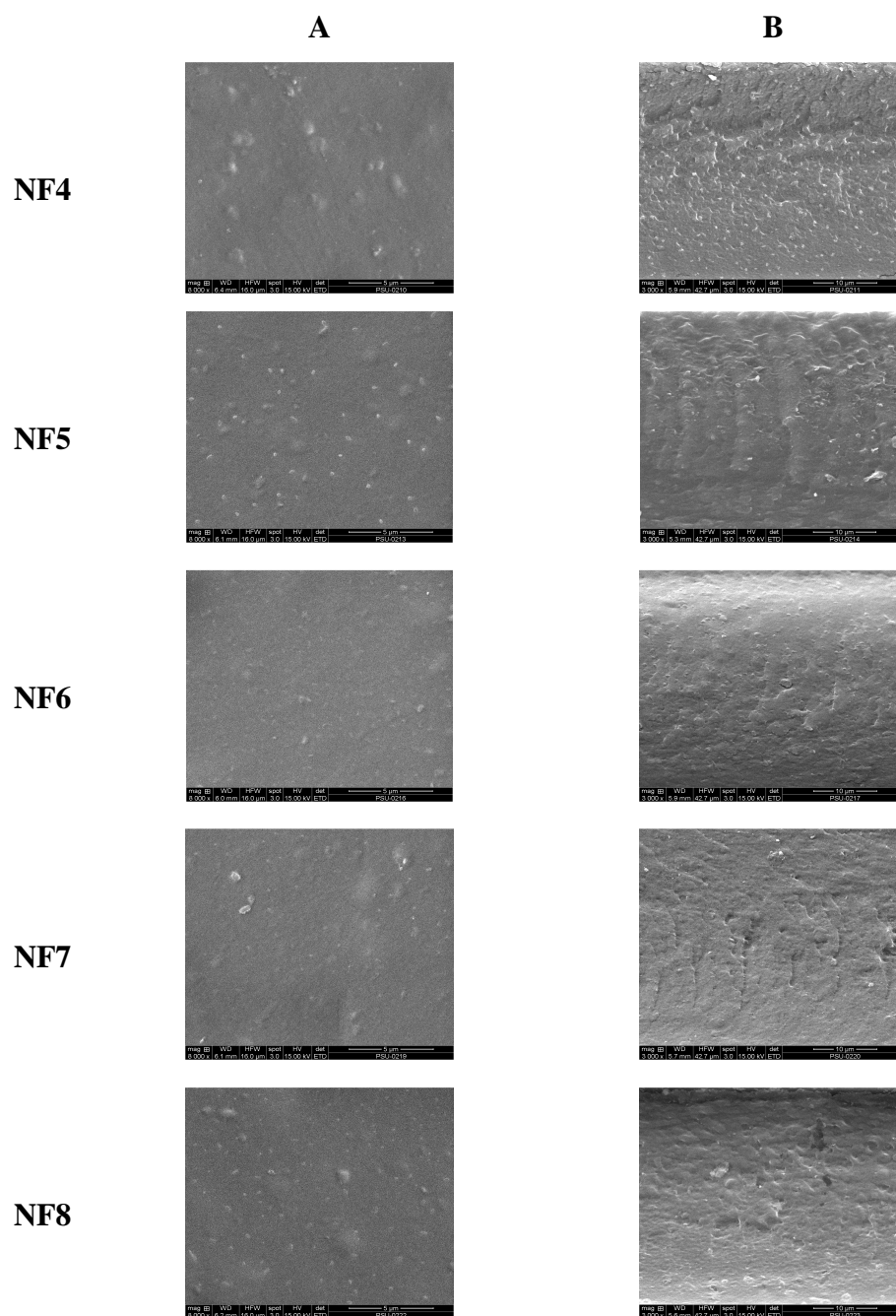


**Figure 36.** SEM micrographs of surface (A) and cryo-fractured cross-section (B) of nanocomposite films from tilapia skin gelatin incorporated with Cloisite Na<sup>+</sup> prepared from FFS at different pH levels. Magnification: 8000x for surface and 3000x for cross-section. NF4, NF5, NF6, NF7 and NF8 represent gelatin nanocomposite films incorporated with Cloisite Na<sup>+</sup> prepared from FFS at pHs 4, 5, 6, 7 and 8, respectively.



microstructure as compared to others. This might be due to the coagulation or aggregation of gelatin chains at pH 7-8. The microstructure results were in agreement with the WAXD results as well as the mechanical and barrier properties. Thus, the microstructures of nanocomposite films were governed by the pH levels of FFS.

#### 8.4.2.8 Thermogravimetric curves

Thermal degradation behaviours of nanocomposite films from tilapia skin gelatin incorporated with Cloisite Na<sup>+</sup> as influenced by pH levels of FFS were determined by TGA analysis and their thermograms are depicted in Figure 37. Their corresponding degradation temperatures (Td) and weight loss ( $\Delta w$ ) are presented in Table 33. Nanocomposite films showed the first stage of weight loss ( $\Delta w_1 = 4.82\text{--}6.30\%$ ) approximately at onset temperatures (Td<sub>1</sub>) of 57.14–69.05 °C, mostly associated with the continuous loss of free moisture absorbed in the films. The second stage of weight loss ( $\Delta w_2 = 71.26\text{--}72.24\%$ ) was observed at the degradation temperatures (Td<sub>2</sub>) of 188.91-207.43 °C, depending on the nanocomposite films. This transition might be due to the degradation of protein matrix as well as plasticiser, glycerol, in the nanocomposite films. Td<sub>2</sub> seemed to increase with increasing pH levels up to pH 6. This was plausibly due to the positively charged gelatin molecules interacted well with negatively charged nanoclay particles, resulting in thermal resistance of the films. Nevertheless, films prepared at pH 6, 7 and 8 showed similar Td<sub>2</sub> (206.38-207.43 °C). NF6 film showed the higher thermal degradation temperature (Td<sub>2</sub>) The strong interaction between gelatin molecules and nanoclay mostly yielded the stronger film network with ordered structures, leading to higher heat resistance of the resulting film.

Additionally, nanocomposite films showed slight differences in residual mass (representing char content) at 600 °C in the range of 21.77-23.81%. This suggested the varying matrix, strengthened by nanoclay to different extents. It was also suggested that the interaction of gelatin and nanoclays could be varied as determined by pH of FFS. Thus, TGA study confirmed that pH levels of FFS had the direct impact on thermal stability of resulting nanocomposite films.

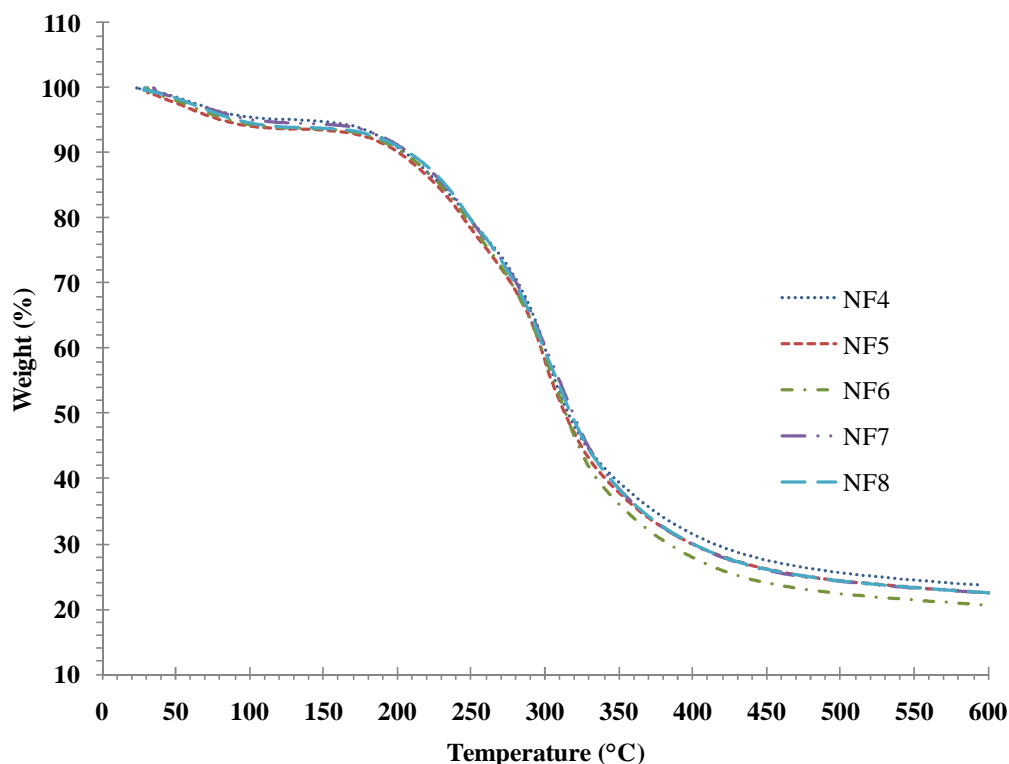


**Figure 37.** Thermogravimetric curves of nanocomposite films from tilapia skin gelatin incorporated with Cloisite Na<sup>+</sup> prepared from FFS at different pH levels. NF4, NF5, NF6, NF7 and NF8 represent gelatin nanocomposite films incorporated with Cloisite Na<sup>+</sup> prepared from FFS at pHs 4, 5, 6, 7 and 8, respectively.

#### 8.4.2.9 Differential scanning calorimetric thermograms

DSC thermograms of the first and second heating scans of films from tilapia skin gelatin incorporated with Cloisite Na<sup>+</sup> using FFS at different pH levels are depicted in Figure 38(a) and 38(b), respectively. Glass transition temperature ( $T_g$ ) of films during the first and second heating scan is presented in Table 33. For the first heating scan, all nanocomposite films exhibited glass transition at the temperature of 48.77-54.71 °C, depending on film samples.  $T_g$  is an important parameter for determining the stability of edible biodegradable polymers (Ghanbarzadeh and Oromiehi, 2009). The  $T_g$  of gelatin nanocomposite films prepared from FFS at pH 4 (NF4) was 48.77 °C, and increased with increasing pH levels of FFS up to pH 6. NF6 film had the highest  $T_g$  (54.71 °C) when compared to other films. The result suggested

**Table 33.** Thermal degradation temperature ( $T_d$ , °C), weight loss ( $\Delta w$ , %) and glass transition temperature ( $T_g$ , °C) of nanocomposite films from tilapia skin gelatin incorporated with Cloisite Na<sup>+</sup> prepared from FFS at different pH levels

Film samples	$\Delta_1$		$\Delta_2$		Residue (%)	$T_g$	
	$T_{d1, \text{onset}}$	$\Delta w_1$	$T_{d2, \text{onset}}$	$\Delta w_2$		1 <sup>st</sup> scan	2 <sup>nd</sup> scan
<b>NF4</b>	61.91	4.82	188.91	71.37	23.81	48.77	104.49
<b>NF5</b>	57.14	6.30	200.82	71.26	22.44	51.22	119.28
<b>NF6</b>	64.29	6.12	207.43	72.11	21.77	54.71	121.42
<b>NF7</b>	69.05	5.44	206.38	72.24	22.32	50.06	108.07
<b>NF8</b>	65.48	6.10	207.07	71.49	22.44	51.35	109.46

$\Delta_1$  and  $\Delta_2$  denote the first and second stage weight loss, respectively of nanofilm during TGA heating scan.

that higher amount of bonding between negative charged nanoclay and positive charged gelatin molecules yielded stronger film network at pH 6 (Figure 39), leading to increased molecular rigidity of gelatin and heat resistance of the resulting film. However,  $T_g$  of nanocomposite films decreased when pH 7 and 8 were used to prepare the films. This might be due to the poor interaction between gelatin molecules and nanoclays. The charged domains were less available for nanoclays binding as a consequence of the strong electrostatic interaction between ionised groups at pH close to pI (Figure 39).  $T_g$  was found to have a positive relationship with the YM and TS of protein films (Pommet *et al.*, 2005). Similar trend was observed in this study for nanocomposite films prepared from FFS at different pH levels (Table 30). Weng *et al.* (2014) reported similar results for tilapia scale gelatin films. The first heating scan of all films also revealed the endothermic peak transition around the temperature of 134.17-149.09 °C. This transition was most likely associated with the evaporation of bound water. Langmaier *et al.* (2008) also reported the similar endothermic peak, which was occurred due to the evaporation of absorbed moisture in collagen hydrolysate films. The absorbed water played an important role in the plasticising effect of gelatin films.

In the thermograms of the second heating scan, glass transition was observed for all nanocomposite films in the temperature range of 104.49-121.42 °C (Figure 38b). It was noticed that the endothermic peak transition disappeared in the second heating scan. This was plausibly because of the absorbed water, acting as plasticiser, was removed during the first heating scan (Hoque *et al.*, 2011c). As a consequence, the interactions between gelatin chains and also between gelatin molecules and nanoclays could be enhanced, in which more rigid film network was formed. Therefore, the glass transition of all films obviously shifted to higher temperature, as compared to that observed in the first heating scan. The result suggested that thermal properties of nanocomposite films from tilapia skin gelatin were affected by the pH levels of FFS.

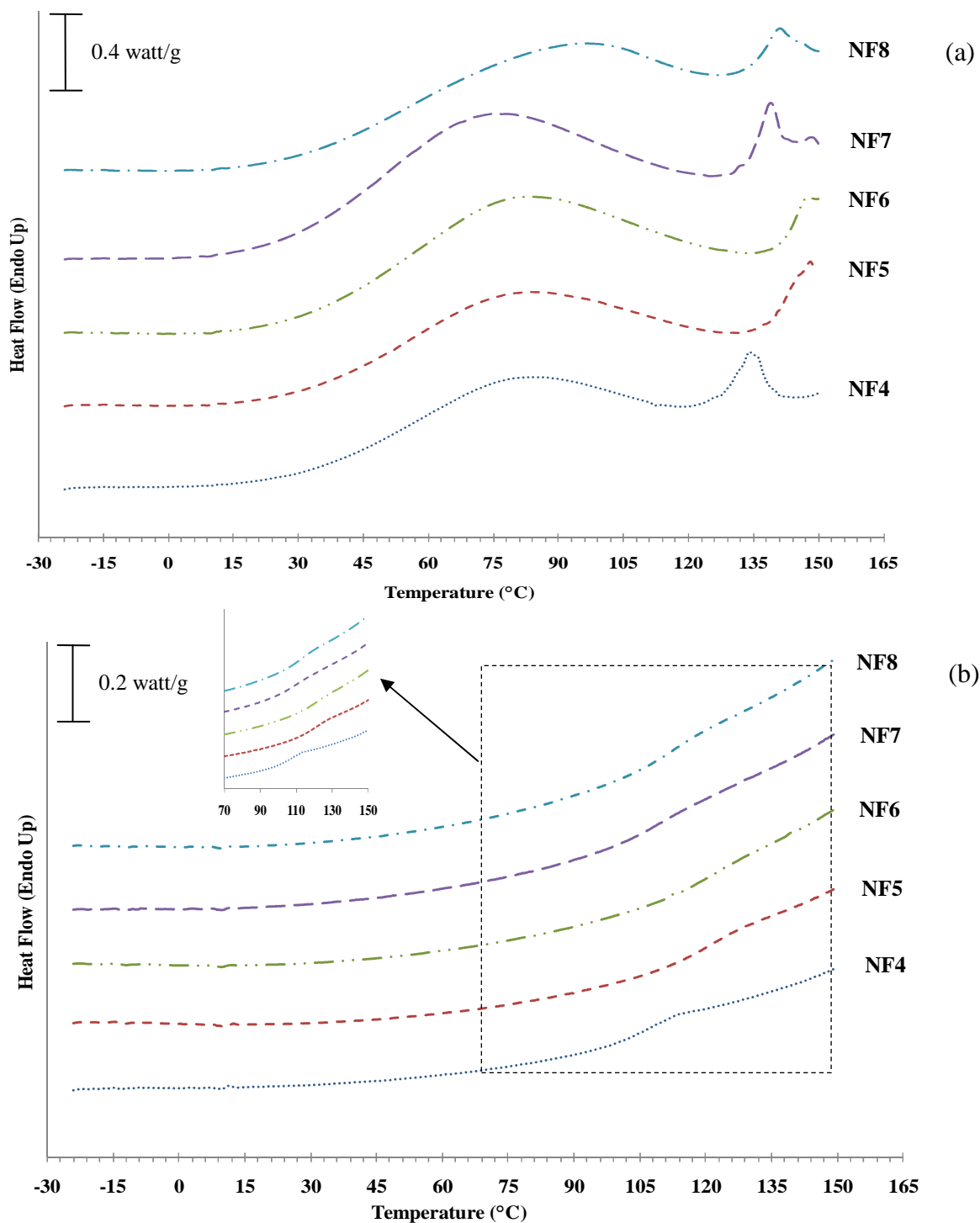


**Figure 38.** DSC thermograms of nanocomposite films from tilapia skin gelatin incorporated with Cloisite Na<sup>+</sup> prepared from FFS at different pH levels. NF4, NF5, NF6, NF7 and NF8 represent gelatin nanocomposite films incorporated with Cloisite Na<sup>+</sup> prepared from FFS at pHs 4, 5, 6, 7 and 8, respectively.

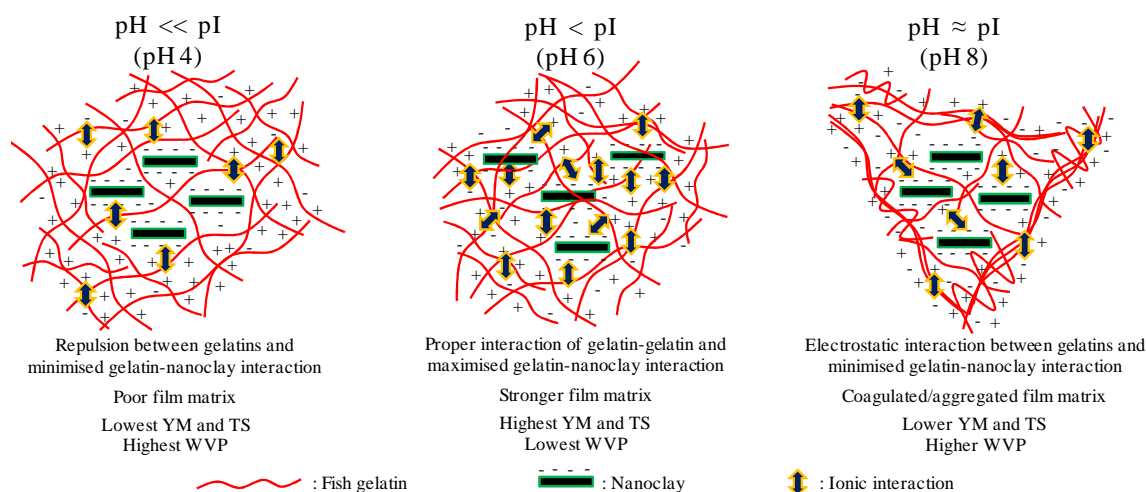


**Figure 39.** Proposed scheme of nanoclay incorporation with gelatin chains at different pH levels of FFS.

## 8.5 Conclusion

Gelatin nanocomposite films from tilapia skin prepared from FFS with different pH levels showed different properties and characteristics. The highest mechanical, water vapour barrier as well as thermal properties were obtained when FFS with pH of 6 was used. Nanocomposite films prepared at pH 6 had the stronger film network, possibly due to the stronger interaction between positively charged gelatin molecules and negatively charged nanoclays. WAXD patterns revealed the intercalated/exfoliated structure of nanocomposite films. Poorer properties of gelatin nanocomposite films were observed at inappropriate pH of FFS, mainly due to excessive electrostatic repulsive forces and the low interaction between nanoclay and gelatin molecules.

## CHAPTER 9

### PROPERTIES AND CHARACTERISTICS OF NANOCOMPOSITE FILMS FROM TILAPIA SKIN GELATIN INCORPORATED WITH ETHANOLIC EXTRACT FROM COCONUT HUSK

#### 9.1 Abstract

Impacts of ethanolic extract from coconut husk (EECH) at 0-0.4% (w/w, on protein basis) on properties of films from tilapia skin gelatin and gelatin/Cloisite Na<sup>+</sup> nanocomposite films were investigated. Young's Modulus, tensile strength and elongation at break of both films decreased with addition of EECH (P<0.05). The lowest water vapour permeability (WVP) was obtained for gelatin film containing 0.05% EECH (w/w) (P<0.05). Nevertheless, the nanocomposite film showed the lowest WVP when incorporated with 0.4% EECH (w/w) (P<0.05). Generally, *L*\*- value (lightness) decreased and *a*\*- value (redness) of films increased (P<0.05) with increasing levels of EECH, regardless of nanoclay incorporation. Transparency of both films generally decreased as the level of EECH increased (P<0.05). Intercalated or exfoliated structure of nanocomposite films was revealed by wide angle X-ray diffraction (WAXD) analysis. Based on scanning electron microscopic (SEM) analysis, the rougher surface was found when EECH was added. EECH had varying impact on thermal stability of films as revealed by thermogravimetric (TGA) and differential scanning calorimetric (DSC) analyses. Thus, the incorporation of EECH determined the properties of both gelatin film and nanocomposite film in which the improved water vapour barrier property could be obtained.

#### 9.2 Introduction

Packaging from biopolymers known as 'bio- or eco- packaging' can be used to replace foods' plastic packaging materials, thereby lowering waste disposal (Tharanathan, 2003). Biodegradable packaging is universally gaining the great

interest for the protection and shelf-life extension of foods (Bao *et al.*, 2009). In recent years, there has been growing public concern about sustainability practices, green chemistry and inherent safe design. Consequently, an urgent need is emerging for the efficient use of natural resources (Gomez-Guillen *et al.*, 2009). Biodegradable films are normally made from renewable biopolymers such as proteins, lipids, polysaccharides (Tharanathan, 2003). Proteins are thermoplastic heteropolymers containing both polar and non-polar amino acids, which are able to form numerous intermolecular linkages (Chinabark *et al.*, 2007). However, resistance of protein films to water vapor transmission is limited due to the inherent hydrophilicity of proteins (Gennadios *et al.*, 1993). Amongst all proteins, gelatin has been attracted the attention for the development of edible films due to its abundance, biodegradability and its broad range of functional properties and applications (Karim and Bhat, 2009). Gelatin films have poor water vapour barrier property; however, they have been found to be very effective UV light and oxygen barriers (Gennadios *et al.*, 1993; Jongjareonrak *et al.*, 2008). The hydrophilic nature of proteins induces interaction with water, causing swelling and apparent thickness alteration (Avena-Bustillos and Krochta, 1993).

Nowadays, one of the most effective alternatives to amelioration of the barrier and mechanical properties of packaging materials, either synthetic or natural, is the formation of nanocomposites (Bae *et al.*, 2009a; Farahnakhy *et al.*, 2014). Montmorillonite nanoclays, such as sodium bentonite, a hydrophilic aluminum phyllosilicate with high water sorption and swelling capacity can be homogeneously dispersed in a polymeric matrix to form the new nanocomposite (Ray and Okamoto, 2003). Its crystal lattice consists of 1 nm thin layers formed by an octahedral alumina sheet sandwiched between two tetrahedral silica sheets. It has a high surface area (aspect ratio of about 100), and is negatively charged (Ray and Okamoto, 2003). The stacking of these layers leads to a Van der Waals gap or gallery, in which alkaline cations, such as  $\text{Na}^+$ ,  $\text{Li}^+$  or  $\text{Ca}_2^+$ , can neutralise the charge. The major problem in preparing these composites is to separate the initially agglomerated clay layers. Therefore, a necessary step, in which the clay layers are well dispersed in the polymer



matrix, is implemented (Nagarajan *et al.*, 2014a). The improved barrier properties could be obtained from well and organised dispersion of nanoclays in the gelatin matrix (Martucci and Ruseckaite, 2010a). In general, the ‘tortuous path’ in nanocomposite films has been reported (Rhim, 2007). Gelatin bio-nanocomposite films have been prepared (Bae *et al.*, 2009a; Farahnakhy *et al.*, 2014; Martucci and Ruseckaite, 2010a; Nagarajan *et al.*, 2014b).

Coconut husk, the fibrous external portion of the fruit of coconut palms, is a by-product of the copra extraction process and is generally considered as a waste (Vazquez-Torres *et al.*, 1992). Vazquez-Torres *et al.* (1992) reported that polymer/antioxidant such as lignin can be successfully extracted from coconut husk. The use of coconut husk extract containing phenolic compounds in gelatin films or nanocomposite films might induce the formation of complex matrix, thereby improving water barrier property. Phenolic compounds from plant origin were reported to improve mechanical property of gelatin-based films (Bitencourt *et al.*, 2014; Hoque *et al.*, 2011c; Kavooosi *et al.*, 2013). The present study aimed to investigate the effect of ethanolic extract from coconut husk on the barrier and mechanical properties as well as thermal stability of tilapia skin gelatin films and nanocomposite films.

## **9.3 Materials and methods**

### **9.3.1 Chemicals**

Fish skin gelatin from tilapia (~240 bloom) was obtained from Lapi Gelatine (Empoli, Italy). MMT-nanoclay, Cloisite<sup>®</sup> Na<sup>+</sup> was purchased from Southern clay products Inc. (Gonzlaes, TX, USA). Glycerol was procured from Merck (Darmstadt, Germany). Ethanol was purchased from RCI Labscan (Pathumwan, Thailand). All chemicals were of analytical grade.

### **9.3.2 Extraction of ethanolic extract from coconut husk**

#### **9.3.2.1 Collection and preparation of coconut husk**

Coconut husk was obtained from a local market in Hat Yai, Songkhla, Thailand and transported to the Department of Food Technology, Prince of Songkla University, Hat Yai, Thailand. Husk sample was prepared as per the method of Vazquez-Torres *et al.* (1992) with slight modifications. Husk sample was dried at 60 °C in the cabinet rotary dryer for 16 h and then defibered. Husk sample was then subjected to grinding using a mill (IKA Labortechnik colloid mill, Selangor, Malaysia). The prepared sample was then sieved with the aid of sieve shaker (Model EVJ1, Endecotts Ltd., London, UK) with a sieve size of 6 mm (Woven wire sieves, Endecotts Ltd., London, UK). This coarse form was further blended using a blender (Panasonic, Model MX-898N, Berkshire, UK) and finally sieved using a stainless steel sieve of 80 mesh. The coconut husk powder obtained was further dried in a hot air oven (Memmert, Schwabach, Germany) at 105 °C overnight. The obtained powder was placed in a polyethylene bag, sealed and kept at room temperature until use.

#### **9.3.2.2 Preparation of the ethanolic extract**

Coconut husk powder was subjected to extraction according to the method of Santoso *et al.* (2004) with a slight modification. Ten grams of husk powder were mixed with 250 ml of 80% ethanol (w/v). The mixture was stirred at room temperature (28–30 °C) using a magnetic stirrer (IKA-Werke, Staufen, Germany) for 3 h. The mixture was then centrifuged at 5000g for 30 min at room temperature using a RC-5B plus centrifuge (Beckman, JE-AVANTI, Fullerton, CA, USA). The supernatant was filtered using a Whatman No. 1 filter paper (Whatman International, Ltd., Maidstone, England). The filtrate was then evaporated at 40 °C using an Eyela rotary evaporator (Tokyo Rikakikai, Co. Ltd., Tokyo, Japan). To remove the residual ethanol, the extract was purged with nitrogen gas. The extract was then dried using a Scanvac Model Coolsafe 55 freeze dryer (Coolsafe, Lyngø, Denmark) to obtain the dry extract. Dried extract was powdered using a mortar and pestle and was kept in an amber bottle and stored in a desiccator until use. The obtained powder was referred to

as 'ethanolic extract from coconut husk, EECH'. EECH had phenolic content of 436.82 mg tannic acid equivalent/g as determined by Folin–Ciocalteu reagent (Slinkard and Singleton, 1977).

### 9.3.3 Preparation of gelatin films and nanocomposite films

Gelatin films and nanocomposite films were prepared as per the methods of Bae *et al.* (2009a) and Hoque *et al.* (2011c) as illustrated in Figure 40. Firstly, gelatin solution was prepared by mixing the gelatin powder with distilled water to obtain protein concentration of 3% (w/v) as determined by the Kjeldhal method (AOAC, 2000). Thereafter, glycerol (25% of protein, w/w) was added into the gelatin solution as a plasticiser. The final volume was made up to 100 ml using the distilled water and referred to as 'film-forming solution'.

To prepare nanocomposite film, nanoclay, Cloisite Na<sup>+</sup> was mixed with distilled water to obtain a final concentration of 1% (w/w, on protein basis). The mixture was stirred at 1000 rpm (IKA Labortechnik stirrer, Selangor, Malaysia) for 5 min at room temperature. Nanoclay suspension was then incubated at 60 °C for 1 h to delaminate the nanoclay in a temperature controlled water bath (W350; Memmert, Schwabach, Germany) with occasional stirring. Nanoclay suspension was cooled down to room temperature and homogenised for 1 min at 5000 rpm (IKA Labortechnik homogeniser, Selangor, Malaysia). Gradually, nanoclay suspension was dropped into the gelatin solution, prepared as mentioned earlier and the mixture was homogenised for 30 sec at 5000 rpm. The mixture was degassed using a desiccator equipped with JEIO Model VE-11 electric aspirator (JEIO TECH, Seoul, Korea). The final volume was made up to 100 ml using the distilled water and referred to as 'film-forming suspension'.

Both film-forming solution and suspension were sonicated for 30 min using the sonicating bath (Elmasonic S 30 H, Singen, Germany), followed by gentle stirring for 24 h at room temperature to obtain a homogenous solution and suspension. Prior to casting, EECH was added to both film-forming solution and suspension at the levels of 0, 0.025, 0.05, 0.1, 0.2 and 0.4% (w/w, on protein basis) and the mixtures

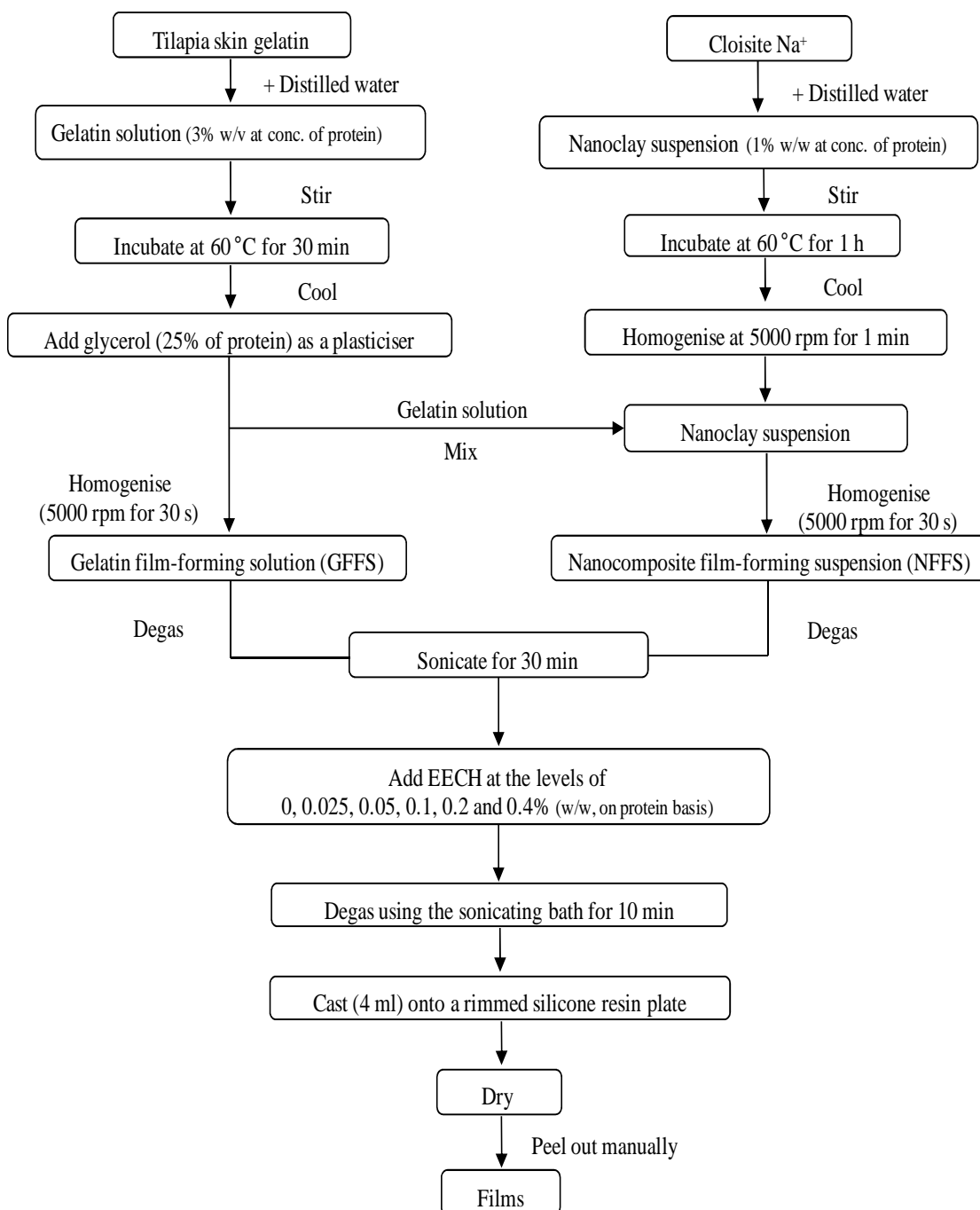


**Figure 40.** Scheme for preparation of gelatin film-forming solutions and nanocomposite film-forming suspensions incorporated with EECH.

were gently stirred for 1 h at room temperature. The mixtures were degassed for 10 min using the sonicating bath and then cast ( $4 \pm 0.01$  ml) onto a rimmed silicone resin plate ( $5 \times 5$  cm<sup>2</sup>), air-blown for 12 h at 25 °C, followed by drying in an environmental chamber (Binder GmbH, Tuttlingen, Germany) at  $25 \pm 0.5$  °C and  $50 \pm 5\%$  relative humidity (RH) for 24 h. Films obtained were manually peeled off. Gelatin films (GF) and nanocomposite films (NF) containing different levels of EECH were subjected to analyses.

#### **9.3.4 Analyses**

Prior to testing, samples were conditioned in an environmental chamber for 48 h at  $50 \pm 5\%$  relative humidity (RH) and  $25 \pm 0.5$  °C. For WAXD, SEM, TGA and DSC studies, films were conditioned in a desiccator containing dried silica gel for 3 weeks at room temperature (28-30 °C) to obtain the most dehydrated films.

##### **9.3.4.1 Thickness**

The thickness of ten film samples of each condition was measured using a digital micrometer (Mitutoyo, Model ID-C112PM, Serial No. 00320, Mituyoto Corp., Kawasaki-shi, Japan). Ten random locations around each film sample were used for determination of thickness.

##### **9.3.4.2 Mechanical properties**

Young's Modulus (YM), tensile strength (TS) and elongation at break (EAB) of film samples were determined as described by Iwata *et al.* (2000) using the Universal Testing Machine (Lloyd Instruments, Hampshire, UK). The test was performed in the controlled room at 25 °C and  $50 \pm 5\%$  RH. Ten film samples ( $2 \times 5$  cm<sup>2</sup>) with the initial grip length of 3 cm were used for testing. The film samples were clamped and deformed under tensile loading using a 100 N load cell with the cross head speed of 30 mm/min until the samples were broken. The initial slope of the

stress-strain curve, the maximum load and final extension at break of the film samples were used to calculate YM, TS and EAB, respectively.

### 9.3.4.3 Water vapour permeability

Water vapour permeability (WVP) was measured using a modified ASTM (American Society for Testing and Materials, 1989) method as described by Shiku *et al.* (2004). Film samples were sealed on an aluminium permeation cup containing dried silica gel (0% RH) with silicone vacuum grease and rubber gasket. The cups were placed at 30 °C in a desiccator containing distilled water, followed by weighing at every 1 h intervals for up to 8 h. Five film samples were used for WVP testing. WVP of the film was calculated as follows:

$$\text{WVP (gmm}^{-2}\text{s}^{-1}\text{Pa}^{-1}) = w/lA^{-1} t^{-1} (P_2 - P_1)^{-1}$$

where,  $w$  is the weight gain of the cup (g);  $l$  is the film thickness (m);  $A$  is the exposed area of film ( $\text{m}^2$ );  $t$  is the time of gain (s);  $(P_2 - P_1)$  is the vapour pressure difference across the film (Pa).

### 9.3.4.4 Color

Colour of five film samples was determined using a CIE colourimeter (Hunter associates laboratory, Inc., Reston, VA, USA). Colour of the film was expressed as  $L^*$ - (lightness or brightness),  $a^*$ - (redness or greenness) and  $b^*$ - (yellowness or blueness) values. Total difference in colour ( $\Delta E^*$ ) was calculated according to Gennadios *et al.* (1996).

$$\Delta E^* = \sqrt{(\Delta L^*)^2 + (\Delta a^*)^2 + (\Delta b^*)^2}$$

where  $\Delta L^*$ ,  $\Delta a^*$  and  $\Delta b^*$  are the difference between the colour parameter of corresponding film samples and that of white standard ( $L^* = 92.81$ ,  $a^* = -1.24$  and  $b^* = 0.49$ ).

### 9.3.4.5 Light transmission and transparency

Light transmission of the films in ultraviolet (UV) and visible range were measured at selected wavelengths between 200 and 800 nm, using a UV-Visible spectrophotometer (model UV-1800, Shimadzu, Kyoto, Japan) according to the method of Jongjareonrak *et al.* (2008). The transparency value of five film samples was calculated by following the equation of Shiku *et al.* (2004).

$$\text{Transparency value} = (-\log T_{600})/x$$

where  $T_{600}$  is the fractional transmittance at 600 nm and  $x$  is the film thickness (mm). The higher transparency value represents the lower transparency of films.

### 9.3.5 Characterisation of selected films

Gelatin films and nanocomposite films incorporated with EECH at the selected levels (GF-0.05% and NF-0.4%) were further characterised, in comparison with the corresponding films.

#### 9.3.5.1 Wide angle x-ray diffraction (WAXD) analysis

WAXD analysis of the film samples was conducted in reflection mode with an incident wavelength ( $\lambda$ ) at 0.154 nm of  $\text{CuK}\alpha$  radiation (Martucci and Ruseckaite, 2010b). Measurements were performed for  $2\theta$  from  $5^\circ$  to  $10^\circ$  at a scan rate of  $1.0^\circ/\text{min}$ . The layer spacing of the clay was calculated from Bragg's law:

$$n\lambda = 2d \sin \theta$$

where  $\lambda$  is the wavelength of the radiation;  $d$  is the c-dimension distance or the interlayer spacing; and  $\theta$  is the diffraction angle (Bae *et al.*, 2009a).

#### 9.3.5.2 Scanning electron microscopic (SEM) analysis

Microstructure of the upper surface and cryo-fractured cross-section of the film samples was visualised using a scanning electron microscope (Quanta 400; FEI, Praha, Czech Republic) at an accelerating voltage of 15 kV, as described by

Farahnaky *et al.* (2014). The gelatin film samples were cryo-fractured by immersion in liquid nitrogen. Prior to visualisation, the film samples were mounted on a brass stub and sputtered with gold in order to make the sample conductive, and photographs were taken at 5000x magnification for surface analysis. For cross-sectional analysis, cryo-fractured films were mounted around stubs perpendicularly using double sided adhesive tape, coated with gold and observed at the 3000x magnification.

#### **9.3.5.3 Thermo-gravimetric analysis (TGA)**

Dried film samples were scanned using a thermogravimetric analyser (TGA-7, Perkin Elmer, Norwalk, CT, USA) from 30 to 600 °C using a heating rate of 10 °C/min (Nuthong *et al.*, 2009). Nitrogen was used as the purge gas at a flow rate of 20 ml/min.

#### **9.3.5.4 Differential scanning calorimetry (DSC)**

Thermal properties of film samples were determined using a differential scanning calorimeter (DSC-7, Perkin Elmer, Norwalk, CT, USA) as per the method of Hoque *et al.* (2011c). Temperature calibration was performed using the Indium thermogram. Film samples (2–5 mg) were accurately weighed into aluminium pans, hermetically sealed, and scanned over the temperature range of –30 to 150 °C with a heating rate of 10 °C/min. Dry ice was used as the cooling medium and the system was equilibrated at –30 °C for 5 min prior to scanning. The empty aluminium pan was used as a reference.

#### **9.3.6 Statistical analyses**

All experiments were performed in triplicates (n=3) and a completely randomised design (CRD) was used. Analysis of variance (ANOVA) was performed and the mean comparisons were done by Duncan's multiple range tests (Steel and Torrie, 1980). Data are presented as mean  $\pm$  standard deviation and the probability value of  $P < 0.05$  was considered as significant. Statistical analysis was performed



using the Statistical Package for Social Sciences (SPSS 17.0 for windows, SPSS Inc., Chicago, IL, USA).

## **9.4 Results and discussion**

### **9.4.1 Properties of gelatin films and nanocomposite films as affected by EECH addition**

#### **9.4.1.1 Thickness**

Thickness of gelatin films and nanocomposite films incorporated with EECH at different levels is shown in Table 34. In general, thickness of the films was not significantly affected by the incorporation of EECH at all levels used ( $P > 0.05$ ). Nanocomposite films generally showed similar thickness to gelatin films ( $P > 0.05$ ), regardless of EECH incorporation. Generally, film thickness is influenced by the solid content of the film forming solution (Han and Krochta, 1999). The results suggested that the thickness of gelatin films and nanocomposite films was not markedly affected by the incorporation of nanoclay and EECH.

#### **9.4.1.2 Mechanical properties**

Mechanical properties, including YM, TS and EAB of gelatin films and nanocomposite films incorporated with EECH at different levels are shown in Table 34. Mechanical properties of films varied with the levels of EECH incorporated ( $P < 0.05$ ). YM of gelatin films increased when EECH at a level of 0.05% (w/w, on protein basis) was added ( $P < 0.05$ ). Further increasing levels of EECH decreased the YM of resulting gelatin films. Nevertheless, protein precipitation obviously occurred in gelatin film-forming solutions and nanocomposite film-forming suspensions when the incorporation level of EECH was higher than 0.04% (w/w). Hydroxyl group of phenolic compounds in EECH possibly acted as hydrogen donor and hydrogen bonds could be formed between phenolic functional groups and gelatin molecules at an appropriate level of EECH. The decrease in YM of gelatin film incorporated with EECH at high amount was probably caused by aggregation of phenolics and gelatin

molecules. This resulted in the lessened integrity of film structure (Jongjareonrak *et al.*, 2008). Haslam (1998) stated that polyphenols have the ability to form complexes with proteins. Kavooosi *et al.* (2013) reported that addition of carvacrol resulted in the lowered interaction between gelatin monomers, and might hinder polymer chain-to-chain interactions. As a consequence, the decrease in mechanical property could be obtained. The formation of complexes between polyphenols and proteins to a high extent led to coagulation of proteins, in which the ordered network of film was not formed. This resulted in the lower YM of resulting films ( $P < 0.05$ ). When considering

**Table 34.** Young's Modulus (YM), tensile strength (TS), elongation at break (EAB), water vapour permeability (WVP) and thickness of gelatin films and nanocomposite films incorporated with EECH at different levels

Film Samples	YM (MPa)	TS (MPa)	EAB (%)	WVP ( $\times 10^{-11} \text{gmm}^{-2} \text{s}^{-1} \text{Pa}^{-1}$ )	Thickness (mm)
GF-0%	1048.03±31.40bB	41.93±0.49bB	7.90±0.03bA	2.76±0.05aA	0.048±0.0053bA
GF-0.025%	1046.27±5.89bB	40.00±0.66cC	7.24±0.13cdC	2.09±0.07gC	0.049±0.0004abA
GF-0.05%	1129.63±25.58aA	43.65±0.68aA	7.63±0.01bcB	1.79±0.02iD	0.050±0.0009abA
GF-0.1%	1030.87±34.09bB	39.33±0.80cC	7.08±0.11dCD	2.10±0.05gC	0.049±0.0003abA
GF-0.2%	977.69±15.81cC	35.61±1.14ghD	6.94±0.30dD	2.17±0.09fBC	0.050±0.0001abA
GF-0.4%	923.98±19.96dD	34.97±0.59hD	6.16±0.01eE	2.25±0.01eB	0.049±0.0002abA
NF-0%	1144.85±1.75aA	43.99±0.48aA	9.20±0.12aA	2.19±0.02efD	0.049±0.0023abC
NF-0.025%	989.67±6.19cC	36.06±0.02fghD	7.57±0.43bcBC	2.50±0.03cdB	0.052±0.0019aA
NF-0.05%	972.16±2.64cC	36.45±0.38fgD	7.61±0.30bcBC	2.56±0.02bcA	0.051±0.0010aABC
NF-0.1%	1037.73±12.73bB	37.90±0.99deBC	7.95±0.19bB	2.59±0.03bA	0.050±0.0013abBC
NF-0.2%	981.10±17.68cC	37.18±0.82efCD	7.89±0.07bB	2.44±0.05dC	0.051±0.0014aABC
NF-0.4%	1044.60±15.70bB	38.82±0.61cdB	7.19±0.50cdC	1.94±0.04hE	0.052±0.0001aAB

Mean ± SD (n=3).

Different lowercase letters in the same column indicate significant differences between the different groups ( $P < 0.05$ ).

Different uppercase letters in the same column indicate significant differences in the same group ( $P < 0.05$ ).

YM between the control gelatin film and nanocomposite film (without EECH addition), latter showed the higher YM than the former ( $P < 0.05$ ). The increase in YM, representing increased stiffness, of gelatin/nanocomposite film might be owing to the uniform dispersion of MMT nanoclay in gelatin matrix and a strong interaction between carbonyl group of gelatin and hydroxyl group of MMT (Martucci and Ruseckaite, 2010a). The enhancement of YM of nanocomposite film was directly attributed to the reinforcement provided by the high aspect ratio and the high surface area of silicate layers, to the good dispersion of clay layers in the gelatin matrix (Gutierrez *et al.*, 2012). It was noted that YM of gelatin nanocomposite films decreased with the addition of EECH. Thus, EECH more likely lowered the stiffness of gelatin film containing nanoclay.

TS is an important mechanical property that expresses the maximum stress developed in a film during tensile testing (Briston, 1988). TS of gelatin films increased when EECH at 0.05% (w/w, based on protein) was incorporated. The decreases in TS were observed when EECH at levels of 0.1-0.4% (w/w) was incorporated ( $P < 0.05$ ). The results indicated that an appropriate level of EECH could strengthen the film matrix by enhancing the interaction between protein chains and phenolics in the extract. Film formation generally takes place by the development of a three dimensional network of protein molecules by ionic, hydrophobic, hydrogen and covalent (non-disulfide) bonds (Hoque *et al.*, 2011c). Hoque *et al.* (2011c) reported that integrity and chain length of gelatin molecules directly contributed to the formation of film network. The decrease in TS was in agreement with the decrease in YM, when higher EECH levels were used. For gelatin nanocomposite films, the similar result was observed. At high concentration of EECH, the aggregation of phenolic compounds in EECH might be enhanced. In general, the reduction in mechanical properties occurred when the higher levels of phenolic compounds were used (Gomez-Estaca *et al.*, 2014). The development of a heterogeneous structure with the presence of discontinuous areas could lower TS (Li *et al.*, 2014). The incorporation of foreign components at an excessive amount is more likely associated with the development of heterogeneous film structure (Hoque *et al.*, 2011c).

EAB, the strain on a film sample when it breaks, decreased with increasing levels of EECH ( $P < 0.05$ ). Control films (GF-0% and NF-0%) showed higher EAB ( $P < 0.05$ ) than those added with EECH. In general, higher EAB was obtained for nanocomposite films ( $P < 0.05$ ) than gelatin films. Similar result was observed by Li *et al.* (2014), who reported that the control gelatin film had the higher EAB than the films incorporated with natural antioxidants. Gelatin–phenolics, gelatin–clay or gelatin–phenolics–clay interactions at various degrees more likely led to the formation of different polymer matrices. These complex systems with reduced molecular mobility might have lower elasticity as indicated by the decreased EAB. Nunez-Flores *et al.* (2012) also reported that the number and size of the lignosulphonate domains led to the greater steric hindrance in gelatin film matrix, which considerably restricted the biopolymer molecular motion. Lignosulphonate was shown to form supra-molecular complexes by inter- and intra-molecular hydrogen bonding of its polar groups. Moreover, the triple-helix content in films might be decreased due to the strong interaction between phenolics and gelatin (Bao *et al.*, 2009). Polyphenolic compounds could form hydrogen and covalent (non-disulphide) bonds with amino and hydroxyl groups of polypeptide in gelatin, which would weaken the protein-protein interactions in protein network (Li *et al.*, 2014). Thus, the incorporation of EECH and nanoclay directly affected the mechanical properties of gelatin films.

#### **9.4.1.3 Water vapour permeability (WVP)**

WVP of gelatin films and nanocomposite films incorporated with EECH at different levels is shown in Table 34. Control gelatin film (GF-0%) showed the highest WVP, compared with others ( $P < 0.05$ ). Gelatin is hydrophilic in nature, due to its polar amino acids and large number of hydroxyl groups (-OH). As a consequence, gelatin film has the lower moisture barrier property. Gelatin film incorporated with EECH at the level of 0.05% (w/w) had the lowest WVP ( $P < 0.05$ ). The interaction between gelatin and phenolic compounds in EECH could lower the available or free charged or polar residues of gelatins and this might result in the decreased water adsorptivity and thus decreasing the WVP of films (Bitencourt *et al.*,

2014). Additionally, incorporation of EECH more likely increased the compactness of films, thereby lowering the adsorptivity as well as diffusivity of water vapour through the film as indicated by lower WVP. Interactions of polymers also reduced the free volume in the film matrix, limiting the diffusion of small molecules through the polymer film. The phenolic compounds were able to form hydrogen and covalent bonds (non-disulphide) with reactive groups of polypeptide in gelatin (Li *et al.*, 2014). These bonds limited the availability of hydrogen groups to bind with water, thereby decreasing the affinity of gelatin films with water. Wu *et al.* (2013) reported that polyphenolic compounds could fit into the gelatin matrix and establish crosslinks through hydrogen bonds or through hydrophobic interactions with the reactive groups of the gelatin. Consequently, the network structure of films became denser and less permeable (Jongjareonrak *et al.*, 2008). The degree of crosslinking also affects the barrier characteristics of gelatin films (Hoque *et al.*, 2011c). However, WVP of gelatin films seemed to increase when EECH was incorporated at the levels higher than 0.05% (w/w). The highest WVP was observed when the highest level of EECH (0.4%, w/w) was incorporated into the gelatin films. The excessive interaction between phenolic compounds and gelatins could bring about the coagulation. As a result, non-uniform film matrix was developed. This might be associated with the increasing number of micro-pores or voids in film networks. Thus, water migration through the films was increased.

For gelatin nanocomposite films, those without and with EECH addition exhibited lower WVP than did the control gelatin film (without nanoclay and EECH addition) ( $P < 0.05$ ). The lowest WVP was observed when EECH at 0.4% (w/w) was incorporated in the gelatin nanocomposite film ( $P < 0.05$ ). The improved barrier properties of the gelatin/nanocomposite films (NF-0%) could be attributed to the hindrance caused by nanoclay (Ray and Okamoto, 2003; Rhim and Ng, 2007). The formation of network induced by the hydrogen bonds between the gelatin chains and phenolics and the exfoliation/intercalation of gelatin molecules into the silicate galleries of nanoclays might lead to the improved water vapour barrier property (Abdollahi *et al.*, 2012). OH groups may form hydrogen linkages between phenolic

compounds and gelatin chains or Cloisite Na<sup>+</sup> (Gutierrez *et al.*, 2012). Furthermore, the incorporation of Cloisite Na<sup>+</sup> to the gelatin matrix provides a ‘tortuous pathway’ for water vapour molecules to pass through (Martucci and Ruseckaite, 2010a). When EECH was added into nanocomposite films, higher WVP was found in comparison with gelatin films. Phenolic compounds might enhance the formation of coagulated gelatins in the matrix or interfere with the interaction between gelatin and nanoclays. This resulted in the discontinuous network with the poorer water vapour barrier property. Thus, gelatin films had varying WVP, depending on the concentration of phenolic compounds as well as the incorporation of nanoclay.

#### 9.4.1.4 Colour

Colour of gelatin films and nanocomposite films incorporated with EECH at different levels is shown in Table 35. The colour of the packaging is an important factor in terms of general appearance and consumer acceptance (Rawdkuen *et al.*, 2012). Lightness ( $L^*$ - value) of both films generally decreased with increasing levels of EECH ( $P < 0.05$ ). However, redness ( $a^*$ - value) and yellowness ( $b^*$ - value) of films increased ( $P < 0.05$ ). This was in accordance with the increases in  $\Delta E^*$  value. The lowest  $L^*$  and the highest  $a^*$  and  $b^*$ - values were obtained for both films incorporated with the highest level (0.4%, w/w) of EECH ( $P < 0.05$ ). Generally,  $\Delta E^*$  was higher in nanocomposite films than gelatin films, especially at high level of EECH. The phenolic compounds in EECH might interact with matrix or nanoclays, in the ways which yielded the higher redness or yellowness. Similar results were observed for gelatin films incorporated with natural spices (Hoque *et al.*, 2011c) and ethanolic extract of curcuma (Bitencourt *et al.*, 2014). Films from cuttlefish (*Sepia pharaonis*) skin gelatin incorporated with cinnamon, clove and star anise extracts and gelatin-based films added with curcuma ethanol extract showed lower  $L^*$  and higher  $b^*$  values than the control gelatin film (without added herbal/curcuma extracts). Thus, colour of films was affected by the incorporation of EECH as well as nanoclay.

**Table 35.** Colour of gelatin films and nanocomposite films incorporated with EECH at different levels

<b>Film samples</b>	<b><i>L</i>*</b>	<b><i>a</i>*</b>	<b><i>b</i>*</b>	<b><math>\Delta E^*</math></b>
<b>GF-0%</b>	90.11±0.01eB	-1.25±0.02ghD	1.92±0.01eB	3.05±0.06gC
<b>GF-0.025%</b>	90.14±0.01dA	-1.24±0.01fgD	1.94±0.02eB	3.04±0.01ghCD
<b>GF-0.05%</b>	90.05±0.01gC	-1.22±0.01efgD	1.75±0.01fC	3.03±0.01hDE
<b>GF-0.1%</b>	90.03±0.01hD	-1.11±0.01cB	1.93±0.02eB	3.14±0.02dB
<b>GF-0.2%</b>	90.15±0.01cA	-1.19±0.02dC	1.92±0.02eB	3.02±0.01hiE
<b>GF-0.4%</b>	89.92±0.01jE	-1.02±0.02bA	2.23±0.01bA	3.38±0.01bA
<b>NF-0%</b>	90.15±0.01cC	-1.25±0.06ghDE	2.04±0.02cC	3.08±0.01fD
<b>NF-0.025%</b>	90.18±0.01bB	-1.27±0.01hE	1.93±0.03eE	3.00±0.01iE
<b>NF-0.05%</b>	90.09±0.00fD	-1.21±0.01defCD	1.99±0.03dD	3.11±0.01eC
<b>NF-0.1%</b>	90.25±0.01aA	-1.20±0.02deC	1.76±0.02fF	2.86±0.01jF
<b>NF-0.2%</b>	89.97±0.01iE	-1.12±0.01cB	2.22±0.01bB	3.33±0.01cB
<b>NF-0.4%</b>	89.25±0.01kF	-0.66±0.02aA	3.08±0.01aA	4.44±0.01aA

Mean ± SD (n=3).

Different lowercase letters in the same column indicate significant differences between the different groups ( $P < 0.05$ ).

Different uppercase letters in the same column indicate significant differences in the same group ( $P < 0.05$ ).

#### 9.4.1.5 Light transmission and transparency

Transmission of UV and visible light at selected wavelengths in the range of 200–800 nm of gelatin films and nanocomposite films incorporated with EECH at various levels is presented in Table 36. Decreases in light transmission of both films at all wavelengths were observed as the levels of EECH increased. However, the degree of decrease varied with the levels of EECH for nanocomposite

films. The transmission of UV light was low at 200 and 280 nm for both gelatin film and nanocomposite film and NF-0.4% had the lowest transmission. It was found that film added with 0.4% EECH (w/w) also showed the lowest transmission in visible range. This might be due to the light scattering effect of gelatin-phenolic complexes (Papadopoulou and Frazier, 2004). The result suggested that film effectively prevented the UV light. High UV light barrier ability was reported for gelatin films (Gomez-Guillen *et al.*, 2009; Hoque *et al.*, 2011c; Jongjareonrak *et al.*, 2008). Hamaguchi *et al.* (2007) reported that protein-based films exhibited the good UV barrier properties, owing to their high content of aromatic amino acids that absorb UV light. In general, light transmission in visible range (350–800 nm) for all films was in the range of 73.12–89.78%. In visible range, gelatin film incorporated with EECH showed higher light transmission, as compared with nanocomposite film containing EECH. The result suggested that phenolic compounds in EECH might form the complex with gelatin or nanoclays in the film network. As a result, light could not pass through the film with ease. Furthermore, nanoclays might result in the light reflection of films, leading to the lower transmission.

Transparency value of both gelatin films and nanocomposite films increased as the level of EECH increased ( $P < 0.05$ ). Both films added with EECH at a level of 0.4% (w/w) showed the highest transparency value ( $P < 0.05$ ), regardless of nanoclay incorporation. Higher transparency value indicated that the films had lower transparency. Transparency of protein-based films is generally affected by additives, processing conditions, thickness as well as compatibility between polymer and nanoclay (Farahnaky *et al.*, 2014; Hoque *et al.*, 2011c; Martucci and Ruseckaite, 2010b; Nagarajan *et al.*, 2014a,b; Rhim, 2007). The aggregation of gelatin molecules due to the incorporation of EECH, especially at higher level might result in large agglomeration (Papadopoulou and Frazier, 2004). Consequently, the films possessed more internal light scattering property and became turbid (Martucci and Ruseckaite, 2008). In general, gelatin films containing EECH were more transparent (lower transparency value) than those incorporated with both EECH and nanoclay ( $P < 0.05$ ). Additionally, phenolic compounds themselves also contributed to the opaqueness of



films. Therefore, the incorporation of EECH and nanoclay had an impact on the appearance and light barrier properties of gelatin films.

**Table 36.** Light transmittance and transparency values of gelatin films and nanocomposite films incorporated with EECH at different levels

Film samples	Transmittance (%)								Transparency values
	200	280	350	400	500	600	700	800	
<b>GF-0%</b>	0.02	41.10	83.27	86.57	88.13	88.79	89.27	89.78	1.02±0.0005kF
<b>GF-0.025%</b>	0.02	41.64	81.18	84.79	86.74	87.61	88.29	88.95	1.15±0.0034jE
<b>GF-0.05%</b>	0.02	43.91	81.84	85.15	86.98	87.88	88.58	89.25	1.21±0.0016iD
<b>GF-0.1%</b>	0.03	43.15	80.56	84.21	86.15	87.06	87.73	88.39	1.27±0.0012hC
<b>GF-0.2%</b>	0.02	40.16	79.36	83.00	85.14	86.26	87.09	87.84	1.28±0.0015gB
<b>GF-0.4%</b>	0.01	32.91	77.13	81.47	83.89	85.13	86.11	86.98	1.42±0.0005eA
<b>NF-0%</b>	0.02	37.52	77.53	81.78	84.68	86.31	87.47	88.44	1.28±0.0026gF
<b>NF-0.025%</b>	0.02	34.45	76.64	80.86	83.84	85.48	86.72	87.76	1.31±0.0024fE
<b>NF-0.05%</b>	0.02	35.99	73.65	77.99	81.15	83.02	84.43	85.65	1.53±0.0017dD
<b>NF-0.1%</b>	0.01	34.91	73.93	78.59	81.95	83.88	85.35	86.55	1.56±0.0010cC
<b>NF-0.2%</b>	0.01	37.61	75.57	79.61	82.46	84.12	85.36	86.43	1.56±0.0016bB
<b>NF-0.4%</b>	0.01	24.96	73.12	78.44	81.98	83.99	85.45	86.61	1.57±0.0006aA

Mean ± SD (n=3).

Different lowercase letters in the same column indicate significant differences between the different groups (P<0.05).

Different uppercase letters in the same column indicate significant differences in the same group (P<0.05).

#### **9.4.2 Characteristics of selected gelatin film and nanocomposite film added with EECH**

Gelatin film and nanocomposite film incorporated with EECH (GF-0.05% and NF-0.4%) were further subjected to characterisation, in comparison with the control gelatin film (GF-0%) and nanocomposite film (NF-0%) (without EECH incorporation).

#### 9.4.2.1 Wide angle x-ray diffraction (WAXD) analysis

WAXD analysis was performed in order to determine the dispersion of Cloisite Na<sup>+</sup> in the films from tilapia skin gelatin incorporated with and without EECH. WAXD patterns of Cloisite Na<sup>+</sup> and the selected films are illustrated in Figure 41a and 41b, respectively. Intercalated or exfoliated structures of different nanocomposite films were normally revealed by the *d*-spacing due to the interlayer spacing of the nanoclay gallery in gelatin matrix (Martucci *et al.*, 2007). Characteristic diffraction peak of Cloisite Na<sup>+</sup> (Figure 41a) was found at  $2\theta$  of  $7.04^\circ$  (*d*-spacing = 1.25 nm, based on Bragg's equation;  $n\lambda = 2d \sin\theta$ ). This result was consistent with previous report and was also quite similar to the suggested value given by manufacturer (Gutierrez *et al.*, 2012; Koh *et al.*, 2010; Pradhan *et al.*, 2012). WAXD patterns of films were different (Figure 41b), compared to hydrophilic nanoclay, Cloisite Na<sup>+</sup>. The characteristic halo peak of amorphous proteins was obtained for control gelatin film (GF-0%) in the  $2\theta$  range of  $6.2$  to  $9.5^\circ$ . Similar WAXD pattern of gelatin-based film was observed (Grevellec *et al.*, 2001; Martucci and Ruseckaite, 2010a). For nanocomposite films incorporated with or without EECH, the absence of characteristic diffraction peak ( $2\theta = 7.04^\circ$ ) of Cloisite Na<sup>+</sup> nanoclay was noticed in their WAXD patterns. This suggested the intercalated/exfoliated structure of obtained nanocomposite films (Abdollahi *et al.*, 2012; Gutierrez *et al.*, 2012). However, WAXD pattern of NF-0.4% was different from that of NF-0% (without EECH addition). This suggested the varying degrees of intercalation or exfoliation of nanoclays in gelatin matrix, as influenced by EECH addition (Gutierrez *et al.*, 2012). In particular, the WAXD pattern of NF-0.4% exhibited broader halo peak of amorphous gelatin. This might be due to the non-homogeneous aggregation of gelatin molecules at highest incorporation level (0.4%, w/w) of EECH. WAXD analysis is a classical method for determining the gallery height (*d*-spacing distance) in clay particles. During intercalation or exfoliation, the insertion of polymer into the organoclay galleries forces the platelets apart and increases the *d*-spacing, resulting in a shift of the diffraction peak to lower angles or even disappeared (Abdollahi *et al.*, 2012; Xu *et al.*, 2006). Therefore, phenolic

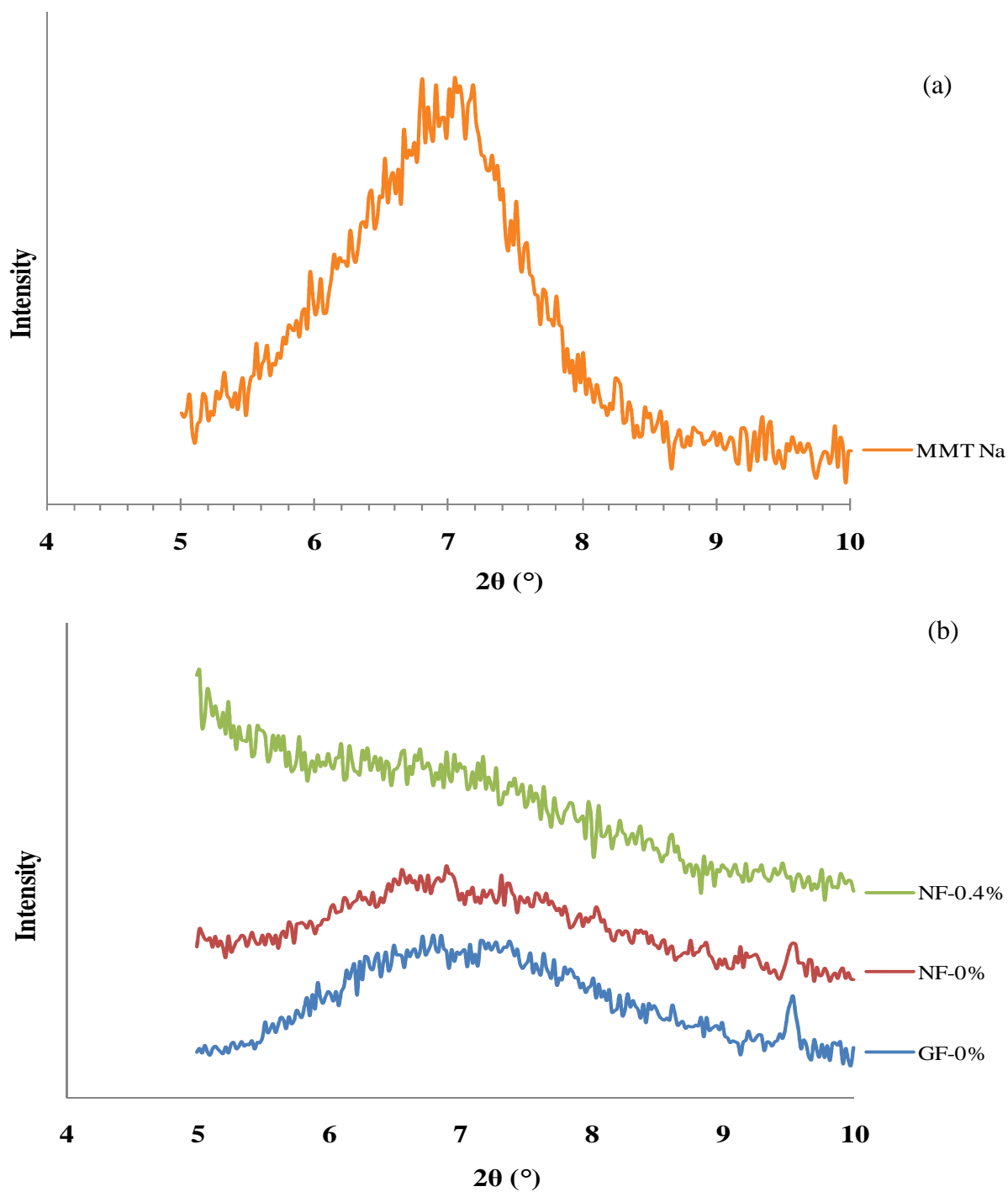


**Figure 41.** WAXD patterns of Cloisite Na<sup>+</sup> (a) and gelatin film and nanocomposite films incorporated with or without EECH (b). MMT Na: Cloisite Na<sup>+</sup>; GF-0% and NF-0%: Control gelatin film and nanocomposite film, respectively; NF-0.4%: nanocomposite film incorporated with 0.4% EECH (w/w).

compounds in EECH more likely affected intercalated or exfoliated structure as well as the organisation of amorphous gelatin in the film matrix. In general, the intercalated or exfoliated structures of gelatin nanocomposite films were dependent on the addition of nanoclay and EECH.

#### 9.4.2.2 Microstructure

SEM micrographs of the surface (5000x) and cryo-fractured cross-section (3000x) of selected gelatin films and nanocomposite films incorporated with or without EECH are shown in Figure 42. All films showed the smooth surface and free of crack or void. Homogeneity and smoothness of film surface were varied upon the inclusion of EECH and nanoclays. The control gelatin film (GF-0%) and Cloisite Na<sup>+</sup> (NF-0%) incorporated film had no differences in film surface morphology. Smooth, homogenous and compact film surface of both films indicated an ordered film matrix. The continuous and strong film network with a great number of junction zones was developed and the thorough dispersion of hydrophilic nanoclay into the hydrophilic polymer was obtained (Bao *et al.*, 2009; Theng, 1979). However, the incorporation of EECH resulted in slightly coarser/non-homogenous film surface. Gelatin film incorporated with both EECH and nanoclay showed larger aggregates or agglomerates on surface (NF-0.4% films). The highest EECH level (0.4%, w/w on protein basis) plausibly induced the formation of coagulation, as evidenced by the increased rougher surface.

For cross-section, gelatin film incorporated with EECH at 0.05% (w/w, on protein basis) level showed a more compact and smoother structure, compared to the control gelatin film (without EECH and nanoclay). Similar result was reported for pig skin gelatin films incorporated with curcuma ethanol extract (Bitencourt *et al.*, 2014). The compact structure regulated by interaction between phenolic compounds of EECH and gelatin was also responsible for the improved mechanical and water vapour barrier properties (Table 34). NF-0% film showed some roughness in the film network. This was plausibly due to the presence of Cloisite Na<sup>+</sup> in the film matrix. Films incorporated with EECH at the level of 0.4% (w/w, on protein basis) along with

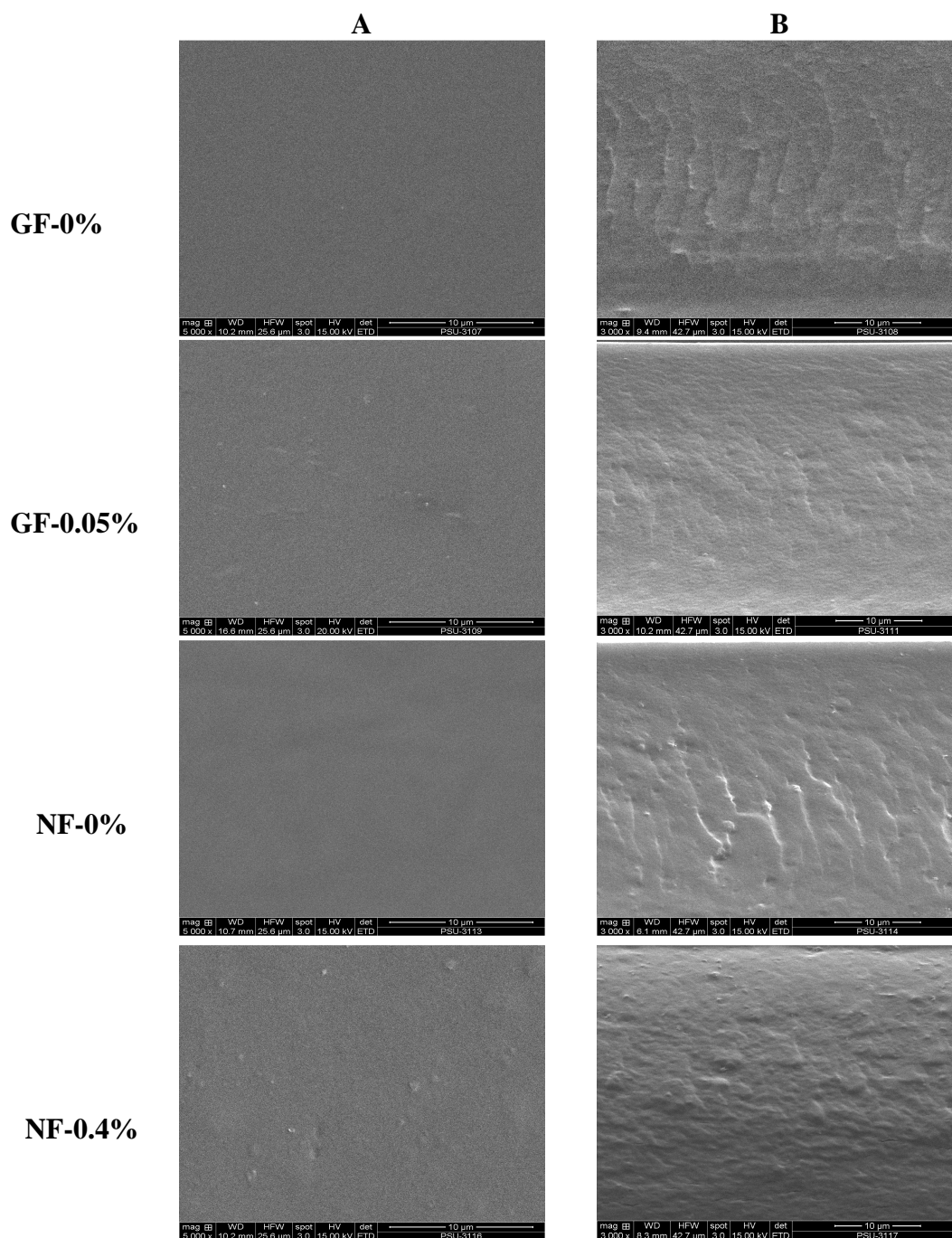


**Figure 42.** SEM micrographs of surface (A) and cryo-fractured cross-section (B) of gelatin films and nanocomposite films incorporated with EECH at different levels. Magnification: 5000x for surface and 3000x for cross-section. GF-0% and NF-0%: Control gelatin film and nanocomposite film, respectively; GF-0.05% and NF-0.4%: gelatin film and nanocomposite film incorporated with EECH at the levels of 0.05 and 0.4% (w/w), respectively.

the nanoclay had the compactness with some protrusions. This result was concomitant with lower mechanical but improved water vapour barrier properties (Table 34). Phenolic compounds in EECH more likely interacted with protein chains and caused protein aggregation. Therefore, the microstructures of gelatin films were governed by the incorporation of EECH and nanoclay.

#### 9.4.2.3 TGA thermograms

TGA curves of selected gelatin films and nanocomposite films incorporated with or without EECH are illustrated in Figure 43. Degradation temperatures ( $T_d$ ) and weight loss ( $\Delta w$ ) of corresponding films are presented in Table 37. In general, two stages of weight loss were observed for all films, irrespective of nanoclay or EECH incorporation. First stage of weight loss ( $\Delta w_1 = 5.64 - 6.98\%$ ) was observed for all films approximately at onset temperatures ( $T_{d1}$ ) of  $52.38 - 71.43$  °C, mostly associated with the continuous loss of free moisture absorbed in the films. At the first stage of weight loss, GF-0.05% films showed higher weight loss than NF-0.4% films at the same onset temperatures. Enhanced interaction between gelatin chains and Cloisite Na<sup>+</sup> sheets plausibly consumed some hydrophilic groups and depressed the water uptake through capillary action at the interface (Li *et al.*, 2003).  $T_{d1}$  of GF-0.05% was higher than that of GF-0%. For all films, the second stage of weight loss ( $\Delta w_2 = 71.49 - 72.70\%$ ) was observed approximately at a temperature ( $T_{d2}$ ) of  $258.33 - 267.86$  °C. Here,  $T_{d2}$  referred to as thermal degradation temperature of the films. This change was most likely due to the degradation or decomposition of protein components and the plasticiser, glycerol. GF-0.05% had the higher  $T_{d2}$  than GF-0%. GF-0% also had higher weight loss (72.70%) with the lower  $T_{d2}$  (258.33 °C). This result revealed that control gelatin film showed higher heat susceptibility than that added with EECH. In general, increasing thermal degradation temperatures ( $T_{d2}$ ) was related with decreasing weight loss ( $\Delta w_2$ ). Nanocomposite films added with EECH showed the slightly higher  $T_{d2}$  than the control nanocomposite film (NF-0%). NF-0% also showed higher  $T_{d1}$  and  $T_{d2}$  than GF-0%. This was possibly due to the decrease in free volume of polymer matrix by stronger interaction between the gelatin molecules and nanoclay (Bae *et al.*, 2009a). Effective crosslinking of gelatin by

phenolics in EECH could lead to the enhancement in thermal stability of films. Higher amount of bondings between phenolic compounds and gelatin molecules yielded stronger film network. As a result, films became stiffer and more compact, thereby improving thermal stability (Hoque *et al.*, 2011c; Wu *et al.*, 2014). The increased thermal stability of nanocomposite films might be due to the thermal resistance of Cloisite Na<sup>+</sup> and the nano-dispersion of montmorillonite sheets in the polymer matrix (Zheng *et al.*, 2002). Martucci and Ruseckaite (2010a) reported the increased thermal stabilisation of gelatin nanocomposite films. Additionally, all films had slight difference in residual mass (representing char content) at 600 °C in the range of 21.08-21.78%. The results suggested that the incorporation of nanoclay and EECH into the films based on tilapia skin gelatin contributed to differences in thermal stability.

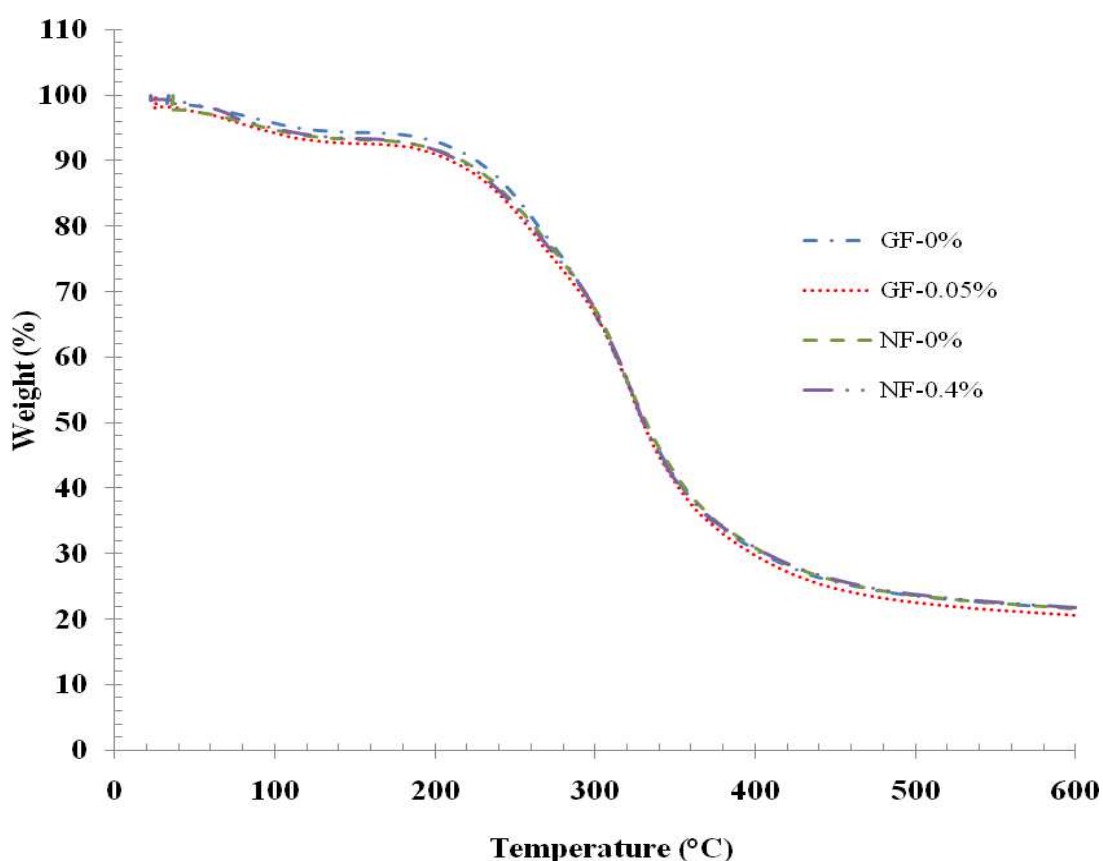


**Figure 43.** Thermogravimetric curves of gelatin films and nanocomposite films incorporated with EECH at different levels. GF-0% and NF-0%: Control gelatin film and nanocomposite film, respectively; GF-0.05% and NF-0.4%: gelatin film and nanocomposite film incorporated with EECH at the levels of 0.05 and 0.4% (w/w), respectively.

**Table 37.** Thermal degradation temperature (Td, °C), weight loss ( $\Delta w$ , %), residue (%) and glass transition temperature (T<sub>g</sub>, °C) of gelatin films and nanocomposite films incorporated with EECH at different levels

<b>Film samples</b>	$\Delta_1$		$\Delta_2$		<b>Residue</b>	<b>T<sub>g</sub></b>
	<b>Td<sub>1</sub></b>	$\Delta w_1$	<b>Td<sub>2</sub></b>	$\Delta w_2$		
<b>GF-0%</b>	52.38	5.64	258.33	72.70	21.66	47.14
<b>GF-0.05%</b>	69.05	6.98	264.29	71.94	21.08	53.57
<b>NF-0%</b>	71.43	6.76	266.66	71.49	21.75	54.99
<b>NF-0.4%</b>	69.05	6.60	267.86	71.62	21.78	58.57

$\Delta_1$  and  $\Delta_2$  denote the first and second stage weight loss, respectively, of films during TGA heating scan.



#### 9.4.2.4 DSC thermograms

DSC thermograms of gelatin films and nanocomposite films incorporated with or without EECH are depicted in Figure 44. Glass transition temperatures ( $T_g$ ) of films are presented in Table 37. Thermograms of the first heating scan of all film samples exhibited step-like or glass transition at temperatures ( $T_g$ ) ranging from 47.14 to 58.57 °C (Figure 44).  $T_g$  is normally correlated to the segmental motion of polymer molecules in the amorphous phase (Slade and Levine, 1991). The control gelatin film (GF-0%) had the lowest  $T_g$  (47.14 °C). In contrast, the incorporation of Cloisite Na<sup>+</sup> (NF-0%) or EECH (GF-0.05%) into the control gelatin film showed higher  $T_g$  (54.99 and 53.57 °C, respectively). However, gelatin film incorporated with both nanoclay and EECH showed the highest  $T_g$  (58.57 °C). Incorporation of EECH along with the nanoclay decreased the molecular mobility of gelatin. For nanocomposite films, nano-dispersion of hydrophilic nanoclay in hydrophilic gelatin matrix might enhance the stronger interaction via hydrogen bonds,

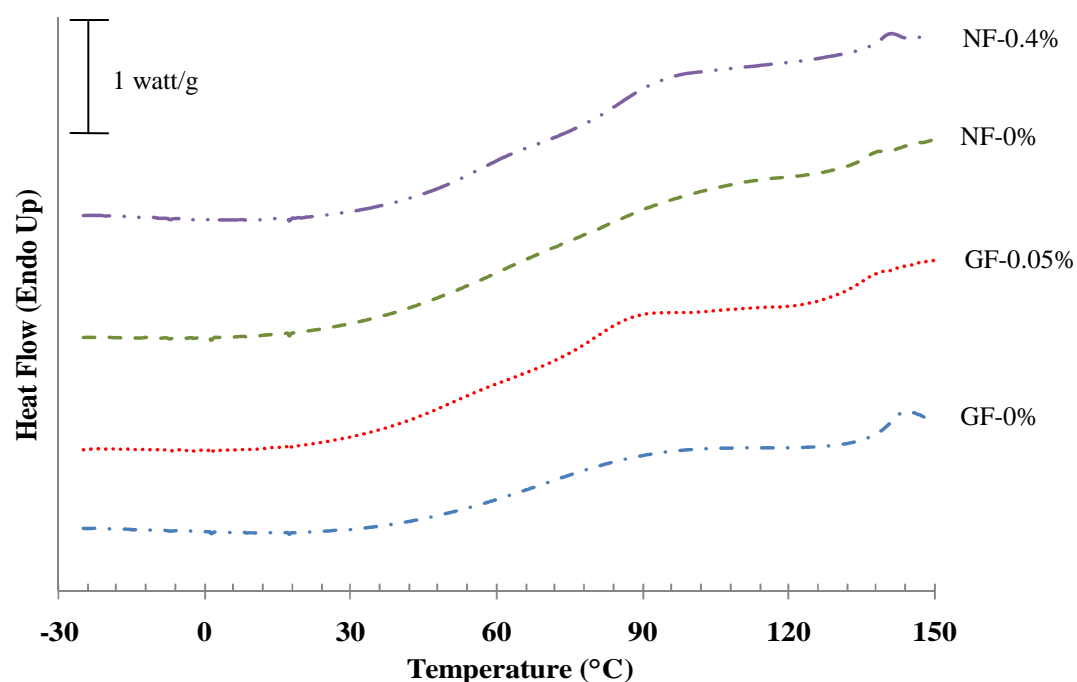


**Figure 44.** DSC thermograms of gelatin films and nanocomposite films incorporated with EECH at different levels. GF-0% and NF-0%: Control gelatin film and nanocomposite film, respectively; GF-0.05% and NF-0.4%: gelatin film and nanocomposite film incorporated with EECH at the levels of 0.05 and 0.4% (w/w), respectively.

thus increasing the rigidity of gelatin molecules in the matrix of film (Martucci *et al.*, 2007). Li *et al.* (2003) reported that Cloisite Na<sup>+</sup> serves as physical crosslinking sites, which could enhance the stability of film network. Moreover, hydrogen bond or hydroxyl group interaction between the gelatin molecules and phenolic compounds in EECH was also responsible for increasing T<sub>g</sub> of NF-0.4% films. Oxford *et al.* (1989) stated that T<sub>g</sub> is one of the important parameters which determines both the mechanical and barrier properties of corresponding films and controls the crystallisation kinetics of the gelatins. In general, the DSC results were correlated well with the mechanical and water vapour barrier properties of films (Table 34). EECH incorporation at higher level might induce cross-linking of gelatin matrix. This resulted in the stronger and more heat stable gelatin film network/matrix.

For the second heating scan, no clear transition was generally observed for both gelatin films and nanocomposite films incorporated with or without EECH (data not shown). Absorbed water, acting as plasticiser, might be removed during the first heating scan. As a consequence, the interactions between gelatin chains and also between gelatin molecules and nanoclays along with the phenolic compounds of EECH could be enhanced by the formation of more rigid film network. Therefore, the solid-state molecular transition was limited and could not be noticed during the second heating scan in the transition temperature range tested.

Gelatin-phenolics-nanoclay interaction occurred by different possible interactions such as hydrogen, hydrophobic, ionic and covalent (non-disulphide) interactions as illustrated in Figure 45. Polyphenolic compounds contain many hydrophobic groups, which can form hydrophobic interaction with hydrophobic region of gelatin molecule and hydroxyl groups of polyphenolic compounds and nanoclay were able to interact via hydrogen bonds (Bae *et al.*, 2009a; Hoque *et al.*, 2011c; Martucci and Ruseckaite, 2010a; Rattaya *et al.*, 2009). As a result, the compact and stronger network with the improved water vapour barrier property could be achieved.

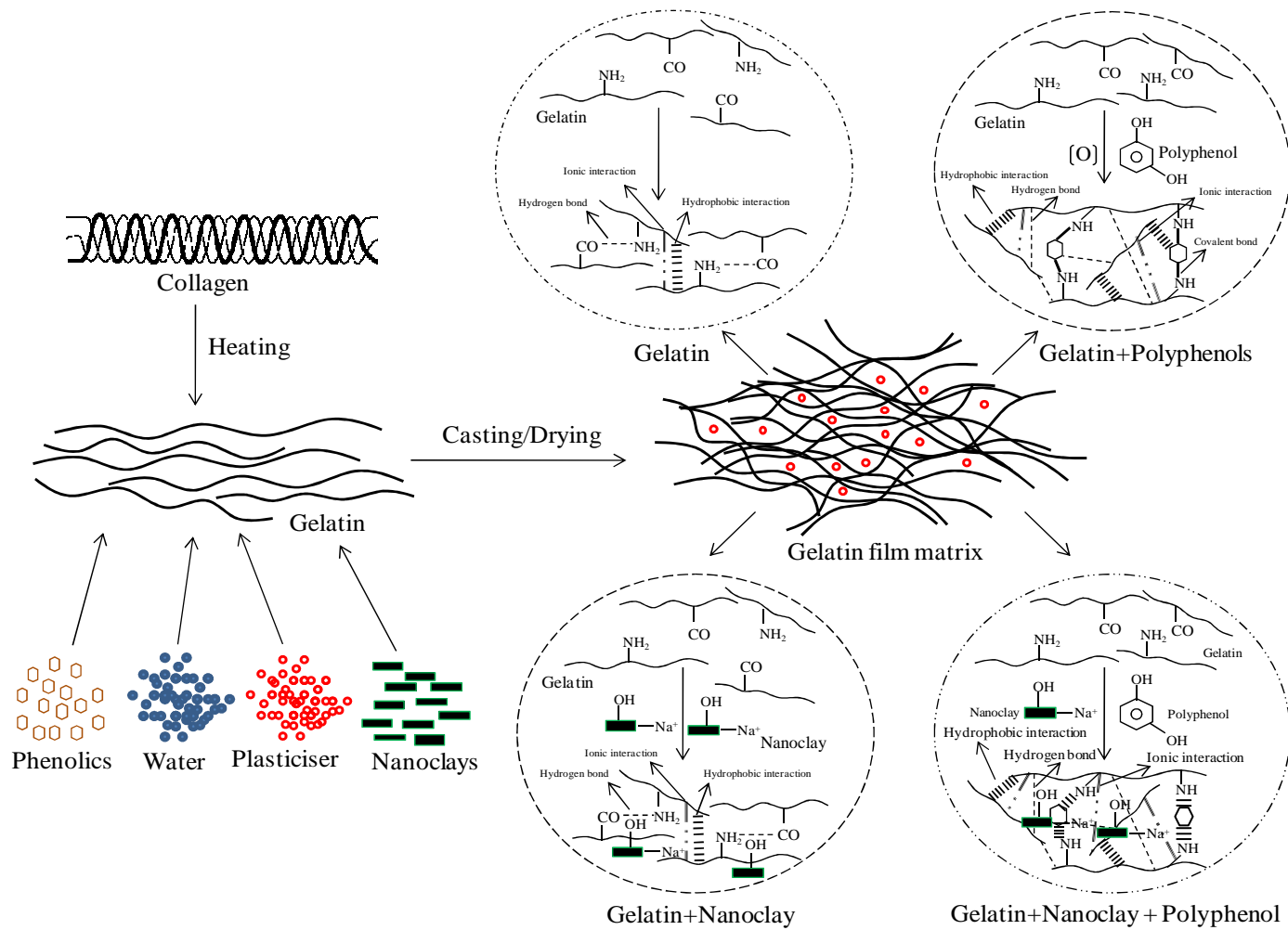


**Figure 45.** Proposed scheme of possible interaction between gelatin, phenolic compounds, and nanoclay in film matrix

## 9.5 Conclusion

Properties of gelatin films and nanocomposite films from tilapia skin gelatin were governed by EECH. Gelatin film and nanocomposite film incorporated with EECH at the levels of 0.05 and 0.4% (w/w, on protein basis), respectively showed the improved water vapour barrier property, possibly due to the augmented interactions between functional group of gelatin and phenolics as well as gelatin, phenolics and nanoclay. Thus, the appropriate level of EECH could effectively improve the film properties, particularly in conjunction with nanoclay incorporation.

## CHAPTER 10

### EFFECTS OF BIO-NANOCOMPOSITE FILMS FROM TILAPIA AND SQUID SKIN GELATINS INCORPORATED WITH ETHANOLIC EXTRACT FROM COCONUT HUSK ON STORAGE STABILITY OF MACKEREL MEAT POWDER

#### 10.1 Abstract

Chemical, physical and sensory changes of mackerel meat powder covered with tilapia and squid skin gelatin films and nanocomposite films incorporated without and with ethanolic extract from coconut husk (EECH) in comparison with that covered with polyethylene (PE) film and the control (without covering) during storage of 30 days at 28-30 °C were investigated. The powder covered with nanocomposite film incorporated with EECH at 0.4% (w/w) (SGF-Na-EECH) generally had the lower moisture content than those covered with other gelatin films throughout the storage ( $P < 0.05$ ). Nevertheless, the lowest moisture content was found in the sample covered with the PE film ( $P < 0.05$ ). The lower PV, TBARS, TVB and pH were observed for SGF-Na-EECH sample than PE sample and the control ( $P < 0.05$ ). Based on SPME-GC-MS analysis, SGF-Na-EECH sample contained the lower volatile lipid oxidation products than the control and that covered with PE film. The lower increases in  $a^*$ ,  $b^*$  and  $\Delta E^*$  values were also obtained for SGF-Na-EECH sample during the storage. Higher overall likeness score was observed for SGF-Na-EECH sample on day 30 of storage. Thus, gelatin film incorporated with both EECH and nanoclay could be an alternative to synthetic commercial film to maintain the quality and extend the shelf-life of mackerel meat powder.

#### 10.2 Introduction

Food packaging has been used to facilitate marketing and to protect food products from harmful environmental factors by providing a barrier to mass

transfer and mechanical protection (Abreu *et al.*, 2011). Several food items susceptible to lipid oxidation could be stored for an extended time by the appropriate packaging (Artharn, *et al.*, 2009). The use of proper packaging technology to minimise quality losses and assure the safety of foods has gained increasing attention (Jongjareonrak *et al.*, 2008). However, packaging materials currently used for food packaging are mostly derived from petroleum by-products, contributing significantly to environmental and ecological problems (Gomez-Guillen *et al.*, 2009). Moreover, there is an increasing concern about the potential risk that plasticiser such as phthalate used in plastics can leach out into foodstuffs. To overcome these problems, biodegradable, non-toxic, natural and renewable sources have been searched to replace the synthetic plastic packaging (Tharanathan, 2003; Weng and Wu, 2014).

Gelatin, the partially hydrolysed form of collagen, is mainly extracted from bovine bones, hides and porcine skin generated as byproducts during animal slaughtering and processing (Karim and Bhat, 2009). Fish gelatin has been paid increasing attention as the alternative of land animal gelatin due to religious constraints of mammalian counterpart (Benjakul *et al.*, 2012). Amongst all biopolymers, gelatin is considered as promising biopolymers under the light of its film-forming ability and applicability (Gomez-Guillen *et al.*, 2009). Due to their inherent hydrophilic properties, gelatin films absorb water at elevated relative humidity (RH) conditions. This results in the plasticised film matrices, but weakens barrier and mechanical properties (Martucci and Ruseckaite, 2009). Several technologies have been implemented for improvement of film properties (Gomez-Guillen *et al.*, 2009; Hoque *et al.*, 2011c; Nunez-Flores *et al.*, 2013b).

Nanoclays, both hydrophilic and hydrophobic were incorporated with gelatin films to improve their mechanical and water vapour barrier properties as well as thermal stability (Farahnaky *et al.*, 2014; Nagarajan *et al.*, 2014a). Due to the enhanced polymer-filler interfacial interaction, nanocomposite films showed improved mechanical and barrier properties and thermal stability (Martucci and Ruseckaite, 2010a). Montmorillonite nanoclays, such as Cloisite Na<sup>+</sup>, with hydrophilic in nature, could be homogeneously dispersed in a hydrophilic polymer

matrix to form the new nanocomposite (Bae *et al.*, 2009a; Nagarajan *et al.*, 2014b). This forces water and gas travelling through the nanocomposite film via an increased ‘tortuous path’ of the film matrix surrounding the nanoclay, thereby increasing the effective path length for diffusion (Ray and Okamoto, 2003; Rhim, 2007).

Coconut husk is the byproduct, which is either burned for energy production or simply disposed (Vazquez-Torres *et al.*, 1992). The preparation of ethanolic extract containing phenolic compounds could increase the value of the husk. Plant phenolics have been used to improve the physical properties of gelatin films (Gomez-Estaca *et al.*, 2014; Hoque *et al.*, 2011c; Rattaya *et al.*, 2009) and to increase bioactivity of resulting films (Nunez-Flores *et al.*, 2013b). Recently, ethanolic extract from coconut husk has been shown to form suitable nanocomposites with gelatin and nanoclay, yielding the films with improved water barrier property (Nagarajan *et al.*, 2014c). The obtained nanocomposites with ethanolic coconut husk extract could therefore serve as the active packaging for shelf-life extension of fishery products rich in polyunsaturated fatty acids.

To the best of our knowledge, there is no information on the uses of nanocomposite films from fish or squid gelatin containing natural extract in fishery products. Thus, the objective of this investigation was to study the quality changes of mackerel meat powder covered with nanocomposite films from tilapia and squid skin gelatins incorporated with ethanolic extract from coconut husk during the storage time of 30 days at 28-30 °C.

## **10.3 Materials and methods**

### **10.3.1 Chemicals**

Fish skin gelatin from tilapia (~240 bloom) was purchased from Lapi Gelatine (Empoli, Italy). MMT-nanoclay, Cloisite<sup>®</sup> Na<sup>+</sup> was obtained from Southern clay products Inc. (Gonzales, TX, USA). Sodium hydroxide, hydrogen peroxide (H<sub>2</sub>O<sub>2</sub>) (30.96% w/v) and glycerol were procured from Merck (Darmstadt, Germany). Ethanol was purchased from RCI Labscan (Bangkok, Thailand). All chemicals were of analytical grade.

### **10.3.2 Preparation of squid skin and extraction of gelatin**

The skin of fresh splendid squid (*Loligo formosana*) was obtained from Sea Wealth Frozen Food Co., Ltd., Songkhla, Thailand and stored in ice using a skin/ice ratio of 1:2 (w/w). The sample was transported to the Department of Food Technology, Prince of Songkla University, Hat Yai, Thailand within 2 h. Upon arrival, the skin was cleaned and washed with iced tap water (0-2 °C). The skin was then cut into small pieces (0.5x0.5 cm<sup>2</sup>), placed in polyethylene bags and stored at -20 °C until use. The skin was stored for not more than 2 months. Prepared skin was subjected to gelatin extraction following the method of Nagarajan *et al.* (2013a). Freeze-dried gelatin contained 97.58% protein (dry weight basis) as determined by the Kjeldhal method (AOAC, 2000).

### **10.3.3 Extraction of ethanolic extract from coconut husk**

#### **10.3.3.1 Collection and preparation of coconut husk**

Coconut husk was obtained from a local market in Hat Yai, Songkhla, Thailand. Husk sample was prepared as per the method of Vazquez-Torres *et al.* (1992) with slight modifications. Husk sample was dried at 60 °C in the cabinet rotary dryer for 16 h and then defibered. Husk sample was then subjected to grinding using a mill (IKA Labortechnik colloid mill, Selangor, Malaysia). The prepared sample was then sieved with the aid of sieve shaker (Model EVJ1, Endecotts Ltd., London, UK) using a sieve size of 6 mm (Woven wire sieves, Endecotts Ltd., London, UK). This coarse form was further blended using a blender (Panasonic, Model MX-898N, Berkshire, UK) and finally sieved using a stainless steel sieve of 80 mesh. The coconut husk powder obtained was further dried in a hot air oven (Mettler, Schwabach, Germany) at 105 °C overnight. The obtained powder was placed in a polyethylene bag, sealed and kept at room temperature until use.

#### **10.3.3.2 Preparation of the ethanolic extract**

Coconut husk powder was subjected to extraction according to the method of Santoso *et al.* (2004) with a slight modification. Ten grams of husk powder



were mixed with 250 ml of 80% ethanol (w/v). The mixture was stirred at room temperature (28–30 °C) using a magnetic stirrer (IKA-Werke, Staufen, Germany) for 3 h. The mixture was then centrifuged at 5000g for 30 min at room temperature using a RC-5B plus centrifuge (Beckman, JE-AVANTI, Fullerton, CA, USA). The supernatant was filtered using a Whatman No. 1 filter paper (Whatman International, Ltd., Maidstone, England). The filtrate was then evaporated at 40 °C using an Eyela rotary evaporator (Tokyo Rikakikai, Co. Ltd., Tokyo, Japan). To remove the residual ethanol, the extract was purged with nitrogen gas. The extract was then dried using a Scanvac Model Coolsafe 55 freeze dryer (Coolsafe, Lyngø, Denmark) to obtain the dry extract. Dried extract was powdered using a mortar and pestle, transferred to an amber bottle and stored in a desiccator until use. The obtained powder was referred to as 'ethanolic extract from coconut husk, EECH'. EECH had phenolic content of 436.82 mg tannic acid equivalent/g as determined by Folin–Ciocalteu reagent (Slinkard and Singleton, 1977).

#### **10.3.4 Preparation of gelatin films and nanocomposite films**

Tilapia and squid skin gelatin films and nanocomposite films were prepared as per the method of Nagarajan *et al.* (2014c). Prior to casting, EECH was added to both film forming solutions and film forming suspensions at the levels of 0.05 and 0.4% (w/w, on protein basis), respectively. The mixtures were gently stirred for 1 h at room temperature. The mixtures were degassed for 10 min using the sonicating bath and then cast ( $4 \pm 0.01$  ml) onto a rimmed silicone resin plate ( $5 \times 5$  cm<sup>2</sup>), air-blown for 12 h at 25 °C, followed by drying in an environmental chamber (Binder GmbH, Tuttlingen, Germany) at  $25 \pm 0.5$  °C and  $50 \pm 5\%$  relative humidity (RH) for 24 h. Films obtained were manually peeled off.

#### **10.3.5 Study on shelf-life extension of mackerel meat powder using gelatin films and nanocomposite films**

##### **10.3.5.1 Preparation of mackerel meat powder**

Fresh mackerel were purchased from a dock, Songkhla, Thailand and kept in ice using a fish/ice ratio of 1:2 (w/w) and then transported to the laboratory

within 1 h. Fish were washed, deskinning, degutted and filleted. Fillets were chopped manually and subjected to drying in a rotary dryer with the air velocity of 1.5 m/s at 60 °C for 8 h. The dried sample was blended with the aid of blender (Panasonic, Model MX-898N, Berkshire, UK) until the uniformity was obtained and referred to as 'mackerel meat powder'.

#### **10.3.5.2 Storage of mackerel meat powder covered with films**

Mackerel meat powder (20 g) was transferred to the cylindrical aluminium cups with a diameter of 30 mm. The aluminium cups were covered with tilapia and squid skin gelatin films or nanocomposite films incorporated with or without EECH as illustrated in Figure 46. Cups were sealed with the aid of silicone vacuum grease and rubber gasket. The samples were stored at room temperature (28-30 °C). For the control, samples were placed in aluminium cups without covering. Samples covered with polyethylene (PE) film (Thickness =  $0.049 \pm 0.001$  mm and  $WVP = 0.04 \pm 0.01 \times 10^{-11}$  gmm<sup>-2</sup>s<sup>-1</sup>Pa<sup>-1</sup>) were also prepared. During storage, the samples were taken for analyses every 5 days up to 30 days. For determination of volatile compounds, the samples stored for 0 and 30 days were used.

#### **10.3.5.3 Analyses**

##### **10.3.5.3.1 Moisture content**

The moisture content of samples was determined according to the method of AOAC (2000).

##### **10.3.5.3.2 pH measurement**

pH measurement was performed by the method described by Lopez-Caballero *et al.* (2007) with a slight modification. Sample (2 g) was homogenised with 10 volumes of deionised water for 1 min using an IKA homogeniser at a speed of 5000 rpm. The homogenate was kept at room temperature for 5 min. The pH was determined using a pH-meter (Sartorius North America, Edgewood, NY, USA).

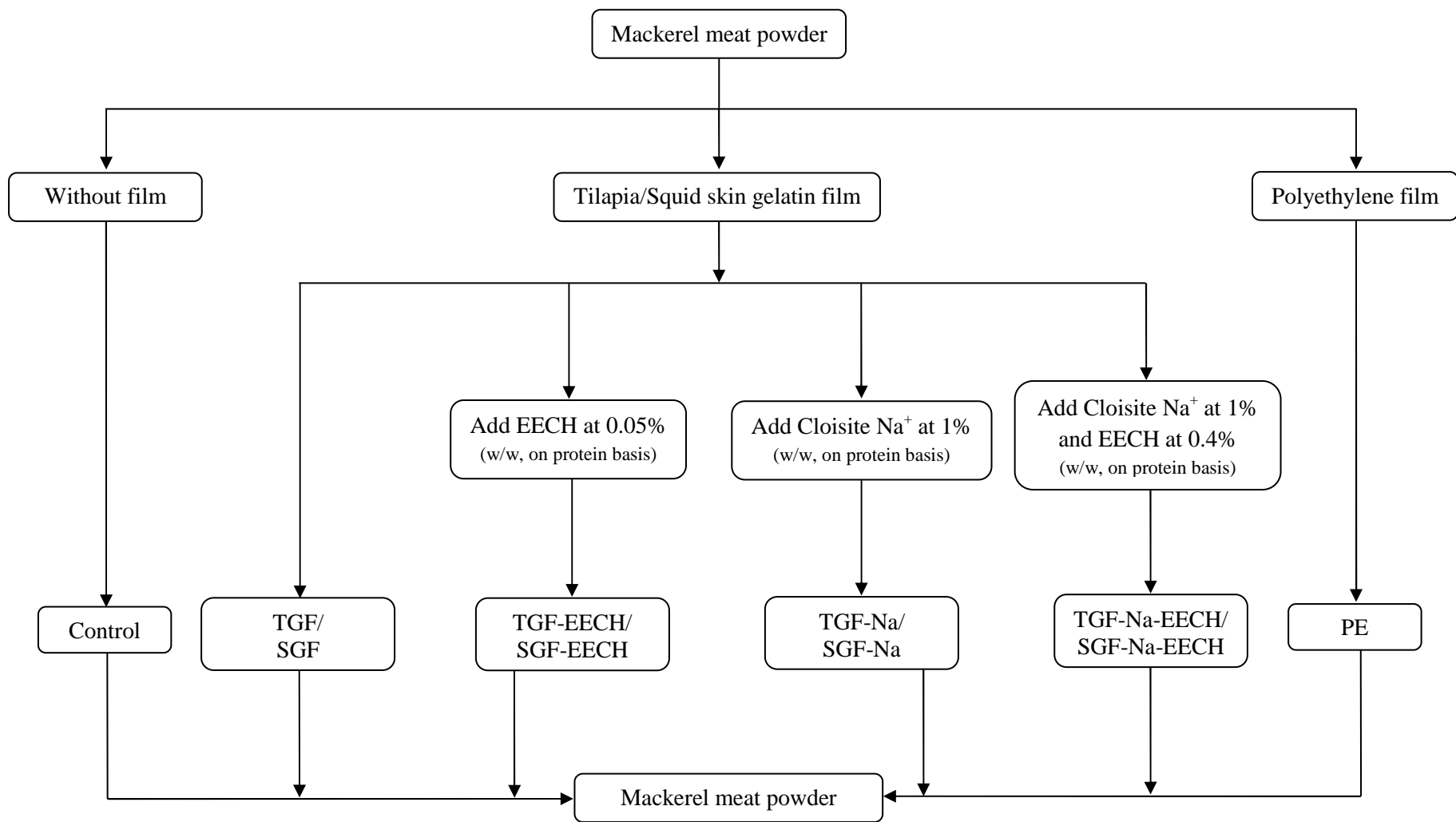


**Figure 46.** Scheme for preparation of mackerel meat powder covered with different films.

#### **10.3.5.3.3 Determination of peroxide value (PV)**

PV was determined as per the method of Richards and Hultin (2002) with a slight modification. Samples (1 g) were mixed with 11 ml of chloroform/methanol (2:1, v/v). The mixtures were homogenised at a speed of 13,500 rpm for 2 min. Homogenates were then filtered using a Whatman No. 1 filter paper. Two millilitres of 0.5% NaCl were then added to 7 ml of the filtrate. The mixtures were vortexed at a moderate speed for 30 s using a Vortex-Genie2 mixer 4 (Bohemia, NY, USA) and then centrifuged at 3000g for 3 min to separate the sample into two phases. Two millilitres of cold chloroform/methanol (2:1, v/v) were added to 3 ml of the lower phase. Twenty-five microlitres of 30% ammonium thiocyanate and 25 µl of 20 mM iron (II) chloride were added to the mixture (Shantha and Decker, 1994). Reaction mixtures were allowed to stand for 20 min at room temperature and the absorbance was read at 500 nm using a UV-1800 spectrophotometer (Shimadzu, Kyoto, Japan). A standard curve was prepared using cumene hydroperoxide with the concentration range of 0.5–2 ppm. PV was calculated and expressed as mg cumene hydroperoxide/kg sample.

#### **10.3.5.3.4 Determination of thiobarbituric acid reactive substances (TBARS)**

TBARS was determined as described by (Buege and Aust, 1978). The sample (0.5 g) was homogenised with 2.5 ml of solution containing 0.375% thiobarbituric acid (w/v), 15% trichloroacetic acid (w/v) and 0.25 M HCl. The mixture was heated in a boiling water bath (95–100 °C) for 10 min to develop a pink colour, cooled with running water and centrifuged at 3600xg at 25 °C for 20 min. The absorbance of the supernatant was measured at 532 nm. A standard curve was prepared using 1,1,3,3-tetramethoxypropane at the concentrations ranging from 0 to 6 ppm. TBARS was calculated and expressed as mg malondialdehyde/kg sample.

#### **10.3.5.3.5 Determination of total volatile base (TVB) content**

TVB content was determined following the method of (Conway and Byrne, 1936). Sample (5 g) was homogenised with 4% of trichloroacetic acid at a ratio of 1: 2 (w/v). The homogenate was filtered through Whatman No. 1 paper (Whatman International, Ltd., Maidstone, England). The filtrate (1 ml) was placed in the outer ring. The inner ring solution (1% boric acid containing the Conway indicator) was pipetted into the inner ring. To initiate the reaction,  $K_2CO_3$  (1 ml) was mixed with the filtrate. The Conway unit was closed tightly with the aid of silicone vacuum grease and incubated at 37 °C for 60 min. The inner ring solution was then titrated with 0.02 N HCl until the green colour turned to pink. TVB content was calculated and expressed as mg-N/100 g sample.

#### **10.3.5.3.6 Determination of colour**

Colour of samples was measured by using a CIE colourimeter (Hunter associates laboratory, Inc., Reston, VA, USA).  $L^*$ ,  $a^*$ ,  $b^*$  and  $\Delta E^*$  indicate lightness or brightness, redness or greenness, yellowness or blueness and total colour difference, respectively. The colourimeter was calibrated with a white standard ( $L^*=92.83$ ,  $a^*=-1.27$  and  $b^*=0.52$ ).

#### **10.3.5.3.7 Sensory evaluation**

Sensory evaluation of the samples was performed by 30 untrained panelists with the ages of 22–32, who were familiar with mackerel consumption. The assessment was conducted for colour, odour and overall likeness (OAL) of samples using a 9-point hedonic scale: 1- dislike extremely; 5- neither like nor dislike; 9- like extremely (Meilgaard *et al.*, 2007). The test was conducted on day 0, 15, and 30 of storage.

#### **10.3.5.3.8 Measurement of volatile compounds**

The volatile compounds in mackerel meat powder at day 0 and the selected samples stored for 30 days were determined using a solid-phase micro

extraction gas chromatography mass spectrometry (SPME-GCMS), following the method of Iglesias and Medina (2008) with a slight modification.

#### **10.3.5.3.8.1 Extraction of volatile compounds by SPME fibre**

To extract volatile compounds, 1 g of selected samples were homogenised with 4 ml of deionised water. Homogenates were then centrifuged at 5000g for 10 min. The supernatants were heated at 60 °C in 20 ml headspace vial (Agilent Technologies, Palo Alto, CA, USA) with equilibrium time of 60 min. The SPME fiber (50/30 µm DVB/Carboxen<sup>TM</sup>/PDMS Stableflex<sup>TM</sup>) (Supelco, Bellefonte, PA, USA) was conditioned at 270 °C for 15 min before use and then was exposed to the headspace. The vials containing the sample extracts and the volatile compounds were allowed to absorb into the SPME fiber at 60 °C for 60 min. The volatile compounds were then desorbed in the GC injector port for 15 min at 270 °C.

#### **10.3.5.3.8.2 GC–MS analysis**

GC–MS analysis was performed in a Gas Chromatograph-Mass Spectrometer (Trace GC Ultra/ISQ MS, Thermo Scientific Inc., USA). Compounds were separated on a Stabilwax capillary column (Restek Corporation, Bellefonte, PA) (30 m x 0.25 mm ID, with film thickness of 0.25 µm). The GC oven temperature program was: 35 °C for 3 min, followed by an increase of 3 °C/min to 70 °C, an increase of 10 °C/min to 200 °C, and finally an increase of 15 °C/min to a final temperature of 250 °C and holding for 10 min. Helium was employed as a carrier gas with a constant flow of 1 ml/min. The injector was operated in the splitless mode and its temperature was set at 270 °C. Transfer line temperature was maintained at 265 °C. The quadrupole mass spectrometer was operated in the electron ionisation (EI) mode and source temperature was set at 250 °C. Initially, full-scan-mode data was acquired to determine appropriate masses for the later acquisition in scan mode under the following conditions: mass range: 35–500 amu and scan rate: 0.220 s/scan. All the analyses were performed with ionisation energy of 70 eV, filament emission current at 150 µA, and the electron multiplier voltage at 500 V.

#### **10.3.5.3.8.3 Analyses of volatile compounds**

Identification of the volatile compounds in the samples was done by consulting ChemStation Library Search (Wiley 275.L). Identification of compounds was performed, based on the retention time and mass spectra in comparison with those of standards from ChemStation Library Search (Wiley 275.L). Quantification limits were calculated to a signal-to-noise (S/N) ratio of 10. Repeatability was evaluated by analysing 3 replicates of each sample. The identified volatile compounds related with lipid oxidation, including aldehydes, alcohols and acids, etc. were presented in the term of abundance.

#### **10.3.6 Statistical analyses**

All experiments were performed in triplicates (n=3) and a completely randomised design (CRD) was used. Analysis of variance (ANOVA) was performed and the mean comparisons were done by Duncan's multiple range tests (Steel and Torrie, 1980). Data are presented as mean  $\pm$  standard deviation and the probability value of  $P < 0.05$  was considered as significant. Statistical analysis was performed using the Statistical Package for Social Sciences (SPSS 17.0 for windows, SPSS Inc., Chicago, IL, USA).

### **10.4 Results and discussion**

#### **10.4.1 Chemical changes of mackerel meat powder during storage**

##### **10.4.1.1 Moisture content**

Moisture content of mackerel meat powder covered with tilapia and squid skin gelatin films and nanocomposite films incorporated without and with EECH during storage of 30 days at 28-30 °C in comparison with those of samples covered with PE and the control (without cover) is depicted in Figure 47a. Moisture content of the powder covered with all films increased up to 20 days of storage ( $P < 0.05$ ). The adsorption of water vapour by dried powder is generally mediated by binding of water molecules to specific hydrophilic sites, such as carboxylic, amino

and hydroxyl residues of proteins, even at low relative humidity (D'Arcy and Watt, 1981). It was noted that the lowest moisture content was found in the samples covered with PE throughout the storage ( $P < 0.05$ ). This might be due to the much higher water vapour barrier property of PE, compared to gelatin films. Cervera *et al.* (2004) stated that water vapour strongly interacts with the hydrophilic polymer film matrix. As a consequence, the permeation of water vapour through film matrix increases. The higher moisture diffusion from the environment through the packaging material increases the moisture content of packed sample (Cervera *et al.*, 2004). In general, the decreases in moisture content of all samples were observed after 20 days of storage ( $P < 0.05$ ). The result suggested that some water in the sample might be evaporated to the head space of container. This led to the lower amount of water retained in the samples. Generally, samples covered with fish gelatin based films incorporated with either EECH or nanoclay exhibited the lower moisture content than those covered with gelatin films from both tilapia and squid skin. The powder covered with nanocomposite film from squid skin gelatin incorporated with 0.4% EECH (SGF-Na-EECH) showed the lowest moisture content ( $P < 0.05$ ) during storage time, except 25 days of storage. Nevertheless, moisture content was still higher than that found in sample covered with PE ( $P < 0.05$ ). This was plausibly due to the combined effect of EECH and nanoclay in formation of more compact film network. The ordered film matrix developed by the strong interaction between OH group of EECH or nanoclay with gelatin chains via hydrogen bonds and the 'tortuous pathway' created by the nanoclay were responsible for prevention of water vapour migration as indicated by the lowered moisture content of samples (Bae *et al.*, 2009a; Hoque *et al.*, 2011c; Martucci and Ruseckaite, 2010a; Ray and Okamoto, 2003). Abdollahi *et al.* (2012) confirmed the formation of hydrogen bonds through Fourier Transform infrared studies (FT-IR) in chitosan/montmorillonite/rosemary essential oil. Reinforcement of thermoplastic starch/montmorillonite composites was also reported (Huang *et al.* 2004). The increases in moisture content were also reported earlier by Artharn *et al.* (2009) for fish meat powder covered with different types of films. It has been known that gelatin based films have excellent barrier property to oxygen, but poor water vapour barrier property (Gomez-Guillen *et al.*, 2009; Hoque *et al.*, 2011c; Jongjareon-



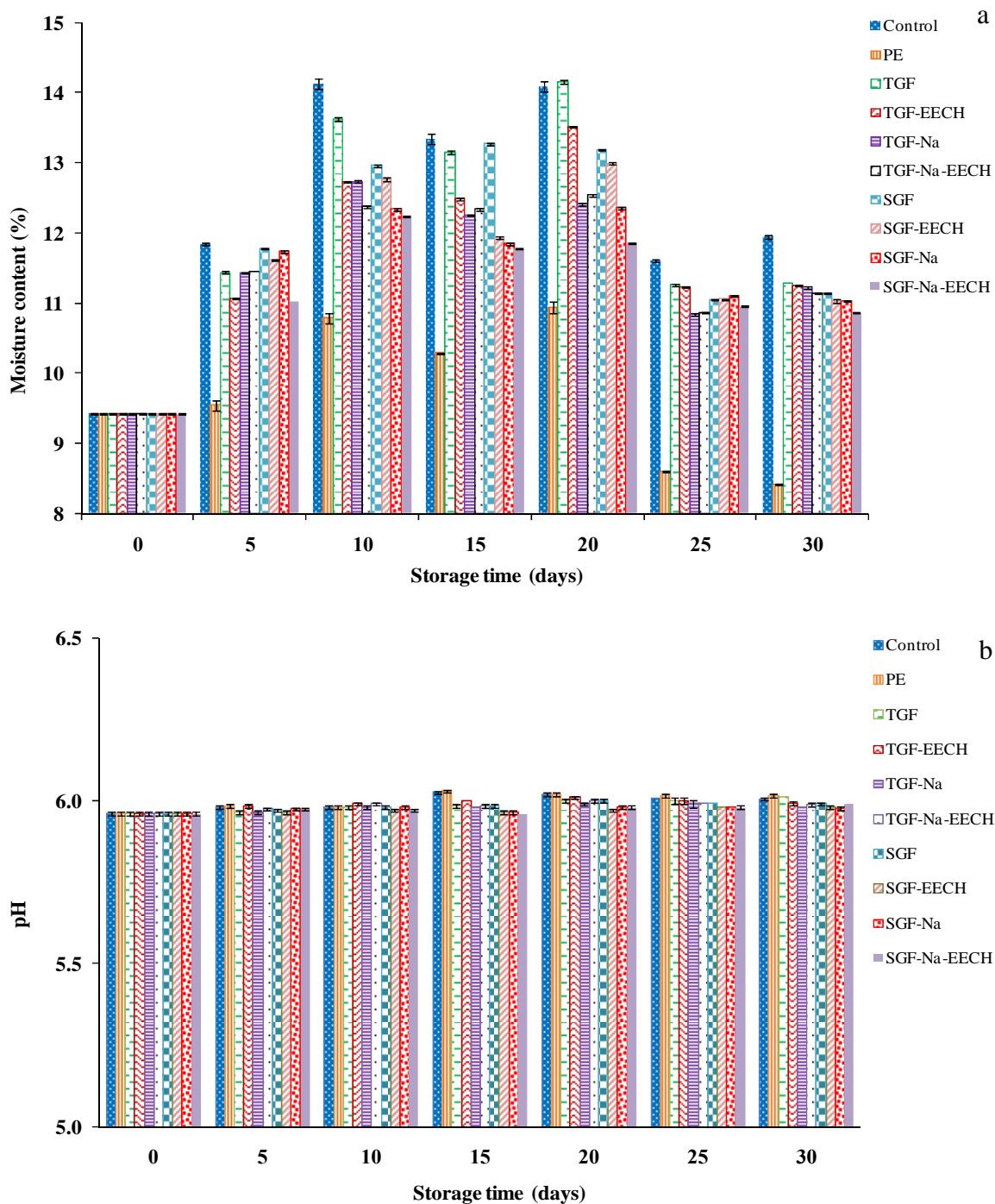


**Figure 47.** Moisture content (a) and pH (b) of mackerel meat powder covered with gelatin films and nanocomposite films incorporated without and with EECH in comparison with that covered polyethylene (PE) film and the control during storage at 28-30 °C. Control and PE: samples covered without any films and with PE film, respectively; TGF, TGF-Na and SGF, SGF-Na: gelatin films and nanocomposite films from tilapia and squid skin, respectively; TGF-EECH, SGF-EECH and TGF-Na-EECH, SGF-Na-EECH: gelatin films and nanocomposite films from tilapia and squid skin incorporated with EECH at 0.05 and 0.4% (w/w, based on protein), respectively.

-rak *et al.*, 2008; Nunez-Flores *et al.*, 2013b). The result therefore suggested that the incorporation of EECH along with the nanoclay could improve moisture barrier property of gelatin film to some extent, in which migration of water vapour to the powder was lowered.

#### **10.4.1.2 pH**

pH of mackerel meat powder covered with gelatin films and nanocomposite films incorporated without and with EECH in comparison with those of sample covered with PE and the control during the storage is shown in Figure 47b. In general, pH of all samples slightly increased when the storage time increased ( $P < 0.05$ ). Generally, the control and PE samples showed higher pH value than other samples, particularly after 10 days of storage. The increase in pH might be related with the increased formation of decomposition products, especially volatile base compounds (Lopez-Caballero *et al.*, 2007). The increase in pH was in accordance with increasing moisture content (Figure 47a). The increased moisture content might favour the microbial growth, more likely related with increased decomposition of nitrogenous compounds caused by spoilage bacteria. With the extended storage time, especially after 20 days of storage, those volatiles might be lost, leading to the decrease in pH.

#### **10.4.1.3 PV**

PV of mackerel meat powder covered with different films in comparison with that of control sample is shown in Figure 48a. Generally, PV of all samples increased continuously during the storage time, indicating the formation of primary products of lipid oxidation in all samples (Yanishlieva and Marinova, 2001). During the storage, a significant increase in PV was observed in the control sample as compared to other samples ( $P < 0.05$ ). The increase in PV was lowered in samples covered with gelatin films in comparison with that of samples covered with PE at day 30 of storage ( $P < 0.05$ ). This result confirmed that oxygen barrier properties of gelatin film might be superior to PE film during the extended storage (Jongjareonrak *et al.*, 2008). Gelatin films had the impressive gas such as oxygen and carbon dioxide barrier

properties, compared to synthetic films (Gomez-Estaca *et al.*, 2014; Jongjareonrak *et al.*, 2008). Gelatin films could retard the lipid oxidation of food products more effectively than PE films during storage time (Artharn *et al.*, 2009; Jongjareonrak *et al.*, 2008). Abreu *et al.* (2011) reported that blue shark samples covered with or without natural extract added films had the lower PV than the control. Gelatin film might function as a barrier to oxygen permeability and only a small amount of oxygen could therefore permeate across the films. As a result, the lower lipid oxidation was obtained. Lower PV was observed for samples covered with gelatin films when EECH or nanoclay was incorporated. This was plausibly due to the strong interaction between phenolic compounds of EECH and nanoclay with gelatin molecules in film matrix. Silicate layers of nanoclay have good barrier to gases such as oxygen and nitrogen (Liu *et al.*, 2003). The improved barrier properties of films were due to functional property of filler (Bae *et al.*, 2009a). Mackerel powder covered with squid skin gelatin films incorporated with both EECH and nanoclay (SGF-EECH-Na) had the lowest PV during storage time, except at day 5 and 15 of storage. Thus, gelatin films could be used as the packaging material to prevent rancidity of foods, especially when incorporated with EECH and nanoclay. They could serve as an alternative for synthetic polymeric films.

#### **10.4.1.4 TBARS value**

TBARS values of mackerel meat powder covered with various films in comparison with the control are depicted in Figure 48b. In general, TBARS values of all samples increased continuously during storage time ( $P < 0.05$ ). The TBARS value has been widely used to determine the secondary lipid oxidation in meat and meat products (Nunez-Flores *et al.*, 2013b), in which malondialdehyde (MDA) content was measured (Benjakul *et al.*, 2005). Lipid oxidation could be initiated and accelerated by different mechanisms including the production of singlet oxygen, enzymatic and non-enzymatic generation of free radicals and active oxygen (Kubow, 1992). It was found that mackerel meat powder had TBARS value of 10.63 mg MDA/kg sample at day 0, suggesting that lipid oxidation took place during drying and preparation of powder. The highest TBARS values were obtained in the control samples ( $P < 0.05$ ). In

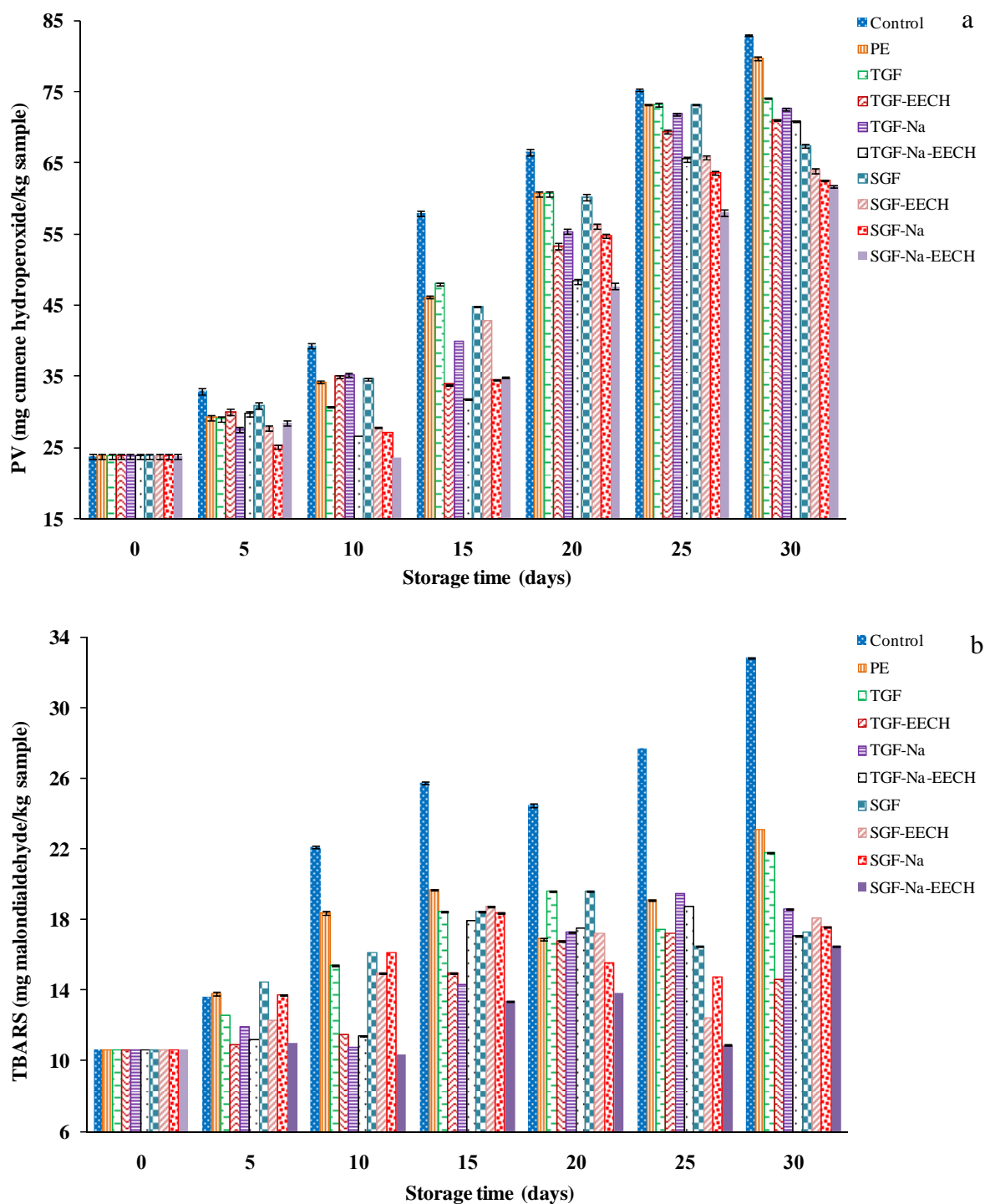


**Figure 48.** PV (a) and TBARS values (b) of mackerel meat powder covered with gelatin films and nanocomposite films incorporated without and with EECH in comparison with that covered PE film and the control during storage at 28-30 °C.

addition, the higher TBARS value was observed for PE samples than those covered with gelatin based films, regardless of incorporation of EECH or nanoclay. This might be due to the superior oxygen barrier properties of gelatin films (Jongjareonrak *et al.*, 2008). In contrast, hydrophobic polymer films such as PE are relatively poor barrier to oxygen but have the excellent barrier property to water vapour (Gomez-Guillen *et al.*, 2009; Jongjareonrak *et al.*, 2008). Gas barrier property of gelatin films had a crucial role in extending the shelf-life of products (Arvanitoyannis, 2002). Amongst gelatin films, those incorporated with EECH or nanoclay or both EECH and nanoclay showed generally lower TBARS value than the gelatin film (without EECH and nanoclay). Gelatin–phenolics, gelatin–clay or gelatin–phenolics–clay interactions more likely led to the formation of matrices with compact structure, which reduced the permeability of gas. The result suggested that lipid oxidation in mackerel meat powder could be retarded when EECH or nanoclay were applied into gelatin films, plausibly caused by the improved oxygen barrier characteristics. Generally, the lowest TBARS values were obtained for SGF-EECH-Na samples up to 25 days of storage ( $P < 0.05$ ). However, the lowest TBARS value was found in sample covered with tilapia gelatin film incorporated with EECH (TGF-EECH) at day 30 of storage ( $P < 0.05$ ). Thus, the different film formulations had the varying impact on TBARS value of fish meat powder during storage at room temperature.

#### **10.4.1.5 TVB content**

TVB content of mackerel meat powder covered with different films during storage at 28-30 °C in comparison with the control is illustrated in Figure 49. Total volatile bases are related with the growth of microorganisms and the formation of basic compounds from their metabolism (Lopez-Caballero *et al.*, 2007). TVB content has been used as the quality index of various seafoods (Abreu *et al.*, 2011). TVB represents the sum of ammonia, dimethylamine (DMA), trimethylamine (TMA) and other basic volatile nitrogenous compounds. DMA and TMA are the degradation products of trimethylamine oxide (TMAO), a typical compound, which has a vital role in osmoregulation of marine fish. DMA is generally produced by endogenous enzymes and TMA is generated by bacterial enzymes (Zeisel *et al.*, 1985). TVB

content of all samples at day 0 was 91.23 mg-N/100 g sample. A continuous increase in TVB content was observed in all samples ( $P < 0.05$ ) throughout the storage but the increasing rate varied upon the films used to cover the samples. However, a rapid increase in TVB content was noticed in the control (WOC samples) during storage time. Generally, the lower TVB content was observed in samples covered with tilapia skin gelatin based films in comparison with those covered with the corresponding squid skin gelatin based films, especially during the first 15 days of storage. Nevertheless, those covered with tilapia skin gelatin film containing both nanoclay and EECH had the lower TVB content than others during 20-30 days of storage ( $P < 0.05$ ). In general, the powder covered with nanocomposite films from tilapia and squid skin gelatin incorporated with EECH at the level of 0.4% (w/w) (TGF-Na-EECH and SGF-Na-EECH) showed the lower TVB content than those covered with gelatin based films. Moisture content of mackerel meat powder might be associated with TVB formation in samples. Moisture content of samples plausibly promoted the

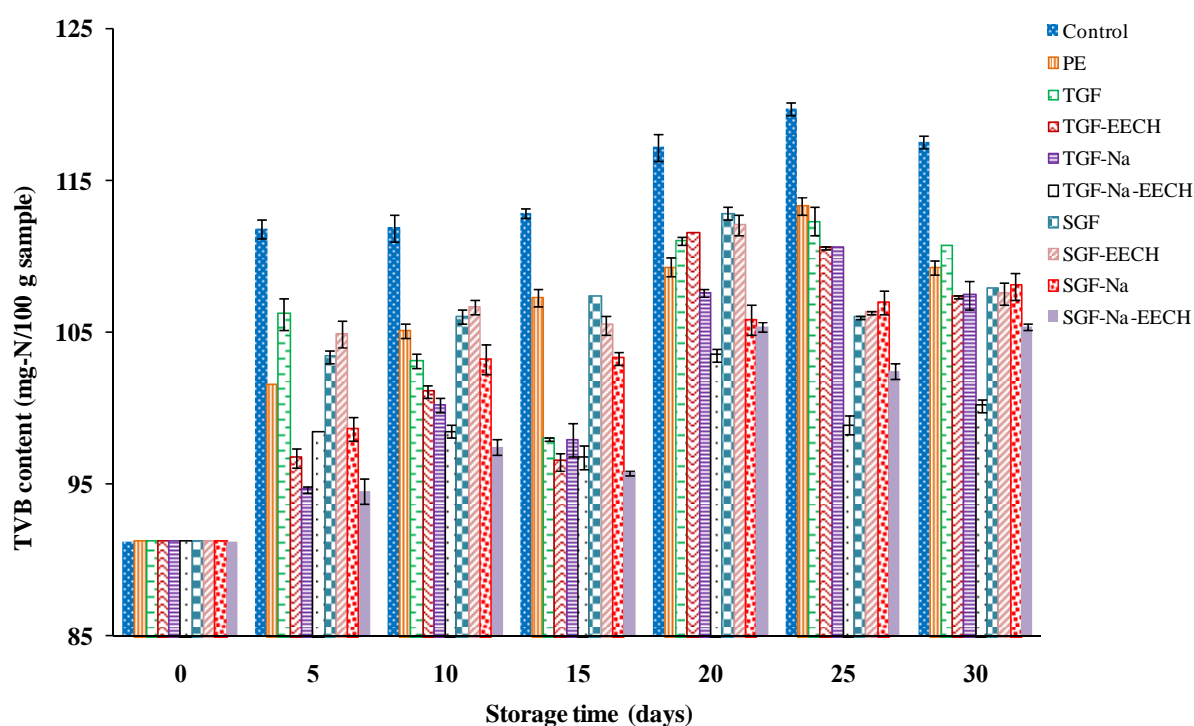


**Figure 49.** TVB content of mackerel meat powder covered with gelatin films and nanocomposite films incorporated without and with EECH in comparison with that covered PE film and the control during storage at 28-30 °C.

growth of microorganisms which were responsible for the production of TVB-N compounds. The increase in TVB content was in accordance with the increases in pH of fish powder during the extended storage (Figure 47b). This phenomenon was in agreement with the higher TVB and moisture content of the control (WOC) throughout the storage ( $P < 0.05$ ). Thus, TVB content of samples was governed by the types of packaging materials.

#### 10.4.2 Changes in colour of mackerel meat powder during storage

Colour of mackerel meat powder covered with various films in comparison with the control (without covering) during storage at 28-30 °C is shown in Figure 50. In general, the increases in  $a^*$ ,  $b^*$  and  $\Delta E^*$ - values were observed for the control sample up to 25 days ( $P < 0.05$ ). At day 30, the decreases in  $a^*$  and  $\Delta E^*$ - values were noticeable ( $P < 0.05$ ). The control samples exhibited the differences in colour parameters in comparison with those of covered with different gelatin based films and PE films. Moreover, the lower  $L^*$ - values were also found with the control compared with others ( $P < 0.05$ ). The increased  $b^*$ - value indicated the formation of yellowish pigment, probably via the Maillard reaction, which might be associated with the increasing moisture content in dried fish meat powder (Artharn *et al.*, 2009). The increase in  $b^*$ - value of mackerel meat powder was more likely related with the increased lipid oxidation, particularly for the control samples. Generally,  $L^*$ - value of PE sample was lower than that covered with fish gelatin films. However, higher  $b^*$ - value was observed for PE sample after 20 days of storage. Carbonyl group such as aldehydes from lipid oxidation might undergo the glycation with amino group of protein and contribute to the non-enzymatic browning reaction (Solomon *et al.*, 1995). Water activity influences rate and extent of non-enzymatic browning reaction and lipid oxidation of food products, and the reaction increased with increasing water activity (Fontana, 2000). Moreover, the browning was likely related with the increased lipid oxidation as indicated by the increase in PV and TBARS values of the control samples (Figure 48a and 48b). This phenomenon was correlated well with the higher  $a^*$ ,  $b^*$  and  $\Delta E^*$ - values of the control samples. The highest rate of increase in

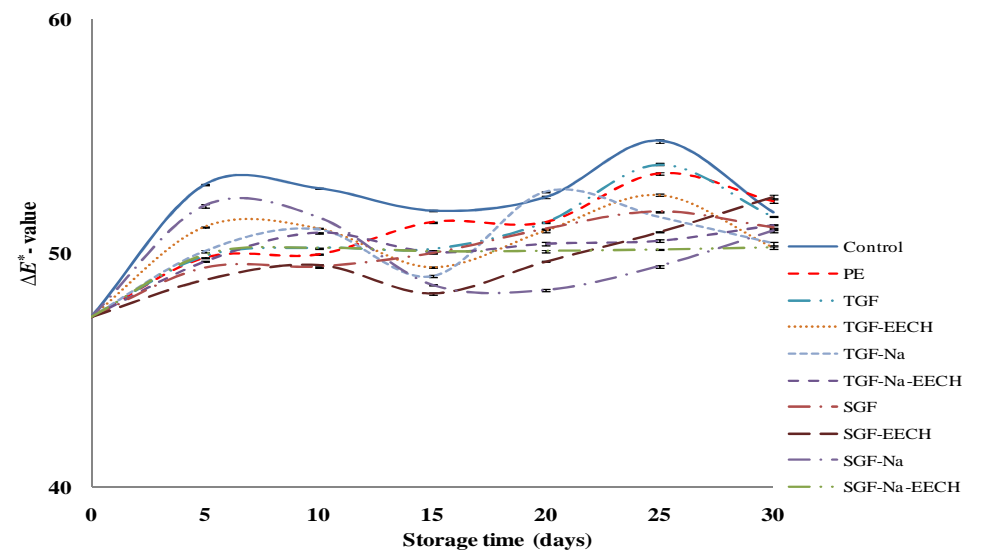
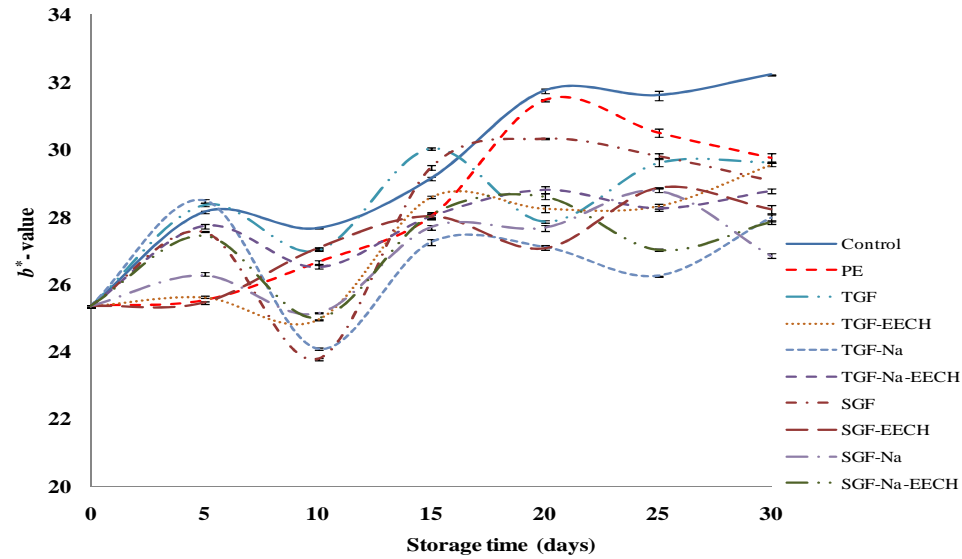
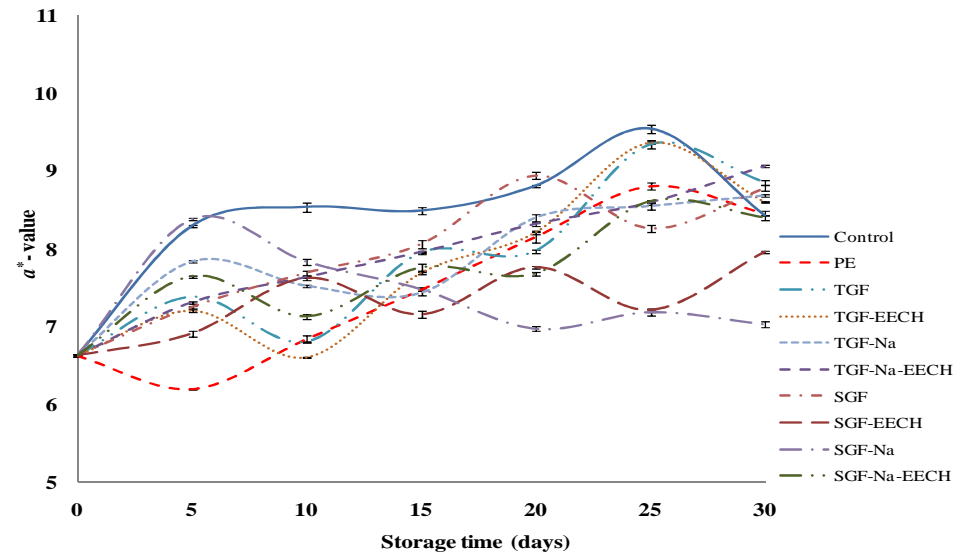
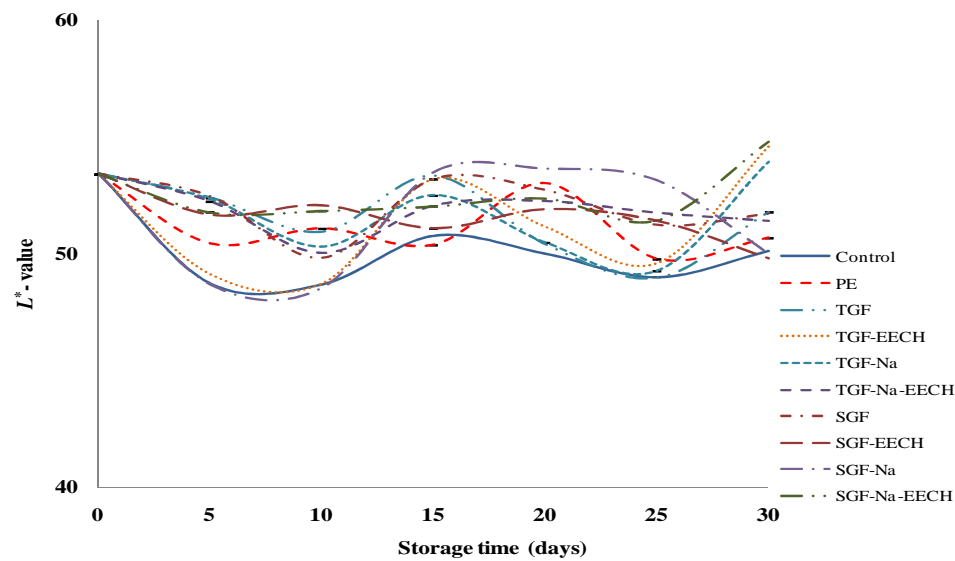


**Figure 50.** Colour of mackerel meat powder covered with gelatin films and nanocomposite films incorporated without and with EECH in comparison with that covered PE film and the control during storage at 28-30 °C.



$a^*$  and  $b^*$ - values was found in the uncovered sample (Artharn *et al.*, 2009). Nunez-Flores *et al.* (2013b) reported that gelatin-lignosulphonate films could not maintain the colour of sardine meat during storage. Salmon meat covered with gelatin-lignin film showed higher  $L^*$ ,  $b^*$  and lower  $a^*$  values than control sample (Ojagh *et al.*, 2011). Thus, the colour of samples was affected by films and was more likely related with the lipid oxidation taken place in the sample.

#### **10.4.3 Changes in sensory property of mackerel meat powder during storage**

Likeness score of mackerel meat powder covered with different films in comparison with the control during storage at 28-30 °C at day 0, 15 and 30 is presented in Table 38. The score for colour, odour and overall likeness was slightly decreased during the storage time ( $P < 0.05$ ). The score of colour likeness of the control sample decreased at day 30 of storage ( $P < 0.05$ ). However, no significant differences were observed in colour of samples that covered with either PE or gelatin films throughout the storage ( $P > 0.05$ ). Odour likeness score of samples covered with EECH or nanoclay or both EECH and nanoclay incorporated gelatin films remained unchanged, except for SGF-Na sample. Nevertheless, powder covered with TGF, SGF, PE films and the control had the decrease in odour likeness score at day 30 ( $P < 0.05$ ). In general, overall likeness score of all samples gradually decreased during the storage time and the rate of decrease varied upon the types of films. Amongst gelatin based films, the highest score of overall likeness was found for SGF-Na-EECH sample and the lowest score was observed for the control samples at day 30 ( $P < 0.05$ ). The result confirmed that the gelatin films added with both EECH and nanoclay could maintain the sensory attributes of fish meat powder to some extent. This was plausibly due to the barrier property of film against oxygen and water vapour. As a result, the deterioration of mackerel meat powder could be retarded. Incorporation of EECH and nanoclay to squid skin gelatin films therefore provided the beneficial effect on overall likeness of the sample during storage.

**Table 38.** Likeness score of mackerel meat powder covered with gelatin films and nanocomposite films incorporated without and with EECH in comparison with that covered PE film and the control during storage at 28-30 °C

Sensory attributes	Storage time (days)	Film samples									
		Control	PE	TGF	TGF-EECH	TGF-Na	TGF-Na-EECH	SGF	SGF-EECH	SGF-Na	SGF-Na-EECH
<b>Colour</b>											
	0	8.33±0.58aA	8.33±0.58aA	8.33±0.58aA	8.33±0.58aA	8.33±0.58aA	8.33±0.58aA	8.33±0.58aA	8.33±0.58aA	8.33±0.58aA	8.33±0.58aA
	15	7.70±0.67aA	8.00±0.00aA	7.90±0.32aA	7.90±0.32aA	7.90±0.32aA	8.00±0.00aA	7.90±0.32aA	8.00±0.47aA	7.90±0.32aA	8.00±0.00aA
	30	6.33±0.58aB	7.00±1.00aA	7.00±1.00aA	7.33±1.15aA	7.33±0.58aA	7.67±0.58aA	7.33±1.15aA	7.33±0.58aA	7.33±0.58aA	7.67±0.58aA
<b>Odour</b>											
	0	7.83±0.29aA	7.83±0.29aA	7.83±0.29aA	7.83±0.29aA	7.83±0.29aA	7.83±0.29aA	7.83±0.29aA	7.83±0.29aA	7.83±0.29aA	7.83±0.29aA
	15	7.00±1.00aAB	7.00±1.00aAB	7.00±1.00aAB	7.33±1.15aA	7.33±1.15aA	7.67±0.58aA	7.00±0.00aAB	7.33±1.53aA	7.67±0.58aA	7.67±0.58aA
	30	6.00±1.00aB	6.00±1.00aB	6.00±1.00aB	6.67±1.15aA	6.67±1.15aA	7.00±1.00aA	6.00±1.00aB	6.67±1.15aA	6.67±0.58aB	7.33±0.58aA
<b>OAL</b>											
	0	8.08±0.25aA	8.08±0.25aA	8.08±0.25aA	8.08±0.25aA	8.08±0.25aA	8.08±0.25aA	8.08±0.25aA	8.08±0.25aA	8.08±0.25aA	8.08±0.25aA
	15	7.35±0.35aB	7.50±0.50aA	7.45±0.45aA	7.62±0.28aA	7.62±0.28aA	7.83±0.17aAB	7.45±0.45aAB	7.67±0.33aA	7.78±0.12aA	7.83±0.17aAB
	30	6.17±0.17dC	6.50±0.50cdB	6.50±0.50cdB	7.00±0.33abcB	7.00±0.33abcB	7.33±0.33abB	6.67±0.67bcdB	7.00±0.33abcB	7.00±0.33abcB	7.50±0.17aB

Mean ± SD (n=30).

Different lower case letters in the same row indicate significant differences (P<0.05).

Different uppercase letters in the same column under the same quality attribute indicate significant differences (P<0.05).

#### **10.4.4 Changes in volatile compounds of mackerel meat powder during storage**

Selected volatile compounds of mackerel meat powder at day 0 and the powder covered with nanocomposite film from squid skin gelatin incorporated with 0.4% EECH (w/w) in comparison with PE sample and the control after storage for 30 days are presented in Table 39. Fish meat powder contained volatile compounds including aldehyde (Hexanal, Nonanal, Octanal, Benzaldehyde), alcohol (1-Heptanol, 1-Octanol, 1-Octene-3-ol, 1-Pentanol, 1-Penten-3-ol, 2-Penten-1-ol), etc. Aldehydes have been used as the indicators of lipid oxidation because they possess low threshold values and are the major contributors to the development of off-flavour and off-odour (Ross and Smith, 2006). Amongst aldehydes, hexanal which are known to be the most predominant volatiles produced during lipid oxidation. Hexanal has been recognised as a reliable indicator of rancidity in meats (Yarnpakdee et al., 2012). Fu, Xu, and Wang (2009) reported that nonanal was responsible for oxidised oil odour as catalysed by hemoglobin. Octanal, the carbonyl compound was responsible for fishy odour (Varlet et al., 2006). Hexanal was the major volatile compound in the control and PE samples after 30 days of storage, whereas in SGF-Na-EECH sample contained hexanal at a lower level. After 30 days of storage, no nonanal and octanal were detected. This was more likely due to the loss of those volatiles after storage. Hexanal and nonanal were reported as the secondary oxidation products of linoleic acid (Grosch, 1987). For benzaldehyde, the highest abundance was found in the control. After 30 days of storage, the highest abundance of 1-Octene-3-ol, 1-Penten-3-ol and 2-Penten-1-ol were found in the control and the lowest abundance was noticeable in the sample covered with SGF-Na-EECH film. After 30 days, 1-Heptanol, 1-Octanol and 1-Pentanol disappeared in all samples. This was more likely owing to their volatilisation during the storage. Aliphatic alcohol contributed to off-flavour produced by oxidative deterioration of lipid, such as 1-octene-3-ol and 1-pentene-3-ol which were described as musty flavour and oxidised, respectively (Badings, 1970). Alcohols are the secondary products produced by the decomposition of hydroperoxide (Girand and Durance, 2000). 8-Carbon alcohols are known to be present in all species of fish

(Josephson et al., 1984). Additionally, 1-alkanols and 1-alkanals (such as pentanol and hexanal) can occur by the decomposition of the primary hydroperoxides of fatty acids (Kellard *et al.*, 1985).

**Table 39.** Volatile compounds of mackerel meat powder at day 0 and powder covered with nanocomposite film from squid skin gelatin incorporated with 0.4% EECH (w/w) in comparison with PE film and the control after 30 days of storage at 28-30 °C

Volatile compounds (abundance x 10 <sup>6</sup> )	Day 0	Day 30		
		Control	PE	SGF-Na-EECH
Hexanal	NA	349	310	29
Nonanal	177	NA	NA	NA
Octanal	118	NA	NA	NA
Benzaldehyde	446	4090	2605	1702
1-Heptanol	163	NA	NA	NA
1-Octanol	78	NA	NA	NA
1-Octene-3-ol	NA	326	294	40
1-Pentanol	103	NA	NA	NA
1-Penten-3-ol	191	814	681	618
2-Penten-1-ol	89	236	222	163
2,3-Dimethyl-5-ethyl pyrazine	NA	627	541	238
2,3,5-Trimethyl pyrazine	NA	1774	1628	970
2,3,5,6-Tetramethyl pyrazine	NA	5585	5522	2485
Butanoic acid	NA	5886	2237	1199
3-Methyl-butanoic acid	NA	6580	2752	559
Propanoic acid	NA	664	217	226

Alkyl pyrazine (2,3-Dimethyl-5-ethyl pyrazine, 2,3,5-Trimethyl pyrazine, 2,3,5,6-Tetramethyl pyrazine) as well as acids (Butanoic acid, Propanoic acid, 3-Methyl-butanoic acid) were also found in the samples. The abundance varied with films used for covering. Alkyl pyrazines are chemical compounds based on pyrazine with different substitution patterns. Some alkyl pyrazines are naturally

occurring highly aromatic substances which often have a very low odor threshold (Mihara and Masuda, 1988). Alkyl pyrazines are also formed during the cooking of some foods via Maillard reactions (Fors and Olofsson, 1985). Generally, those pyrazine compounds found at higher levels in the control and PE samples than SGF-Na-EECH sample after 30 days of storage. All acids were lowest in abundance when SGF-Na-EECH film was used to cover the sample. In general, the formation of volatile compounds was in agreement with TBARS value of corresponding samples (Figure 48b). The result reconfirmed that nanocomposite films from squid skin gelatin incorporated with EECH at 0.4% (w/w) could retard oxidative deterioration and prevent the formation of offensive odorous compounds in mackerel meat powder by preventing the gas and light as well as water vapour migration.

## **10.5 Conclusion**

Mackerel meat powder was susceptible to moisture absorption and lipid oxidation throughout the storage time. The uses of nanocomposite films from squid skin gelatin incorporated with EECH at 0.4% (w/w) could retard the moisture permeation across the film as well as lipid oxidation more effectively than other films. Thus, SGF-Na-EECH film can be an alternative to synthetic films in maintaining the quality and extend the shelf-life of mackerel meat powder.

## CHAPTER 11

### SUMMARY AND FUTURE WORKS

#### 11.1 Summary

1. Splendid squid skin gelatin extracted at 60 °C had superior gelling and film-forming abilities. Higher extraction temperature yielded the gelatin with darker colour and lower functional properties. Gelatin extracted at higher temperature had weaker film network, associated with lower mechanical and water barrier properties.

2. Gelatin from squid skin bleached with H<sub>2</sub>O<sub>2</sub> at a concentration of 2% had the improved colour. H<sub>2</sub>O<sub>2</sub> at higher concentration resulted in the increasing yield, however negatively affected gelling property and colour of gelatin. Gelatin from squid skin bleached with H<sub>2</sub>O<sub>2</sub> at higher concentrations yielded the films with lower WVP but higher extensibility.

3. Tilapia skin gelatin film incorporated with hydrophilic nanoclay had a stronger film network than hydrophobic nanoclay. Cloisite Na<sup>+</sup> at a level of 1% (w/w) could effectively improve the water vapour barrier and mechanical properties as well as the thermal stability of films.

4. Homogenisation under appropriate shear force, especially the conventional homogenisation (CH) could improve the mechanical resistance, water vapour barrier property, transparency and thermal stability of nanocomposite fish gelatin films. The decrease in overall properties of the nanocomposite films was obtained when high pressure homogenisation (HPH) under higher pressures with more than 2 passes was implemented.

5. Highest mechanical, water vapour barrier properties as well as the thermal stability were obtained when FFS with pH of 6 was used for preparation of nanocomposite films.

6. Fish gelatin film and nanocomposite film incorporated with EECH at 0.05% and 0.4% (w/w, on protein basis), respectively showed the improved water vapour barrier property.

7. Nanocomposite films from squid skin gelatin incorporated with EECH at 0.4% (w/w) could retard lipid oxidation more effectively than other films. Thus, SGF-Na-EECH film can be an alternative to synthetic films in maintaining the quality and extend the shelf-life of mackerel meat powder.

## **11.2 Future works**

1. Shelf-life and storage stability of bio-nanocomposite gelatin films should be examined.

2. Migration of nanoclays from bio-nanocomposite gelatin films to food must be investigated.

3. Biodegradability of bio-nanocomposite gelatin films should be studied.

## REFERENCES

- Abdollahi, M., Rezaei, M. and Farzi, G. 2012. A novel active bionanocomposite film incorporating rosemary essential oil and nanoclay into chitosan. *J. Food. Eng.* 111: 343-350.
- Abreu, D. A. P. D., Losada, P. P., Maroto, J. and Cruz., J. M., 2011. Natural antioxidant active packaging film and its effect on lipid damage in frozen blue shark (*Prionace glauca*). *Innov. Food Sci. Emerg.* 12: 50–55.
- Aewsiri, T., Benjakul, S., Visessanguan, W., Wierengac, P. A. and Gruppen. H. 2011. Surface activity and molecular characteristics of cuttlefish skin gelatin modified by oxidized linoleic acid. *Int. J. Biol. Macromol.* 48: 650-660.
- Aewsiri, T., Benjakul, S. and Visessanguan, W. 2009. Functional properties of gelatin from cuttlefish (*Sepia pharaonis*) skin as affected by bleaching using hydrogen peroxide. *Food Chem.* 115: 243–249.
- Ahmad, M., Benjakul, S., Prodpran, T. and Agustini, T. W. 2012. Physico-mechanical and antimicrobial properties of gelatin film from the skin of unicorn leatherjacket incorporated with essential oils. *Food Hydrocolloid.* 28: 189-199.
- Ahmad, M. and Benjakul, S. 2011. Characteristics of gelatin from the skin of unicorn leatherjacket (*Aluterus monoceros*) as influenced by acid pretreatment and extraction time. *Food Hydrocolloid.* 25: 381-388.
- Ahvenainen, R. 2003. Active and intelligent packaging. Novel food packaging techniques. CRC Press. New York.
- Ajandouz, E. H. and Puigserver, A. 1999. Nonenzymatic Browning Reaction of Essential Amino Acids: Effect of pH on Caramelization and Maillard Reaction Kinetics. *J. Agric. Food Chem.* 47: 1786-1793.



- Akagunduz, Y., Mosquera, M., Gimenez, B., Aleman, A., Montero, P. and Gomez-Guillen, M. C. 2014. Sea bream bones and scales as a source of gelatin and ACE inhibitory peptides. *LWT-Food Sci. Technol.* 55: 579-585.
- Alamsi, H., Ghanbarzadeh, B. and Entezami, A. A. 2010. Physicochemical properties of starch-CMC-nanoclay biodegradable films. *Int. J. Biol. Macromol.* 46: 1–5.
- Alboofetileh, M., Rezaei, M., Hosseini, H. and Abdollahi, M. 2013. Effect of montmorillonite clay and biopolymer concentration on the physical and mechanical properties of alginate nanocomposite films. *J. Food Eng.* 117: 26–33.
- Aleman, A., Gimenez, B., Montero, P. and Gomez-Guillen, M. C. 2011. Antioxidant activity of several marine skin gelatins. *LWT-Food Sci. Technol.* 44: 407-413.
- Alfaro, A. T., Biluca, F. C., Marquetti, C., Tonial, I. B. and de Souza, N. E. 2014. African catfish (*Clarias gariepinus*) skin gelatin: Extraction optimization and physical–chemical properties. *Food Res. Int.* DOI: <http://dx.doi.org/10.1016/j.foodres.2014.05.070>
- AOAC. 2000. Official methods of analysis. 17th ed. Association of Official Analytical Chemists. Gaithersberg, MD.
- Appendini, P. and Hotchkiss, J. H. 2002. Review of antimicrobial food packaging. *Innov. Food Sci. Emerg. Technol.* 3: 113-126.
- Arcan, I. and Yemenicioglu, A. 2011. Incorporating phenolic compounds opens a new perspective to use zein films as flexible bioactive packaging materials. *Food Res. Int.* 44: 550-556.
- Arnao, M. B., Cano, A. and Acosta, M. 2001. The hydrophilic and lipophilic contribution to total antioxidant activity. *Food Chem.* 73: 239–244.

- Arnesen, J. A. and Gildberg, A. 2007. Extraction and characterisation of gelatin from Atlantic salmon (*Salmo salar*) skin. *Biores. Technol.* 98: 53–57.
- Arnesen, J. A. and Gildberg, A. 2006. Extraction of muscle proteins and gelatin from cod head. *Process Biochem.* 41: 697–700.
- Artharn, A., Prodpran, T. and Benjakul, S. 2009. Round scad protein-based film: Storage stability and its effectiveness for shelf-life extension of dried fish powder. *LWT-Food Sci. Technol.* 42: 1238–1244.
- Artharn, A., Benjakul, S., Prodpran, T. and Tanaka, M. 2007. Properties of a protein-based film from round scad (*Decapterus maruadsi*) as affected by muscle types and washing. *Food Chem.* 103: 867-874.
- Arvanitoyannis, I.S. 2002. Formation and properties of collagen and gelatin films and coatings. *In Protein-based films and coatings* (Gennadios, A., ed.). p. 275-304. CRC Press. Florida.
- Arvanitoyannis, I. S., Nakayama, A. and Aiba, S. 1998. Chitosan and gelatin based edible films: state diagrams, mechanical and permeation properties. *Carbohydr. Polym.* 37: 371–382.
- Arvanitoyannis, I., Psomiadou, E., Nakayama, A., Aiba, S. and Yamamoto, N. 1997. Edible films made from gelatin, soluble starch and polyols, Part 3. *Food Chem.* 60: 593-604.
- As'habi, L., Jafari, S. H., Khonakdar, H. A. and Baghaei, B. 2011. Morphological, rheological and thermal studies in melt processed compatibilized PA6/ABS/clay nanocomposites. *J. Polym. Res.* 18: 197–205.
- ASTM, 1989. Standard test methods for water vapor transmission of materials (E96–E80). Annual book of ASTM standards. Philadelphia, PA. ASTM 730–739.

- Audic, J. L. and Chaufer, B. 2005. Influence of plasticizers and crosslinking on the properties of biodegradable films made from sodium caseinate. *Eur. Polym. J.* 41: 1934–1942.
- Auerbach, S. M., Carrado, K. A. and Dutta, P. K. 2004. *Handbook of layered materials*. Marcel Dekker, Inc. New York.
- Avena-Bustillos, R. J. and Krochta, J. M. 1993. Water vapor permeability of caseinate-based edible films as affected by pH, calcium crosslinking and lipid content. *J. Food Sci.* 58: 904-907.
- Averous, L. 2004. Biodegradable multiphase systems based on plasticised starch: a review. *J. Macromol. Sci. Polym. Rev.* C44: 231–274.
- Badings, H. T. 1970. Cod storage defects in butter and their relation to the autoxidation of unsaturated fatty acids. *Neth. Milk Dairy J.* 24: 147-256.
- Bae, H. J., Park, H. J., Hong, S. I., Byun, Y. J., Darby, D. O., Kimmel, R. M., Whiteside, W. S. 2009a. Effect of clay content, homogenisation RPM, pH, and ultrasonification on mechanical and barrier properties of fish gelatin/montmorillonite nanocomposite films. *LWT-Food Sci. Technol.* 42: 1179–1186.
- Bae, H. J., Darby, D. O., Kimmel, R. M., Park, H. J. and Whiteside, W. S. 2009b. Effects of transglutaminase-induced cross-linking on properties of fish gelatin-nanoclay composite film. *Food Chem.* 114: 180-189.
- Bae, I., Osatomi, K., Yoshida, A., Osaka, K., Yamaguchi, A. and Hara, K. 2008. Biochemical properties of acid-soluble collagens extracted from the skins of underutilized fishes. *Food Chem.* 108: 49-54.

- Balti, R., Jridi, M., Sila, A., Souissi, N., Nedjar-Arroume, N., Guillochorn, D. and Nasri, M. 2011. Extraction and functional properties of gelatin from the skin of cuttlefish (*Sepia officinalis*) using smooth hound crude acid protease-aided process. *Food Hydrocolloid*. 25: 943-950.
- Bama, P., Vijayalakshmi, M., Jayasimman, R., Kalaichelvan, P. T., Deccaramani, M. and Sankaranarayanan, S. 2010. Extraction of collagen from cat fish (*Tachysurus maculatus*) by pepsin digestion and preparation and characterisation of collagen chitosan sheet. *Int. J. Pharm. Pharmaceut. Sci.* 2: 133-137.
- Bandekar, J. 1992. Amide modes and protein conformation. *BBA-Protein Struct. M*: 1120: 123-143.
- Bao, S., Xu, S. and Wang, Z. 2009. Antioxidant activity and properties of gelatin films incorporated with tea polyphenol-loaded chitosan nanoparticles. *J. Sci. Food Agric.* 89: 2692–2700.
- Barbosa-Pereira, L., Angulo, I., Lagaron, J. M., Paseiro-Losada, P. and Cruz, J. M. 2014. Development of new active packaging films containing bioactive nanocomposites. *Innov. Food Sci. Emerg.* DOI: <http://dx.doi.org/10.1016/j.ifset.2014.06.002>.
- Barnett, I. 2010. The packaging materials future outlook: Key trends in new materials, light weighting and emerging applications. Business Insights Ltd. UK.
- Baron, C. P., Kjaersgard, I. V. H., Jessen, F. and Jacobsen, C. 2007. Protein and lipid oxidation during frozen storage of rainbow trout (*Oncorhynchus mykiss*). *J. Agric. Food Chem.* 55: 8118–8125.

- Bates, L., Ames, J. M., MacDougall, D. B. and Taylor, P. C. 1998. Laboratory reaction cell to model maillard color development in a starch-glucose-lysine system. *J. Food Sci.* 63: 991-996.
- Benjakul, S., Kittiphattanabawon, P. and Regenstein, J. M. 2012a. Fish Gelatin. *In* Food Biochemistry and Food Processing (Simpson, B. K., ed.). p. 388-405. John Wiley & Sons, Inc. USA.
- Benjakul, S., Nalinanon, S. and Shahidi, F. 2012b. Fish Collagen. *In* Food Biochemistry and Food Processing (Simpson, B. K., ed.). pp. 365-387. John Wiley & Sons, Inc. USA.
- Benjakul, S., Oungbho, K., Visessanguan, W., Thiansilakul, Y. and Roytrakul, S. 2009. Characteristics of gelatin from the skins of bigeye snapper, *Priacanthus tayenus* and *Priacanthus macracanthus*. *Food Chem.* 116: 445-451.
- Benjakul, S., Visessanguan, W., Phongkanpai, V. and Tanaka, M. 2005. Antioxidative activity of caramelisation products and their preventive effect on lipid oxidation in fish mince. *Food Chem.* 90: 231-239.
- Benjakul, S. and Morrissey, M. T. 1997. Protein hydrolysates from Pacific whiting solid wastes. *J. Agric. Food Chem.* 45: 3423-3430.
- Benzie, I. F. F. and Strain, J. J. 1996. The ferric reducing ability of plasma (FRAP) as a measure of antioxidant power the FRAP assay. *Anal. Biochem.* 239: 70-76.
- Bergo, P. and Sobral, P. J. A. 2007. Effects of plasticiser on physical properties of pig skin gelatin films. *Food Hydrocolloid.* 21: 1285-1289.
- Bertan, L. C., Tanada-Palmua, P. S., Sianib, A. C. and Grosso, C. R. F. 2005. Effect of fatty acids and 'Brazilian elemi' on composite films based on gelatin. *Food Hydrocolloid.* 19: 73-82.

- Bianco, A., Chiacchio, U., Rescifina, A., Romeo, G. and Uccella, N. 1997. Biomimetic supramolecular biophenol-carbohydrate and biophenol-protein models by NMR experiments. *J. Agric. Food Chem.* 45: 4281-4285.
- Bigi, A., Panzavolta, S. and Rubini, K. 2004. Relationship between triple-helix content and mechanical properties of gelatin films. *Biomaterials.* 25: 5675–5680.
- Bigi, A., Cojazzi, G., Panzavolta, S., Roveri, N. and Rubini, K. 2002. Stabilization of gelatin films by crosslinking with genipin. *Biomaterials.* 23: 4827-4832.
- Bigi, A., Cojazzi, G., Panzavolta, S., Rubini, K. and Roveri, N. 2001. Mechanical and thermal properties of gelatin films at different degrees of glutaraldehyde crosslinking. *Biomaterials.* 22: 763-768.
- Bigi, A., Borghi, M., Cojazzi, G., Fichera, A. M., Panzavolta, S. and Roveri, N. 2000. Structural and mechanical properties of cross-linked drawn gelatin films. *J. Thermal Anal. Calorimetry.* 61: 451–459.
- Bigi, A., Bracci, B., Cojazzi, G., Panzavolta, S. and Roveri, N. 1998. Drawn gelatin films with improved mechanical properties. *Biomaterials.* 19: 2335–2340.
- Binsi, P. K., Shamasundar, B. A., Dileep, A. O., Badii, F. and Howell, N. K. 2009. Rheological and functional properties of gelatin from the skin of Bigeye snapper (*Priacanthus hamrur*) fish: Influence of gelatin on the gel-forming ability of fish mince. *Food Hydrocolloid.* 23: 132-145.
- Bitencourt, C. M., Favaro-Trindade, C. S., Sobral, P. J. A. and Carvalho, R. A. 2014. Gelatin-based films additivated with curcuma ethanol extract: Antioxidant activity and physical properties of films. *Food Hydrocolloid.* 40: 145-152.

- Bonilla, J., Atares, L., Vargas, M. and Chiralt, A. 2012. Edible films and coatings to prevent the detrimental effect of oxygen on food quality: possibilities and limitations. *J. Food Eng.* 110: 208-213.
- Bonner, P. L. R. 2007. *Protein purification*. Taylor & Francis Group. UK.
- Bower, C. K., Avena-bustillos, R. J., Olsen, C. W., McHugh, T. H. and Bechtel, P. J. 2006. Characterisation of fish-skin gelatin gels and films containing the antimicrobial enzyme lysozyme. *J. Food Sci.* 71: 141-145.
- Brinckmann, J. 2005. Collagens at a glance. *Top. Curr. Chem.* 247: 1–6.
- Briston, J. H. 1988. *Plastics Films*. Wiley. NY.
- Buege, J. A. and Aust, S. D. 1978. Microsomal lipid peroxidation. *Method. Enzymol.* 52: 302–310.
- Burnside, S. D. and Giannelis, E. P. 1995. Synthesis and properties of new poly(Dimethylsiloxane) nanocomposites. *Chem. Mater.* 7: 1597-1600.
- Byun, Y., Ward, A. and Whiteside, S. 2012. Formation and characterisation of shellac-hydroxypropyl methylcellulose composite films. *Food Hydrocolloid.* 27: 364-370.
- Byun, Y., Kim, Y. T. and Scott, W. 2010. Characterisation of an antioxidant polylactic acid (PLA) film prepared with  $\alpha$ -tocopherol, BHT and polyethylene glycol using film cast extruder. *J. Food Eng.* 100: 239-244.
- Cao, N., Fu, Y. and He, J. 2007a. Mechanical properties of gelatin films cross-linked, respectively, by ferulic acid and tannin acid. *Food Hydrocolloids.* 21: 575-584.
- Cao, N., Fu, Y. and He, J. 2007b. Preparation and physical properties of soy protein isolate and gelatin composite films. *Food Hydrocolloid.* 21: 1153-1162.

- Carvalho, R. A., Sobral, P. J. A., Thomazine, M., Habitante, A. M. Q. B., Gimenez, B., Gomez-Guillen, M. C. and Montero, P. 2008. Development of edible films based on differently processed Atlantic halibut (*Hippoglossus hippoglossus*) skin gelatin. *Food Hydrocolloid*. 22: 1117-1123.
- Carvalho, R. A. and Grosso, C. R. F. 2004. Characterisation of gelatin based films modified with transglutaminase, glyoxal and formaldehyde. *Food Hydrocolloid*. 18: 717-726.
- Cervera, M. F., Karjalainen, M., Airaksinen, S., Rantanen, J., Krogars, K. and Heinamaki, T. 2004. Physical stability and moisture sorption of aqueous chitosan–amylose starch films plasticised with polyols. *Eur. J. Pharm. Biopharm.* 58: 69–76.
- Chambi, H. and Grosso, C. 2006. Edible films produced with gelatin and casein cross-linked with transglutaminase. *Food Res. Int.* 39: 458–466.
- Chen, L., Ma, L., Zhou, M., Liu, Y. and Zhang, Y. 2014. Effects of pressure on gelatinization of collagen and properties of extracted gelatins. *Food Hydrocolloid*. 36: 316-322.
- Cheow, C. S., Norizah, M. S., Kyaw, Z. Y. and Howell, N. K. 2007. Preparation and characterisation of gelatins from the skins of sin croaker (*Johnius dussumieri*) and shortfin scad (*Decapterus macrosoma*). *Food Chem.* 101: 386-391.
- Chick, J. and Ustunol, Z. 1998. Mechanical and barrier properties of lactic acid and rennet-precipitated casein-based edible films. *J. Food Sci.* 63: 1024-1027.
- Chinabark, K., Benjakul, S. and Prodpran, T. 2007. Effect of pH on the properties of protein-based film from bigeye snapper (*Priacanthus tayenus*) surimi. *Bioresource Technol.* 98: 221-225.



- Chiou, B. S., Avena-Bustillos, R. J., Bechtel, P. J., Jafri, H., Narayan, R., Imam, S. H., Glenn, G. M. and Orts, W. J. 2008. Cold water fish gelatin films: Effects of cross-linking on thermal, mechanical, barrier, and biodegradation properties. *Eur. Polym. J.* 44: 3748-3753.
- Chiou, B. S., Avena-Bustillos, R. J., Shey, J., Yee, E., Bechtel, P. J., Imam, S. H., Glenn, G. M. and Orts, W. J. 2006. Rheological and mechanical properties of cross-linked fish gelatins. *Polymer.* 47: 6379-6386.
- Cho, S. H., Jahncke, M. L., Chin, K. B. and Eun, J. B. 2006. The effect of processing conditions on the properties of gelatin from skate (*Raja Kenojei*) skins. *Food Hydrocolloid.* 20: 810-816.
- Cho, S. M., Gu, Y. S. and Kim, S. B. 2005. Extracting optimisation and physical properties of yellowfin tuna (*Thunnus albacares*) skin gelatin compared to mammalian gelatins. *Food Hydrocolloid.* 19: 221-229.
- Cho, S. M., Kwak, K. S., Park, D. C., Gu, Y. S., Ji, C. I., Jang, D. H., Lee, Y. B. and Kim, S. B. 2004. Processing optimization and functional properties of gelatin from shark (*Isurus oxyrinchus*) cartilage. *Food Hydrocolloid.* 18: 573-579.
- Cientifica Report. 2006. "Nanotechnologies in the Food Industry"; published August 2006. Available: [www.cientifica.com/www/details.php?id=47](http://www.cientifica.com/www/details.php?id=47). Accessed: 24 October 2006.
- Cole, C. G. B. and Roberts, J. J. 1997. Gelatine colour measurement. *Meat Sci.* 45: 23-31.
- Conway, E. J. and Byrne, A. 1936. An absorption apparatus for the micro-determination of certain volatile substances I. The micro-determination of ammonia. *J. Biochem.* 27: 419-429.

- Courts, A. 1961. Structural changes in collagen. *Biochem. J.* 81: 356–365.
- Cuq, B., Gontard, N., Cuq, J. L. and Guilbert, S. 1997. Selected functional properties of fish myofibrillar protein-based films as affected by hydrophilic plasticisers. *J. Agric. Food Chem.* 45: 622-626.
- Cuq, B., Aymad, C., Cuq, J. and Quilbert, S. 1995. Edible packaging films based on fish myofibrillar proteins: formulation and functional properties. *J. Food Sci.* 60: 1369-1373.
- Cyras, V. P., Manfredi, L. B., Ton-That, M. and Vazquez. A. 2008. Physical and mechanical properties of thermoplastic starch/montmorillonite nanocomposite films. *Carbohydr. Polym.* 73: 55–63.
- Damodaran, S. 1997. Protein-stabilized foams and emulsions. *In* Food proteins and their applications (Damodaran. S. and Paraf. A., ed.). p. 57–110. Marcel Dekker Inc. New York.
- D'Arcy, R. L. and Watt, I. C. 1981. Water Actiuity: Influences on food quality. *In* Water vapour sorption isotherms on macromolecular substrates (Rockland, L. B. and Stewart, G. F., ed.). p. 111-142. Academic Press. New York.
- Dawson, P. L., Acton, J. C. and Ogale, A. A. 2002. Biopolymer films and potential applications to meat and poultry products. *Proceedings of the 55th Reciprocal Meat Conference*, pp. 75–81.
- Decker, E. A., Xiong, Y. L., Calvert, J. T., Crum, A. D. and Blanchart, S. P. 1993. Chemical, physical and functional properties of oxidised turkey white muscle myofibrillar proteins. *J. Agric. Food Chem.* 41: 186–189.
- Denavi, G. A., Perez-Mateos, M., Anon, M. C., Montero, P., Mauri, A. N. and Gomez-Guillen, M. C. 2009. Structural and functional properties of soy protein isolate and cod gelatin blend films. *Food Hydrocolloid.* 23: 2094-2101.

- Di, Y., Chang-Feng, C., Bin, W., Guo-Fang, D. and Zhong-Rui, L. 2014. Characterization of acid- and pepsin-soluble collagens from spines and skulls of skipjack tuna (*Katsuwonus pelamis*). *Chin. J. Nat. Med.* 12: 712-720.
- Diak, O. A, Bani-Jaber, A., Amro, B., Jones, D. and Andrews, G. P. 2007. The manufacture and characterization of casein films as novel tablet coatings. *Food Bioprod. Process.* 85: 284-290.
- Donhowe, I. G. and Fenema, O. 1994. *In* Edible coatings and films to improve food quality. (Kroachta, J. M., Baldwin, E. A. and Nisperos-Carriedo, M., eds.). p. 1–25. Technomic Publishing Co. Lancaster.
- Donnelly, T. H. and McGinnis, R. S. 1977. Gelatin manufacture; peroxide liquefaction process. US Patent 40,43,996.
- Doyle, B. B., Blout, E. R. and Bendit, E. G. 1975. Infrared spectroscopy of collagen and collagen like polypeptides. *Biopolymers.* 14: 937–57.
- D'Souza, L., Devi, P., Shridhar, M. P. D. and Naik, C. G. 2008. Use of Fourier transform infrared (FTIR) spectroscopy to study cadmium-induced changes in *Padina tetrastromatica* (Hauck). *Anal. Chem. Insights.* 3: 135–143.
- Duan, R., Zhang, J., Xing, F., Konno, K. and Xu, B. 2011. Study on the properties of gelatins from skin of carp (*Cyprinus carpio*) caught in winter and summer season. *Food Hydrocolloid.* 25: 368-373.
- Duan, R., Zhang, J., Du, X., Yao, X. and Konno, K. 2009. Properties of collagen from skin, scale and bone of carp (*Cyprinus carpio*). *Food Chem.* 112: 702-706.
- Ensminger, L. E. and Giesecking, J. E. 1941. The adsorption of proteins by montmorillonitic clays and its effect on base-exchange capacity. *Soil Sci.* 51: 125–132.

- Eysturskar, J., Haug, I. J., Elharfaoui, N., Djabourov, M. and Draget, K. I. 2009. Structural and mechanical properties of fish gelatin as a function of extraction conditions. *Food Hydrocolloid*. 23: 1702-1711.
- Farahnaky, A., Dadfar, S. M. M. and Shahbazi, M. 2014. Physical and mechanical properties of gelatin-clay nanocomposite. *J. Food Eng.* 122: 78-83.
- Fernandez-Diaz, M. D., Montero, P. and Gomez-Guillen, M. C. 2003. Effect of freezing fish skins on molecular and rheological properties of extracted gelatin. *Food Hydrocolloid*. 17: 281-286.
- Fernandez-Diaz, M. D., Montero, P. and Gomez-Guillen, M. C. 2001. Gel properties of collagens from skins of cod (*Gadus morhua*) and hake (*Merluccius merluccius*) and their modification by the coenhancers magnesium sulphate, glycerol and transglutaminase. *Food Chem.* 74: 161-167.
- Foegeding, E. A., Lanier, T. C. and Hultin, H. O. 1996. Characteristics of Edible Muscle Tissue. *In Food Chemistry*. 3rd ed. (Fennema, O. R., ed.). p. 879-942. Marcel Dekker. New York.
- Fontana, A. J. 2000. Understanding the importance of water activity in food. *Cereal Food. World.* 45: 8-10.
- Fors, S. M. and Olofsson, B. K. 1985. Alkylpyrazines, volatiles formed in the Maillard reaction. I. Determination of odour detection thresholds and odour intensity functions by dynamic olfactometry. *Chem. Sense.* 10: 287-296.
- Fratzl, P. 2008. Structure and Mechanics, an Introduction. *In Collagen, Structure and Mechanics*. (Fratzl, P., ed.). p. 1-12. Springer. New York.
- Fu, Z., Wang, L., Li, D., Wei, Q. and Adhikari, B. 2011. Effects of high-pressure homogenisation on the properties of starch-plasticiser dispersions and their films. *Carbohydr. Polym.* 86: 202-207.

- Fu, X. J., Xu, S. Y. and Wang, Z. 2009. Kinetics of lipid oxidation and off-odor formation in silver carp mince: The effect of lipoxygenase and haemoglobin. *Food Res. Int.* 42: 85–90.
- Ganno, S., Hamano, Y. and Kobayashi, J. 1985. Single-column separation of aminoethylcysteine other amino acids. *J. Chromatogr. A.* 332: 275-282.
- Gennadios, A., Hanna, M. A. and Kurth, L. B. 1997. Application of edible coatings on meats, poultry and seafoods: a review. *LWT- Food Sci. Technol.* 30: 337-350.
- Gennadios, A., Weller, C. L., Hanna, M. A. and Froning, G. W. 1996. Mechanical and barrier properties of egg albumen films. *J. Food Sci.* 61: 585-589.
- Gennadios, A., Brandenburg, A. H., Park, J. W., Weller, C. L. and Testin, R. F. 1994. Water vapor permeability of wheat gluten and soy protein isolate films. *Ind. Crop. Prod.* 2: 189-195.
- Gennadios, A., Brandenburg, A. H., Weller, C. L. and Testin, R. F. 1993. Effect of pH on properties of wheat gluten and soy protein isolate films. *J. Agric. Food Chem.* 41: 1835–1839.
- Ghanbarzadeh, B. and Oromiehi, A. R. 2009. Thermal and mechanical behavior of laminated protein films. *J. Food Eng.* 90: 517-524.
- Gilsenan, P. M. and Ross Murphy, S. B. 2000. Viscoelasticity and thermoreversible gelatin gels from animal and piscine collagens. *J. Rheol.* 44: 871-883.
- Gimenez, B., Gomez-Guillen, M.C., Perez-Mateos, M., Montero, P. and Marquez-Ruiz, G. 2011. Evaluation of lipid oxidation in horse mackerel patties covered with borage-containing film during frozen storage. *Food Chem.* 124: 1393-1403.

- Gimenez, B., Gomez-Estaca, J., Aleman, A., Gomez-Guillen, M. C. and Montero, M. P. 2009a. Improvement of the antioxidant properties of squid skin gelatin films by the addition of hydrolysates from squid gelatin. *Food Hydrocolloid*. 23: 1322-1327.
- Gimenez, B., Gomez-Estaca, J., Aleman, A., Gomez-Guillen, M. C. and Montero, M. P. 2009b. Physico-chemical and film forming properties of giant squid (*Dosidicus gigas*) gelatin. *Food Hydrocolloid*. 23: 585-592.
- Gimenez, B., Aleman, A., Montero, P. and Gomez-Guillen, C. 2009c. Antioxidant and functional properties of gelatin hydrolysates obtained from skin of sole and squid. *Food Chem*. 114: 976–983.
- Gimenez, B., Gomez-Guillen, M. C. and Montero, P. 2005a. The role of salt washing of fish skins in chemical and rheological properties of gelatin extracted. *Food Hydrocolloid*. 19: 951-957.
- Gimenez, B., Turnay, J., Lizarbe, M. A., Montero, P., and Gomez-Guillen, M. C. 2005b. Use of lactic acid for extraction of fish skin gelatin. *Food Hydrocolloid*. 19: 941-950.
- Girand, B. and Durance, T. 2000. Headspace volatiles of sockeye and pink salmon as affected by retort process. *J. Food Sci*. 65: 34–39.
- GME. 2005. Standard Methods for the Testing of Edible Gelatine, *Gelatine Monograph*, Gelatin Manufacturers of Europe.
- Goldschmid, O. 1971. *In* Lignins: Occurrence, formation, structure and reactions. (Sarkanen, K. V. and Ludwig. C. H., eds.). p. 259. Wiley-Interscience. New York.

- Gomez-Estaca, J., Lopez-de-Dicastillo, C., Hernandez-Munoz, P., Catala, R. and Gavara, R. 2014. Advances in antioxidant active food packaging. *Trends Food Sci. Tech.* 35: 42-51.
- Gomez-Estaca, J., Gomez-Guillen, M. C., Fernandez-Martin, F. and Montero, P. 2011. Effects of gelatin origin, bovine-hide and tuna-skin, on the properties of compound gelatin–chitosan films. *Food Hydrocolloid.* 25: 1461–1469.
- Gomez-Estaca, J., Lopez de Lacey, A., Lopez-Caballero, M. E., Gomez-Guillen, M. C. and Montero, P. 2010. Biodegradable gelatin-chitosan films incorporated with essential oils as antimicrobial agents for fish preservation. *Food Microbiol.* 27: 889–896.
- Gomez-Estaca, J., Bravo, L., Gomez-Guillen, M. C., Aleman, A. and Montero, P. 2009a. Antioxidant properties of tuna-skin and bovine-hide gelatin films induced by the addition of oregano and rosemary extracts. *Food Chem.* 112: 18-25.
- Gomez-Estaca, J., Montero, P., Fernandez-Martin, F., Aleman, A. and Gomez-Guillen, M. C. 2009b. Physical and chemical properties of tuna-skin and bovinehide gelatin films with added aqueous oregano and rosemary extracts. *Food Hydrocolloid.* 23: 1334-1341.
- Gomez-Estaca, J., Gimenez, B., Montero, P. and Gomez-Guillen, M. C. 2009c. Incorporation of antioxidant borage extract into edible films based on sole skin gelatin or a commercial fish gelatin. *J. Food Eng.* 92: 78-85.
- Gomez-Estaca, J., Montero, P., Gimenez, B. and Gomez-Guillen, M. C. 2007. Effect of functional edible films and high pressure processing on microbial and oxidative spoilage in cold-smoked sardine (*Sardina pilchardus*). *Food Chem.* 105: 511–520.

- Gomez-Guillen, M. C., Porez-Mateos, M., Gomez-Estaca, J., Lopez-Caballero, E., Gimenez, B., Montero, P., 2009. Fish gelatin: a renewable material for developing active biodegradable films. *Trends Food Sci. Technol.* 20, 3–16.
- Gomez-Guillen, M. C., Ihl, M., Bifani, V., Silva, A. and Montero, P. 2007. Edible films made from tuna-fish gelatin with antioxidant extracts of two different murta ecotypes leaves (*Ugni molinae Turcz.*). *Food Hydrocolloid.* 21: 1133–1143.
- Gomez-Guillen, M. C., Gimenez, B., and Montero, P. 2005. Extraction of gelatin from fish skins by high pressure treatment. *Food Hydrocolloid.* 19: 923-928.
- Gomez-Guillen, M. C., Turnay, J., Fernandez-Diaz, M. D., Ulmo, N., Lizarbe, M. A. and Montero, P. 2002. Structural and physical properties of gelatin extracted from different marine species: a comparative study. *Food Hydrocolloid.* 16: 25–34.
- Gomez-Guillen, M. C. and Montero, P. 2001. Extraction of gelatin from megrim (*Lepidorhombus boscii*) skins with several organic acids. *J. Food Sci.* 66: 213-216.
- Gontard, N., Thibault, R., Cuq, B. and Guilbert, S. 1996. Influence of relative humidity and film composition on oxygen and carbon dioxide permeabilities of edible films. *J. Agric. Food Chem.* 44: 1064–1069.
- Gontard, N., Guilbert, S. and Cuq, J. L. 1993. Water and glycerol as plasticizers affect mechanical and water vapor barrier properties of an edible wheat gluten film. *J. Food Sci.* 58: 206-211.
- Grevellec, J. I., Marquie, C., Ferry, L., Crespy, A. and Vialettes, V. 2001. Processability of cottonseed proteins into biodegradable materials. *Biomacromolecules.* 2: 1104–1109.



- Grosch, W. 1987. Low-MW products of hydroperoxide reactions. *In* Autoxidation of unsaturated lipids (Chan, H. W. S., ed.). p. 95-139. Academic Press. London.
- Gudmundsson. 2002. Rheological properties of fish gelatin. *J. Food Sci.* 67, 2172–2176.
- Gudmundsson, M. and Hafsteinsson, H. 1997. Gelatin from cod skins as affected by chemical treatment. *J. Food Sci.* 62: 37-47.
- Guenther, E. 1948. *The Essential Oils*. D. Van Nostrand. New York.
- Guerrero, P., Retegi, A., Gabilondo, N. and de-la-Caba, K. 2010. Mechanical and thermal properties of soy protein films processed by casting and compression. *J. Food Eng.* 100: 145-151.
- Guilbert, S., Cuq, B. and Gontard, N. 1997. Recent innovations in edible and/or biodegradable packaging materials. *Food Add. Contam.* 14: 741-751.
- Guilbert, S. and Gontard, N. 1995. Edible and biodegradable food packaging. *In* Foods and packaging materials-chemical interactions. (Ackermann, P. et al., eds.). p. 159-168. The Royal Society of Chemistry. Cambridge, England.
- Gutierrez, M. Q., Echeverria, I., Ihl, M., Bifani, V. and Mauri, A.N., 2012. Carboxymethylcellulose–montmorillonite nanocomposite films activated with murta (*Ugni molinae Turcz*) leaves extract. *Carbohydr. Polym.* 87: 1495– 1502.
- Hagermen, A. E. 1992. Tanin-protein interactions. *In* Phenolic compounds in food and their effects on health. I-Analysis, occurrence and chemistry (Ho, P., Lee, C. Y. and Huang, M. T. ed.). p. 237-247. American Chemical Society. Washington, DC.
- Halling, P. J. 1981. Protein stabilized foams and emulsions. *Crit. Rev. Food Sci.* 12: 155–203.

- Hamaguchi, P. Y., Yin, W. W. and Tanaka, M. 2007. Effect of pH on the formation of edible films made from the muscle proteins of Blue marlin (*Makaira mazara*). *Food Chem.* 100: 914-920.
- Han, J. H., Aristippos, G. and Jung, H. H. 2005. Edible films and coatings: A review. *In Innovations in Food Packaging*, p. 239-262. Academic Press. London.
- Han, J. H. and Floros, J. D. 1997. Casting antimicrobial packaging films and measuring their physical properties and antimicrobial activity. *J. Plast. Film Sheet.* 13: 287–298.
- Han, J. H. and Krochta, J. M. 1999. Water vapor permeability and wetting properties of whey protein coating on paper. *AM. Soc. Agric. Engineer.* 42: 1375–1382.
- Hanani, Z. A. N, Roos, Y. H. and Kerry, J. P. 2012. Use of beef, pork and fish gelatin sources in the manufacture of films and assessment of their composition and mechanical properties. *Food Hydrocolloid.* 29: 144-151.
- Hao, S., Li, L., Yang, X., Cen, J., Shi, H., Bo, Q. and He, J. 2009. The characteristics of gelatin extracted from sturgeon (*Acipenser baeri*) skin using various pretreatments. *Food Chem.* 115: 124-128.
- Haslam, E. 1998. Practical polyphenolics. From structure to molecular recognition and physiological action. Cambridge University Press. Cambridge.
- Haug, I. J., Draget, K. I. and Smidsrod, O. 2004. Physical and rheological properties of fish gelatin compared to animal gelatin. *Food Hydrocolloid.* 18: 203-213.
- Hawkins, C. L. and Davies, M. J. 1997. Oxidative damage to collagen and related substrates by metal ion/hydrogen peroxide systems: random attack or site-specific damage?. *BBA.* 1360: 84-96.

- Heng, P. W. S., Chan, L. W. and Ong, K. T. 2003. Influence of storage conditions and type of plasticizers on ethylcellulose and acrylate films formed from aqueous dispersions. *J. Pharm. Pharm. Sci.* 6: 334-344.
- Henning, S., Metz, R. and Hammes, W. 1986. New aspects for the application of nisin to food products based on its mode of action. *Int. J. Food Microbiol.* 3: 135–141.
- Holzer, D. 1996. “Gelatin production” U.S. Pat. 5, 484,888.
- Hoque, M. S., Benjakul, S. and Prodpran, T. 2011a. Effects of partial hydrolysis and plasticiser content on the properties of film from cuttlefish (*Sepia pharaonis*) skin gelatin. *Food Hydrocolloid.* 25: 82-90.
- Hoque, M. S., Benjakul, S. and Prodpran, T. 2011b. Effects of hydrogen peroxide and Fenton’s reagent on the properties of film from cuttlefish (*Sepia pharaonis*) skin gelatin. *Food Chem.* 128: 878-888.
- Hoque, M. S., Benjakul, S. and Prodpran, T. 2011c. Properties of film from cuttlefish (*Sepia pharaonis*) skin gelatin incorporated with cinnamon, clove and star anise extracts. *Food Hydrocolloid.* 25: 1085-1097.
- Hoque, M. S., Benjakul, S., Prodpran, T. and Songtipya, P. 2011d. Properties of blend film based on cuttlefish (*Sepia pharaonis*) skin gelatin and mungbean protein isolate. *Int. J. Biol. Macromol.* 49: 663–673.
- Hoque, M. S., Benjakul, S. and Prodpran, T. 2010. Effect of heat treatment of film forming solution on the properties of film from cuttlefish (*Sepia pharaonis*) skin gelatin. *J. Food Eng.* 96: 66-73.
- Huang, Y.-R., Shiau, C.-Y., Chen, H.-H. and Huang, B.-C. 2011. Isolation and characterization of acid and pepsin-solubilized collagens from the skin of balloon fish (*Diodon holocanthus*). *Food Hydrocolloid.* 25: 1507-1513.

- Iglesias, J. and Medina, I. 2008. Solid-phase microextraction method for the determination of volatile compounds associated to oxidation of fish muscle. *J. Chromatograph.* 1192A: 9–16.
- Ikoma, T., Kobayashi, H., Tanaka, J., Walsh, D. and Mann, S. 2003. Physical properties of Type I collagen extracted from fish scales of *Pagrus major* and *Oreochromis nilotica*. *Int. J. Biol. Macromol.* 32: 199-204.
- Intarasirisawat, R., Benjakul, S., Visessanguan, W., Prodpran, T., Tanaka, M. and Howell, N. K. 2007. Autolysis study of bigeye snapper (*Priacanthus macracanthus*) skin and its effect on gelatin. *Food Hydrocolloid.* 21: 537-544.
- Iwata, K. I., Ishizaki, S. H., Handa, A. K. and Tanaka, M. U. 2000. Preparation and characterisation of edible films from fish water-soluble proteins. *Fish. Sci.* 66: 372–378.
- Jackson, M., Choo, L. P., Watson, P. H., Halliday, W. C. and Mantsch, H. H. 1995. Beware of connective tissue proteins: assignment and implications of collagen absorptions in infrared spectra of human tissues. *BBA-Mol. Basis Dis.* 1270, 1–6.
- Jamilah, B., Tan, K. W., Umi Hartina, M. R. and Azizah, A. 2011. Gelatins from three cultured freshwater fish skins obtained by liming process. *Food Hydrocolloid.* 25: 1256-1260.
- Jamilah, B. and Harvinder, K. G. 2002. Properties of gelatins from skins of fish–black tilapia (*Oreochromis mossambicus*) and red tilapia (*Oreochromis nilotica*). *Food Chem.* 77: 81–84.
- Jang, S. A., Shin, Y. J., Seo, Y. B. and Song, K. B. 2011. Effects of various plasticisers and nanoclays on the mechanical properties of red algae film. *J. Food Sci.* 76: N30-N34.

- Jeevithan, E., Wu, W., Nanping, W., Lan, H. and Bao, B. 2014. Isolation, purification and characterization of pepsin soluble collagen isolated from silvertip shark (*Carcharhinus albimarginatus*) skeletal and head bone. *Process Biochem.* 49: 1767–1777.
- Jellouli, K., Balti, R., Bougatef, A., Hmidet, N., Barkia, A. and Nasri, M. 2011. Chemical composition and characteristics of skin gelatin from grey triggerfish (*Balistes capriscus*). *LWT-Food Sci. Technol.* 44: 1965-1970.
- Jo, C., Kang, H., Lee, N. Y., Kwon, J. H. and Byun, M. W. 2005. Pectin- and gelatin-based film: effect of gamma irradiation on the mechanical properties and biodegradation. *Rad. Phys. Chem.* 72: 745-750.
- Johnston-Banks, F. A. 1990. Gelatin. *In Food gels.* (Harris, P., ed.). p. 233-289. Elsevier Applied Science. London.
- Jones, N. R. 1977. Uses of gelatin in edible products. *In The science and technology of gelatins* (Ward, A. G. and Courts., A., ed.). p. 365-394. Academic Press. New York.
- Jongjareonrak, A., Rawdkuen, S., Chaijan, M., Benjakul, S., Osako, K. and Tanaka, M. 2010. Chemical compositions and characterisation of skin gelatin from farmed giant catfish (*Pangasianodon gigas*). *LWT-Food Sci. Technol.* 43: 161-165.
- Jongjareonrak, A., Benjakul, S., Visessanguan, W. and Tanaka, M. 2008. Antioxidant activity and properties of skin gelatin films incorporated with BHT and  $\alpha$ -tocopherol. *Food Hydrocolloid.* 22: 449–458.

- Jongjareonrak, A., Benjakul, S., Visessanguan, W. and Tanaka, M. 2006a. Skin gelatin from bigeye snapper and brownstripe red snapper: Chemical compositions and effect of microbial transglutaminase on gel properties. *Food Hydrocolloid*. 20: 1216-1222.
- Jongjareonrak, A., Benjakul, S., Visessanguan, W., Prodpran, T. and Tanaka, M. 2006b. Characterisation of edible films from skin gelatin of brownstripe red snapper and bigeye snapper. *Food Hydrocolloid*. 20: 492–501.
- Jorge, M. F. C., Flaker, C. H. C., Nassar, S. F., Moraes, I. C. F., Bittante, A. M. Q. B. and Sobral, P. J. d. A. 2014. Viscoelastic and rheological properties of nanocomposite-forming solutions based on gelatin and montmorillonite. *J. Food Eng.* 120: 81–87.
- Jorge, M. F. C., Vanin, F. M., Carvalho, R. A. d, Moraes, I. C. F., Bittante, A. M. Q. B., Nassar, S. F. and Sobral, P. J. d. A. 2011. Mechanical properties of gelatin nanocomposite films prepared by spreading: effect of montmorillonite concentration. *International Congress on Engineering and Food. ICEF11 Publications. Greece.*
- Josephson, D. B., Lindsay, R. C. and Stuibler, D. A. 1984. Variation in the occurrences of enzymatically derived volatile aroma compounds in salt and freshwater fish. *J. Agric. Food Chem.* 32. 1344–1347.
- Jridi, M., Hajji, S., Ayed, H. B., Lassoued, I., Mbarek, A., Kammoun, M., Souissi, N. and Nasri, M. 2014. Physical, structural, antioxidant and antimicrobial properties of gelatin–chitosan composite edible films. *Int. J. Biol. Macromol.* 67: 373–379.

- Jridi, M., Lassoued, I., Kammoun, A., Nasri, R., Chaabouni, M., Nasri, M. and Souissi, N. 2014b. Screening of factors influencing the extraction of gelatin from the skin of cuttlefish using supersaturated design. *Food Bioprod. Process.* DOI: <http://dx.doi.org/10.1016/j.fbp.2014.07.010>.
- Jung, D., Bodyfelt, F. and Daeschel, M. 1992. Influence of fat emulsifiers on the efficacy of nisin in inhibiting *Listeria monocytogenes* in fluid milk. *J. Dairy Sci.* 75: 387–393.
- Kaewruang, P., Benjakul, S. and Prodpran, T. 2014. Effect of phosphorylation on gel properties of gelatin from the skin of unicorn leatherjacket. *Food Hydrocolloid.* 35: 694-699.
- Kaewruang, P., Benjakul, S. and Prodpran, T. 2013. Molecular and functional properties of gelatin from the skin of unicorn leatherjacket as affected by extracting temperatures. *Food Chem.* 138: 1431–1437.
- Karayannakidis, P. D. and Zotos, A. 2014. Physicochemical properties of yellowfin tuna (*Thunnus albacares*) skin gelatin and its modification by the addition of various coenhancers. *J. Food Process. Pres.* DOI: 10.1111/jfpp.12258.
- Karim, A. A. and Bhat, R. 2009. Fish gelatin: properties, challenges, and prospects as an alternative to mammalian gelatins. *Food Hydrocolloid.* 23: 563-576.
- Kasankala, L. M., Xue, Y., Weilong, Y., Hong, S. D. and He, Q. 2007. Optimisation of gelatin extraction from grass carp (*Ctenopharyngodon idella*) fish skin by response surface methodology. *Biores. Technol.* 98: 3338-3343.
- Kavoosi, G., Dadfar, S. M. M., Purfard, A. M. and Mehrabi, R. 2013. Antioxidant and antibacterial properties of gelatin films incorporated with carvacrol. *J. Food Safety.* 33: 423–432.

- Kellard, B., Busfield, D. M. and Kinderlerer, J. L. 1985. Volatile off-flavour compounds in desiccated coconut. *J. Sci. Food Agric.* 36: 415-420.
- Kim, Y.T. 2005. Development and characterization of gelatin film as active packaging layer. Clemson University. Clemson.
- Kim, J. S. and Park, J. W. 2005. Partially purified collagen from refiner discharge of Pacific Whiting surimi processing. *J. Food Sci.* 70: C511–C516.
- Kimura, S., Zhu, X., Matsui, R., Shijoh, M. and Takamizawa, S. 1988. Characterisation of fish muscle Type I collagen. *J. Food Sci.* 53: 1315-1318.
- Kinsella, J. E. 1979. Functional properties of soy proteins. *J. Am. Oil Chem. Soc.* 56: 242-258.
- Kittiphattanabawon, P., Benjakul, S., Visessanguan, W. and Shahidi, F. 2012. Cryoprotective effect of gelatin hydrolysate from blacktip shark skin on surimi subjected to different freeze-thaw cycles. *LWT-Food Sci. Technol.* 47: 437-442.
- Kittiphattanabawon, P., Benjakul, S., Visessanguan, W., Kishimura, H. and Shahidi, F. 2010a. Isolation and characterisation of collagen from the skin of brownbanded bamboo shark (*Chiloscyllium punctatum*). *Food Chem.* 119: 1519-1526.
- Kittiphattanabawon, P., Benjakul, S., Visessanguan, W. and Shahidi, F. 2010b. Comparative study on characteristics of gelatin from the skins of brownbanded bamboo shark and blacktip shark as affected by extraction conditions. *Food Hydrocolloid.* 24: 164–171.



- Kocha, T., Yamaguchi, M., Ohtaki, H., Fukuda, T. and Aoyagi, T. 1997. Hydrogen peroxide-mediated degradation of protein: Different oxidation modes of copper- and iron-dependent hydroxyl radicals on the degradation of albumin. *BBA-Protein Struct. M.* 1337: 319–326.
- Koh, M. J., Hwang, H. Y., Kim, D. J., Kim, H. J., Hong, Y. T. and Nam, S. Y. 2010. Preparation and characterization of porous PVdF-HFP/clay nanocomposite membranes. *J. Mater. Sci. Technol.* 26: 633-638.
- Koli, J. M., Basu, S., Kannuchamy, N. and Gudipati, V. 2013. Effect of pH and ionic strength on functional properties of fish gelatin in comparison to mammalian gelatin. *Fishery Technol.* 50: 126–132.
- Koli, J. M., Basu, S., Nayak, B. B., Surendra B. Patange, S. B., Pagarkar, A.U. and Gudipati, V. 2012. Functional characteristics of gelatin extracted from skin and bone of Tiger-toothed croaker (*Otolithes ruber*) and Pink perch (*Nemipterus japonicus*). *Food Biopro. Proc.* 90: 555-562.
- Kolodziejska, I., Skierka, E., Sadowska, M., Kolodziejski, W. and Niecikowska, C. 2008. Effect of extracting time and temperature on yield of gelatin from different fish offal. *Food Chem.* 107: 700-706.
- Kolodziejska, I., Piotrowska, B., Bulge, M. and Tylingo, R. 2006. Effect of transglutaminase and 1-ethyl-3-(3-dimethylaminopropyl) carbodiimide on the solubility of fish gelatin–chitosan films. *Carbohydr. Polym.* 65: 404–409.
- Kolodziejska, I., Kaczorowski, K., Piotrowsia, B. and Sadowska, M. 2004. Modification of properties of gelatin from skins of Baltic cod (*Gadus morhua*) with transglutaminase. *Food Chem.* 86: 203-209.

- Kolodziejska, I., Sikorski, Z. E. and Niecikowska, C. 1999. Parameters affecting the isolation of collagen from squid (*Illex argentinus*) skin. *Food Chem.* 66: 153–157.
- Krishna, M., Nindo, C. I. and Min, S. C. 2012. Development of fish gelatin edible films using extrusion and compression molding. *J. Food Eng.* 108: 337–344.
- Krochta, J. M. 2002. Protein as raw materials for films and coatings: definitions, current status, and opportunities. *In Protein-Based Films and Coating* (Gennadios, A., ed.). p. 1-39. CRC Press. New York.
- Krochta, J. M., Baldwin, E. A. and Nisperos-Carriedo, M. O. 1994. Edible coatings and films to improve food quality. Technomic Publishing. Lancaster, PA.
- Ktari, N., Jridi, M., Nasri, R., Lassoued, I., Ayed, H. B., Barkia, A. and Nasri, M. 2014. Characteristics and functional properties of gelatin from zebra blenny (*Salaria basilisca*) skin. *LWT-Food Sci. Technol.* 58: 602-608.
- Kubow, S. 1992. Routes of formation and toxic consequences of lipid oxidation in foods. *Free Radical Bio. Med.* 12: 63–81.
- Kumar, P., Sandeep, K. P., Alavi, S., Truong, V. D. and Gorga, R. E. 2010. Preparation and characterisation of bio-nanocomposite films based on soy protein isolate and montmorillonite using melt extrusion. *J. Food Eng.* 100: 480–489.
- Kwak, K., Cho, S., Ji, C., Lee, Y. and Kim, S. 2009. Changes in functional properties of shark (*Isurus oxyrinchus*) cartilage gelatin produced by different drying methods. *I. J. Food Sci. Technol.* 44: 1480-1484.
- Laemmli, U. K. 1970. Cleavage of structural proteins during assembly of head of bacteriophage T4. *Nature.* 227: 680-685.

- Langmaier, F., Mokrejs, P., Kolomaznik, K. and Mladek, M. 2008. Plasticising collagen hydrolysate with glycerol and low-molecular weight poly(ethylene glycols). *Thermochim. Acta.* 469: 52-58.
- Lassoued, I., Jridi, M., Nasri, R., Dammak, A., Hajji, M., Nasri, M. and Barkia, A. 2014. Characteristics and functional properties of gelatin from thornback ray skin obtained by pepsin-aided process in comparison with commercial halal bovine gelatin. *Food Hydrocolloid.* 41: 309-318.
- LeBaron, P. C., Wang, Z. and Pinnavaia, T. J. 1999. Polymer-layered silicate nanocomposites: an overview. *Appl. Clay Sci.* 15: 11-29.
- Ledward, D. A. 1986. Gelation of gelatin. *In Functional Properties of Food Macromolecules* (Mitchell, J. R. and Ledward, D. A. eds.). p. 171-201. Elsevier Applied Science Publishers. London.
- Lehninger, A. L. 1982. Fibrous proteins. *In Principles of Biochemistry.* (Lehninger, A. L., ed.). p. 147-168. CBS Publishers and Distributors Pvt. Ltd., New Delhi, India.
- Levine, R. L., Garland, D., Oliver, C. N., Amici, A., Climent, I., Lenz, A. G., Ahn, B. W., Shaltiel, S. and Stadtman, E. R. 1990. Determination of carbonyl content in oxidatively modified proteins. *Method. Enzymol.* 186, 464-478.
- Lewis, M. S. and Piez, K. A. 1964. The characterisation of collagen from the skin of the dogfish shark, *Squalus acanthias*. *J. Biol. Chem.* 239: 3336-3340.
- Li, J., Miao, J., Wu, J., Chen, S. and Zhang, Q. 2014. Preparation and characterisation of active gelatin-based films incorporated with natural antioxidants. *Food Hydrocolloid.* 37: 166-173.

- Li, Z.-R., Wang, B., Chi, C.-F., Zhang, Q.-H., Gong, Y.-D., Tang, J.-J., Luo, H.-Y. and Ding, G.-F. 2013. Isolation and characterization of acid soluble collagens and pepsin soluble collagens from the skin and bone of Spanish mackerel (*Scomberomorus niphonius*). Food Hydrocolloid. 31: 103-113.
- Li, P., Zheng, J. P., Ma, Y. L. and Yao, K. D. 2003. Gelatin/montmorillonite hybrid nanocomposite. II. Swelling behavior. J. Appl. Polym. Sci. 88: 322-326.
- Liang, Q., Wang, L., Sun, W., Wang, Z., Xu, J. and Ma, H. 2014. Isolation and characterization of collagen from the cartilage of Amur sturgeon (*Acipenser schrenckii*). Process Biochem. 49: 318–323.
- Lim, G., Jang, S. and Song, K. Physical and antimicrobial properties of *Gelidium corneum*/nano-clay composite film containing grapefruit seed extract or thymol. J. Food Eng. 98: 415–420.
- Limpisophon, K., Tanaka, M. and Osako, K. 2010. Characterisation of gelatin–fatty acid emulsion films based on blue shark (*Prionace glauca*) skin gelatin. Food Chem. 122, 1095–1101.
- Limpisophon, K., Tanaka, M., Weng, W., Abe, S. and Osako, K. 2009. Characterisation of gelatin films prepared from under-utilized blue shark (*Prionace glauca*) skin. Food Hydrocolloid. 23: 1993-2000.
- Liu, D., Wei, G., Li, T., Hu, J., Lu, N., Regenstein, J. M. and Zhou, P. 2015. Effects of alkaline pretreatments and acid extraction conditions on the acid-soluble collagen from grass carp (*Ctenopharyngodon idella*) skin. Food Chem. 172: 836–843.

- Liu, D., Liang, L., Regenstein, J. M. and Zhou, P. 2012. Extraction and characterisation of pepsin-solubilised collagen from fins, scales, skins, bones and swim bladders of bighead carp (*Hypophthalmichthys nobilis*). Food Chem. 133: 1441-1448.
- Liu, H. Y., Han, J. and Guo, S. D. 2009. Characteristics of the gelatin extracted from Channel Catfish (*Ictalurus Punctatus*) head bones. LWT-Food Sci. Technol. 42: 540–544.
- Liu, H. Y., Li, D. and Guo, S. D. 2008a. Extraction and properties of gelatin from channel catfish (*Ictalurus punctatus*) skin. LWT - Food Sci. Technol. 41: 414-419.
- Liu, L. S., Jin, T., Liu, C. K., Hicks, K., Mohanty, A. K., Bhardwal, R. and Misra, M. 2008b. A preliminary study on antimicrobial edible films from pectin and other food hydrocolloid by extrusion method. J. Nat. Fibre. 5: 366–382.
- Liu, H., Li, D. and Guo, S. 2007. Studies on collagen from the skin of channel catfish (*Ictalurus punctatus*). Food Chem. 101: 621-625.
- Liu, T. X., Liu, Z. H., Ma, K. X., Shen, L. Zeng, K. Y. and He, C. B. 2003. Compos. Sci. Technol. 63: 331.
- Liu, G. and Xiong, Y. L. 2000a. Oxidatively induced chemical changes and interactions of mixed myosin,  $\beta$ -lactoglobulin and soy 7S globulin. J. Sci. Food Agric. 80: 1601–1607.
- Liu, G. and Xiong, Y. L. 2000b. Electrophoretic pattern, thermal denaturation, and *in vitro* digestibility of oxidized myosin. J. Agric. Food Chem. 48: 624–630.
- Liu, D. and Zhang, L. 2006. Structure and properties of soy protein plastics plasticised with acetamide. Macromol. Mater. Eng. 291: 820–828.

- Liu, J., Xu, G., Yuan, S. and Jiang, P. 2003. The effect of macromolecules on foam stability in sodium dodecyl sulfate/cetylpyridinium bromide mixtures. *J. Disper. Sci. Technol.* 24: 779–787.
- Lopez-De-Dicastillo, C., Gomez-Estaca, J., Catala, R., Gavara, R. and Hernandez-Munoz, P. 2012. Active antioxidant packaging films: development and effect on lipid stability of brined sardines. *Food Chem.* 131: 1376-1384.
- Lopez-Caballero, M. E., Martinez-Alvarez, O., Gomez-Guillen, M. C. and Montero, P. 2007. Quality of thawed deepwater pink shrimp (*Parapenaeus longirostris*) treated with melanosis-inhibiting formulations during chilled storage. *Int. J. Food Sci. Tech.* 42: 1029–1038.
- Ma, W., Tang, C., Yin, S., Yang, X., Qi, J. and Xia, N. 2012. Effect of homogenisation conditions on properties of gelatin–olive oil composite films. *J. Food Eng.* 113: 136–142.
- Majdzadeh-Ardakani, K., Navarchian, A. H. and Sadeghi., F. 2010. Optimization of mechanical properties of thermoplastic starch/clay nanocomposites. *Carbohydr. Polym.* 79: 547–554.
- Martins, C. G., Larocca, N. M., Paul, D. R. and Pessan, L. A. 2009. Nanocomposites formed from polypropylene/EVA blends. *Polymer.* 50: 1743–1754.
- Martucci, J. F. and Ruseckaite, R. A. 2010a. Biodegradable bovine gelatin/Na<sup>+</sup> montmorillonite nanocomposite films. structure, barrier and dynamic mechanical properties. *Polymer-Plast. Technol. Eng.* 49: 581-588.
- Martucci, J. F. and Ruseckaite, R. A. 2010b. Biodegradable three-layer film derived from bovine gelatin. *J Food Eng.* 99: 377–383.

- Martucci, J. F. and Ruseckaite, R. A. 2009. Biodegradation of three-layer laminate films based on gelatin under indoor soil conditions. *Polym. Degrad. Stabil.* 94: 1307–1313.
- Martucci, J. F. 2008. Structure–properties relationship in materials based on gelatin. Doctoral Thesis, Universidad Nacional de Mar del Plata, Argentina.
- Martucci, J. F. and Ruseckaite, R. A. 2008. Structure and properties of gelatine/montmorillonite nanocomposite films. *In* Recent Advances in Research on Biodegradable Polymers and Sustainable Polymers. (Jimenez, A. and Zaikov, G. E., ed.). p. 27–36. Nova Publishers. NY.
- Martucci, J. F., Vazquez, A. and Ruseckaite, R. A. 2007. Nanocomposites based on gelatin and montmorillonite: morphological and thermal studies. *J. Therm. Anal. Calorim.* 89: 117-122.
- Mathew, S. 2002. Fish Collagens. CIFT Technology Advisory Series: 8. Agricultural Technology Information Centre. CIFT, Kochi, India.
- McGlashan, S. A. and Halley, P. J. 2003. Preparation and characterisation of biodegradable starch-based nanocomposite materials. *Polym. Int.* 52: 1767–1773.
- McHugh, T. H. and Krochta, J. M. 1994. Milk protein based edible film and coatings. *Food Technol.* 48: 97-103.
- Mclaren, A. D., Peterson, G. H. and Barshad, I. 1958. The adsorption and reactions of enzymes and proteins on clay minerals. IV. Kaolinite and montmorillonite. *Soil Sci. Soc. AM. Proc.* 22: 239–244.
- Meilgaard, M., Civille, G. V. and Carr, B. T. 2007. Sensory evaluation techniques. CRC Press. Florida.

- Mihara, S. and Masuda, H. 1988. Structure-odor relationships for disubstituted pyrazines. *J. Agric. Food Chem.* 36: 1242–1247.
- Mine, Y. 1995. Recent advances in the understanding of egg white protein functionality. *Trend. Food Sci. Technol.* 6: 225-232.
- Montero, P. and Gomez-Guillen, M. C. 2000. Extracting conditions for megrim (*Lepidorhombus boscii*) skin collagen affect functional properties of the resulting gelatin. *J. Food Sci.* 65: 434-438.
- Morales, J., Moral, A. and Montero, P. 2000. Isolation and partial characterization of two types of muscle collagen in some cephalopods. *J. Agric. Food Chem.* 211: 2142–2148.
- Muyonga, J. H., Cole, C. G. B. and Duodu, K. G. 2004a. Characterisation of acid soluble collagen from skins of young and adult Nile perch (*Lates niloticus*). *Food Chem.* 85: 81–89.
- Muyonga, J. H., Cole, C. G. B. and Duodu, K. G. 2004b. Extraction and physico-chemical characterisation of Nile perch (*Lates niloticus*) skin and bone gelatin. *Food Hydrocolloid.* 18: 581-592.
- Muyonga, J. H., Cole, C. G. B. and Duodu, K. G. 2004c. Fourier transform infrared (FTIR) spectroscopic study of acid soluble collagen and gelatin from skins and bones of young and adult Nile perch (*Lates niloticus*). *Food Chem.* 86: 325–333.
- Nagai, T. and Suzuki, N. 2000. Isolation of collagen from fish waste material- skin, bone and fins. *Food Chem.* 68: 277-281.
- Nagarajan, M., Benjakul, S., Prodpran, T. and Songtipya, P. 2014a. Characteristics of bio-nanocomposite films from tilapia skin gelatin incorporated with hydrophilic and hydrophobic nanoclays. *J. Food Eng.* 143: 195-204.



- Nagarajan, M., Benjakul, S., Prodpran, T. and Songtipya, P. 2014b. Properties of bio-nanocomposite films from tilapia skin gelatin as affected by different nanoclays and homogenising conditions. *Food Bioprocess Tech.* 7: 3269-3281.
- Nagarajan, M., Benjakul, S., Prodpran, T. and Songtipya, P. 2014c. Properties and characteristics of nanocomposite films from tilapia skin gelatin incorporated with ethanolic extract from coconut husk. *J. Agric. Food Chem.* (Submitted).
- Nagarajan, M., Benjakul, S., Prodpran, T. and Songtipya, P. 2013a. Effects of bleaching on characteristics and gelling property of gelatin from splendid squid (*Loligo formosana*) skin. *Food Hydrocolloid.* 32: 447-452.
- Nagarajan, M., Benjakul, S., Prodpran, T., Songtipya, P. and Nuthong, P. 2013b. Film forming ability of gelatins from splendid squid (*Loligo formosana*) skin bleached with hydrogen peroxide. *Food Chem.* 138: 1101-1108.
- Nagarajan, M., Benjakul, S., Prodpran, T., Songtipya, P. and Kishimura, H. 2012a. Characteristics and functional properties of gelatin from splendid squid (*Loligo formosana*) skin as affected by extraction temperatures. *Food Hydrocolloid.* 29: 389-397.
- Nagarajan, M., Benjakul, S., Prodpran, T. and Songtipya, P. 2012b. Properties of film from splendid squid (*Loligo formosana*) skin gelatin with various extraction temperatures. *Int. J. Biol. Macromol.* 51: 489-496.
- Nalinanon, S., Benjakul, S., Kishimura, H. and Osako, K. 2011. Type I collagen from the skin of ornate threadfin bream (*Nemipterus hexodon*): Characteristics and effect of pepsin hydrolysis. *Food Chem.* 125: 500-507.
- Nalinanon, S., Benjakul, S., Visessanguan, W. and Kishimura, H. 2008. Improvement of gelatin extraction from bigeye snapper skin using pepsin-aided process in combination with protease inhibitor. *Food Hydrocolloid.* 22: 615-622.

- Nalinanon, S., Benjakul, S., Visessanguan, W. and Kishimura, H. 2007. Use of pepsin for collagen extraction from the skin of bigeye snapper (*Priacanthus tayenus*). *Food Chem.* 104: 593-601.
- Nikoo, M., Benjakul, S., Bashari, M., Alekhorshied, M., Cissouma, A. I., Yang, N. and Xu, X. 2014. Physicochemical properties of skin gelatin from farmed Amur sturgeon (*Acipenser schrenckii*) as influenced by acid pretreatment. *Food Biosci.* 5: 19–26.
- Ninan, G., Abubacker, Z. and Jose, J. 2011a. Physico-chemical and texture properties of gelatins and water gel desserts prepared from the skin of freshwater carps. *Fish Technol.* 48: 67-74.
- Ninan, G., Jose, J. and Abubacker, Z. 2011b. Preparation and characterisation of gelatin extracted from the skins of rohu (*Labeo rohita*) and common carp (*Cyprinus carpio*). *J. Food Process. Pres.* 35: 143-162.
- Ninan, G., Joseph, J. and Abubacker, Z. 2010. Physical, mechanical, and barrier properties of carp and mammalian skin gelatin films. *J. Food Sci.* 75: E620-E626.
- Niu, L., Zhou, X., Yuan, C., Bai, Y., Lai, K., Yang, F. and Huang, Y. 2013. Characterization of tilapia (*Oreochromis niloticus*) skin gelatin extracted with alkaline and different acid pretreatments. *Food Hydrocolloid.* 33: 336-341.
- Nunez-Flores, R., Gimenez, B., Fernandez-Martin, F., Lopez-Caballero, M. E., Montero, M. P. and Gomez-Guillen, M. C. 2013a. Physical and functional characterization of active fish gelatin films incorporated with lignin. *Food Hydrocolloid.* 30: 163-172.

- Nunez-Flores, R., Castro, A. X., Lopez-Caballero, M. E., Montero, P. and Gomez-Guillen, M. C. 2013b. Functional stability of gelatin–lignosulphonate films and their feasibility to preserve sardine fillets during chilled storage in combination with high pressure treatment. *Innov. Food Sci. Emerg.* 19: 95–103.
- Nunez-Flores, R., Gimenez, B., Fernandez-Martin, F., Lopez-Caballero, M. E., Montero, M. P. and Gomez-Guillen, M. C. 2012. Role of lignosulphonate in properties of fish gelatin films. *Food Hydrocolloid.* 27: 60-71.
- Nuthong, P., Benjakul, S. and Prodpran, T. 2009. Characterisation of porcine plasma protein-based films as affected by pretreatment and cross-linking agents. *Int. J. Biol. Macromol.* 44: 143-148.
- Ofori, R. A. 1999. Preparation of gelatin from fish skin by an enzyme aided process. Master of Science thesis. Macdonald Campus of McGill University, Montreal, Canada.
- Ojagh, S. M., Nunez-Flores, R., Lopez-Caballero, M. E., Montero, M. P. and Gomez-Guillen, M. C. 2011. Lessening of high-pressure-induced changes in Atlantic salmon muscle by the combined use of a fish gelatin-lignin film. *Food Chem.* 125: 595-606.
- Ojagh, S. M., Rezaei, M., Razavi, S. H., Hosseini, S. M. H., 2010. Effect of chitosan coatings enriched with cinnamon oil on the quality of refrigerated rainbow trout. *Food Chem.* 120: 193–198.
- Olabarrieta, I., Gallstedl, M., Ispizua, I., Sarasua, J.-R., Hedenqvist, M. S. 2006. Properties of aged montmorillonite-wheat gluten composite films. *J. Agric. Food Chem.* 54: 1283–1288.

- Ou, S. Y., Kwok, K. C. and Kang, Y. J. 2004. Changes in *in vitro* digestibility and available lysine of soy protein isolate after formation of film. *J. Food Eng.* 64: 301-305.
- Oussalah, M., Caillet, S., Salmieri, S., Saucier, L. and Lacroix, M. 2004. Antimicrobial and antioxidant effects of milk protein-based film containing essential oils for the preservation of whole beef muscle. *J. Agric. Food Chem.* 52: 5598–5605.
- Oxford, P., Parker, R. and Ring, S. 1989. Effect of water as a diluent on the glass transition behaviour of malto-oligosaccharides, amylase and amylopectin. *Int. J. Biol. Macromol.* 11: 91–96.
- Padgett, T., Han, I. Y. and Dawson, P. L. 1998. Incorporation of food-grade antimicrobial compounds into biodegradable packaging films. *J. Food Prot.* 61: 1330–1335.
- Padgett, T., Han, I. Y. and Dawson, P. L. 1995. Incorporation of lysozyme into biodegradable packaging films. *Poult. Sci.* 74: 165.
- Pandey, J. K., Singh, R. P. 2005. Green nanocomposites from renewable resources: effect of plasticiser on the structure and material properties of clay-filled starch. *Starch.* 57: 8–15.
- Papadokostaki, K. G., Amanratos, S. G. and Petropoulos, J. H. 1997. Kinetics of release of particules solutes incorporated in cellulosic polymer matrices as a function of solute solubility and polymer swellability. I. Sparingly soluble solutes. *J. Appl. Polym. Sci.* 67: 277–287.
- Papadopoulou, A. and Frazier, R. A. 2004. Characterisation of protein–polyphenol interactions. *Trends Food Sci. Technol.* 15: 186–190.

- Park, J. W., Whiteside, W. S. and Cho, S. Y. 2008. Mechanical and water vapor barrier properties of extruded and heat-pressed gelatin films. *Food Sci. Technol.* 41: 692–700.
- Park, H. M., Lee, W. K., Park, C. Y., Cho, W. J. and Ha, C. S. 2003. Environmentally friendly polymer hybrids: part I – mechanical, thermal, and barrier properties of thermoplastic starch/clay nanocomposites. *J. Mat. Sci.* 38: 909–915.
- Park, H. M., Li, X., Jin, C. Z., Park, C. Y., Cho, W. J., Ha, C. S. 2002. Preparation and properties of biodegradable thermoplastic starch/clay hybrids. *Macromol. Mater. Eng.* 287: 553–558.
- Pearce, K. N. and Kinsella, J. E. 1978. Emulsifying properties of proteins: evaluation of a turbidimetric technique. *J. Agric. Food Chem.* 26: 716-723.
- Penke, B., Ferenczi, R. and Kovacs, K. 1974. A new acid hydrolysis method for determining tryptophan in peptides and proteins. *Anal. Biochem.* 60, 45-50.
- Pereda, M., Ponce, A. G., Marcovich, N. E., Ruseckaite, R. A. and Martucci, J. F. 2011. Chitosan-gelatin composites and bi-layer films with potential antimicrobial activity. *Food Hydrocolloid.* 25: 1372-1381.
- Pereira de Abreu, D. A., Paseiro Losada, P. Maroto, J. and Cruz, J. M. 2011. Natural antioxidant active packaging film and its effect on lipid damage in frozen blue shark (*Prionace glauca*). *Innov. Food Sci. Emerg. Technol.* 12: 50-55.
- Perkins, W. S. 1996. Advances made in bleaching practice. *Alexander Technol. Int.* 4: 92–94.
- Piez, K. A. and Gross, J. 1960. The amino acid composition of some fish collagens: The relation between composition and structure. *J. Biol. Chem.* 235: 995-998.

- Pinnavaia, T. J. 1983. Intercalated clay catalysts. *Science*. 220: 365-371.
- Pommet, M., Redl, A., Guilbert, S. and Morel, M. H. 2005. Intrinsic influence of various plasticizers on functional properties and reactivity of wheat gluten thermoplastic materials. *J. Cereal Sci.* 42: 81-91.
- Pommet, M., Redl, A., Morel, M. H. and Guilbert, S. 2003. Study of wheat plasticisation with fatty acids. *Polymer*. 44: 115–122.
- Pradhan, N. K., Das, M., Palve, Y. P. and Nayak, P. L. 2012. Synthesis and characterization of soya protein isolate/cloisite 30B (MMT) nanocomposite for controlled release of anticancer drug curcumin. *Int. J. Res. Pharm. Biomed. Sci.* 3: 1513-1522.
- Pranoto, Y., Lee, C. M. and Park, H. J. 2007. Characterisations of fish gelatin films added with gellan and  $\kappa$ -carrageenan. *LWT–Food Sci. Technol.* 40: 766–774.
- Prigent, S. V. E., Gruppen, H., Visser, A. J. W. G., van Koningsveld, G. A., de Jong, G. A. H. and Voragen, A. G. J. 2003. Effects of non-covalent interactions with 5-O-caffeoylquinic acid (chlorogenic acid) on the heat denaturation and solubility of globular proteins. *J. Agric. Food Chem.* 51: 5088-5095.
- Qin, Z., Guo, X., Lin, Y., Chen, J., Liao, X., Hu, X. and Wu, J. 2013. Effects of high hydrostatic pressure on physicochemical and functional properties of walnut (*Juglans regia L.*) protein isolate. *J. Sci. Food Agric.* 93: 1105-1111.
- Rahman, M. S., Al-Saidi, G. S. and Guizani, N. 2008. Thermal characterisation of gelatin extracted from yellowfin tuna skin and commercial mammalian gelatin. *Food Chem.* 108: 472-481.
- Rao, Y. 2007. Gelatin-clay nanocomposites of improved properties. *Polymer*, 48, 5369–5375.

- Rattaya, S., Benjakul, S. and Prodpran, T. 2009. Properties of fish skin gelatin film incorporated with seaweed extract. *J. Food Eng.* 95: 151–157.
- Rawdkuen, S., Suthiluk, P., Kamhangwong, D. and Benjakul, S. 2012. Mechanical, physico-chemical, and antimicrobial properties of gelatin-based film incorporated with catechin-lysozyme. *Chem. Cent. J.* 6: 1-10.
- Ray, S. S. and Okamoto, M. 2003. Polymer/layered silicate nanocomposites: a review from preparation to processing. *Prog. Polym. Sci.* 28: 1539–1641.
- Rhim, J. 2012. Physical-Mechanical Properties of Agar/ $\kappa$ -Carrageenan Blend Film and Derived Clay Nanocomposite Film. *J. Food Sci.* 77: N66-N73.
- Rhim, J. 2011. Effect of clay contents on mechanical and water vapor barrier properties of agar-based nanocomposite films. *Carbohydr. Polym.* 86: 691–699.
- Rhim, J. 2007. Potential use of biopolymer-based nanocomposite films in food packaging applications. *Food Sci. Biotech.* 16: 691–709.
- Rhim, J. and Ng, P. 2007. Natural biopolymer-based nanocomposite films for packaging applications. *Crit. Rev. Food Sci. Nut.* 47: 411–433.
- Rhim, J., Hong, S. and Ha, C. 2009. Tensile, water vapor barrier and antimicrobial properties of PLA/nanoclay composite films. *LWT- Food Sci. Technol.* 42: 612-617.
- Rhim, J. W., Lee, J. H. and Ng, P. K. W. 2007. Mechanical and barrier properties of biodegradable soy protein isolate-based films coated with polylactic acid. *LWT-Food Sci. Technol.* 40: 232–238.

- Rhim, J., Hong, S., Park, H. and Ng, P. 2006a. Preparation and characterization of chitosan-based nanocomposite films with antimicrobial activity. *J. Agric. Food Chem.* 54: 5814–5822.
- Rhim, J., Mohanty, K. A., Singh, S. P. and Ng, P. K. W. 2006b. Preparation and properties of biodegradable multilayer films based on soy protein isolate and poly(lactide). *Ind. Eng. Chem. Res.* 45: 3059-3066.
- Rhim, J., Lee, J. H. and Kwak, H. S. 2005. Mechanical and barrier properties of soy protein and clay mineral composite films. *Food Sci. Biotechnol.* 14: 112–116.
- Richards, M. P. and Hultin, H. O. 2002. Contribution of blood and blood components to lipid oxidation in fish muscle. *J. Agric. Food Chem.* 50: 555–564.
- Robinson, H. W. and Hogden, C. G. 1940. The Biuret reaction in the determination of serum protein: I. A study of the condition necessary for the production of the stable color which bears a quantitative relationship to the protein concentration. *J. Biol. Chem.* 135, 707–725.
- Rodziewicz-Motowidlo, S., Sładewska, A., Mulkiewicz, E., Kolodziejczyk, A., Aleksandrowicz, A., Miskiewicz, J. and Stepnowski, P. 2008. Isolation and characterisation of a thermally stable collagen preparation from the outer skin of the silver carp *Hypophthalmichthys molitrix*. *Aquaculture.* 285: 130-134.
- Ross, C. F. and Smith, D. M. 2006. Use of volatiles as indicators of lipid oxidation in muscle foods. *Compr. Rev. Food Sci. Food Safe.* 5: 18–25.
- Ruiz-Hitzky, E., Darder, M. and Aranda, P. 2005. Functional biopolymer nanocomposites based on layered solids. *J. Mater. Chem.* 15: 3650–3662.
- Santoso, J., Yoshie-stark, Y. and Suzuki, T. 2004. Antioxidant activity of methanol extracts from Indonesian seaweeds in an oil emulsion model. *Fisheries Sci.* 70: 183–188.



- Sato, K., Ohashi, C., Muraki, M., Itsuda, H., Yokoyama, Y., Kanamori, M., Ohtsuki, K. and Kawabata, M. 1998. Isolation of intact Type V collagen from fish intramuscular connective tissue. *J. Food Biochem.* 22: 213-225.
- Sha, X., Tu, Z., Liu, W., Wang, H., Shi, Y., Huang, T. and Mana, Z. 2014. Effect of ammonium sulfate fractional precipitation on gel strength and characteristics of gelatin from bighead carp (*Hypophthalmichthys nobilis*) scale. *Food Hydrocolloid.* 36: 173-180.
- Shahidi, F., Xiao-Qing, H. and Synowiecki, J. 1995. Production and characteristics of protein hydrolysates from capelin (*Mallotus villosus*). *Food Chem.* 53, 285-293.
- Shahidi, F. 1994. Seafood processing by-products. *In* Seafoods chemistry, processing, technology and quality. (Shahidi, F. and Botta, J. R., eds.) .p. 11–26. Blackie Academic Professional. Glasgow.
- Shakila, R. J, Jeevithan, E., Varatharajakumar, A., Jeyasekaran, G. and Sukumar, D. 2012a. Functional characterisation of gelatin extracted from bones of red snapper and grouper in comparison with mammalian gelatin. *LWT–Food Sci. Technol.* 48: 30–36.
- Shakila, R. J., Jeevithan, E., Varatharajakumar, A., Jeyasekaran, G. and Sukumar, D. 2012b. Comparison of the properties of multi-composite fish gelatin films with that of mammalian gelatin films. *Food Chem.* 135, 2260-2267.
- Shankar, S., Reddy, J. P., Rhim, J. W. and Kim, H.-Y. 2015. Preparation, characterization, and antimicrobial activity of chitin nanofibrils reinforced carrageenan nanocomposite films, *Carbohydr. Polym.* DOI: <http://dx.doi.org/10.1016/j.carbpol.2014.10.010>.

- Shantha, N. C. and Decker, E. A. 1994. Rapid, sensitive, iron-based spectrophotometric methods for determination of peroxide values of food lipids. *J. AM. Oil Chemists' Soc.* 77: 421–424.
- Shiku, Y., Hamaguchi, P. Y., Benjakul, S., Visessanguan, W. and Tanaka, M. 2004. Effect of surimi quality on properties of edible films based on Alaska pollock. *Food Chem.* 86, 493–499.
- Shiku, Y., Hamaguchi, P. Y. and Tanaka, M. 2003. Effect of pH on the preparation of edible films based on fish myofibrillar proteins. *Fish. Sci.* 69: 1026-1032.
- Shon, J., Eo, J., Hwang, J. and Eun, J. 2011. Effect of processing conditions on functional properties of collagen powder from Skate (*Raja kenojei*) skins. *Food Sci. Biotechnol.* 20: 99-106.
- Shukla, R. and Cheryan, M. 2001. Zein: The industrial protein from corn. *Ind. Crop. Prod.* 13: 171-192.
- Shyni, K., Hema, G. S., Ninan, G., Mathew, S., Joshy, C. G. and Lakshmanan. P. T. 2014. Isolation and characterization of gelatin from the skins of skipjack tuna (*Katsuwonus pelamis*), dog shark (*Scoliodon sorrakowah*), and rohu (*Labeo rohita*). *Food Hydrocolloid.* 39: 68-76.
- Sikorski, Z. E. 2001. Functional properties of proteins in food systems. *In* Chemical and functional properties of food proteins. (Sikorski, Z. E., eds.). p. 113-136. Technomic publishing Co., Inc. Lancaster, PA.
- Sila, A., Martinez-Alvarez, O., Haddar, A., Gomez-Guillen, M. C., Nasri, M., Montero, M. P. and Bougatef, A. 2015. Recovery, viscoelastic and functional properties of Barbel skin gelatine: Investigation of anti-DPP-IV and anti-prolyl endopeptidase activities of generated gelatine polypeptides. *Food Chem.* 168: 478–486.

- Silva, R. S. G., Bandeira, S. F. and Pinto, L. A. A. 2014. Characteristics and chemical composition of skins gelatin from cobia (*Rachycentron canadum*). LWT-Food Sci. Technol. 57: 580-585.
- Singh, P., Benjakul, S., Maqsood, S. and Kishimura, H. 2011. Isolation and characterisation of collagen extracted from the skin of striped catfish (*Pangasianodon hypophthalmus*). Food Chem. 124: 97-105.
- Singleton, V. L. and Rossi, J. A. 1965. Colometric of total phenolics with phosphomolybdic-phosphotungstic acid reagents. Am. J. Enol. Vitic. 16: 144-158.
- Sinthusamran, S., Benjakul, S. and Kishimura, H. 2014. Characteristics and gel properties of gelatin from skin of seabass (*Lates calcarifer*) as influenced by extraction conditions. Food Chem. 152: 276-284.
- Sinthusamran, S., Benjakul, S. and Kishimura, H. 2013. Comparative study on molecular characteristics of acid soluble collagens from skin and swim bladder of seabass (*Lates calcarifer*). Food Chem. 138: 2435-2441.
- Skierka, E. and Sadowska, M. 2007. The influence of different acids and pepsin on the extractability of collagen from the skin of Baltic cod (*Gadus morhua*). Food Chem. 105: 1302-1306.
- Slade, L. and Levine, H. 1991. Beyond water activity: recent advances based on an alternative approach to the assessment of food quality and safety. Crit. Rev. Food Sci. Nut. 30: 115-360.
- Slavutsky, A. M., Bertuzzi, M. A. and Armada, M. 2012. Water barrier properties of starch-clay nanocomposite films. Braz. J. Food Sci. Techn. 15: 208-218.
- Slinkard, K. and Singleton, V. L. 1977. Total phenol analysis: automation and comparison with manual methods. AM. J. Enol. Viticult. 28: 49-55.

- Sobral, P. J. A., Menegalli, F. C., Hubinger, M. D. and Roques, M. A. 2001. Mechanical, water vapor barrier and thermal properties of gelatin based edible films. *Food Hydrocolloid*. 15: 423–432.
- Solomon, O., Svanberg, H. and Sahlstr, M. A. 1995. Effect of oxygen and fluorescent light on the quality of orange juice during storage at 8 °C. *Food Chem*. 53: 363–368.
- Song, N., Jo, W., Song, H., Chung, K., Won, M. and Song, K. B. 2013. Effects of plasticizers and nano-clay content on the physical properties of chicken feather protein composite films. *Food Hydrocolloid*. 31: 340-345.
- Songchotikunpan, P., Tattiyakul, J. and Supaphol, P. 2008. Extraction and electrospinning of gelatin from fish skin. *Int. J. Biol. Macromol*. 42: 247–255.
- Sothornvit, R., Hong, S., An, D. J. and Rhim, J. 2010. Effect of clay content on the physical and antimicrobial properties of whey protein isolate/organo-clay composite films. *LWT-Food Sci. Technol*. 43: 279–284.
- Sothornvit, R., Rhim, J. and Hong, S. 2009. Effect of nano-clay type on the physical and antimicrobial properties of whey protein isolate/clay composite films. *J. Food Eng*. 91: 468-473.
- Sothornvit, R. and Krochta, J. M. 2005. Plasticisers in edible films and coatings. *In*. *Innovations in food packaging*. Vol. 403-433. (Han J. H, ed.). Elsevier Academic Press. San Diego, Calif.
- Sothornvit, R. and Krochta, J. M. 2000. Plasticiser effect on oxygen permeability of  $\beta$ -lactoglobulin films. *J. Agric. Food Chem*. 48: 6298-6302.
- Southern Clay Products Cloisite nanoclay technical report, [www.scprod.com](http://www.scprod.com).

- Sozer, N. and Kokini, J. L. 2009. Nanotechnology and its applications in the food sector. *Trend. Biotechnol.* 27: 82-89.
- Stainsby, G. 1987. Gelatin gels. *In* Advances in meat research. (Pearson, A. M. and Dutson T. R. eds.). Vol 4. Ch. 11. p. 209-220. Van Nostrand Reinhold Company. New York.
- Stadtman, E. R. 2001. Protein oxidation in aging and age-related diseases. *Ann. NY. Acad. Sci.* 928: 22–38.
- Stadtman, E. R. 1997. Free radical mediated oxidation of proteins. *In* Free radicals, oxidative stress, and antioxidants: Pathological and physiological significance. (Ozben. T., ed.). p. 51–65. Plenum Press Inc. New York.
- Steel, R. G. D. and Torrie, J. H. 1980. Principles and procedures of statistics: A biometrical approach (2nd ed.). McGraw-Hill. New York.
- Stuchell, Y. M. and Krochta, J. M. 1994. Enzymatic treatments and thermal effects on edible soy protein films. *J. Food Sci.* 59: 1332-1337.
- Surewicz, W. K. and Mantsch, H. H. 1988. New insight into protein secondary structure from resolution-enhanced infrared spectra. *BBA-Protein Struct. M.* 952: 115–130.
- Taheri, A., Abedian Kenari, A. M., Gildberg, A. and Behnam, S. 2009. Extraction and physicochemical characterization of greater lizardfish (*Saurida tumbil*) skin and bone gelatin. *J. Food Sci.* 74: 160-165.
- Thanonkaew, A., Benjakul, S., Visessanguan, W. and Decker, E. A. 2008. The effect of antioxidants on the quality changes of cuttlefish (*Sepia pharaonis*) muscle during frozen storage. *LWT-Food Sci. Technol.* 41: 161–169.

- Tharanathan, R. N. 2003. Biodegradable films and composite coatings: past, present and future. *Trend. Food Sci. Technol.* 1: 71-78.
- Theng, B. K. G. 1979. Formation and properties of clay–polymer complexes. Elsevier Scientific Publishing Company. NY.
- Thiansilakl, Y., Benjakul, S. and Shahidi, F. 2007. Compositions, functional properties and Antioxidative activity of protein hydrolysates prepared from round scad (*Decapterus maruadsi*). *Food Chem.* 103: 1385- 1394.
- Thomazine, M., Carvalho, R. A. and Sobral, P. J. A. 2005. Physical properties of gelatin films plasticised by blends of glycerol and sorbitol. *J. Food Sci.* 71: 172–176.
- Tongnuanchan, P., Benjakul, S. and Prodpran, T. 2013. Physico-chemical properties, Morphology and antioxidant activity of film from fish skin gelatin incorporated with root essential oils. *J. Food Eng.* 117: 350–360.
- Tongnuanchan, P., Benjakul, S. and Prodpran, T. 2012. Properties and antioxidant activity of fish skin gelatin film incorporated with citrus essential oils. *Food Chem.* 134: 1571–1579.
- Tongnuanchan, P., Benjakul, S., Prodpran, T. and Songtipya, P. 2011. Characteristics of film based on protein isolate from red tilapia muscle with negligible yellow discoloration. *Int. J Biol. Macromol.* 48: 758–767.
- Torrezan, R., Tham, W. P., Bell, A. E., Frazier, R. A. and Cristianini, M. 2007. Effects of high pressure on functional properties of soy protein. *Food Chem.* 104: 140-147.
- Tunc, S., Angellier, H., Cahyana, Y., Chalier, P., Gontard, N. and Gastaldi, E. 2007. Functional properties of wheat gluten/montmorillonite nanocomposite films processed by casting. *J. Membrane Sci.* 289: 159–168.

- United States Pharmacopeia, 1990. Gelatin. Official Monographs for USP XXII/NF.
- Uriarte-Montoya, M. H., Santacruz-Ortega, H., Cinco-Moroyoqui, F. J., Rouzaud-Sández, O., Plascencia-Jatomea, M. and Ezquerra-Brauer, J. M. 2011. Giant squid skin gelatin: Chemical composition and biophysical characterisation. *Food Res. Int.* 44: 3243–3249.
- Van der Ven, C., Gruppen, H., de Bont, D. B. A. and Voragen, A. G. J. 2002. Optimisation of the angiotensin converting enzyme inhibition by whey protein hydrolysates using response surface methodology. *Int. Dairy J.* 12: 813–820.
- Vanin, F. M., Hirano, M. H., Carvalho, R. A., Moraes, I. C. F., Bittante, A. M. Q. B. and Sobral, P. J. d. A. 2014. Development of active gelatin-based nanocomposite films produced in an automatic spreader. *Food Res. Int.* 63: 16–24.
- Vanin, F. M., Sobral, P. J. A., Menegalli, F. C., Carvalho, R. A. and Habitante, A. M. Q. B. 2005. Effects of plasticisers and their concentrations on thermal and functional properties of gelatin-based films. *Food Hydrocolloid.* 19: 899–907.
- Vargas, M., Perdonés, A., Chiralt, A., Chafer, M. and Gonzalez-Martinez, C. 2011. Effect of homogenisation conditions on physicochemical properties of chitosan-based film-forming dispersions and films. *Food Hydrocolloid.* 25: 1158–1164.
- Varlet, V., Knockaer, C., Prost, C. and Serot, T. 2006. Comparison of odor-active volatile compounds of fresh and smoked salmon. *J. Agric. Food Chem.* 54: 3391–3401.

- Vartiainen, J., Tammelin, T., Pere, J., Tapper, U. and Harlin, A. 2010. Biohybrid barrier films from fluidized pectin and nanoclay. *Carbohydr. Polym.* 82: 989–996.
- Vazquez-Torres, H., Canche-Escamilla, G. and Cruz-Ramos, C. A. 1992. Coconut husk lignin. I. Extraction and characterisation. *J. Appl. Polym. Sci.* 45: 633–644.
- Veeruraj, A., Arumugam, M., Ajithkumar, T. and Balasubramanian, T. 2014. Isolation and characterization of collagen from the outer skin of squid (*Doryteuthis singhalensis*). *Food Hydrocolloid.* 1-9.  
DOI: <http://dx.doi.org/10.1016/j.foodhyd.2014.07.025>
- Vermeiren, L., Devlieghere, F., Van Beest, M., De Kruijf, N. and Debevere, J. 1999. Developments in the active packaging of foods. *Trend. Food Sci. Technol.* 10: 77-86.
- Vichasilp, C., Sai-Ut, S., Benjakul, S. and Rawdkuen, S. 2014. Effect of Longan Seed Extract and BHT on Physical and Chemical Properties of Gelatin Based Film. *Food Biophysics.* DOI 10.1007/s11483-014-9345-4.
- Vojdani, F. and Torres, J.A. 1989. Potassium sorbate permeability of methylcellulose and hydroxypropyl methylcellulose multi-layer films. *J. Food Process. Preserv.* 13: 417–430.
- Wang, Y., Liu, A., Ye, R., Wang, W. and Li, X. 2015. Transglutaminase-induced crosslinking of gelatin–calcium carbonate composite films. *Food Chem.* 166: 414-422.
- Wang, L., An, X., Yang, F., Xin, Z., Zhao, L. and Hu, Q. 2008. Isolation and characterisation of collagens from the skin, scale and bone of deep-sea red fish (*Sebastes mentella*). *Food Chem.* 108: 616-623.



- Weng, W. and Zheng, H. 2015. Effect of transglutaminase on properties of tilapia scale gelatin films incorporated with soy protein isolate. *Food Chem.* 169: 255–260.
- Weng, W. and Wu, F. 2014. Water resistance and mechanical property improvement of tilapia (*Tilapia zillii*) scale gelatin films by dehydrated thermal treatment. *J. Food Sci. Tech.* DOI 10.1007/s13197-014-1401-z.
- Weng, W., Zheng, H. and Su, W. 2014. Characterisation of edible films based on tilapia (*Tilapia zillii*) scale gelatin with different extraction pH. *Food Hydrocolloid.* 41: 19-26.
- Wihodo, M. and Moraru, C. I. 2013. Physical and chemical methods used to enhance the structure and mechanical properties of protein films: A review. *J. Food Eng.* 114: 292–302.
- Wilesmith, J. W., Ryan, J. B. M. and Atkinson, M. J. 1991. Bovine spongiform encephalopathy: epidemiological studies on the origin. *Vet. Rec.* 128: 199-203.
- Woodward, S. A. 1990. Egg Protein Gels. *In Food Gels.* (Harris, P., ed.). p. 175-199. Elsevier Science Publishers Ltd. Essex, England.
- Wu, J., Ge, S., Liu, H., Wang, S., Chen, S., Wang, J., Li, J. and Zhang, Q. 2014. Properties and antimicrobial activity of silver carp (*Hypophthalmichthys molitrix*) skin gelatin-chitosan films incorporated with oregano essential oil for fish preservation. *Food Pack. Shelf Life.* 2: 7–16.
- Wu, J., Chen, S., Ge, S., Miao, J., Li, J. and Zhang, Q. 2013. Preparation, properties and antioxidant activity of an active film from silver carp (*Hypophthalmichthys molitrix*) skin gelatin incorporated with green tea extract. *Food Hydrocolloid.* 32: 42-51.

- Wu, H. C., Chen, H. M. and Shiau, C. Y. 2003. Free amino acids and peptides as related to antioxidant properties in protein hydrolysates of mackerel (*Scomber austriasicus*). Food Res. Int. 36: 949–957.
- Xu, Y., Ren, X., & Hanna, M., 2006. Chitosan/clay nanocomposite film preparation and characterization. J. Appl. Polym. Sci. 99: 1684–1691.
- Yakimets, I., Wellner, N., Smith, A. C., Wilson, R. H., Farhat, I. and Mitchell, J. 2005. Mechanical properties with respect to water content of gelatin films in glassy state. Polymer. 46: 12577–12585.
- Yamauchi, K., Schimizu, M. and Kamiya, T. 1980. Emulsifying properties of whey proteins. J. Food Sci. 45: 1237-1244.
- Yan, M., Li, B., Zhao, X. and Qin, S. 2012. Effect of concentration, pH and ionic strength on the kinetic self-assembly of acid-soluble collagen from walleye pollock (*Theragra chalcogramma*) skin. Food Hydrocolloid. 29: 199-204.
- Yan, M., Li, B., Zhao, X. and Yi, J. 2011. Physicochemical properties of gelatin gels from walleye pollock (*Theragra chalcogramma*) skin cross-linked by gallic acid and rutin. Food Hydrocolloid. 25: 907-914.
- Yan, M., Li, B., Zhao, X., Ren, G., Zhuang, Y., Hou, H., Zhang, X., Chen, L. and Fan, Y. 2008. Characterisation of acid-soluble collagen from the skin of walleye pollock (*Theragra chalcogramma*). Food Chem. 107: 1581-1586.
- Yang, H., Wang, Y., Jiang, M., Oh, J. H., Herring, J. and Zhou, P. 2007. 2-step optimization of the extraction and subsequent physical properties of Channel Catfish (*Ictalurus punctatus*) skin gelatin. J. Food Sci. 72: C188–C195.
- Yanishlieva, N. V. and Marinova, E. M. 2001. Stabilisation of edible oils with natural antioxidants. Eur. J. Lipid Sci. Tech. 103: 752-767.

- Yarnpakdee, S., Benjakul, S., Nalinanon, S. and Kristinsson, H. G. 2012. Lipid oxidation and fishy odour development in protein hydrolysate from Nile tilapia (*Oreochromis niloticus*) muscle as affected by freshness and antioxidants. *Food Chem.* 132: 1781–1788.
- Yoshinaka, R., Sato, K., Sato, M. and Anbe, H. 1990. Distribution of collagen in body of several fishes. *Nippon Suisan Gakkaishi.* 56: 549.
- Yudi, P., Chong, M. L. and Hyun, J. P. 2007. Characterisations of fish gelatin films added with gellan and  $\kappa$ -carrageenan. *LWT- Food Sci. Technol.* 40: 766-774.
- Zarai, Z., Balti, R., Mejdoub, H., Gargouri, Y. and Sayari, A. 2012. Process for extracting gelatin from marine snail (*Hexaplex trunculus*): Chemical composition and functional properties. *Process Biochem.* 47: 1779-1784.
- Zayas, J. F. 1997. *Functionality of proteins in food.* Springer. Berlin.
- Zeisel, S. H., Dacosta, K. A. and Fox, J. G. 1985. Endogenous formation of dimethylamine. *Biochem. J.* 232: 403–408.
- Zeng, S.-k., Zhang, C.-h., Lin, H., Yang, P., Hong, P.-z. and Jiang, Z. 2009. Isolation and characterisation of acid-solubilised collagen from the skin of Nile tilapia (*Oreochromis niloticus*). *Food Chem.* 116: 879-883.
- Zeng, Q. H., Yu, A. B., Lu, G. Q. and Paul, D. R. 2005. Clay-based polymer nanocomposites: Research and commercial development. *J. Nanosci. Nanotechnol.* 5: 1574–1592.
- Zhang, C., Ma, Y., Guo, K. and Zhao, X. 2012. High-pressure homogenisation lowers water vapor permeability of soybean protein isolate–beeswax films. *J. Agric. Food Chem.* 60: 2219–2223.

- Zhang, F., Xu, S. and Wang, Z. 2011. Pre-treatment optimisation and properties of gelatin from freshwater fish scales. *Food Bioprod. Process.* 89: 185–193.
- Zhang, M., Liu, W. and Li, G. 2009. Isolation and characterisation of collagens from the skin of largefin longbarbel catfish (*Mystus macropterus*). *Food Chem.* 115: 826-831.
- Zheng, J. P., Li, P., Ma, Y. L. and Yao, K. D. 2002. Gelatin/montmorillonite hybrid nanocomposite. I. Preparation and properties. *J. Appl. Polym. Sci.* 86: 1189-1194.
- Zhou, P. and Regenstein, J. M. 2005. Effects of alkaline and acid pretreatments on Alaska pollock skin gelatin extraction. *J. Food Sci.* 70: C392-C396.
- Zhou, P. and Regenstein, J. M. 2004. Optimisation of extraction conditions for pollock skin gelatin. *J. Food Sci.* 69: C393–C398.
- Zhou, P. and Regenstein, J. M. 2003. Extraction of gelatin from pollock skin. Session 76A, Aquatic Food Products: General. IFT Annual Meeting–Chicago.

## VITAE

**Name** Mr. Muralidharan Nagarajan

**Student ID** 5411030022

### **Educational Attainment**

<b>Degree</b>	<b>Name of Institution</b>	<b>Year of Graduation</b>
Bachelor of Fisheries Science	Tamil Nadu Veterinary and Animal Sciences University, Chennai, India	2007
Master of Fisheries Science	Tamil Nadu Veterinary and Animal Sciences University, Chennai, India	2009

### **Scholarship Awards during Enrollment**

ICAR-International Fellowship granted by Indian Council of Agricultural Research (ICAR), New Delhi, India.

### **List of Publication and Proceedings**

#### **Publications**

1. Nagarajan, M., Benjakul, S., Prodpran, T., Songtipya, P. and Kishimura, H. 2012. Characteristics and functional properties of gelatin from splendid squid (*Loligo formosana*) skin as affected by extraction temperatures. Food Hydrocolloid. 29: 389-397.
2. Nagarajan, M., Benjakul, S., Prodpran, T. and Songtipya, P. 2012. Properties of film from splendid squid (*Loligo formosana*) skin gelatin with various extraction temperatures. Int. J. Biol. Macromol. 51: 489–496.
3. Nagarajan, M., Benjakul, S., Prodpran, T. and Songtipya, P. 2013. Effects of bleaching on characteristics and gelling property of gelatin from splendid squid (*Loligo formosana*) skin. Food Hydrocolloid. 32: 447-452.

4. Nagarajan, M., Benjakul, S., Prodpran, T., Songtipya, P. and Nuthong, P. 2013. Film forming ability of gelatins from splendid squid (*Loligo formosana*) skin bleached with hydrogen peroxide. *Food Chem.* 138: 1101-1108.
5. Nagarajan, M., Benjakul, S., Prodpran, T. and Songtipya, P. 2014. Characteristics of bio-nanocomposite films from tilapia skin gelatin incorporated with hydrophilic and hydrophobic nanoclays. *J. Food Eng.* 143: 195-204.
6. Nagarajan, M., Benjakul, S., Prodpran, T. and Songtipya, P. 2014. Properties of bio-nanocomposite films from tilapia skin gelatin as affected by different nanoclays and homogenising conditions. *Food Bioprocess Tech.* 7: 3269-3281.
7. Nagarajan, M., Benjakul, S., Prodpran, T. and Songtipya, P. 2014. Effects of pHs on properties of bio-nanocomposite based on tilapia skin gelatin and Cloisite Na<sup>+</sup>. *Eur. Polym. J.* (Submitted).
8. Nagarajan, M., Benjakul, S., Prodpran, T. and Songtipya, P. 2014. Properties and characteristics of nanocomposite films from tilapia skin gelatin incorporated with ethanolic extract from coconut husk. *Food Hydrocolloid.* (Submitted).
9. Nagarajan, M., Benjakul, S., Prodpran, T. and Songtipya, P. 2014. Effects of bio-nanocomposite films from tilapia and squid skin gelatins incorporated with ethanolic extract from coconut husk on storage stability of mackerel meat powder. *Food Pack. Shelf Life.* (Submitted).

#### **Proceedings/presentations**

1. Nagarajan, M., Benjakul, S., Prodpran, T. and Songtipya, P. Effect of extraction temperature on characteristics and film forming ability of gelatin from splendid squid (*Loligo formosana*) skin. 15<sup>th</sup> Food Innovation Asia Conference (FIAC2013), BITEC Bangna, Bangkok, Thailand, 13-14 June 2013. Oral presentation.
2. Nagarajan, M., Benjakul, S., Prodpran, T. and Songtipya, P. Characteristics and film forming ability of gelatin from splendid squid (*Loligo formosana*) skin

bleached with hydrogen peroxide. 13<sup>th</sup> ASEAN Food Conference (AFC2013), Max Atria, Singapore Expo, 9-11 September 2013. Poster presentation.

3. Nagarajan, M., Benjakul, S., Prodpran, T. and Songtipya, P. Characteristics of biocomposite films from tilapia skin gelatin incorporated with hydrophilic and hydrophobic nanoclays. Joint Postgraduate Seminar USM-PSU-UNAND, Universiti Sains Malaysia, Penang, Malaysia, 4 April 2014. Oral presentation.

### **Book chapter**

Benjakul, S., Nagarajan, M. and Prodpran, T. 2014. Films & coatings from collagen and gelatin. II. Biopolymeric matrices “Traditional and alternative sources for biopolymeric film and coating matrices”. *In* Edible films and coatings: Fundamentals and applications (M.P. Montero, M.C. Gomez-Guillen, M.E. Lopez-Caballero, G.V. Barbosa-Canovas, Eds.). Florida, US: CRC press, Taylor & Francis Group. (In revision).